SPIN-ORBIT COUPLING IN ITINERANT-ELECTRON MAGNETISM

A thesis presented for the degree of Doctor of Philosophy of the University of London and the Diploma of Imperial College

by

John William Aidan Millar

Department of Mathematics
Imperial College of Science and Technology
London SW7 2BZ

CONTENTS

ACKNOWLEDGEMENTS

I am very grateful to Dr. D.M. Edwards, my supervisor, for suggesting the problem and for his constant ability to supply enthusiasm, inspiration and new ideas.

Thanks are due to Dr. R.B. Muniz and Dr. R. Zeller for the provision of computer code which partitions a Brillouin zone into tetrahedra. I should also like to thank many members of the Departments of Mathematics and of Physics for valuable discussions.

Financial support from the Science and Engineering Research Council is gratefully acknowledged.

ABSTRACT

The thesis seeks to establish some of the effects of strong spin-orbit coupling on itinerant-electron magnetism. It derives its motivation from the unusual magnetic properties of light actinide chalcogenides and pnictides, as in these systems the 5f electrons contribute to bonding and the Fermi surface, and the spin-orbit coupling is very important.

For simplicity the detailed calculations are made for a tight-binding d band in a face centred cubic lattice, rather than an f band, and in the presence of large spin-orbit coupling only a $j = 3/2$ subband is considered. The electrons are assumed to interact only when on the same atom and in the ground state this interaction is treated self-consistently via the Hartree-Fock approximation.

For sufficiently large values of the interaction the paramagnetic state is unstable against the formation of states with magnetic or quadrupolar ordering. In the magnetically ordered states the magnetic anisotropy is investigated. In the localized limit of an integral number of electrons per atom and large electron-electron interaction, the discussion is clearly related to the work of Cooper on cerium and actinide compounds.

To compare the model qualitatively with inelastic neutron scattering results the dynamical susceptibility $\chi^{\alpha\beta}(q,\omega)$ is calculated within the random phase approximation in both the paramagnetic and ordered states. For a system close to an antiferromagnetic instability the critical scattering is found to be very anisotropic, as is observed in uranium pnictides near the Néel temperature. It is shown that under certain circumstances spin-

wave modes in magnetically-ordered systems are very strongly damped as observed in uranium nitride and uranium sulphide.

Another possible application of the present work is to heavy fermion systems such as UPt_3 and UBe_{13}. These systems exhibit large quasi-particle mass enhancement and appear to be near a non-magnetic instability of the paramagnetic state. It is found that near a quadrupolar instability the present model leads to substantial mass enhancement due to interaction between the electrons and quadrupolar fluctuations.

CHAPTER 1

Magnetic response in light actinide compounds

1.1 Introduction

In an itinerant model of magnetism the electrons are taken to occupy Bloch states, so that the state of the system is described by the bandstructure calculated from the chosen Hamiltonian. The system may remain paramagnetic, or order in some magnetic or nonmagnetic sense; magnetic transitions involve a splitting of the bandstructure as Kramers' degeneracy is broken (that is invariance under time reversal no longer holds). A consequence of the Pauli exclusion principle and the exchange interaction is that electrons of parallel spin are kept apart. Hence instability with respect to a magnetic state is determined by the increase in electronic kinetic energy on transitions to Bloch states of higher energy and opposite spin, compared with the decrease in the electron-electron interaction energy produced by aligning the spins.

The exchange interaction and degeneracy are fundamental to magnetic properties in itinerant systems, and govern the ground state formed. Corresponding to the possible magnetic or nonmagnetic ordering there are magnetic or nonmagnetic excitations from the ground state. Spin flip excitations across the Fermi surface constitute spin waves in a spin-$\frac{1}{2}$ system with no degeneracy, and this involves creation of pairs of an electron and a hole of opposite spin. The magnetic excitation dispersion relation consists of a continuum of Stoner (single-particle) excitations together with spin wave (low-lying collective) excitations

at small values of momentum transfer, as shown by Izuyama et al. (1963). They calculate the magnetic transverse dynamic susceptibility which has poles corresponding to the excitation modes.

The multiband generalization of such a spin-$\frac{1}{2}$ RPA calculation has been developed by Cooke (1973) who has studied spin waves, and spin-wave disappearance, in d-band systems such as iron and nickel. The disappearance of spin waves at larger $\underset{\sim}{q}$ can be understood, as they can decay into Stoner excitations provided their energies are comparable and there is sufficient coupling. The spin-wave lifetime will depend on the details of the coupling between these excitations and on the density of Stoner excitations into which the spin wave can decay. The calculations of Cooke (1973), Cooke et al. (1980) assume zero spin-orbit coupling, and so whilst being suitable for lighter d-block elements cannot realistically model the properties of heavier elements. The presence of spin-orbit coupling in an itinerant system produces unusual effects, however, and real systems exist in which this occurs, for example some light actinide compounds.

The 5f electrons in some light actinide compounds contribute to bonding and the Fermi surface, and so in calculating magnetic response functions it is appropriate to use an itinerant formalism. Other important aspects of the problem are that the high atomic number of the actinides gives rise to large spin-orbit effects, and the existence of magnetic moments, indicating that the correlation between electrons is important.

The experiments by Fournier (1980) on the effects of pressure on the moments of uranium nitride also indicate that the electrons in some of these systems are itinerant and agree with calculations by Brooks and Kelly (to be published) on the effects of pressure on itinerant systems and their magnetic moments.

1.2 Experimental situation

The electronic structure of the uranium rock-salt structure pnictide and chalcogenides is characterized by hybridized 5f and 6d electrons and conduction electrons close to the Fermi energy, giving rise to metallic character, high electronic specific heat and susceptibility. A general review of the properties of actinide compounds is given in Erdös and Robinson (1983) and Buyers and Holden (1985). These compounds show extremely unusual magnetic behaviour in the following respects, observed experimentally. Firstly, the neutron critical scattering close to the onset of magnetic ordering has strongly anisotropic spin correlations characteristic of a two-dimensional system although these materials are cubic (Lander et al. (1978)). Secondly, the equilibrium magnetic behaviour is unusual, favouring $<001>$ alignment of moments and exhibiting transitions between unusual linear magnetic structures (Siemann and Cooper (1980)). Thirdly, the magnetic excitation behaviour is anomalous both with respect to the characteristics of the dispersion curves when well-defined excitations are observed, and to the occurrence of very strong damping especially in the uranium pnictides and chalcogenides with smaller lattice spacing (Buyers et al. (1980, 1981)).

Measurements on the critical neutral scattering of UN have revealed that it is essentially longitudinal (Holden et al. (1982b)), implying that the fluctuations are permitted parallel to the incipient moments of the low-temperature phase, while perpendicular spin fluctuations were highly suppressed. Spatial anisotropy was also present with the scattering in reciprocal space having a cigar-shaped distribution whose long axis lay along the domain

direction. The range of these correlations was much longer than in Heisenberg systems and was still observable at 1.6 T_N. Anisotropic critical scattering has also been observed in USb (Lander et al. (1978)) and UAs (Sinha et al.(1981)).

The static magnetic properties of these compounds are summarized in Table 1.1 (Buyers and Holden (1984)). Uranium nitride has an antiferromagnetic Type 1 structure with [001] ordering wavevector and has the lowest Néel temperature T_N and lowest ordered moment of the pnictides, together with the lowest uranium-uranium distance. The Type 1 structure has like moments arranged in sheets, with an up-down-up-down sequence by sheets, whereas the Type 1A structure has an up-up-down-down sequence.

Despite their high magnetic ordering temperatures magnetic pnictides show no detectable lattice distortion associated with magnetic ordering (Lander et al. (1974), Knott et al. (1979)). In contrast, the chalcogenides, which have ferromagnetic ordering along [111], do show significant distortions.

The neutron scattering experiments performed on uranium pnictides and chalcogenides such as UN, UP, UAs, USb, US, USe and UTe leave considerable difficulty in characterizing the dynamical properties of these systems. In experiments on those compounds with smaller lattice spacings such as UN, UP, UAs, US which possess itinerant character well-defined magnetic excitations (spin-waves) are not observed, whereas in those with larger lattice spacings and more localized character such as USb, UTe well-defined excitations are found.

Work by Buyers et al. (1981) on single crystals of UN has revealed a broad feature lacking sharp peaks, centred around 18 meV

TABLE I.1
Magnetic properties of uranium rocksalt structure compounds

Compound	Lattice parameter (A)	T_N or T_C (K)	Magnetic structure	Easy direction	Ordered moment[a] (μ_B)	Ordered moment[b] (μ_B)	μ_{eff} (μ_B)	θ (K)
UBi	6 34	285	AF I		3 0			
USb	6 205	213 ± 1	AF I triple k	⟨111⟩	2 82 ± 0 05		3 64	140
UAs	5 779	127 ± 1	T > 64 AF I single k	⟨001⟩	1 92 ± 0 04		3 46	42
			T < 64 AF IA double k	⟨110⟩	2 24 ± 0 04			
UP	5 589	125	T > 23 AF I single k	⟨100⟩	1 7		3 25	35
			T < 23 AF I double k	⟨110⟩	1 9			
UN	4 89	50	AF I single k	⟨001⟩	0 75 ± 0 10		2 9	−270
UTe	6 155	104	F	⟨111⟩	2 25 ± 0 05	1 91 ± 0 05	2 7	120
USe	5 744	160	F	⟨111⟩	2 0 ± 0 10	1 82	2 5	165
US	5 489	180	F	⟨111⟩	1 70 ± 0 03	1 55 ± 0 03	2 25	180
UC	4 960	—	Nonmagnetic					

[a] Measured by neutron diffraction
[b] Measured by magnetometer

and displaying longitudinal character. Lander and Stirling (1980) have found a discrete spin wave in the more localized USb; it was longitudinal in nature, and at higher temperature disappeared into a broad continuum of magnetic scattering. UAs appears to have no sharp excitations or crystal-field levels below about 30 meV (Stirling et al. (1980)), and this has been confirmed by more recent work (Loewenhaupt et al. (1982)), which investigated the energy spectrum up to about 60 meV. The latter experiments indicate that the average halfwidth at half maximum for the magnetic scattering found around 10-20 meV in UAs is about 15 meV at all temperatures.

Thus the properties of these uranium compounds fall into two regimes which may be related to the lattice parameter and hence degree of itinerancy. For USb (a_o = 6.18 Å) and UTe (a_o = 6.16 Å, Buyers et al. (1980)) well-defined excitations are present in the ordered state, whereas in UN (a_o = 4.89 Å, Holden et al. (1982b)), US (a_o = 5.49 Å, Holden et al. (1982a)) and UAs (a_o = 5.78 Å) the scattering is broad and ill-defined, containing no sharp features. At high temperatures (300 K) even in USb (Lander and Stirling (1980)) and UTe broad magnetic scattering is found. Loewenhaupt et al. (1982) conclude that their neutron scattering experiments show the strong influence of the itinerant conduction electrons on the dynamic properties of these materials, which have ordered moments ranging from $0.75\mu_B$ in UN to $2.2\mu_B$ in UAs and about $3.0\mu_B$ in USb.

1.3 Model of actinide magnetism

We shall now consider how a simple model may be established, in order to see how the results of applying the formalism to it bears upon substances such as uranium rock-salt compounds, and the inelastic neutron scattering measurements by Buyers and Holden (1985) and Holden et al. (1982a, 1982b) in UN and US.

Bandstructure calculations on a variety of actinide compounds by Brooks (1984) and Weinberger et al. (1980) yields 5f bandwidths of the order of 2eV; this agrees with the photoemission experiments by Norton et al. (1980) and is in contrast to the calculations of Adachi et al. (1969). The spin-orbit splitting between the $j = 7/2$ and $j = 5/2$ orbital levels in UN is about 0.7 eV. In compounds such as UN and US there is a tendency for the 5f band to split into two subbands, with the upper one lying above the Fermi level.

The work on the electronic bandstructure of uranium nitride by Weinberger et al. (1980) and Brooks (1984) has demonstrated that spin-orbit coupling is very important, and as a consequence that the 5f band has a tendency to split into $5f_{5/2}$ and $5f_{7/2}$ subbands divided by the Fermi level. Brooks finds that in the Γ_8 valance band states of UN the electron density is 3% $6p_{1/2}$, 26% $5f_{5/2}$, 14% $5f_{7/2}$ and 55% $2p_{3/2}$, whereas Weinberger et al. found 8% $6p_{1/2}$, 15% $5f_{5/2}$, 7% $5f_{7/2}$ and 54% $2p_{3/2}$. The ratio of the $5f_{5/2}$ to $5f_{7/2}$ occupation numbers is 2.7 according to Brooks (2.5 according to Weinberger) and the partial density of states $N_{f_{5/2}}(E_f) = 66$ states/Ry/f.u. and $N_{f_{7/2}}(E_f) = 6$ states/Ry/f.u. Thus the $5f_{5/2}$ band partially splits away from the $5f_{7/2}$. Hence a purely spin description of the states near the Fermi level is

unlikely to reveal the nature of actinide itinerant electron magnetism.

The model adopted considered only the uranium atoms of the rock-salt structures (therefore distributed on a face centred cubic lattice) and considered only the 5f band of the bandstructure with only first nearest neighbour hopping of electrons. Infinite spin-orbit coupling rather than a large value was assumed, as this completely splits the 5f band into a partially filled j = 5/2 subband and unfilled j = 7/2 subband. Hence the number of bands that must be considered is much smaller, and this allows the self-consistent ground state calculations and the dynamical susceptibility calculations to be carried out on the model. However, the ability to examine the effects of the spin-orbit coupling varying from small to large is lost, which would indicate how the effects found arise.

The treatment of the problem adopted was to combine the essential features of itinerancy spin-orbit interaction and correlation by assuming the long-range correlation reduces the Coulomb interaction to a screened interaction (predominantly intra-atomic) and then writing the Hamiltonian as containing a tight-binding kinetic energy term plus a Hubbard interaction term with parameter U.

In order to diagonalize the spin-orbit interaction it is convenient to use a basis of atomic orbitals of definite angular momentum $\mu = (j,m)$ for the Hamiltonian H' containing a general interaction U:

$$H' = \sum_{\mu\nu\underline{k}} T_{\mu\nu}(\underline{k})\, c^{+}_{\mu\underline{k}} c_{\nu\underline{k}} + \frac{1}{2} \sum_{\substack{\xi\eta \\ \mu\nu}} \sum_{\underline{k}\underline{p}\underline{q}} \langle \xi\underline{k}, \eta\underline{p}+\underline{q} \,|\, U \,|\, \mu\underline{p}, \nu\underline{k}+\underline{q} \rangle\, c^{+}_{\xi\underline{k}} c^{+}_{\eta\underline{p}+\underline{q}} c_{\mu\underline{p}} c_{\nu\underline{k}+\underline{q}} \qquad (1.1)$$

where $c^{+}_{\mu\underline{k}}$ creates an electron in a Bloch state of wavevector $\underline{k}$ formed from an atomic orbital μ. The term $T_{\mu\nu}(\underline{k})$ is a kinetic energy matrix, as used by Slater and Koster (1954) and Hodges et al. (1966), and the $T_{\mu\mu}$ are taken to include the spin-orbit interaction. The interaction U is assumed to be short-range (on site), reducing the Hamiltonian to a Hubbard Hamiltonian H,

$$H = \sum_{\mu\nu\underline{k}} T_{\mu\nu}(\underline{k}) c^{+}_{\mu\underline{k}} c_{\nu\underline{k}} + U \sum_{i} \sum_{\mu<\nu} n_{\mu i} n_{\nu i} \qquad (1.2)$$

$$= \sum_{\mu\nu\underline{k}} T_{\mu\nu}(\underline{k}) c^{+}_{\mu\underline{k}} c_{\nu\underline{k}} + \frac{U}{2N} \sum_{\mu\neq\nu} \sum_{\underline{k}\underline{k}'\underline{p}} c^{+}_{\mu\underline{k}} c^{+}_{\nu\underline{p}+\underline{k}'} c_{\nu\underline{p}} c_{\mu\underline{k}+\underline{k}'} \qquad (1.3)$$

as would be reasonable for a paramagnet or for the transverse susceptibility of a ferromagnet, where the long-range Coulomb interaction plays no role. Strictly, the longitudinal susceptibility requires inclusion of the long-range forces, but these are omitted in this model despite the spin-orbit coupling mixing the longitudinal and transverse responses.

Having assumed that the short-range correlation can be taken care of by replacing strong U interactions by weaker effective ones, the model is then treated at the Hartree-Fock (HF) and Random Phase Approximation (RPA) level, deriving the ground state self-consistently.

The one-electron HF Hamiltonian H" corresponding to equation (1.2) will be derived and can be diagonalized; the transformation from the original definite angular momentum basis $|\mu\underline{k}\rangle$, denoted by Greek symbols from this point to the HF eigenstates $|n\underline{k}\rangle$, denoted by Roman symbols, is defined by

$$c^{+}_{\mu\underline{k}} = \sum_{n} a^{*}_{n\mu}(\underline{k})\, c^{+}_{n\underline{k}} \qquad (1.4)$$

where for the N sites i at positions $\underline{R}_i$:

$$c^+_{\mu i} = \frac{1}{\sqrt{N}} \sum_{\underline{k}} e^{i\underline{k}\cdot\underline{R}_i} c^+_{\mu \underline{k}} \tag{1.5}$$

Also

$$H'' |n\underline{k}\rangle = E_{n\underline{k}} |n\underline{k}\rangle \tag{1.6}$$

so that the eigenstates $|n\underline{k}\rangle$ have energy $E_{n\underline{k}}$.

1.4 Hartree-Fock equations

The HF equations that we require as a single-particle approximation to this Hamiltonian H' in equation (1.1) may be derived by putting H' into the equation of motion:

$$\left[\sum_{\mu} a_{n\mu}(\underline{k}) c^+_{\mu\underline{k}} , H' \right] = - E_{n\underline{k}} \sum_{\mu} a_{n\mu}(\underline{k}) c^+_{\mu\underline{k}} \tag{1.7}$$

from which we obtain, by decoupling the expression, an HF equation taking account of the direct and exchange interaction:

$$E_{n\underline{k}} c^+_{n\underline{k}} = \sum_m \langle m\underline{k} | T | n\underline{k} \rangle c^+_{m\underline{k}}$$

$$+ \sum_{mi\underline{p}} \left\{ \langle m\underline{k}, i\underline{p} | U | i\underline{p}, n\underline{k} \rangle - \langle m\underline{k}, i\underline{p} | U | n\underline{k}, i\underline{p} \rangle \right\} f_{i\underline{p}} c^+_{m\underline{k}}$$

where $f_{i\underline{p}}$ is the occupation number of $|i\underline{p}\rangle$.

More specifically, for the Hubbard Hamiltonian H in equation (1.2), on expanding in the $|\lambda\underline{k}\rangle$ basis by using

$$a_{m\lambda}(\underline{k}) = \langle \lambda \underline{k} \mid m \underline{k} \rangle \tag{1.9}$$

we obtain on summing over the complete set of states $|m\underline{k}\rangle$

$$E_{n\underline{k}} a_{n\lambda}(\underline{k}) = \langle \lambda \underline{k} | T | n \underline{k} \rangle + \sum_{mi\underline{p}} a_{m\lambda}(\underline{k}) \frac{U}{N} \sum_{\mu \neq} \sum_{\nu}$$

$$\left\{ a^*_{m\mu}(\underline{k}) a^*_{i\nu}(\underline{p}) a_{i\nu}(\underline{p}) a_{n\mu}(\underline{k}) - a^*_{m\mu}(\underline{k}) a^*_{i\nu}(\underline{p}) a_{n\nu}(\underline{k}) a_{i\mu}(\underline{p}) \right\} f_{i\underline{p}} \tag{1.10}$$

$$= \sum_{\mu} \langle \lambda \underline{k} | T | \mu \underline{k} \rangle a_{n\mu}(\underline{k}) + \frac{U}{N} \sum_{i\underline{p}} \sum_{\mu \neq} \sum_{\nu} \delta_{\lambda\mu}$$

$$\left\{ a^*_{i\nu}(\underline{p}) a_{i\nu}(\underline{p}) a_{n\mu}(\underline{k}) - a^*_{i\nu}(\underline{p}) a_{n\nu}(\underline{k}) a_{i\mu}(\underline{p}) \right\} f_{i\underline{p}} \tag{1.11}$$

Hence

$$E_{n\underline{k}} a_{n\lambda}(\underline{k}) = \sum_{\mu} \langle \lambda \underline{k} | T | \mu \underline{k} \rangle a_{n\mu}(\underline{k}) + \frac{U}{N} \sum_{i\underline{p}} \sum_{\mu}$$

$$\left\{ \sum_{\nu \neq \lambda} \delta_{\lambda\mu} |a_{i\nu}(\underline{p})|^2 f_{i\underline{p}} a_{n\mu}(\underline{k}) - (1-\delta_{\mu\lambda}) a^*_{i\mu}(\underline{p}) a_{i\lambda}(\underline{p}) f_{i\underline{p}} a_{n\mu}(\underline{k}) \right\} \tag{1.12}$$

so that combining the diagonal component of the last term with the preceding one we have

$$E_{n\underline{k}} a_{n\lambda}(\underline{k}) = \sum_{\mu} \left\{ \langle \lambda \underline{k} | T | \mu \underline{k} \rangle + \frac{U}{N} \delta_{\lambda\mu} \sum_{i\underline{p}\nu} |a_{i\nu}(\underline{p})|^2 f_{i\underline{p}} \right.$$

$$\left. - \frac{U}{N} \sum_{i\underline{p}} a^*_{i\mu}(\underline{p}) a_{i\lambda}(\underline{p}) f_{i\underline{p}} \right\} a_{n\mu}(\underline{k}) \tag{1.13}$$

Thus, using $\langle n_{\lambda\mu} \rangle = \langle c^{+}_{\mu i} c_{\lambda i} \rangle$ given by

$$\langle n_{\lambda\mu} \rangle = \frac{1}{N} \sum_{i\underline{\rho}} a^{*}_{i\mu}(\underline{\rho}) a_{i\lambda}(\underline{\rho}) f_{i\underline{\rho}} \tag{1.14}$$

the HF equations can be written

$$E_{n\underline{k}} a_{n\lambda}(\underline{k}) = \sum_{\mu} \left\{ T_{\lambda\mu}(\underline{k}) + Un\delta_{\lambda\mu} - U\langle n_{\lambda\mu} \rangle \right\} a_{n\mu}(\underline{k}) \tag{1.15}$$

where n is the total number of electrons per atom. This single-particle HF Hamiltonian H" is, from equation (15),

$$H'' = \sum_{\mu\nu\underline{k}} \left\{ T_{\mu\nu}(\underline{k}) + U(n\delta_{\mu\nu} - \langle n_{\mu\nu} \rangle) \right\} c^{+}_{\mu\underline{k}} c_{\nu\underline{k}} \tag{1.16}$$

and can be solved self-consistently, with the $\langle n_{\mu\nu} \rangle$ being the parameters to be made consistent, and with the constraint that $\sum_{\mu} \langle n_{\mu\mu} \rangle = n$. Furthermore, it is shown in Appendix A that in the paramagnetic state or for ordering with respect to one of the cubic symmetry axes $\langle n_{\mu\nu} \rangle$ only has diagonal finite elements so that $\langle n_{\mu\nu} \rangle = \delta_{\mu\nu} \langle n_{\mu\mu} \rangle$.

It should be noted that the effective Coulomb interaction introduced by the Hubbard term in equation (2) has energy $\frac{1}{2}Un_i(n_i-1)$ where n_i is the total number of electrons on site i; this term commutes with all total spin and orbital angular momentum operators $\underline{S}_i$, $\underline{L}_i$ and the total angular momentum operator $\underline{J}_i$. It therefore has the correct rotational symmetry to correspond to a screened Coulomb interaction. However, Hund's rule exchange is not included, and this is discussed in Appendix B.

The total energy per atom E of a given solution can then be found from the cumulative density of states $\rho_{cum}(E)$, calculated

from the bandstructure, as, if m is the band index for N atoms,

$$E = \frac{1}{N} \sum_{m\underline{k}} E_{m\underline{k}} n_{m\underline{k}} - \frac{1}{2} U \sum_{\mu \neq \upsilon} \langle n_{\mu\mu} \rangle \langle n_{\upsilon\upsilon} \rangle \tag{1.17}$$

where the second term removes the double counting of the interaction term. Thus

$$E = \frac{1}{N} \int_{-\infty}^{E_f} dE \sum_{mk} E\, \delta(E - E_{mk}) - \frac{U}{2} \sum_{\mu \neq \upsilon} \langle n_{\mu\mu} \rangle \langle n_{\upsilon\upsilon} \rangle \tag{1.18}$$

and writing this as a surface integral, with i denoting tetrahedral points in $\underline{k}$-space:

$$E = \frac{1}{N} \int_{-\infty}^{E_f} dE\; E \sum_{mi} \frac{dS_{mi}(E)}{|\nabla E_{mk}|_i} - \frac{U}{2} \sum_{\mu \neq \upsilon} \langle n_{\mu\mu} \rangle \langle n_{\upsilon\upsilon} \rangle \tag{1.19}$$

where $dS_{mi}(E)$ is a linear surface element corresponding to energy E. The density of states $\rho(E)$ is then

$$\rho(E) = \frac{d}{dE} \rho_{cum}(E) \tag{1.20}$$

so that

$$E = \left[E\, \rho_{cum}(E) \right]_{-\infty}^{E_f} - \int_{-\infty}^{E_f} \rho_{cum}(E)\, dE - \frac{U}{2} \sum_{\mu \neq \upsilon} \langle n_{\mu\mu} \rangle \langle n_{\upsilon\upsilon} \rangle \tag{1.21}$$

$$= n E_f - \int_{-\infty}^{E_f} \rho_{cum}(E)\, dE - \frac{U}{2} \sum_{\mu \neq \upsilon} \langle n_{\mu\mu} \rangle \langle n_{\upsilon\upsilon} \rangle \tag{1.22}$$

where n is the number of electrons per atom and E_f the Fermi energy.

1.5 Basis functions and the Hartree-Fock matrix

The Slater-Koster kinetic energy matrix $T_{\mu\nu}(\underline{k})$ for the $\ell = 2$, $s = \frac{1}{2}$ d states splits into a j = 3/2 and j = 5/2 subband under large spin-orbit coupling. The canonical values of the dd hopping integrals are given in Anderson (1978) amongst other places and allow $dd\pi$, $dd\delta$ to be given in terms of $dd\sigma$:

$$dd\sigma = -1$$

$$dd\pi = 2/3$$

$$dd\delta = -1/6$$

The model was used making the approximation $dd\delta = 0$ with $dd\pi$ to be varied, and $dd\sigma = -1$.

The basis states chosen are the functions

$$\phi_1 = \sqrt{\left(\frac{15}{4\pi}\right)} \frac{xy}{r^2} f(r) \qquad \phi_2 = \sqrt{\left(\frac{15}{4\pi}\right)} \frac{yz}{r^2} f(r)$$

$$\phi_3 = \sqrt{\left(\frac{15}{4\pi}\right)} \frac{xz}{r^2} f(r) \qquad \phi_4 = \sqrt{\left(\frac{15}{4\pi}\right)} \frac{x^2-y^2}{2r^2} f(r)$$

$$\phi_5 = \sqrt{\left(\frac{15}{4\pi}\right)} \frac{3z^2-r^2}{2\sqrt{3}r^2} f(r)$$

and using only the j = 3/2 subband the $|j\, m_j\rangle$ states are resolved into $|m_L s\rangle$ states according to

$$|3/2\ 3/2\rangle = \sqrt{\tfrac{4}{5}}\,|2\ -1/2\rangle - \sqrt{\tfrac{1}{5}}\,|1\ 1/2\rangle$$

$$|3/2\ 1/2\rangle = \sqrt{\tfrac{3}{5}}\,|1\ -1/2\rangle - \sqrt{\tfrac{2}{5}}\,|0\ 1/2\rangle$$

$$|3/2\ -1/2\rangle = \sqrt{\tfrac{2}{5}}\,|0\ -1/2\rangle - \sqrt{\tfrac{3}{5}}\,|-1\ 1/2\rangle$$

$$|3/2\ -3/2\rangle = \sqrt{\tfrac{1}{5}}\,|-1\ -1/2\rangle - \sqrt{\tfrac{4}{5}}\,|-2\ 1/2\rangle$$

Therefore, as the states of definite m_L are

m_L	function
0	ϕ_5
+1	$-\frac{1}{\sqrt{2}}(\phi_3 + i\phi_2)$
−1	$\frac{1}{\sqrt{2}}(\phi_3 - i\phi_2)$
+2	$\frac{1}{\sqrt{2}}(\phi_4 + i\phi_1)$
−2	$\frac{1}{\sqrt{2}}(\phi_4 - i\phi_1)$

the form of $T_{\mu\nu}(\underline{k})$ using Slater and Koster (1954) and in the basis $|^3/_2\,^3/_2\rangle, |^3/_2\,^1/_2\rangle, |^3/_2\,^{-1}/_2\rangle, |^3/_2\,^{-3}/_2\rangle$ is

$$T_{\mu\nu}(\underline{k}) = \begin{pmatrix} a(\underline{k}) & c(\underline{k}) & d(\underline{k}) & 0 \\ c^*(\underline{k}) & b(\underline{k}) & 0 & d(\underline{k}) \\ d^*(\underline{k}) & 0 & b(\underline{k}) & -c(\underline{k}) \\ 0 & d^*(\underline{k}) & -c^*(\underline{k}) & a(\underline{k}) \end{pmatrix} \tag{1.23}$$

The definition of the spherical harmonics contains a factor $(-1)^m$ for $m > 0$ and + 1 otherwise so that

$$|1\,s\rangle = -\langle -1\,s\,|^*$$

If we have, for an fcc crystal of lattice constant a

$$\xi = a k_x$$

$$\eta = a k_y$$

$$\zeta = a k_z$$

we define $A = \cos\xi\cos\eta$, $B = \cos\xi\cos\zeta$, $C = \cos\eta\cos\zeta$, $D = \sin\eta\sin\zeta$, $E = \sin\xi\sin\zeta$, $F = \sin\xi\sin\eta$:

$$a(\underline{k}) = w\left(\left(\tfrac{6}{5}dd\sigma + 2dd\pi\right)A + \left(\tfrac{3}{5}dd\sigma + \tfrac{7}{5}dd\pi\right)(B+C)\right)$$

$$b(\underline{k}) = w\left(\left(\tfrac{2}{5}dd\sigma + \tfrac{6}{5}dd\pi\right)A + \left(dd\sigma + \tfrac{9}{5}dd\pi\right)(B+C)\right)$$

$$c(\underline{k}) = -w\,\tfrac{2\sqrt{3}}{5}(dd\sigma + dd\pi)(-E + iD)$$

$$d(\underline{k}) = w\,\tfrac{\sqrt{3}}{5}\left(-(dd\sigma + dd\pi)(B-C) - 2i(dd\sigma + dd\pi)F\right)$$

using $w = (15/4)^{1/2}$ to denote the normalization constant.

The fact that $\langle n_{\lambda\lambda}\rangle$ belongs to a single Γ_8^+ representation for the j = 3/2 subband implies (by Schurr's lemma) that in the paramagnetic state which has full cubic symmetry,

$$\langle n_{\lambda\lambda} \rangle = \frac{n}{4}$$

For U greater than a critical value the equations have possible solutions (e.g. a ferromagnetic solution) with the $\langle n_{\lambda\lambda} \rangle$ unequal.

1.6 Bandstructure and wave functions in the paramagnetic regime

In the paramagnetic regime with

$$H = T_{\lambda\mu} + U\,(n\delta_{\lambda\mu} - \langle n_{\lambda\mu} \rangle) \tag{1.24}$$

$$= T_{\lambda\mu} + \delta_{\lambda\mu}\,\frac{3Un}{4} \tag{1.25}$$

the eigenvalues ~~solutions~~ of H are

$$\lambda_{1,2}(\underline{k}) = \frac{1}{2}\left\{ a(\underline{k}) + b(\underline{k}) \pm \sqrt{\left((a(\underline{k}) - b(\underline{k}))^2 + 4\left(|c(\underline{k})|^2 + |d(\underline{k})|^2\right)\right)} \right\} + \frac{3Un}{4} \tag{1.26}$$

and have Kramers' degeneracy due to the Hamiltonian being invariant under time reversal; if i = 1,2 denotes the energy in the eigenvalue of H $\lambda_i(\underline{k})$ then the eigenvectors $y_i^{(1)}$, $y_i^{(2)}$ are

$$y_i^{(1)}(\underline{k}) = \left[(a-\lambda_i)(a+b-2\lambda_i)\right]^{-1/2} \begin{pmatrix} d \\ 0 \\ -(a-\lambda_i) \\ -c^* \end{pmatrix} \tag{1.27}$$

$$y_i^{(2)}(\underline{k}) = \left[(a-\lambda_i)(a+b-2\lambda_i)\right]^{-1/2} \begin{pmatrix} c \\ -(a-\lambda_i) \\ 0 \\ d^* \end{pmatrix} \tag{1.28}$$

where the superscript identifies each of the two Kramers-degenerate eigenvectors. These eigenvectors are then the coefficients $a^*_{n\mu}(\underline{k})$ where n is the band index (from i and 1,2) and μ the component index.

1.7 RPA calculations of the dynamical susceptibility

Given the ground state, the dynamical susceptibility $\chi^{\alpha\beta}(q,\omega)$ may be calculated within the RPA. The equations in both the RPA and in Spin Density Functional Theory (SDFT) have the same structure, as shown in Vosko and Perdew (1975), coming from an integral equation relating the spin density (in the spin only case) induced at $\underline{r}$ by a field at $\underline{r}'$ to that field. The interacting spin susceptibility $\chi(\underline{r}, \underline{r}')$ and non-interacting susceptibility $\chi^0(\underline{r}, \underline{r}_1)$ are related by

$$\chi(\underline{r},\underline{r}') = \chi^0(\underline{r},\underline{r}') + \int\int d^3\underline{r}_1 d^3\underline{r}_2 \chi^0(\underline{r},\underline{r}_1) I_{xc}(\underline{r}_1,\underline{r}_2) \chi(\underline{r}_2,\underline{r}') \qquad (1.29)$$

where

$$I_{xc}(\underline{r},\underline{r}') = -\frac{\delta^2 E_{xc}}{\delta m(\underline{r}) \delta m(\underline{r}')} \qquad (1.30)$$

E_{xc} is the exchange-correlation energy and $m(\underline{r})$ the magnetization at $\underline{r}$. The RPA calculation is similar to that of Cooke (1973) and Cooke et al. (1980), and this will be described in detail.

By considering the magnetic scattering of neutrons by both the spin and angular momentum of the electron, the neutron scattering cross-sections for solid angle Ω and energy E may be shown

to be (see Marshall and Lovesey (1971), pp. 107) for scattering from wavevector $\underline{k}$ to $\underline{k}'$, for a neutron of mass m with gyromagnetic moment γ,

$$\frac{d^2\sigma}{d\Omega dE'} = \left(\frac{m}{2\pi\hbar}\right)^2 (2\gamma\mu_N\mu_B)^2 (4\pi)^2 \sum_{\lambda\lambda'\sigma\sigma'} p_\lambda p_\sigma \frac{k'}{k}$$

$$\langle\lambda\sigma | (\underline{\sigma}\cdot\underline{Q})^+ | \lambda'\sigma'\rangle\langle\lambda'\sigma' | \underline{\sigma}\cdot\underline{Q} | \lambda\sigma\rangle \delta(\hbar\omega + E_{\lambda\sigma} - E_{\lambda'\sigma'}) \quad (1.31)$$

where p_λ is the neutron spin probability and where $|\lambda\sigma\rangle$ and $|\lambda'\sigma'\rangle$ are the initial and final states of the target and and $E_{\lambda\sigma}, E_{\lambda'\sigma'}$ the corresponding energies. The operator $\underline{Q}$ is defined by

$$\underline{Q} = \sum_i e^{i\underline{\kappa}\cdot\underline{r}_i} \left\{ \hat{\underline{\kappa}} \wedge (\underline{s}_i \wedge \hat{\underline{\kappa}}) - \frac{i}{\hbar\kappa} \hat{\underline{\kappa}} \wedge \underline{p}_i \right\} \quad (1.32)$$

$$\hat{\underline{\kappa}} = \frac{\underline{\kappa}}{\kappa} \quad (1.33) \qquad \underline{\kappa} = \underline{k} - \underline{k}' \quad (1.34)$$

where $\underline{r}_i$ is the position of the electron, and $\underline{\sigma}$ the Pauli spin operator; $\underline{p}_i$ is the momentum and $\underline{s}_i$ the magnetic moment operator.

An approximation to the cross-section may be obtained by assuming that $|\underline{\kappa}|^{-1}$ is much greater than the mean radius of the wave function of the unpaired electrons, so that $\underline{Q}$ has the form (using the dipole approximation)

$$\underline{Q} \simeq \sum_i e^{i\underline{\kappa}\cdot\underline{r}_i} \left\{ \bar{j}_0 \underline{s}_i + \frac{1}{2}(\bar{j}_0 + \bar{j}_2)\underline{L}_i \right\} \quad (1.35)$$

where $\underline{L}_i$ is the angular momentum operator for an atom at the site $\underline{r}_i$. The coefficient $\bar{j}_n(\kappa)$ is a radial integral given by

$$\bar{j}_n(\kappa) = \int_0^\infty dr\, r^2\, j_n(\kappa r)\, |f(r)|^2 \tag{1.36}$$

where j_n is a Bessel function of order n. In the limit of small κ the scattering amplitude in the forward direction is proportional to the total magnetic moment per atom, with Landé factor g:

$$\bar{j}_0 \underline{S} + \tfrac{1}{2}(\bar{j}_0 + \bar{j}_2)\underline{L} \longrightarrow \tfrac{1}{2}(\underline{L} + 2\underline{S}) \tag{1.37}$$

$$\tfrac{1}{2}(\underline{L} + 2\underline{S}) = \tfrac{1}{2} g \underline{J} \tag{1.38}$$

Therefore, if $F(\underline{\kappa})$ is the form factor and $\underline{J}_i$ the angular momentum operator and $\underline{J}_{\underline{\kappa}}$ its Fourier transform, then

$$Q \simeq \tfrac{1}{2} g F(\underline{\kappa}) \sum_i e^{i\underline{\kappa}\cdot\underline{r}_i} \underline{J}_i \tag{1.39}$$

and

$$\frac{d^2\sigma}{d\Omega dE'} \simeq \left(\frac{\gamma e^2}{mc^2}\right)^2 \left\{\tfrac{1}{2} g F(\underline{\kappa})\right\}^2 \frac{k'}{k} \sum_{\alpha\beta} (\delta_{\alpha\beta} - \hat{\kappa}_\alpha \hat{\kappa}_\beta)$$

$$\times \sum_{\lambda\lambda'\sigma\sigma'} P_\lambda \sum_{ii'} e^{i\underline{\kappa}\cdot(\underline{r}_{i'} - \underline{r}_i)} \langle \lambda\sigma | J_i^\alpha | \lambda'\sigma' \rangle \langle \lambda'\sigma' | J_{i'}^\beta | \lambda\sigma \rangle \delta(\hbar\omega + E_{\lambda\sigma} - E_{\lambda'\sigma'}) \tag{1.40}$$

$$\simeq \left(\frac{\gamma e^2}{mc^2}\right)^2 \frac{k'}{k} \sum_{\alpha\beta} (\delta_{\alpha\beta} - \hat{\underline{\kappa}}_\alpha \hat{\underline{\kappa}}_\beta) \frac{1}{2\pi\hbar} \int_{-\infty}^{\infty} dt\, e^{-i\omega t} \langle J_{\underline{\kappa}}^\alpha(0)\, J_{-\underline{\kappa}}^\beta(t) \rangle \tag{1.41}$$

as in Marshall and Lovesey (1971, p. 235).

Hence, it will be convenient in calculating the scattering cross-section and susceptibility $\chi^{\alpha\beta}(\underline{q},\omega)$ to use the retarded two-particle Green's function $G^R_{\alpha\beta}$ referring to $\underline{J}-\underline{J}$ response.

The susceptibility $\chi^{\alpha\beta}(q,\omega)$, where α = +, - or z (i.e. +1, -1, or 0), is proportional to the retarded two-particle Green's function $G^R_{\alpha\beta}$, which can be obtained from the time-ordered Green's function $G_{\alpha\beta}$ defined by

$$G_{\alpha\beta}(q,t) = -i\langle T\, J^{\alpha}_{q}(t)\, J^{\beta}_{-q}(0)\rangle \tag{1.42}$$

where T is the time-ordering operator. The relation between these Green's functions, which are discussed in Zubarev (1960), is

$$2i\, \mathrm{Im} G^R_{\alpha\beta}(q,\omega) = G_{\alpha\beta}(q,\omega+i\eta) - G_{\alpha\beta}(q,\omega-i\eta) \tag{1.43}$$

$$= -2\pi i\, \rho_{\alpha\beta}(q,\omega) \tag{1.44}$$

where $\rho_{\alpha\beta}(q,\omega)$ is the spectral density.

An angular momentum operator J^{α}_{q} which is the Fourier transform of the total angular momentum J^{α}_{i} of an electron on site i may be defined in terms of the operators $c^{+}_{\mu\underline{k}}$ defined by equation (1.4) above

$$J^{\alpha}_{q} = \sum_{\substack{\mu\underline{k}\\ jj'}} {}_{jj'}f^{\alpha}_{\mu}\; c^{+}_{(j,\mu+\alpha)\,\underline{k}}\; c_{(j',\mu)\,\underline{k}+q} \tag{1.45}$$

where j, j' are the various j manifolds within the set of available states and $\mu = (j, m_j)$; ${}_{jj'}f^{\alpha}_{\mu}$ is a scalar, where for just one manifold j = j'

$${}_{jj}f^{\alpha}_{\mu} = f^{\alpha}_{\mu} = \begin{cases} \mu & \alpha = 0, z \\ \sqrt{((j-\mu)(j+\mu+1))} & \alpha = + \\ \sqrt{((j+\mu)(j-\mu+1))} & \alpha = - \end{cases} \tag{1.46}$$

Therefore ρ^{α}_{q} may be expanded as

$$\rho^{\alpha}_{q} = \sum_{\mu \underline{k}} \sum_{\substack{mn \\ jj'}} jj' f^{\alpha}_{\mu} a^{*}_{n(j,\mu+\alpha)}(\underline{k}) a_{m(j'\mu)}(\underline{k}) c^{+}_{n\underline{k}} c_{m\underline{k}+q} \qquad (1.47)$$

using the expansion coefficients $a^{*}_{n\mu}(\underline{k})$ of equation (1.4) above and using the notation $\mu = (j, m_j)$.

If we define the Green's function $\hat{G}_{\alpha\beta}(n\underline{k}, m\underline{k}+q; t)$ to be

$$\hat{G}_{\alpha\beta}(n\underline{k}, m\underline{k}+q; t) = -i \langle T c^{+}_{n\underline{k}}(t) c_{m\underline{k}+q}(t) \rho^{\beta}_{-q}(0) \rangle \qquad (1.48)$$

then $G_{\alpha\beta}$ may be expressed in terms of $\hat{G}_{\alpha\beta}$

$$G_{\alpha\beta}(q,t) = \sum_{\mu \underline{k}} \sum_{\substack{mn \\ jj'}} jj' f^{\alpha}_{\mu} a^{*}_{n(j,\mu+\alpha)}(\underline{k}) a_{m(j'\mu)}(\underline{k}+q) \hat{G}_{\alpha\beta}(n\underline{k}, m\underline{k}+q; t) \qquad (1.49)$$

The equation of motion of this two-particle Green's function $\hat{G}_{\alpha\beta}$ is therefore

$$i\hbar \dot{\hat{G}}_{\alpha\beta}(n\underline{k}, m\underline{k}+q; t) = \delta(t) \langle [c^{+}_{n\underline{k}}(t) c_{m\underline{k}+q}(t), \rho^{\beta}_{-q}(0)] \rangle$$

$$- i \langle T [H, c^{+}_{n\underline{k}}(t) c_{m\underline{k}+q}(t)] \rho^{\beta}_{-q}(0) \rangle \qquad (1.50)$$

Substituting into equation (50) the general Hamiltonian (1.1) expressed in the $|m\underline{k}\rangle$ basis

$$H = \sum_{mn\underline{k}} \langle n\underline{k} | T + V | m\underline{k} \rangle c^{+}_{n\underline{k}} c_{m\underline{k}}$$

$$+ \frac{1}{2} \sum_{ijnm} \sum_{\underline{k}\underline{p}\underline{K}} \langle i\underline{k}, j\underline{p}+\underline{K} | u | n\underline{p}, m\underline{k}+\underline{K} \rangle c^{+}_{i\underline{k}} c_{j\underline{p}+\underline{K}} c_{n\underline{p}} c_{m\underline{k}+\underline{K}} - V \qquad (1.51)$$

we can use RPA linearization to restrict the equation to terms of the same order as $\hat{C}_{\alpha\beta}$, and to solve for this (and hence $\chi^{\alpha\beta}(q,\omega)$). From

$$H = \sum_{mn\underline{k}} E_{n\underline{k}}\,\delta_{mn}\,c^{+}_{m\underline{k}}c_{n\underline{k}} + \frac{1}{2}\sum_{\substack{ijnm\\ \underline{k}\underline{p}\underline{K}}} \langle i\underline{k}, j\underline{p}+\underline{K}\,|U|\,n\underline{p}, m\underline{k}+\underline{K}\rangle \qquad (1.52)$$
$$c^{+}_{i\underline{k}}c_{j\underline{p}+\underline{K}}c_{n\underline{p}}c_{m\underline{k}+\underline{K}} - V$$

and the HF (single-particle approximation) Hamiltonian derived above and given in equation (1.16), the potential V is

$$V = U\sum_{\underline{k}\lambda\mu}(n\delta_{\lambda\mu} - \langle n_{\lambda\mu}\rangle)\,c^{+}_{\lambda\underline{k}}\,c_{\mu\underline{k}} \qquad (1.53)$$

$$= U\sum_{\underline{k}\lambda\mu}\sum_{h\ell}(n\delta_{\lambda\mu} - \langle n_{\lambda\mu}\rangle)a^{*}_{h\lambda}(\underline{k})\,a_{\ell\mu}(\underline{k})\,c^{+}_{h\underline{k}}c_{\ell\underline{k}} \qquad (1.54)$$

If this Hamiltonian in equation (1.52) is substituted into the equation of motion the commutators required are

$$\langle[c^{+}_{n\underline{k}+\underline{q}}c_{m\underline{k}}\,,\,c^{+}_{h\underline{p}}c_{\ell\underline{p}+\underline{q}}]\rangle = \delta_{\underline{k}\underline{p}}\,\delta_{mh}\,\delta_{\ell n}(f_{n\underline{k}+\underline{q}} - f_{m\underline{k}}) \qquad (1.55)$$

$$[c^{+}_{n\underline{k}+\underline{q}}c_{m\underline{k}}\,,\sum_{m'\underline{k}}E_{m'\underline{k}}\,c^{+}_{m'\underline{k}}c_{m'\underline{k}}] = (E_{m\underline{k}} - E_{n\underline{k}+\underline{q}})\,c^{+}_{n\underline{k}+\underline{q}}\,c_{m\underline{k}} \qquad (1.56)$$

and the interaction term gives

$$U\sum_{\substack{h,\ell,m,n,\\ \underline{k},\underline{p},\underline{q}}}[c^{+}_{n\underline{k}+\underline{q}}c_{m\underline{k}}\,,\,c^{+}_{h,\underline{k}_1}c_{\ell,\underline{p}+\underline{q}_1}c_{n,\underline{p}}c_{m,\underline{k}_1+\underline{q}_1}] = \sum_{\underline{p},m,n,}\Big\{\langle m\underline{k}, n,\underline{p}_1\,|U|\,n,\underline{p}_1, m,\underline{k}\rangle$$

$$-\langle n,\underline{p}_1, m\underline{k}\,|U|\,n,\underline{p}_1, m,\underline{k}\rangle\Big\}f_{n,\underline{p}}\,c^{+}_{n\underline{p}+\underline{q}}c_{m,\underline{k}} - \sum_{h,\underline{k}_1,\ell_1}\Big\{\langle h,\underline{k}_1,\ell,\underline{k}+\underline{q}\,|U|\,n\underline{k}+\underline{q}, h,\underline{k}_1\rangle$$

$$-\langle h,\underline{k}_1,\ell,\underline{k}+\underline{q}\,|U|\,h,\underline{k}_1, n\underline{k}+\underline{q}\rangle\Big\}f_{h,\underline{k}_1}\,c^{+}_{\ell,\underline{k}+\underline{q}}c_{m\underline{k}} + (f_{n\underline{k}+\underline{q}} - f_{m\underline{k}})\,x$$

$$\sum_{p,m_1,n_1} \left(\langle m\underline{k}, n_1\underline{p}+\underline{q} | U | m_1\underline{p}, n\underline{k}+\underline{q} \rangle - \langle m\underline{k}, n_1\underline{p}+\underline{q} | U | n\underline{k}+\underline{q}, m_1\underline{p} \rangle \right) c^{+}_{n_1\underline{p}+\underline{q}} c_{m_1\underline{p}} \quad (1.57)$$

The first two terms of the right-hand side of this equation cancel with

$$\left[c^{+}_{n\underline{k}+\underline{q}} c_{m\underline{k}}, V \right] = U \sum_{\lambda\mu} (n\delta_{\lambda\mu} - \langle n_{\lambda\mu} \rangle) \Big\{ \sum_{l} a^{*}_{h\lambda}(\underline{k}) a_{l\mu}(\underline{k})$$

$$\times c^{+}_{n\underline{k}+\underline{q}} c_{l\underline{k}} - \sum_{h} a^{*}_{h\lambda}(\underline{k}+\underline{q}) a_{n\mu}(\underline{k}+\underline{q}) c^{+}_{h\underline{k}+\underline{q}} c_{m\underline{k}} \Big\} \quad (1.58)$$

The equation of motion then simplifies to the equation

$$i\hbar \frac{d}{dt} \ll c^{+}_{n\underline{k}+\underline{q}} c_{m\underline{k}} ; c^{+}_{h\underline{p}} c_{l\underline{p}+\underline{q}} \gg = \delta(t) \delta_{\underline{k}\underline{p}} \delta_{mh} \delta_{ln} (f_{m\underline{k}} - f_{n\underline{k}+\underline{q}})$$

$$+ (E_{m\underline{k}} - E_{n\underline{k}+\underline{q}}) \ll c^{+}_{n\underline{k}+\underline{q}} c_{m\underline{k}} ; c^{+}_{h\underline{p}} c_{l\underline{p}+\underline{q}} \gg + (f_{n\underline{k}+\underline{q}} - f_{m\underline{k}})$$

$$\times \sum_{\underline{k}'m'n'} \left(\langle m\underline{k}, n'\underline{k}'+\underline{q} | U | m'\underline{k}', n\underline{k}+\underline{q} \rangle - \langle m\underline{k}, n'\underline{k}'+\underline{q} | U | n\underline{k}+\underline{q}, m'\underline{k}' \rangle \right)$$

$$\times \ll c^{+}_{n'\underline{k}'+\underline{q}} c_{m'\underline{k}'} ; c^{+}_{h\underline{p}} c_{l\underline{p}+\underline{q}} \gg \quad (1.59)$$

and on taking the Fourier transform this becomes

$$(-\hbar\omega + E_{n\underline{k}+\underline{q}} - E_{m\underline{k}}) \ll c^{+}_{n\underline{k}+\underline{q}} c_{m\underline{k}} ; c^{+}_{h\underline{p}} c_{l\underline{p}+\underline{q}} \gg_{\omega} = \delta_{\underline{k}\underline{p}} \delta_{mh} \delta_{ln}$$

$$\times (f_{m\underline{k}} - f_{n\underline{k}+\underline{q}}) + (f_{n\underline{k}+\underline{q}} - f_{m\underline{k}}) \sum_{\underline{k}'m'n'} \left(\langle m\underline{k}, n'\underline{k}'+\underline{q} | U | m'\underline{k}', n\underline{k}+\underline{q} \rangle \right.$$

$$\left. - \langle m\underline{k}, n'\underline{k}'+\underline{q} | U | n\underline{k}+\underline{q}, m'\underline{k}' \rangle \right) \ll c^{+}_{n'\underline{k}'+\underline{q}} c_{m'\underline{k}'} ; c^{+}_{h\underline{p}} c_{l\underline{p}+\underline{q}} \gg \quad (1.60)$$

which is the most general RPA result for any interaction U.

For the spin-only transverse case, without spin-orbit coupling, n and m correspond to opposite spins and only the exchange term is non-zero.

Considering equation (1.60), and the specific on-site Hubbard interaction in the Hamiltonian (1.2), it is useful to define the interaction $\omega_{\mu\nu,\eta\xi}$ (see comments in Edwards (1984)) where

$$\omega_{\mu\nu,\eta\xi} = \frac{1}{N}\left(\langle\mu\eta|U|\xi\nu\rangle - \langle\mu\eta|U|\nu\xi\rangle\right) \tag{1.61}$$

$$= \frac{U}{N}\left(\delta_{\mu\nu}\delta_{\eta\xi} - \delta_{\mu\xi}\delta_{\nu\eta}\right) \tag{1.62}$$

This then allows the equation for $\hat{G}$ to be written

$$(\hbar\omega - E_{m\underline{k}+\underline{q}} + E_{n\underline{k}})\,\hat{G}(n\underline{k}, m\underline{k}+\underline{q};\omega) = \sum_{\nu} f_{\nu}^{\beta}\, a^{*}_{m\nu+\beta}(\underline{k}+\underline{q})\, a_{n\nu}(\underline{k})$$

$$\times (f_{n\underline{k}} - f_{m\underline{k}+\underline{q}}) - (f_{n\underline{k}} - f_{m\underline{k}+\underline{q}}) \sum_{ij\beta} \sum_{\xi\eta\mu\nu} a^{*}_{m\mu}(\underline{k}+\underline{q})\, a_{n\nu}(\underline{k})$$

$$\times a_{i\eta}(\underline{p})\, a_{j\xi}(\underline{p}+\underline{q})\, \omega_{\mu\nu,\eta\xi}\, \hat{G}(i\underline{p}, j\underline{p}+\underline{q};\omega) \tag{1.63}$$

having expressed it as

$$(\hbar\omega - E_{m\underline{k}+\underline{q}} + E_{n\underline{k}})\,\hat{G}(n\underline{k}, m\underline{k}+\underline{q};\omega) = \sum_{\mu} \langle m\underline{k}+\underline{q}|f_{\mu}^{\beta}|n\underline{k}\rangle$$

$$\times (f_{n\underline{k}} - f_{m\underline{k}+\underline{q}}) + (f_{n\underline{k}} - f_{m\underline{k}+\underline{q}}) \sum_{ij\beta} (\langle m\underline{k}+\underline{q}, i\underline{p}|U|j\underline{p}+\underline{q}, n\underline{k}\rangle$$

$$- \langle m\underline{k}+\underline{q}, i\underline{p}|U|n\underline{k}, j\underline{p}+\underline{q}\rangle)\,\hat{G}(i\underline{p}, j\underline{p}+\underline{q};\omega) \tag{1.64}$$

which clearly shows the inclusion of the direct and exchange diagram for the interaction. Using the definitions for an interacting susceptibility $\underline{\underline{G}}$

$$G_{\mu\nu,\eta\xi}(q,\omega) = \sum_{\underline{k}'\underline{p}} \ll c^{+}_{\mu\,\underline{k}'+\underline{q}}\, c_{\nu\underline{k}'} ; c^{+}_{\eta\underline{p}}\, c_{\xi\underline{p}+\underline{q}} \gg \tag{1.65}$$

and non-interacting susceptibility $\underline{\underline{\Gamma}}$

$$\Gamma_{\mu\nu,\eta\xi}(q,\omega) = \sum_{nm\underline{k}} \frac{a^{*}_{n\mu}(\underline{k}+\underline{q})\, a_{m\nu}(\underline{k})\, a^{*}_{m\xi}(k)\, a_{n\eta}(k+q)}{(E_{n\underline{k}+\underline{q}} - E_{m\underline{k}} - \hbar\omega)} (f_{n\underline{k}} - f_{m\underline{k}+\underline{q}}) \tag{1.66}$$

then equation (1.64) can be written in terms of these matrices

$$G_{\mu+\alpha\mu,\nu+\beta\nu}(q,\omega) = \Gamma_{\mu+\alpha\mu,\nu\nu+\beta}(q,\omega)$$

$$- \frac{U}{N} \sum_{\xi\eta} \left(\Gamma_{\mu+\alpha\mu,\xi\xi}\, G_{\eta\eta,\nu+\beta\nu} - \Gamma_{\mu+\alpha\mu,\xi\eta}\, G_{\xi\eta,\nu+\beta\nu} \right) \tag{1.67}$$

so that

$$\chi^{\alpha\beta}(q,\omega) = G_{\alpha\beta}(q,\omega) = \sum_{\mu\nu} f^{\alpha}_{\mu}\, G_{\mu+\alpha\mu,\nu+\beta\nu}\, f^{\beta}_{\nu}$$

$$= \sum_{\mu\nu\eta\xi} f^{\alpha}_{\mu} \left(\underline{\underline{1}} + \underline{\underline{\Gamma}}\,\underline{\underline{\omega}} \right)^{-1}_{\mu+\alpha\mu,\eta\xi} \Gamma_{\eta\xi,\nu\nu+\beta}\, f^{\beta}_{\nu} \tag{1.68}$$

This is the required solution for the interacting susceptibility, with U and the hopping integrals in $T_{\mu\nu}$ being the only free parameters.

Incidentally, the interaction is equivalent to that in the spin only case appearing in the transverse susceptibility derived in the Local Density Approximation (LDA) by Callaway et al. (to be published), and as the Spin Density Functional Theory (SDFT) in principle includes all correlation effects this gives a funda-

mental justification to calculations at the HF-RPA level. However, strictly this applies only to static properties, but hopefully implies that the dynamical $\chi^{\alpha\beta}(q,\omega)$ is meaningful (see Rajogopal and Callaway (1973)). Finally, it should be pointed out that the correspondence between the SDFT and RPA goes beyond the LDA as $I_{xc}(\underline{r},\underline{r}')$ can be defined, and parametrized, for a non-local functional.

1.8 The paramagnetic susceptibility

As shown above, in the paramagnetic state the HF eigenstates are as given in equations (1.27) and (1.28) so that the form of $\Gamma_{\alpha\beta,\gamma\delta}(q,\omega)$ can be derived.

Hence, writing equation (1.66) with m = (ij), n = (i'j') and i denoting the energy band and j separating Kramers-degenerate pairs:

$$\Gamma_{\alpha\beta,\gamma\delta}(q,\omega) = \sum_{\underline{k}} \sum_{ij i'j'} a^{*}_{(i'j')\alpha}(\underline{k}+q)\, a_{(ij)\beta}(\underline{k}) \times a^{*}_{(ij)\delta}(\underline{k})\, a_{(i'j')\gamma}(\underline{k}+q) \left(\frac{f_{i\underline{k}} - f_{i'\underline{k}+q}}{\lambda_{i'\underline{k}+q} - \lambda_{i\underline{k}} - \hbar\omega} \right) \quad (1.69)$$

we can use the eigenvectors as given in equation (1.39) above with

$$\sum_{j} a_{(ij)\beta}(\underline{k})\, a^{*}_{(ij)-\beta}(\underline{k}) = 0 \quad (1.70)$$

for degenerate pairs $(\beta,-\beta)$ and do the sum over j,j'.

Furthermore, as we sum over $\underline{k}$ points with q = 0 and full cubic symmetry in the paramagnetic state only a restricted number

of the elements of the 16x16 matrix $\underline{\underline{\Gamma}}$ are non-zero.

This may be shown by considering $\Gamma_{\alpha\beta,\gamma\delta}(0,\omega)$ in terms of the representation $D_{\mu\nu}(R) = \delta_{\mu\nu} D_{\mu}(R)$ for a symmetry operation R about a symmetry axis (as in Appendix A):

$$\Gamma_{\alpha\beta,\gamma\delta}(0,\omega) = \sum_{\substack{nm\underline{k} \\ (IBZ)}} \sum_{R} \frac{a^*_{n\alpha}(R\underline{k}) a_{m\beta}(R\underline{k}) a^*_{m\delta}(R\underline{k}) a_{n\gamma}(R\underline{k})}{(\hbar\omega - E_{m\underline{k}} + E_{n\underline{k}})} (f_{n\underline{k}} - f_{m\underline{k}})$$

$$= \sum_{\substack{nm\underline{k} \\ (IBZ)}} \sum_{R} D^*_{\alpha}(R) D_{\beta}(R) D^*_{\delta}(R) D_{\gamma}(R) \frac{a^*_{n\alpha}(\underline{k}) a_{m\beta}(\underline{k}) a^*_{m\delta}(\underline{k}) a_{n\gamma}(\underline{k})}{(\hbar\omega - E_{m\underline{k}} + E_{n\underline{k}})} (f_{n\underline{k}} - f_{m\underline{k}})$$

where $\underline{k}$(IBZ) indicates a sum over $\underline{k}$ points in the irreducible Brillouin zone.

In the paramagnetic regime the $E_{m\underline{k}}$ and $f_{m\underline{k}}$ have full cubic symmetry, so that $E_{mR\underline{k}} = E_{m\underline{k}}$ and $f_{mR\underline{k}} = f_{m\underline{k}}$ giving

$$\Gamma_{\alpha\beta,\gamma\delta}(0,\omega) = \sum_{R} D^*_{\alpha}(R) D_{\beta}(R) D^*_{\delta}(R) D_{\gamma}(R) \Gamma^{IBZ}_{\alpha\beta,\gamma\delta}(0,\omega)$$

where $\Gamma^{IBZ}_{\alpha\beta,\gamma\delta}(0,\omega)$ is the contribution to $\underline{\underline{\Gamma}}$ from summing only over the IBZ. On summing over R using the $D_{\alpha}(R)$ in Appendix A we can find the restricted set of the $\Gamma_{\alpha\beta,\gamma\delta}(0,\omega)$ which are non-zero.

For the case of fourfold rotational symmetry these are of the form $\Gamma_{\alpha\beta,\alpha'\beta'}$ where for α and β if

$\mu = 3/2$	$\mu' = 3/2, 1/2, -1/2$
$1/2$	$1/2, 3/2, -3/2$
$-1/2$	$-1/2, 3/2, -3/2$
$-3/2$	$-3/2, 1/2, -1/2$

and for the paramagnetic case we can eliminate Kramers-degenerate orthogonal pairs (α,β) also. If $\underline{q}$ is finite but along a symmetry axis, or there is a magnetic moment present which is along a symmetry axis (and any finite $\underline{q}$ vector is along that axis), then again only a subset of the elements is non-zero.

When q = 0 sufficient elements of $\underline{\underline{\Gamma}}$ and $\underline{\underline{G}}$ vanish for $\underline{\underline{G}}$ to become block diagonal.

The type of states $(\alpha\beta)$ which occur in $G_{\alpha\beta,\gamma\delta}(0,\omega)$ are shown in Table 1.3. There is a 4x4 matrix $G_{\alpha\alpha,\beta\beta}$ associated with χ^{zz}, a 2x2 matrix $G_{\alpha\beta,\gamma\delta}$ associated with χ^{+-} and χ^{-+} where $(\alpha\beta)$ and $(\gamma\delta)$ each differ by one, together with a 4x4 matrix $G_{\alpha\beta,\gamma\delta}$ where $(\alpha\beta)$ and $(\gamma\delta)$ each differ by two. Also, there are two 2x2 matrices arising from $(\alpha\beta)$, $(\gamma\delta)$ differing by one; and for one of these and one 2x2 matrix where they differ by three they are of the form $(\alpha\beta) = (\alpha,-\alpha)$. By equation (1.70) these $G_{\alpha-\alpha,\beta-\beta}=0$ in the paramagnetic state, but they are non-zero once Kramers' degeneracy is broken.

Therefore, turning to q = 0 we can calculate the susceptibility

$$\chi^{zz}(0,\omega) = \sum_{\alpha\gamma} \alpha\gamma\, G_{\alpha\alpha,\gamma\gamma}(0,\omega)$$

as from equation (1.67), using the restricted set of finite $\Gamma_{\alpha\beta,\gamma\delta}(0,\omega)$

$$G_{\alpha\alpha,\gamma\gamma}(0,\omega) = \Gamma_{\alpha\alpha,\gamma\gamma}(0,\omega) - \sum_{\xi\nu\eta} \Gamma_{\alpha\alpha,\xi\xi}(0,\omega)\,\omega_{\xi\xi,\nu\eta}\,G_{\nu\eta,\gamma\gamma}(0,\omega)$$

$$= \Gamma_{\alpha\alpha,\gamma\gamma} - \frac{u}{N}\sum_{\eta}\left(\sum_{\xi}\Gamma_{\alpha\alpha,\xi\xi} - \Gamma_{\alpha\alpha,\eta\eta}\right)G_{\eta\eta,\gamma\gamma}$$

as $\Gamma_{\alpha\alpha,\gamma\delta}(0,\omega)$ is only non-zero if $\gamma=\delta$

and the result for $\Gamma_{\alpha\alpha,\gamma\gamma}(0,\omega\neq 0)$ is, summing on i,i' (no i = i' terms contribute),

$$\frac{1}{N}\Gamma_{\alpha\alpha,\gamma\gamma}(0,\omega\neq 0) = \begin{pmatrix} P+Q & -P & -Q & 0 \\ -P & P+Q & 0 & -Q \\ -Q & 0 & P+Q & -P \\ 0 & -Q & -P & P+Q \end{pmatrix} \tag{1.71}$$

where

$$P(\omega) = \frac{1}{N}\sum_{k}\frac{|c|^2}{(a-b)^2+4(|c|^2+|d|^2)}\left\{\frac{f_{1k}-f_{2k}}{\lambda_{2k}-\lambda_{1k}-\hbar\omega}+\frac{f_{2k}-f_{1k}}{\lambda_{1k}-\lambda_{2k}-\hbar\omega}\right\} \tag{1.72}$$

$$Q(\omega) = \frac{1}{N}\sum_{k}\frac{|d|^2}{(a-b)^2+4(|c|^2+|d|^2)}\left\{\frac{f_{1k}-f_{2k}}{\lambda_{2k}-\lambda_{1k}-\hbar\omega}+\frac{f_{2k}-f_{1k}}{\lambda_{1k}-\lambda_{2k}-\hbar\omega}\right\} \tag{1.73}$$

If we now consider the response function for $\underline{q} = 0$, $\omega = 0$, as $\underline{q} \to 0$ in equation (1.69), the i = i' terms make a singular contribution to $\Gamma_{\alpha\beta,\gamma\delta}(0,0)$. The critical values of U and the associated modes of instability can be calculated by a Stoner criterion method. Using the expression for $G_{\alpha\alpha,\gamma\gamma}$ above, $\chi^{zz}(0,0)$ diverges if $\det|\underline{\underline{1}}+\underline{\underline{\Gamma}}\,\underline{\underline{\omega}}|=0$ and this indicates a second-order phase transition to the corresponding ordered state.

Using

$$P^S = \frac{1}{N}\sum_{i\underline{k}}\frac{|c|^2}{(a-b)^2+4(|c|^2+|d|^2)}\,\delta(\lambda_{i\underline{k}}-E_f(\underline{k})) \tag{1.74}$$

$$Q^S = \frac{1}{N}\sum_{i\underline{k}}\frac{|d|^2}{(a-b)^2+4(|c|^2+|d|^2)}\,\delta(\lambda_{i\underline{k}}-E_f(\underline{k})) \tag{1.75}$$

the total $\Gamma_{\beta\beta,\gamma\gamma}(0,0)$ is

$$\frac{1}{N}\Gamma_{\beta\beta,\gamma\gamma}(0,0) = \begin{pmatrix} P+Q+3Q^s & P^s-P & Q^s-Q & 0 \\ P^s-P & P+Q+3Q^s & 0 & Q^s-Q \\ Q^s-Q & 0 & P+Q+3Q^s & P^s-P \\ 0 & Q^s-Q & P^s-P & P+Q+3Q^s \end{pmatrix} \quad (1.76)$$

Putting

$$\Gamma'_{\beta\beta,\gamma\gamma} = \sum_{\xi} \Gamma_{\beta\beta,\xi\xi} - \Gamma_{\beta\beta,\gamma\gamma} \quad (1.77)$$

$$\underline{\underline{G}} = \left(\underline{\underline{1}} + \frac{U}{N}\underline{\underline{\Gamma}}'\right)^{-1}\underline{\underline{\Gamma}} \quad (1.78)$$

the Stoner criterion is that

$$\det\left|\underline{\underline{1}} + \frac{U}{N}\underline{\underline{\Gamma}}'(0,0)\right| = 0 \quad (1.79)$$

This gives, if we define

$$R = 4Q^s + P^s = \frac{1}{2N}\sum_{i\underline{k}} \delta(\lambda_{i\underline{k}} - E_f(\underline{k})) = \frac{1}{4}N(E_f) \quad (1.80)$$

where $N(E_f)$ is the density of states at the Fermi level, the following three instabilities and associated eigenvectors of the matrix $\left(\underline{\underline{1}} + \frac{U}{N}\underline{\underline{\Gamma}}'\right)$ indicating the criteria for various modes of ordering.

$$1 = U_p(2Q - 2Q^s + R) \quad \text{parallel moment } (1,1,-1,-1) \quad (1.81)$$

$$1 = U_c(2P - 2P^s + R) \quad \text{compensated moment } (1,-1,1,-1) \quad (1.82)$$

$$1 = U_m(2P - 2P^s + 2Q - 2Q^s + R) \quad \text{non-magnetic (quadrupolar) } (1,-1,-1,1) \quad (1.83)$$

where U_P, U_c and U_{nm} are the three critical values of U for the various modes and the remaining eigenvector (1,1,1,1) is clearly related to the number operator. If P^s, Q^s and R dominate, as at high $N(E_f)$, then the magnetic transitions are favoured, whereas at low $N(E_f)$ the non-magnetic transition is favoured. The criterion corresponding to the lowest value of U is the one which will occur, provided no first order phase transition occurs first. The eigenvectors indicate the mode of ordering and are proportional to

$$\left(\delta\langle n_{3/2\,3/2}\rangle , \delta\langle n_{1/2\,1/2}\rangle , \delta\langle n_{-1/2\,-1/2}\rangle , \delta\langle n_{-3/2\,-3/2}\rangle \right)$$

Considering the non-magnetic mode, this is quadrupolar ordering of the $\langle O_2^0 \rangle$ type with finite order parameter Q given by

$$Q = \langle J_z^2 - \tfrac{1}{3} J(J+1) \rangle$$

$$= \sum_{\lambda} (\lambda^2 - \tfrac{5}{4}) \langle n_{\lambda\lambda} \rangle = \langle n_{3/2\,3/2}\rangle - \langle n_{1/2\,1/2}\rangle - \langle n_{-1/2\,-1/2}\rangle + \langle n_{3/2\,3/2}\rangle$$

It is also purely orbital ordering, without spin ordering so that as no magnetic moment is formed Kramers' degeneracy is not broken, and the Hamiltonian still commutes with the time reversal operator. Quadrupolar ordering is an important feature of the model, arising naturally in an orbitally degenerate system, and is discussed further in the following chapter.

The matrix $G_{\alpha\alpha',\beta\beta}(q \to 0,0)$ can be written in terms of

$$P' = P - P^s \tag{1.84}$$

$$Q' = Q - Q^s \tag{1.85}$$

and is of the form

$$G_{\alpha\alpha,\beta\beta}(0,0) = \left(\underline{\underline{1}} + u\underline{\underline{\Gamma}}'\right)^{-1}\underline{\underline{\Gamma}}$$

$$= \frac{1}{4}\begin{pmatrix} V & W & X & Y \\ W & V & Z & X \\ X & Z & V & W \\ Y & X & W & V \end{pmatrix} \qquad (1.86)$$

where

$$V = \frac{R}{1+3uR} + \frac{2Q'+R}{1-2uQ'-uR} + \frac{2P'+2Q'+R}{1-2uP'-2uQ'-uR} + \frac{2P'+R}{1-2uP'-uR} \qquad (1.87)$$

$$W = \frac{R}{1+3uR} + \frac{2Q'+R}{1-2uQ'-uR} - \frac{2P'+2Q'+R}{1-2uP'-2uQ'-uR} - \frac{2P'+R}{1-2uP'-uR} \qquad (1.88)$$

$$X = \frac{R}{1+3uR} - \frac{2Q'+R}{1-2uQ'-uR} - \frac{2P'+2Q'+R}{1-2uP'-2uQ'-uR} + \frac{2P'+R}{1-2uP'-uR} \qquad (1.89)$$

$$Y = \frac{R}{1+3uR} - \frac{2Q'+R}{1-2uQ'-uR} + \frac{2P'+2Q'+R}{1-2uP'-2uQ'-uR} - \frac{2P'+R}{1-2uP'-uR} \qquad (1.90)$$

$$Z = \frac{R}{1+3uR} - \frac{2Q'+R}{1-2uQ'-uR} + \frac{2P'+2Q'+R}{1-2uP'-2uQ'-uR} - \frac{2P'+R}{1-2uP'-uR} \qquad (1.91)$$

It is then possible to calculate $\chi^{zz}(q\to 0,0)$ in terms of P(0), Q(0) as

$$\chi^{zz}(q\to 0,0) = \sum_{\mu\nu} \mu\nu\, G_{\mu\mu,\nu\nu} = 4\left(\frac{2Q'+R}{1-2uQ'-uR} + \frac{2P'+R}{1-2uP'-uR}\right)$$

$$= 4\left(\frac{2Q(0)-2Q^s+R}{1-2u(Q(0)-Q^s)-uR}\right) + \frac{2P(0)-2P^s+R}{1-2u(P(0)-P^s)-uR} \qquad (1.93)$$

and $\chi^{zz}(0,\omega\neq 0)$ in the interacting case is

$$\chi^{zz}(0,\omega\neq 0) = \frac{8Q(\omega)}{1-2UQ(\omega)} + \frac{2P(\omega)}{1-2UP(\omega)} \tag{1.94}$$

By cubic symmetry $\chi^{+-}(0,\omega)=\chi^{-+}(0,\omega)=2\chi^{zz}(0,\omega)$ in the paramagnetic state.

Similarly, for the quadrupolar mode we can calculate an appropriate susceptibility $\chi_Q(0,0)$ defined by

$$\chi_Q(0,0) = \sum_{\mu\nu} A_\mu A_\nu C_{\mu\mu,\nu\nu}(0,0) \tag{1.95}$$

where $A_\mu = (1,-1,-1,1)$, and we obtain

$$\chi_Q(0,0) = 4\left(\frac{2P' + 2Q' + R}{1 - 2UP' - 2UQ' - UR}\right) \tag{1.96}$$

The remaining quadrupolar modes are given by

$$\begin{pmatrix} C_{3/2,-3/2,\gamma\delta} \\ C_{1/2,-3/2,\gamma\delta} \\ C_{-1/2,3/2,\gamma\delta} \\ C_{-3/2,1/2,\gamma\delta} \end{pmatrix} = \begin{pmatrix} 1-3UQ' & UP' & U(Q'-P') & 0 \\ UP' & 1-3UQ' & 0 & U(Q'-P') \\ U(Q'-P') & 0 & 1-3UQ' & UP' \\ 0 & U(Q'-P') & UP' & 1-3UQ' \end{pmatrix}^{-1} \begin{pmatrix} \Gamma_{3/2,-1/2,\delta\gamma} \\ \Gamma_{1/2,-3/2,\delta\gamma} \\ \Gamma_{-1/2,3/2,\delta\gamma} \\ \Gamma_{-3/2,1/2,\delta\gamma} \end{pmatrix} \tag{1.97}$$

where $(\gamma\delta) = (-1/2, 3/2)$ or $(-3/2, 1/2)$ and the eigenvectors and corresponding Stoner criteria of these modes are:

$$1 = 2UQ' \qquad (1,1,1,1) \tag{1.98}$$

$$1 = 2U(P' + Q') \qquad (1,-1,1,-1) \tag{1.99}$$

$$1 = 4UQ' \qquad (1,-1,-1,1) \tag{1.100}$$

$$1 = 4UQ' - 2UP' \qquad (1,1,-1,-1) \tag{1.101}$$

These criteria are generally much higher values of U than those of equations (1.81) - (1.83).

1.9 Computational methods

From the formalism developed, for example that of the RPA dynamical susceptibility calculation and the Stoner criterion, it has emerged that two distinct types of integration over $\underline{k}$-space need to be performed. These are of the form of a density of states integral (Lehmann and Taut, 1972) and of a susceptibility integral (Rath and Freeman, 1975), and are themselves very similar. The Brillouin zone integration program was developed by J.F. Cooke, and modified by R. Zeller and R. Muniz.

The computational method adopted was an extension of this previous work to the multi-band calculations required. Simple analytic expressions using linear interpolation in energy are used for the integral inside a tetrahedral microzone of the Brillouin zone (BZ); they depend only on the volume of the tetrahedron and the differences of the energies at its corners for each band. Considering the Green's function $G(\omega)$ which is a spectral distribution function in terms of an energy-like variable ω:

$$G(\omega) = \lim_{\eta \to 0+} \frac{1}{N} \sum_{\underline{k}}' \frac{F(\underline{k})}{\omega - \omega(\underline{k}) - i\eta} \tag{1.102}$$

the real and imaginary parts are

$$\mathrm{Re}\, G(\omega) = \frac{1}{N} \sum_{\underline{k}}' \frac{F(\underline{k})}{\omega - \omega(\underline{k})} \tag{1.103}$$

$$\mathrm{Im}\, G(\omega) = \frac{\pi}{N} \sum_{\underline{k}}' F(\underline{k})\, \delta(\omega - \omega(\underline{k})) \tag{1.104}$$

where $F(\underline{k})$ is a general function of $\underline{k}$, and $\sum\!\!\!\!\!\!-_{\underline{k}}$ denotes the principal part of the summation over $\underline{k}$. The form of $\mathrm{Im}\,G(\omega)$ is that of a density of states integral, and that of $\mathrm{Re}\,G(\omega)$ is (on including the $\underline{q}$ dependence) a generalized susceptibility; these two forms are the Hilbert transforms of each other. The quantities we have calculated are almost always of one of these two forms.

The irreducible Brillouin zone (IBZ) is divided into $2^{(m-2)}$ tetrahedra, where the fineness of the mesh m is chosen according to the accuracy required weighed against the amount of computation that is acceptable. Values of m between 3 and 12 were used, with m = 7 usually adopted. By using the transformation properties of $E_{n\underline{k}}$ and $a_{n\mu}(\underline{k})$ under the cubic group O_h we may reduce the sum over the BZ to a sum over an irreducible region of the zone. Under broken symmetry the residual symmetry may be used, for example, for moment formation along an axis, transformations under rotations about that axis.

The density-of-states type integral N(E) that arises from the form of $\mathrm{Im}\,G(\omega)$ on making the usual replacement

$$\frac{1}{N}\sum_{\underline{k}} \rightarrow \frac{1}{V}\int d^3\underline{k}$$

where V is the volume of the original Brillouin zone, can be transformed into an integral over surfaces of constant energy S

$$N(E) = \frac{2}{(2\pi)^3}\int_{E(\underline{k})=E} \frac{dS}{|\nabla_{\underline{k}} E|} \qquad (1.105)$$

This can now be approximated by a sum over tetrahedra i and bands n

$$N(E) \simeq \frac{2}{(2\pi)^3}\sum_{ni} \frac{S_n(E,\underline{k}_i)}{|\nabla_{\underline{k}} E_n(\underline{k}_i)|} \qquad (1.106)$$

and evaluated in terms of energies at the tetrahedral vertices.

For the generalized susceptibility integral the fractional volume of a given tetrahedron that contributes is determined by the intersection of the constant energy planes corresponding to $E_n(\underline{k})$ and $E_{n'}(\underline{k} + \underline{q})$; the Fermi factor $f(E_n(\underline{k}))[1 - f(E_{n'}(\underline{k}+\underline{q}))]$ must be unity also. The resulting fractional volume is a sum of one, or at most nine, tetrahedra, taking account of the rather few ways that the planes may intersect a tetrahedron.

The integral that is performed in recalculating the occupation numbers of the orbitals $\langle n_{\mu\mu} \rangle$ from a previous set is also of the form of a (cumulative) density of states. Self-consistency was achieved in a three-dimensional (for a j = 3/2 d band) or five-dimensional (for a j = 5/2 f band) parameter space, normally to a sum of squares of the errors of roughly 10^{-9} taking about twenty to forty iterations. The dependence upon starting point and the possibility of several solutions (metastable states) was considered. When U is not close to a critical value U_c corresponding to a phase change a tetrahedral mesh with m = 6 was used, and this was increased to m = 7 when $U \simeq U_c$ as too coarse a mesh had the effect of giving apparently well converged solutions that smoothed out sharp phase changes. The iterative scheme used a direct mixing of (usually) 90% of the new solution and 10% of the old solution to give the next trial solution.

m	$2^{(m-2)}$
12	1024
11	512
10	256
9	128
8	64
7	32
6	16
5	8
4	4

1.10 Computational results

In Table 1.2 there is a set of Stoner criteria where for a given $dd\pi/dd\sigma$ value the number of electrons per atom n has been varied. Figures 1.1 and 1.2 display Stoner criteria for a variety of $dd\pi/dd\sigma$ values for n = 1 and n = 2. For n = 1 magnetic solutions are generally favoured, and by the density of states curves given in Figure 1.3 for four values of $dd\pi/dd\sigma$ indicate that the value of $R = \frac{1}{4} N(E_F)$ is generally high for a quarter-filled band. In contrast, it is generally much lower for a half-filled band, and the n = 2 Stoner criteria mainly favour a non-magnetic (quadrupolar) solution.

Figures 1.4-1.7 show the integrals $P(\omega)$ and $Q(\omega)$ for a variety of paramagnetic ground states. When q = 0 there is a range of ω for which $\mathrm{Im}\, P(\omega)$ and $\mathrm{Im}\, Q(\omega)$ are non-zero and also therefore $\mathrm{Im}\, \chi^{zz}(0,\omega) \neq 0$. This continuum (corresponding to Stoner or single-particle excitations) starts when $P(\omega), Q(\omega)$ go through a turning point and the second derivative with respect to ω is zero, and ends at another turning point. From the examples, the continuum may be made narrow or broad, and extending down to low ω or starting at quite high ω.

From consideration of the Stoner criteria, indicating the maximum extent of the paramagnetic regime, and the equations for the zero of $\det \left| \underline{\underline{1}} + \frac{U}{N} \underline{\underline{\Gamma'}} \right|$ we can use the $P(\omega), Q(\omega)$ curves to give the energy $\hbar\omega$ of the q = 0 excitation of each mode at each value of U. This calculation reveals that the modes generally lie in the continuum, and do not in most cases move down to sufficiently low ω (with increasing U) to leave the continuum before instability with respect to ordering of the ground state occurs.

Table 1.2 Stoner Criteria

$\alpha = dd\sigma, \beta = dd\pi$	n	U_p	U_c	U_{nm}	R
$-\beta/\alpha = 0.25$	0.85	2.22	2.29	2.56	0.498
	1.27	1.97	1.85	1.91	0.525
	1.63	1.69	1.46	1.50	0.609
	1.97	1.43	1.16	1.20	0.728
	2.22	1.97	1.73	1.31	0.322
	2.31	2.43	2.45	1.47	0.138
	2.44	2.37	2.49	1.60	0.196
	2.64	2.17	2.42	1.79	0.315
	3.71	1.28	1.36	3.19	1.20
$-\beta/\alpha = 0.6667$	0.177	1.46	1.11	1.98	
	1.0	0.85	1.06	1.02	
	2.0	0.67	0.79	0.65	
	2.82	1.15	1.12	1.16	
	3.71	2.47	2.65	2.97	
$-\beta/\alpha = 0.60$	0.684	0.416	0.393	0.771	
	0.770	0.401	0.381	0.727	
	0.817	0.418	0.401	0.740	
	0.728	0.402	0.380	0.738	
	0.744	0.400	0.379	0.732	
$-\beta/\alpha = 0.55$	1.91	1.33	1.26	0.73	
	1.97	1.34	1.24	0.69	
	2,32	0.660	0.535	0.560	
	3.74	1.55	2.40	6.11	
	3.97	4.98	9.34	79.6	

However, for the model the mode found to lie at lowest energy is quadrupolar, and examples can be found where on approaching a quadrupolar instability at U_{nm} (with R relatively small) the quadrupolar mode separates from and moves to lower energies than the continuum region.

Table 1.3

α	β	Kramers degenerate $(\alpha,-\alpha)$ pair	$\|(\alpha - \beta)\|$
3/2	3/2		0
1/2	1/2		0
- 1/2	- 1/2		0
- 3/2	- 3/2		0
3/2	1/2		1
1/2	- 1/2	*	1
- 1/2	- 3/2		1
- 3/2	- 1/2		1
- 1/2	1/2	*	1
1/2	3/2		1
3/2	- 1/2		2
1/2	- 3/2		2
- 1/2	3/2		2
- 3/2	1/2		2
3/2	- 3/2	*	3
- 3/2	3/2	*	3

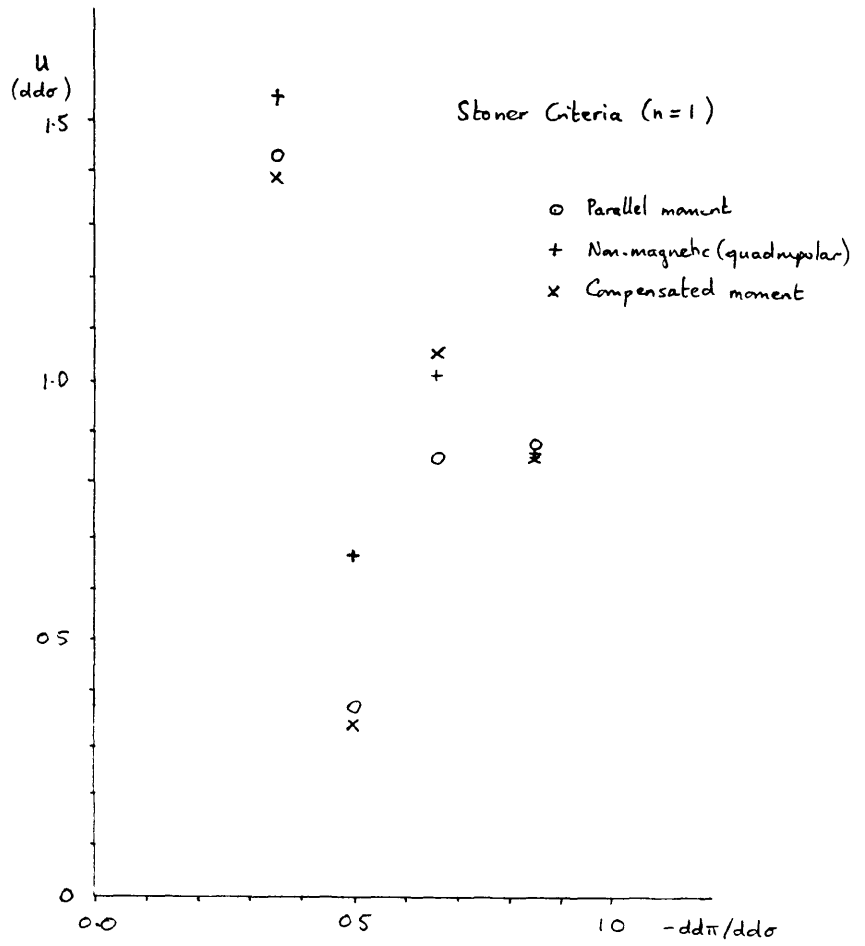

Figure 11

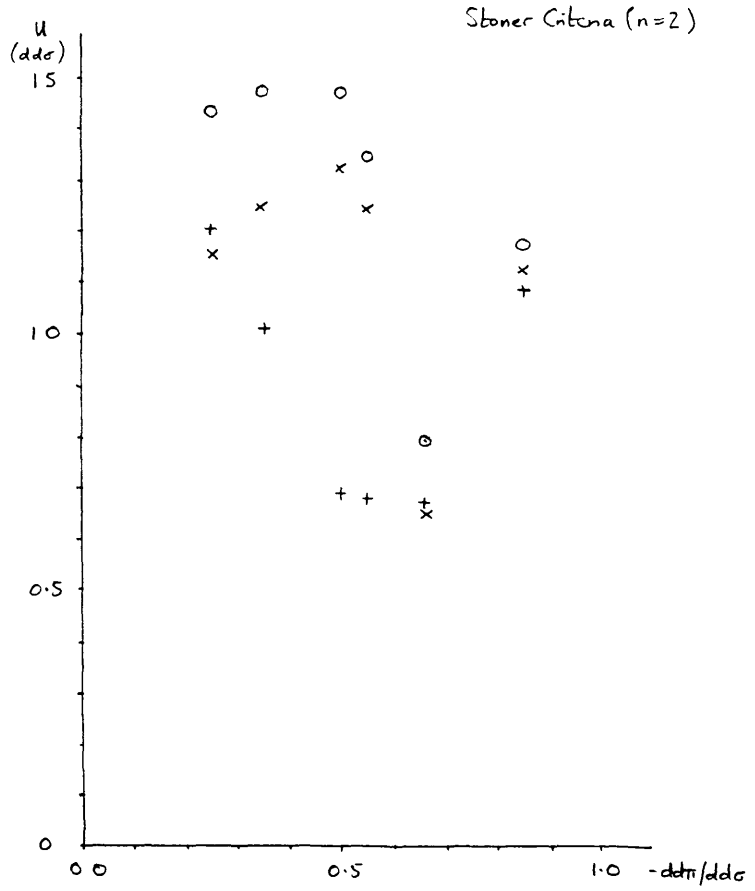

Figure 12

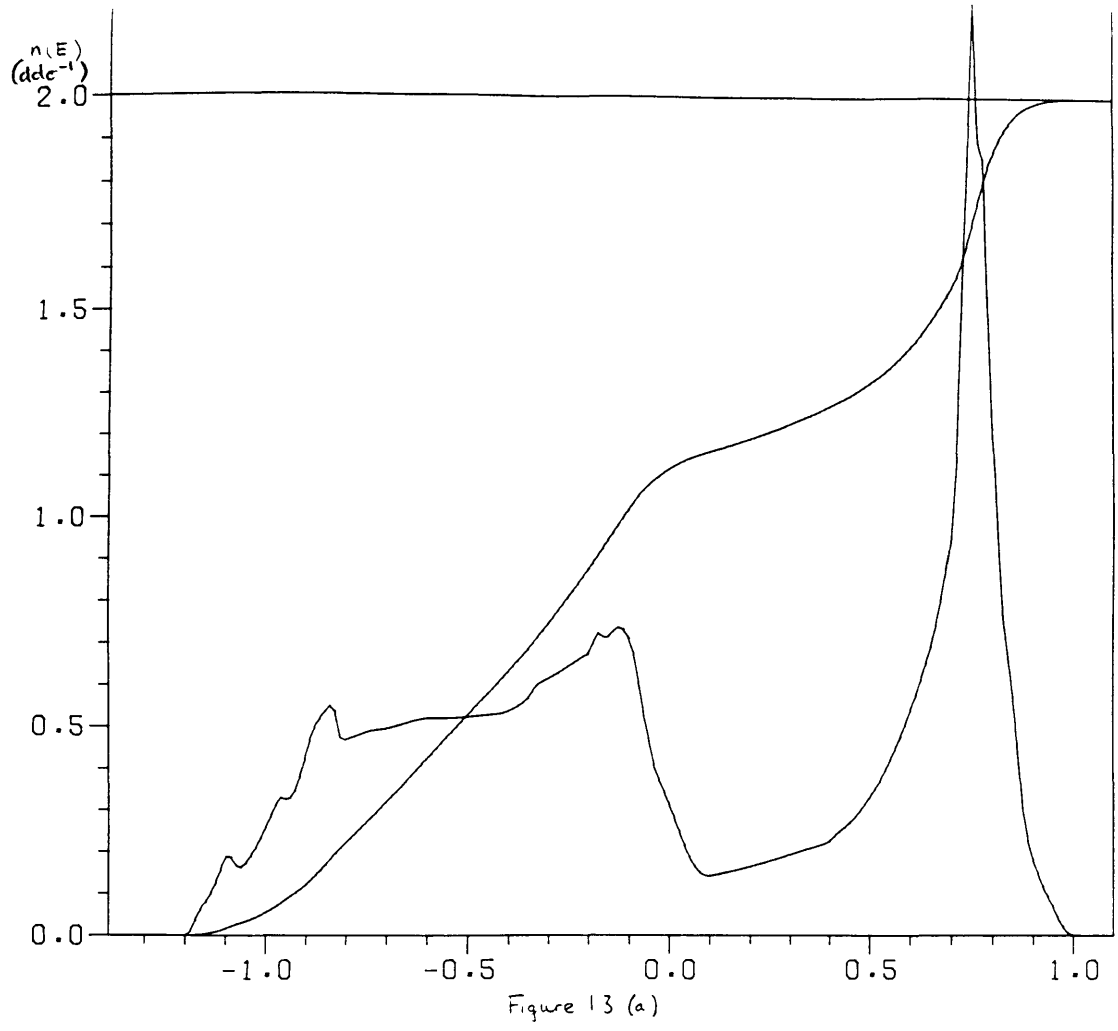

Figure 13 (a)

Density of states
$dd\sigma = -1$, $dd\pi = 0.25$, $U = 0$

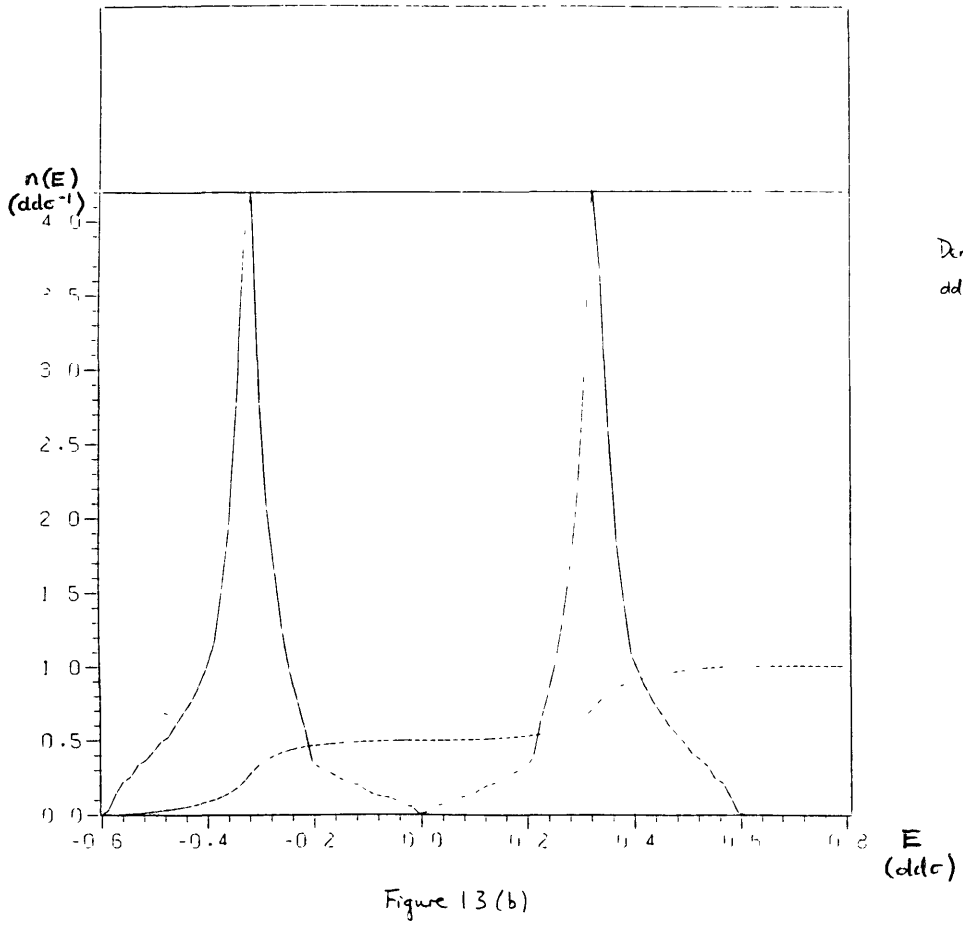

Figure 13 (b)

Density of states
$dd\sigma = -1$, $dd\pi = 1/2$, $U = 0$

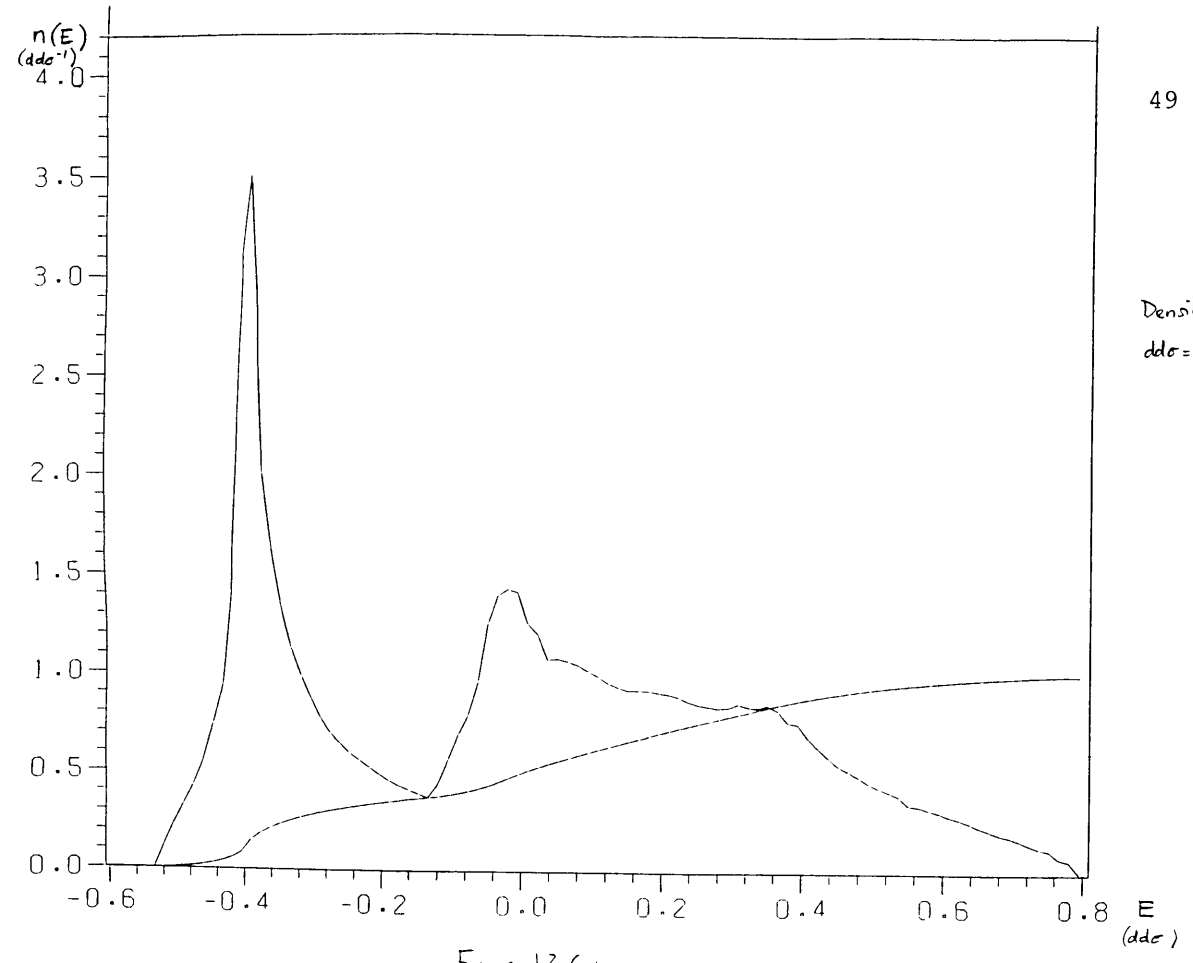
n(E)
(ddσ⁻¹)
4.0
3.5
3.0
2.5
2.0
1.5
1.0
0.5
0.0
-0.6
-0.4
-0.2
0.0
0.2
0.4
0.6
0.8
E
(ddσ)
Density of states
ddσ = -1, ddπ = ⅔

Figure 13 (c)

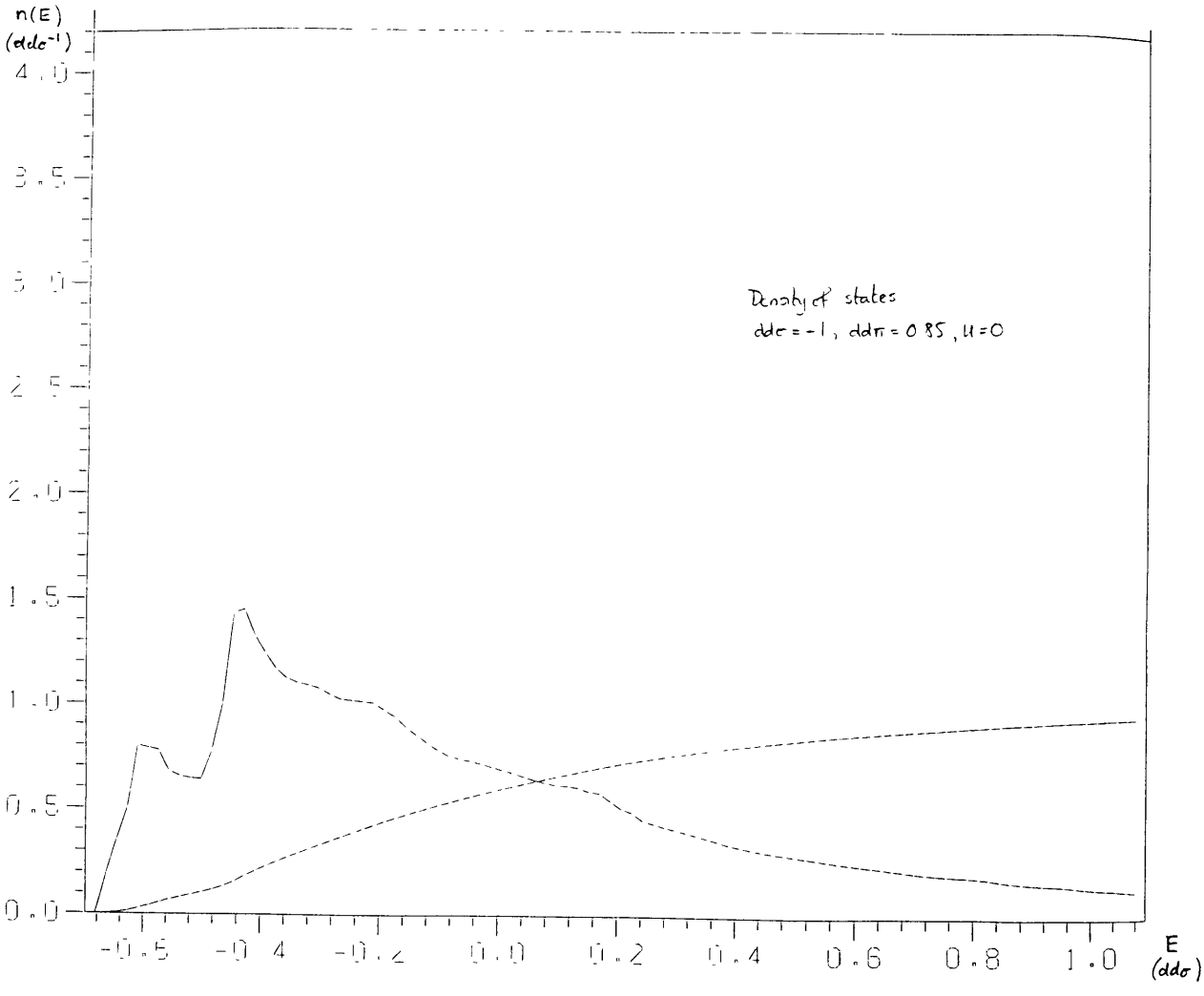
n(E)
(ddσ⁻¹)
4.0
3.5
3.0
2.5
2.0
1.5
1.0
0.5
0.0
-0.5
-0.4
-0.2
0.0
0.2
0.4
0.6
0.8
1.0
E
(ddσ)
Density of states
ddσ = -1, ddπ = 0.85, U = 0

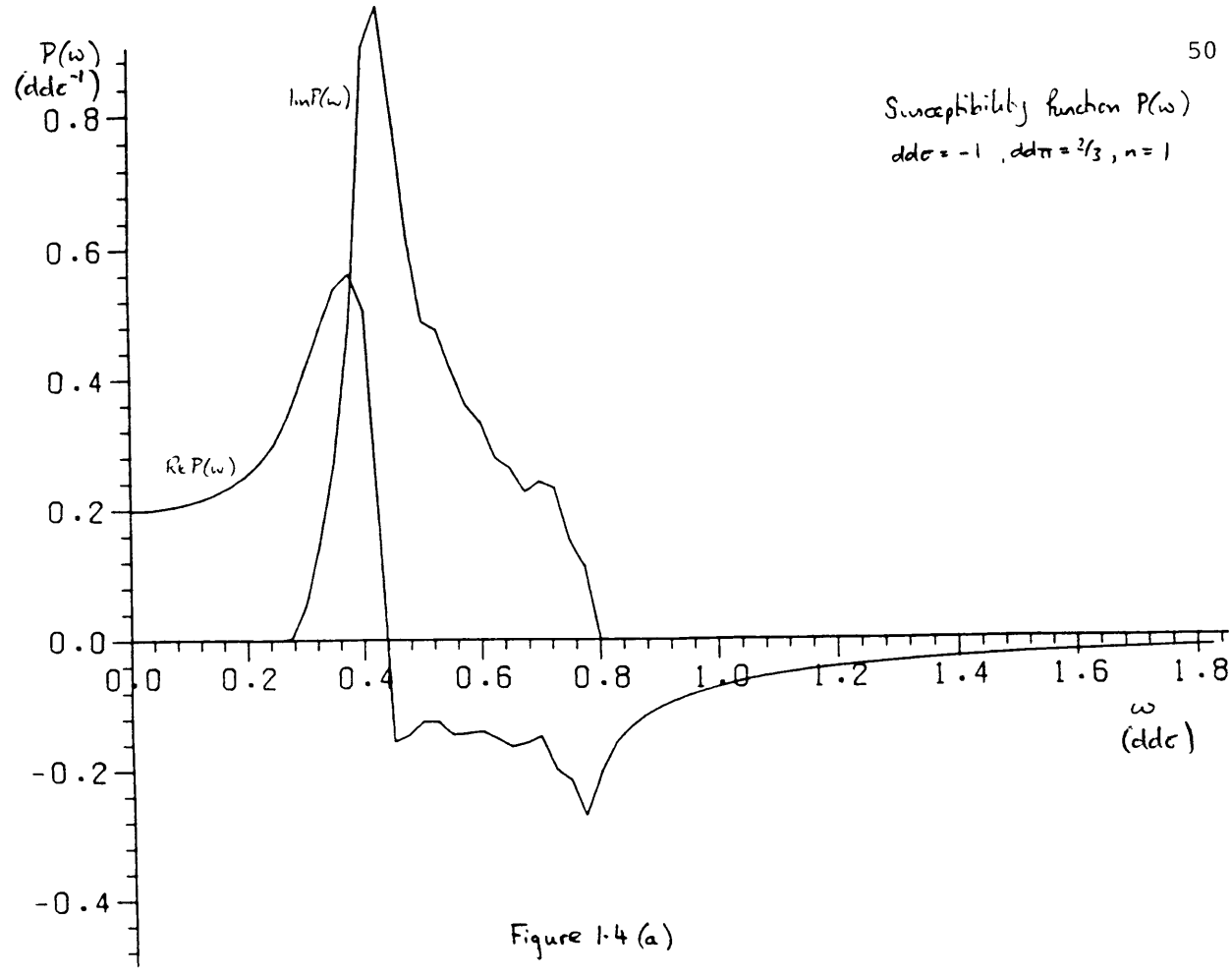

Figure 1.4 (a)

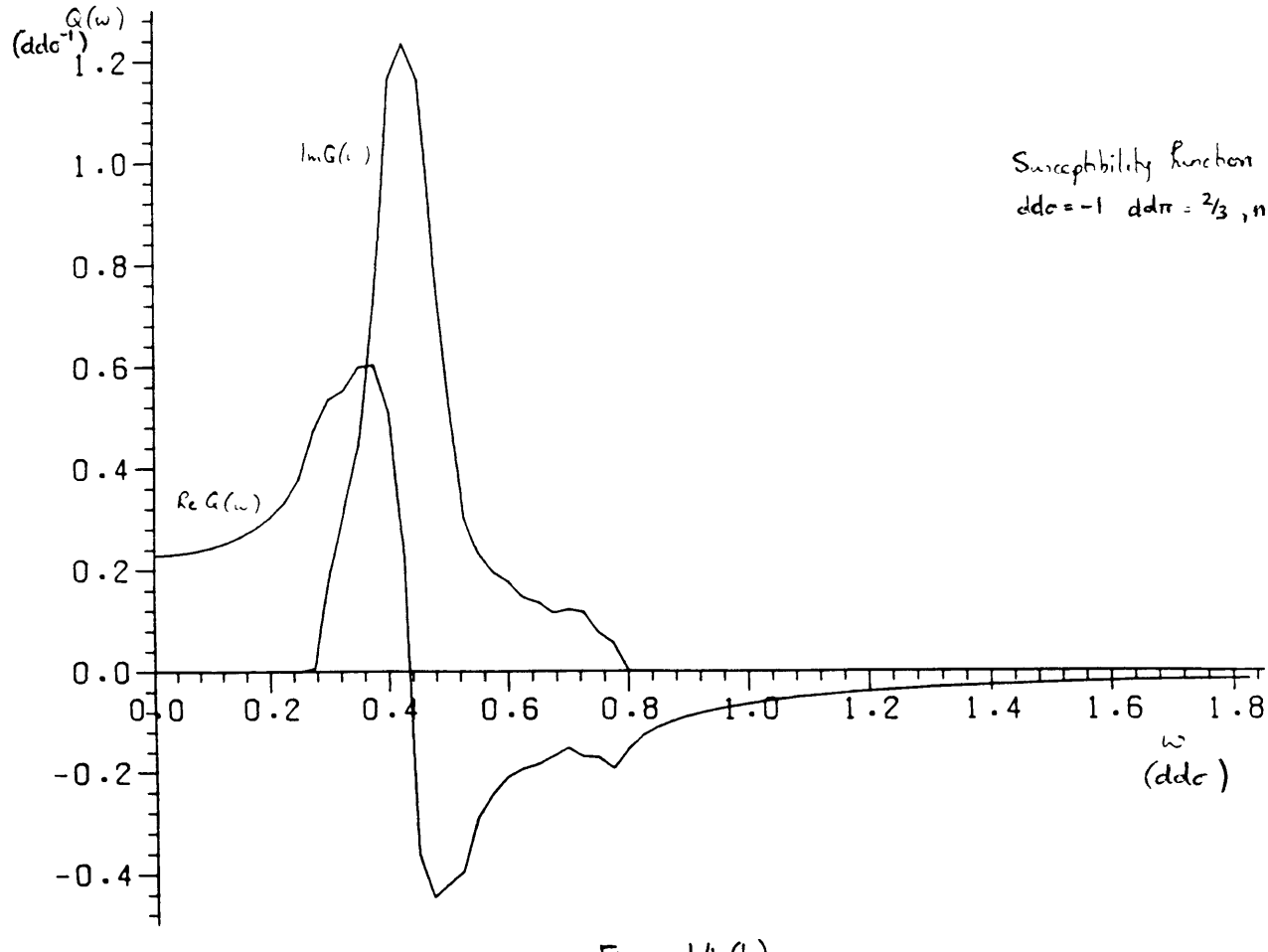

Figure 1.4 (b)

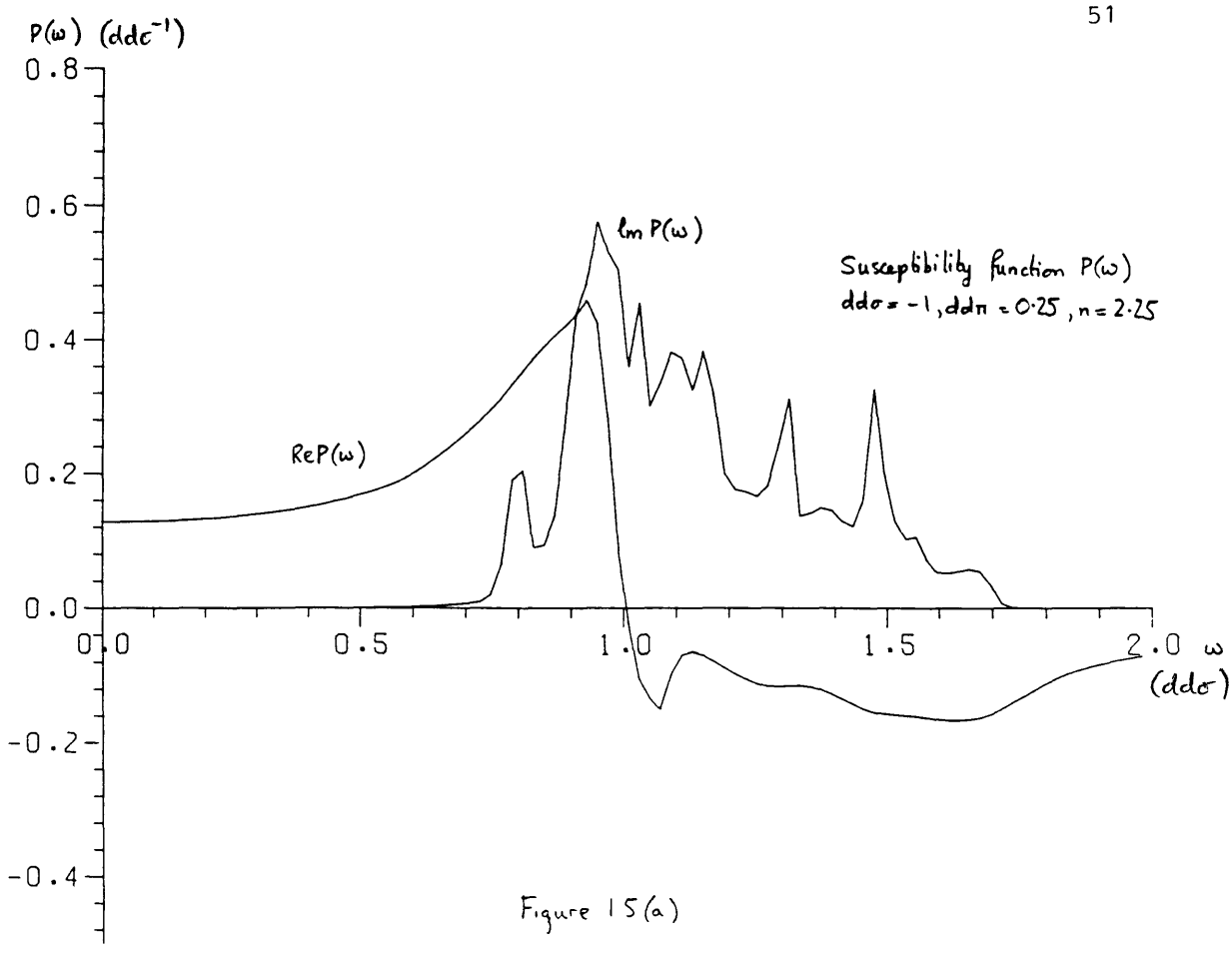

Figure 15(a)

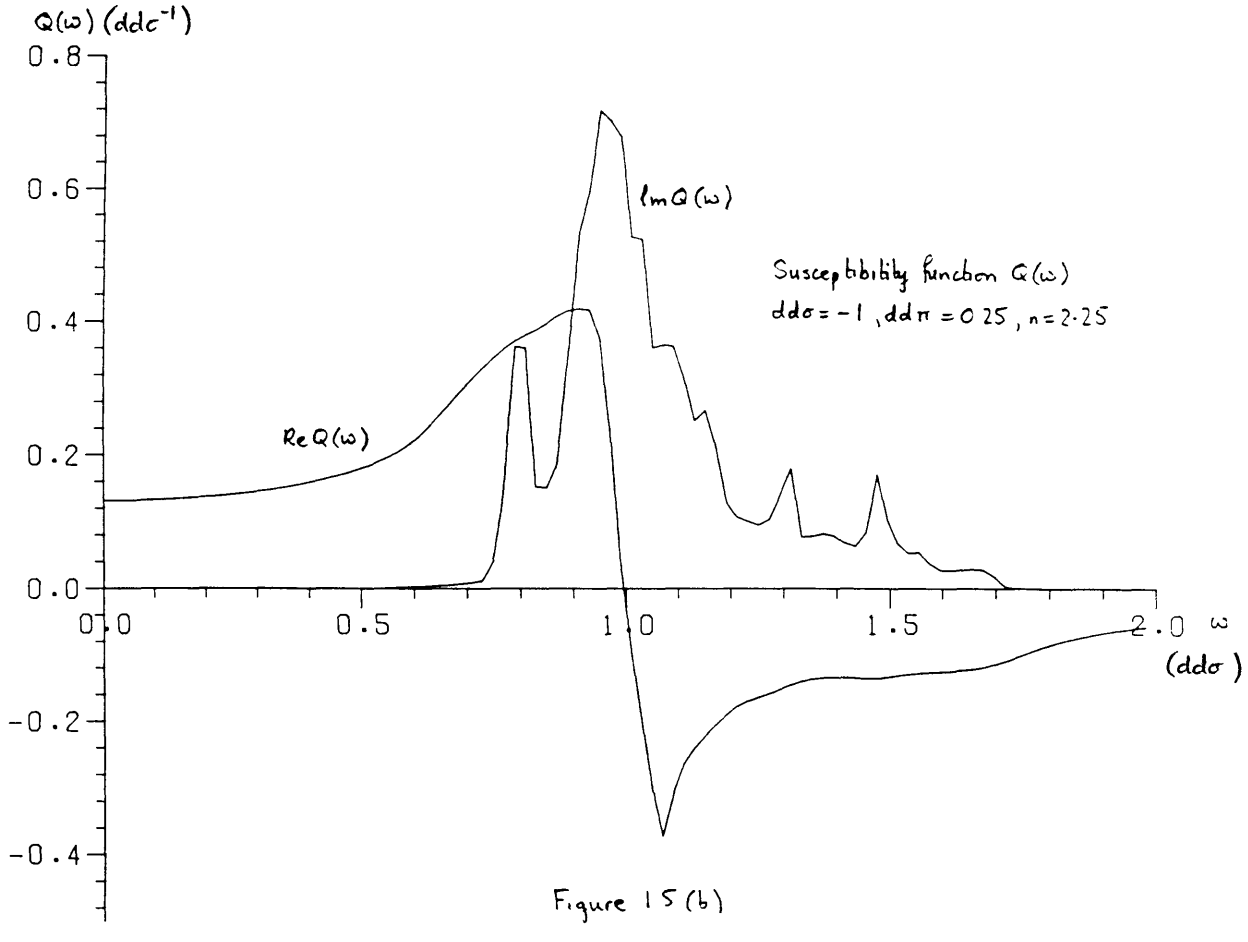

Figure 15(b)

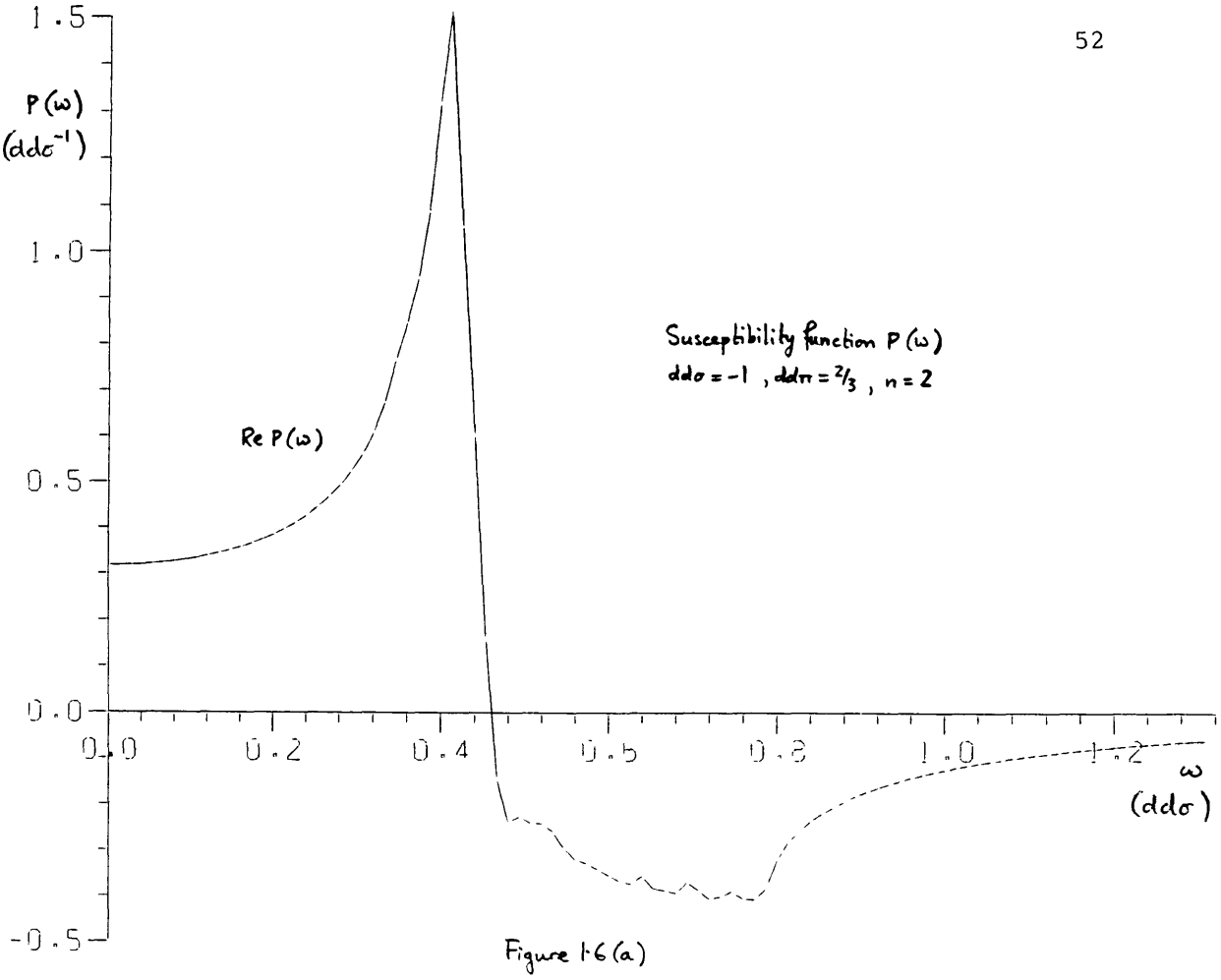

Figure 1.6 (a)

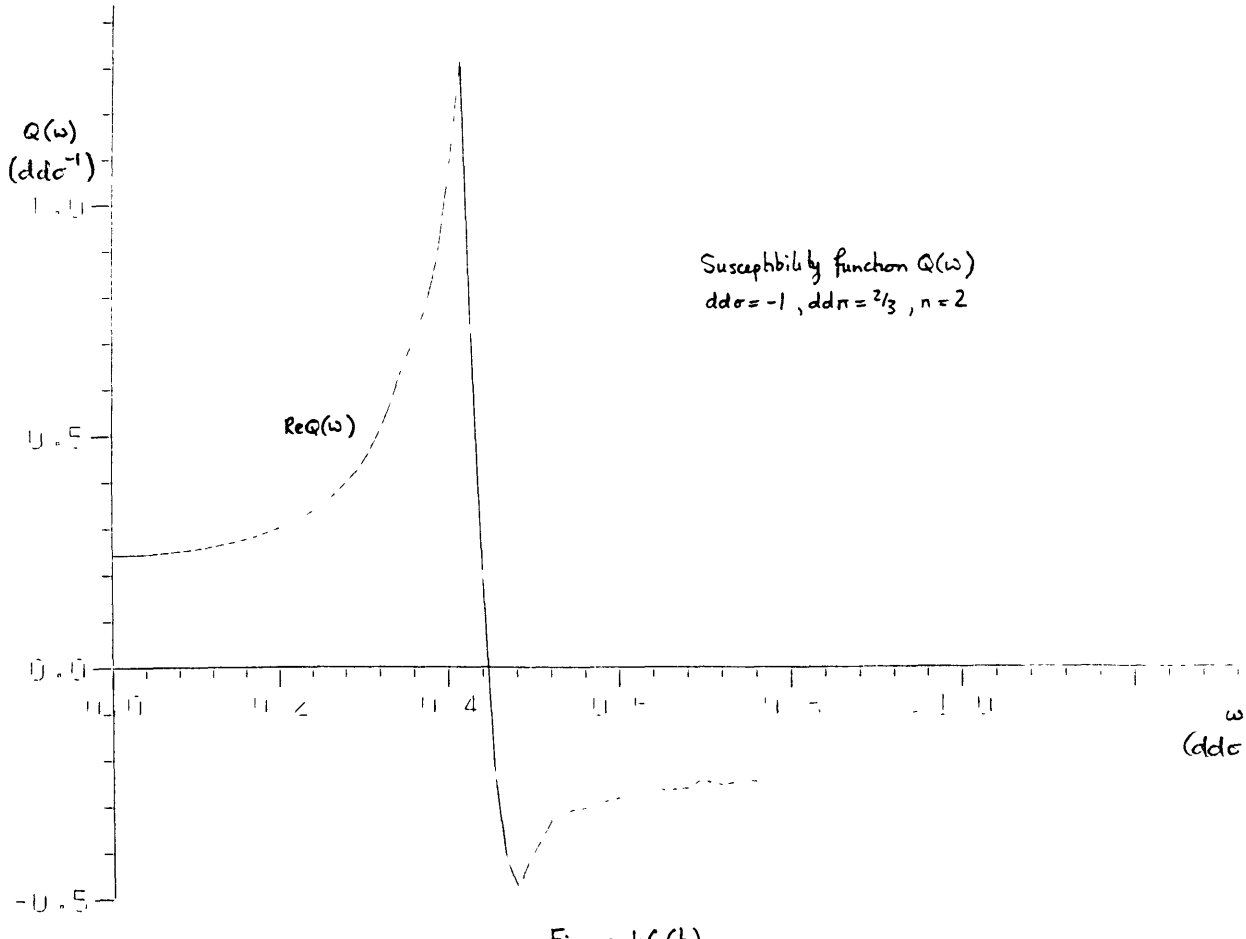

Figure 1.6 (b)

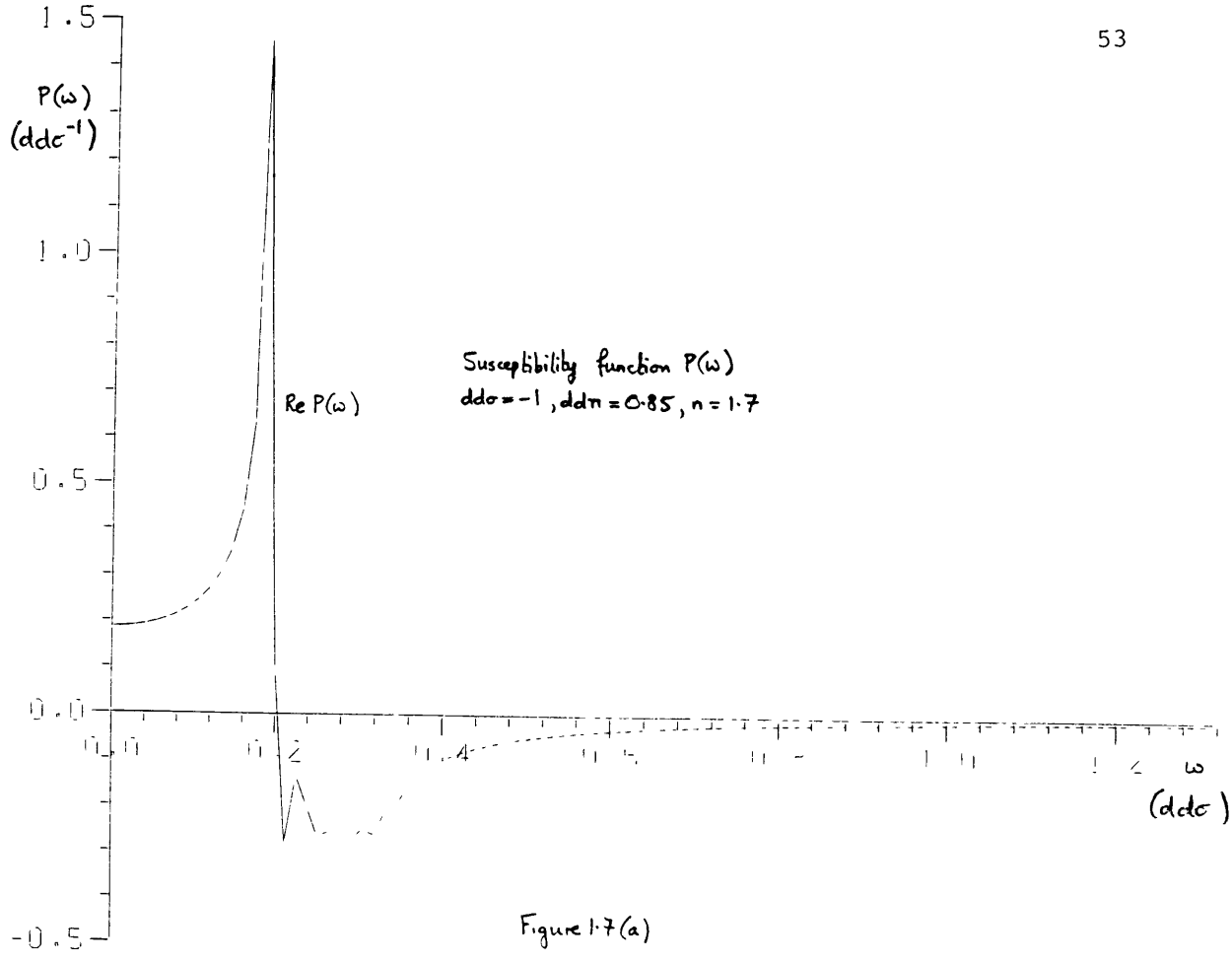

Figure 1.7(a)

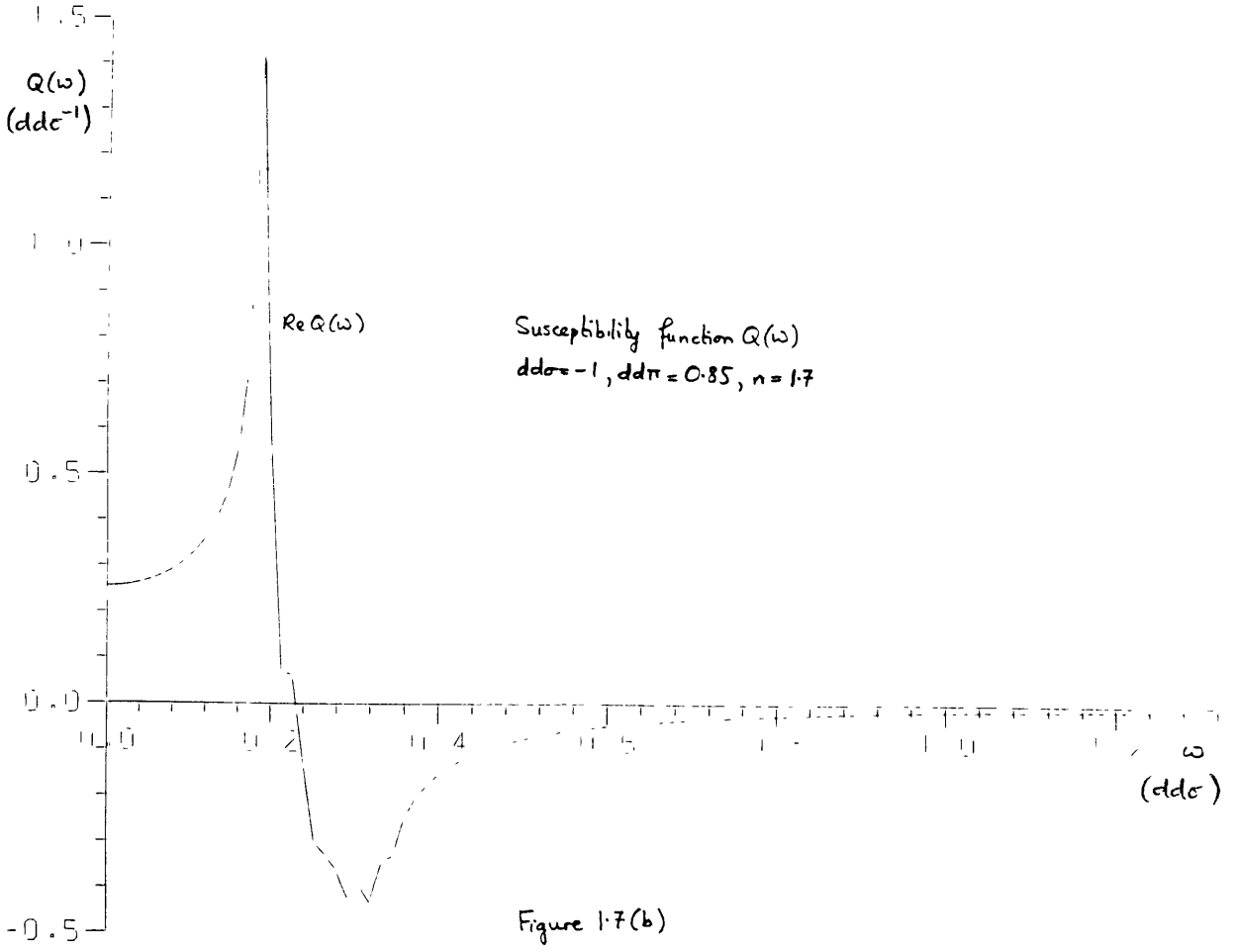

Figure 1.7(b)

CHAPTER 2

Self-consistent ground states and the anisotropy of the model

2.1 Introduction

In the previous chapter we established a simple model which might apply to actinide magnetism, as it contained the essential features of itinerancy and spin-orbit coupling. Having derived the equations for the HF ground state and the RPA dynamic susceptibility, several solutions of the model in the paramagnetic regime were examined. In this chapter we consider possible ordered ground states and the anisotropy of moment formation which is a fundamental characteristic of the model.

The most general ordering in the j = 3/2 manifold involves 15 order parameters, as can be seen from the general form of $\langle n_{\mu\upsilon} \rangle$:

$$\langle n_{\mu\upsilon} \rangle = \begin{pmatrix} n_1 & z_1 & z_2 & z_3 \\ z_1^* & n_2 & z_4 & z_5 \\ z_2^* & z_4^* & n_3 & z_6 \\ z_3^* & z_5^* & z_6^* & n_4 \end{pmatrix}$$

where the n_i are real and the z_i complex, and there is the constraint that $\sum_\mu \langle n_{\mu\mu} \rangle = n$. The order parameters consist of three components arising from dipolar ordering $\underline{\mu} = (\mu_x, \mu_y, \mu_z)$

$$\underline{\mu} = \langle \underline{J}_i \rangle = \langle (J_x, J_y, J_z) \rangle$$

where $\underline{J}_i$ is the angular momentum operator for a particle i on a particular site, together with five quadrupolar order parameters

$$Q = \langle J_z^2 - \tfrac{1}{3} J(J+1) \rangle$$

$$Q' = \frac{1}{\sqrt{3}} \langle J_x^2 - J_y^2 \rangle$$

$$Q'' = \frac{2}{\sqrt{3}} \langle J_x J_y \rangle$$

$$Q''' = \frac{2}{\sqrt{3}} \langle J_y J_z \rangle$$

$$Q^{(4)} = \frac{2}{\sqrt{3}} \langle J_x J_z \rangle$$

and seven octupolar order parameters

$$\bar{O} = \langle J_z^3 - \tfrac{3}{5} J_z J(J+1) \rangle$$

$$O' = \langle J_y^3 - \tfrac{3}{5} J_y J(J+1) \rangle$$

$$O'' = \langle J_x^3 - \tfrac{3}{5} J_x J(J+1) \rangle$$

$$O''' = 2\sqrt{\tfrac{3}{5}} \langle J_x J_y J_z \rangle$$

$$O^{(4)} = \sqrt{\tfrac{3}{5}} \langle J_z (J_x^2 - J_y^2) \rangle$$

$$O^{(5)} = \sqrt{\tfrac{3}{5}} \langle J_y (J_z^2 - J_x^2) \rangle$$

$$O^{(6)} = \sqrt{\tfrac{3}{5}} \langle J_x (J_y^2 - J_z^2) \rangle$$

These form the first three terms ζ of a 2^ζ -order multipole expansion. The order parameters are related to $\langle n_{\mu\nu} \rangle = \langle c_\nu^+ c_\mu \rangle$ by being expectation values of one-particle operators, so that

$$\mu = \sum_{\lambda\nu} \langle \lambda | J^z | \nu \rangle \langle c_\lambda^+ c_\nu \rangle$$

$$= \sum_\lambda \lambda \langle n_{\lambda\lambda} \rangle = \tfrac{3}{2} \langle n_{3/2\,3/2} \rangle + \tfrac{1}{2} \langle n_{1/2\,1/2} \rangle - \tfrac{1}{2} \langle n_{-1/2\,-1/2} \rangle - \tfrac{3}{2} \langle n_{-3/2\,-3/2} \rangle$$

$$Q = \sum_\lambda (\lambda^2 - \tfrac{5}{4}) \langle n_{\lambda\lambda} \rangle = \langle n_{3/2\,3/2} \rangle - \langle n_{1/2\,1/2} \rangle - \langle n_{-1/2\,-1/2} \rangle + \langle n_{-3/2\,-3/2} \rangle$$

$$\bar{O} = \sum_\lambda (\lambda^3 - \tfrac{9}{4}\lambda) \langle n_{\lambda\lambda} \rangle = \langle n_{-1/2\,-1/2} \rangle - \langle n_{1/2\,1/2} \rangle$$

and the μ and $\bar{O}$ modes of ordering are coupled, so that they always occur together. The other order parameters in terms of single-particle operators are:

$$\mu_x = \frac{\sqrt{3}}{2}\left(c^+_{3/2}c_{1/2} + c^+_{1/2}c_{3/2} + c^+_{-1/2}c_{-3/2} + c^+_{-3/2}c_{-1/2}\right) + c^+_{1/2}c_{-1/2} + c^+_{-1/2}c_{1/2}$$

$$\mu_y = \frac{\sqrt{3}}{2i}\left(c^+_{3/2}c_{1/2} - c^+_{1/2}c_{3/2} + c^+_{-1/2}c_{-3/2} - c^+_{-3/2}c_{-1/2}\right) - i\left(c^+_{1/2}c_{-1/2} - c^+_{-1/2}c_{1/2}\right)$$

$$Q' = c^+_{3/2}c_{-1/2} + c^+_{1/2}c_{-3/2} + c^+_{-1/2}c_{3/2} + c^+_{-3/2}c_{1/2}$$

$$Q'' = -i\left(c^+_{3/2}c_{-1/2} + c^+_{1/2}c_{-3/2} - c^+_{-1/2}c_{3/2} - c^+_{-3/2}c_{1/2} - \frac{\sqrt{3}}{2}c^+_{3/2}c_{3/2} - \frac{1}{2\sqrt{3}}c^+_{1/2}c_{1/2} + \frac{1}{2\sqrt{3}}c^+_{-1/2}c_{-1/2} + \frac{\sqrt{3}}{2}c^+_{-3/2}c_{-3/2}\right)$$

$$Q''' = -i\left(\frac{1}{2}c^+_{3/2}c_{1/2} - \frac{3}{2}c^+_{1/2}c_{3/2} - \frac{3}{2}c^+_{-1/2}c_{-3/2} + \frac{1}{2}c^+_{-3/2}c_{-1/2} - \frac{1}{3}c^+_{1/2}c_{-1/2} - \frac{1}{3}c^+_{-1/2}c_{1/2}\right)$$

$$Q^{(4)} = -i\left(\frac{1}{2}c^+_{3/2}c_{1/2} + \frac{3}{2}c^+_{1/2}c_{3/2} - \frac{3}{2}c^+_{-1/2}c_{-3/2} - \frac{1}{2}c^+_{-3/2}c_{-1/2} - \frac{1}{3}c^+_{1/2}c_{-1/2} - \frac{1}{3}c^+_{-1/2}c_{1/2}\right)$$

$$O' = -\frac{1}{8i}\left(6c^+_{3/2}c_{-3/2} + 2c^+_{-1/2}c_{1/2} - 2\sqrt{3}c^+_{-3/2}c_{-1/2} + 2\sqrt{3}c^+_{3/2}c_{1/2} - 2c^+_{1/2}c_{-1/2} + 2\sqrt{3}c^+_{-1/2}c_{-3/2} - 6c^+_{-3/2}c_{3/2} - 2\sqrt{3}c^+_{1/2}c_{3/2}\right)$$

$$O'' = \frac{1}{8}\left(6c^+_{3/2}c_{-3/2} + 2c^+_{-1/2}c_{1/2} + 2\sqrt{3}c^+_{-3/2}c_{-1/2} + 2\sqrt{3}c^+_{3/2}c_{1/2} + 2c^+_{1/2}c_{-1/2} + 2\sqrt{3}c^+_{-1/2}c_{-3/2} + 6c^+_{-3/2}c_{3/2} + 2\sqrt{3}c^+_{1/2}c_{3/2}\right)$$

$$O''' = \frac{1}{2i}\sqrt{\frac{3}{5}}\left(-3\sqrt{3}c^+_{1/2}c_{-3/2} - \sqrt{3}c^+_{3/2}c_{-1/2} - \sqrt{3}c^+_{-3/2}c_{1/2} - 3\sqrt{3}c^+_{-1/2}c_{3/2} - \frac{9}{2}c^+_{3/2}c_{3/2} - \frac{9}{2}c^+_{-3/2}c_{-3/2} - \frac{1}{2}c^+_{1/2}c_{1/2} - \frac{1}{2}c^+_{-1/2}c_{-1/2}\right)$$

$$O^{(4)} = \frac{3}{2\sqrt{5}}\left(3c^+_{3/2}c_{1/2} + c^+_{1/2}c_{-3/2} - c^+_{-1/2}c_{3/2} - 3c^+_{-3/2}c_{1/2}\right)$$

$$O^{(5)} = -\frac{1}{8}\sqrt{\frac{3}{5}}\left(6c^+_{3/2}c_{-3/2} + 10\sqrt{3}c^+_{1/2}c_{3/2} + 6c^+_{-1/2}c_{1/2} + 6\sqrt{3}c^+_{3/2}c_{1/2} + 6c^+_{1/2}c_{-1/2} + 10\sqrt{3}c^+_{-1/2}c_{-3/2} + 6c^+_{-3/2}c_{3/2} + 6\sqrt{3}c^+_{-3/2}c_{-1/2}\right)$$

$$O^{(c)} = -\frac{1}{8}\sqrt{\frac{3}{5}}\,(6\,c^{+}_{3/2}c_{-3/2} - 6\sqrt{3}\,c^{+}_{3/2}c_{1/2} - 6\,c^{+}_{1/2}c_{-1/2} + 10\sqrt{3}\,c^{+}_{-1/2}c_{-3/2}$$
$$+ 6\,c^{+}_{-3/2}c_{3/2} - 6\sqrt{3}\,c^{+}_{-3/2}c_{-1/2} - 6\,c^{+}_{-1/2}c_{1/2} + 10\sqrt{3}\,c^{+}_{1/2}c_{3/2})$$

It is reasonable to examine the ordering of the uniform system with no sublattice, and retaining rotational symmetry about a selected axis. In particular, if we retain invariance under fourfold rotation about the [001] axis then we can write $\langle n_{\mu\nu}\rangle$ in terms of representations of this rotation (as in Appendix A) and sum over them, using the great orthogonality theorem. This shows that $\langle n_{\mu\nu}\rangle$ is diagonal and as there is also the constraint that $n = \sum_{\lambda}\langle n_{\lambda\lambda}\rangle$ there are just three order parameters which are non-zero. These three are μ, Q and $\bar{O}$ which express dipolar, quadrupolar and octupolar ordering aligned with the axis [001]. It can be seen from the definition of the 15 order parameters above that all but three are zero if fourfold rotation is to leave the Hamiltonian invariant.

It is also of interest to consider ordering with respect to the trigonal axis [111] as well as the tetragonal. On rotating the axis of quantization to align along [111] and once again summing over representations of the threefold rotation, as in Appendix A, $\langle n_{\mu\nu}\rangle$ is found to be diagonal, giving three order parameters. On examining the above order parameters these three are

$$\mu_1 = \sqrt{3}\langle J_x\rangle = \sqrt{3}\langle J_y\rangle = \sqrt{3}\langle J_z\rangle$$

$$Q_1 = Q'' = Q''' = Q^{(a)} = \frac{2}{\sqrt{3}}\langle J_x J_y\rangle$$

$$\bar{O}_1 = O''' = 2\sqrt{\frac{3}{5}}\langle J_x J_y J_z\rangle$$

and all others are zero. Similarly, we can consider ordering

with respect to the [110] axis, and by virtue of the two-fold rotational symmetry examine the diagonal $\langle n_{\mu\nu} \rangle$, and find the three order parameters.

It is convenient in comparing ordering about different axes to use the dipolar, quadrupolar and octupolar moment aligned along that axis; thus we can compare magnetic moment formation along [001] , [111] and [110] axes, and investigate the anisotropy of moment formation.

2.2 Related studies of quadrupolar ordering

Ordering in a simple orbitally degenerate itinerant model has also been investigated by Inagaki and Kubo (1973). They use two doubly degenerate bands with intra-atomic Coulomb and exchange interactions, but do not include spin-orbit coupling. Their Hamiltonian is

$$H = \sum_{ij\sigma} t_{ij} \left(c^{+}_{i\sigma} c_{j\sigma} + d^{+}_{i\sigma} d_{j\sigma} \right) + U \sum_{i} \left(n_{i\sigma} n_{i-\sigma} + m_{i\sigma} m_{i-\sigma} \right) + U' \sum_{i\sigma\sigma'} n_{i\sigma} m_{i\sigma'} - V \sum_{i\sigma\sigma'} c^{+}_{i\sigma} c_{i\sigma'} d^{+}_{i\sigma'} d_{i\sigma}$$

$$n_{i\sigma} = c^{+}_{i\sigma} c_{i\sigma} \qquad m_{i\sigma} = d^{+}_{i\sigma} d_{i\sigma}$$

where $c^{+}_{i\sigma}$ and $d^{+}_{i\sigma}$ create a σ-spin electron in orbitals 1 and 2 respectively at the i-th atomic site; t_{ij} is the transfer integral between the states on the i-th and j-th sites, with mixing transfer terms (such as $c^{+}_{i\sigma} d_{j\sigma}$) being ignored. The interaction between two electrons is assumed to act only when they come onto the same atomic sites: U, U' and V are respectively the intraband Coulomb, interband Coulomb and exchange energies on an atom. They examine possible modes of ordering of orbital and spin states

including sublattice structures, and construct a phase diagram of the lowest energy states by numerical calculation, varying the number of electrons and the ratio of the intra-atomic interactions against the bandwidth. The total energies of various states were calculated within the Hartree-Fock approximation and response functions within the RPA. Three types of ferromagnetism were found whose orbital states ordered in different patterns (one having an orbital sublattice structure); without intra-atomic exchange one of these is degenerate with a paramagnetic state which possesses some ferromagnetic ordering in the orbital states (quadrupolar ordering). Orbital ordering with a sublattice was also studied by Cyrot and Lyon-Caen (1975).

However, considering now the role of quadrupolar interactions in the magnetism of actinide compounds or rare-earth compounds (which are much more localized) some of the earliest work was done by Allen (1968). This author established a model of the magnetism of UO_2, considering the spin-lattice interaction and using a Jahn-Teller description; a second paper then examined how the quadrupole-lattice interaction of the ground state produces a first-order phase transition, which is observed.

Another uranium compound (UP) was then the subject of a paper by Long and Wang (1971) in which they showed how the introduction of a quadrupole-quadrupole interaction term, of the electrostatic multipole interactions (EMI), greatly improved a simple model of UP, correctly giving a first-order phase transition.

Sivardière and Blume (1972) considered an $s = 3/2$ Ising system and its dipolar and quadrupolar modes of ordering (neglecting the octupolar mode). The molecular-field approximation is used,

followed by self-consistent solution for the ground state, in order to construct the phase diagram. A variety of possible combinations of phase transitions of the dipolar and quadrupolar order parameters was found. Finally, the effects of a magnetic field and of a sublattice were studied.

Khomskii and Kugel (1973) and Kugel and Khomskii (1974) found that exchange may lead to cooperative orbital (quadrupolar) ordering as well as magnetic ordering when examining a Jahn-Teller Hamiltonian, and also one with a superexchange mechanism, in order to explain the structure of two-dimensional ferromagnets of the K_2CuF_4 type.

The role of indirect multipole interactions, such as RKKY, in a system with itinerant conduction electrons and ions with an incomplete shell was examined by Teitelbaum and Levy (1976), using an s-f Hamiltonian. They determined the full effective coupling by including the direct Coulomb interaction as well as the exchange interaction, and found that high-degree couplings can be important in metallic materials in which the orbital angular momentum is unquenched.

Levy, Morin and Schmitt (1979) then published a significant paper concerned with large quadrupolar interactions in rare-earth intermetallic compounds. Several such compounds undergo structural phase transitions, and in many cases this has been found to be a consequence of the cooperative Jahn-Teller effect. However, they have shown that this is not the reason in TmZn and TmCd, and in these systems the lattice ordering follows quadrupolar ordering in the conduction electrons, being driven by the quadrupolar pair interaction, and the lattice distorts in such a way as to minimize the Jahn-Teller coupling energy. TmCd and TmZn were found to be the first examples of magnetic materials in which

quadrupolar interactions dominate over magnetic and magnetoelastic interactions, and are capable of producing a ferroquadrupolar ordering, even in a clamped or rigid lattice, before the system orders magnetically. The quadrupolar coupling of an exchange or indirect Coulomb origin was found to be larger than the bilinear spin coupling.

The study of the quadrupolar interaction was extended by Morin and Schmitt (1981) using the third-order magnetic susceptibility, and considering various possible lattice distortions. Even when the quadrupolar interaction was less strong than the bilinear ones, driving the magnetic ordering, it nonetheless deeply modified the magnetic properties, especially the magnetic moment and the anisotropy of the energy (Morin and Schmitt (1978)).

2.3 Phase transitions and the formation of ordered states

Self-consistent solutions of the Hartree-Fock equations for our model derived in the previous chapter allow numerical investigation of the phase changes and modes of ordering as the interaction strength U is increased, for various values of the number of electrons per atom n and hopping integral ratio $dd\pi/dd\sigma$. In order to consider the anisotropy of moment formation a canonical band-structure ($dd\sigma = -1$, $dd\pi = 2/3$, $dd\delta = 0$) containing one electron per atom was used, and moment formation investigated along the symmetry axes [001], [110] and [111].

The Stoner criteria indicate the position of second order phase transitions, and with which mode the paramagnetic state is unstable, provided no first order phase transition has occurred up to that point. For the canonical one-electron case the lowest

instability is with respect to a parallel moment and occurs when $U_p = 0.85$ (using the notation of the previous chapter to denote Stoner criteria). In Figure 2.1 the order parameters μ and Q are plotted against U for ordering along the [001] direction, and in Figures 2.2 and 2.3 for symmetry breaking with respect to the [110] and [111] directions with μ , Q calculated along those axes. Figure 2.1 shows a second order phase transition for the magnetic moment at a value agreeing well with U_p. Moment formation breaks invariance of the Hamiltonian under time reversal, so that Kramers' degeneracy is no longer present; in this manner a quadrupole moment is induced by moment formation, and it can be seen that a second order phase transition in the order parameter Q occurs at U_p (when $\mu \neq 0$, $Q \neq 0$).

In contrast, if quadrupolar ordering occurs before the state is unstable with respect to moment formation, then with no moment present time reversal symmetry is not broken and Kramers' degeneracy is retained (as in Figure 2.6). As quadrupolar ordering does not break time reversal symmetry, it does not directly induce dipolar ordering and moment formation so that we can have $Q \neq 0$ whilst $\mu = 0$.

If the paramagnetic state orders in the quadrupole mode (1,-1,-1,1), referred to in equation (1.83), without U being sufficiently large for a magnetic moment to form, then as time reversal symmetry is not broken, the Hamiltonian H may be solved analytically in a manner similar to the paramagnetic state, as we can define new elements of $T_{\mu\nu}(\underline{k})$ with

$$a'(\underline{k}) = a(\underline{k}) + U(n - \langle n_{3/2\,3/2} \rangle) = a - UQ/4 + 3Un/4$$

$$b'(\underline{k}) = b(\underline{k}) + U(n - \langle n_{1/2\,1/2} \rangle) = b + UQ/4 + 3Un/4$$

using the notation of the previous chapter, so that

$$H = \sum_{\mu\nu\underline{k}} \left(T_{\mu\nu}(\underline{k}) + U\left(n\delta_{\mu\nu} - \langle n_{\mu\nu}\rangle\right)\right) c^{+}_{\mu\underline{k}} c_{\nu\underline{k}}$$

$$= \begin{pmatrix} a'(Q) & c & d & 0 \\ c^{*} & b'(Q) & 0 & d \\ d^{*} & 0 & b'(Q) & -c \\ 0 & d^{*} & -c^{*} & a'(Q) \end{pmatrix}$$

where the quadrupole moment Q is given by

$$Q = 2\left(\langle n_{3/2\,3/2}\rangle - \langle n_{1/2\,1/2}\rangle \right)$$

and $\langle n_{\mu\mu}\rangle = \langle n_{-\mu-\mu}\rangle$. The bandstructure $\lambda_i(\underline{k})$ and susceptibility $\chi^{\alpha\beta}(0,\omega)$ are then known provided that the quadrupole moment Q is known:

$$\lambda_{1,2}(\underline{k}) = \frac{1}{2}\left\{ a'(\underline{k}) + b'(\underline{k}) \pm \sqrt{\left(a'(\underline{k}) - b'(\underline{k})\right)^2 + 4\left(|c(\underline{k})|^2 + |d(\underline{k})|^2\right)}\right\} \qquad (2.1)$$

$$y_i^{(1)}(\underline{k}) = \left[(a'-\lambda_i)(a'+b'-2\lambda_i)\right]^{-1/2} \begin{pmatrix} d \\ 0 \\ -(a'-\lambda_i) \\ -c^{*} \end{pmatrix}; \quad y_i^{(2)}(\underline{k}) = \left[(a'-\lambda_i)(a'+b'-2\lambda_i)\right]^{-1/2} \begin{pmatrix} c \\ -(a'-\lambda_i) \\ 0 \\ d^{*} \end{pmatrix}$$

The value of Q is determined from the self-consistency condition.

From the expression for $\lambda_{1,2}(\underline{k})$ we see that Kramers' degeneracy is retained on going from the paramagnetic to quadrupolar state. Also from this analysis it emerges that a set of Stoner criteria for the instability of the quadrupolar state with respect to moment formation could be derived, as was done for the paramagnetic state, and would have the same form. However, these criteria would now also depend on Q, which is a function of U; therefore the point at which a second order phase transition in μ will occur,

after Q has become non-zero, will no longer be U_p as calculated for the paramagnetic state, and may be significantly less than or greater than U_p. Figure 2.4 is a case ($dd\sigma = -1$, $dd\pi = 1/2$, $n = 2$) of the quadrupolar ordering occurring below U_p ($U_{nm} < U_c, U_p$) and no magnetic moment being induced; even when $U > U_p, U_c$ no ordering in μ takes place as the nearly saturated quadrupolar ordering resists this. With a different set of parameters ($dd\sigma = -1$, $dd\pi = 0.25$, $n = 2.64$) in Figure 2.5 the model again has $U_{nm} < U_p, U_c$, but when it orders in Q the new ground state is such that by its new Stoner criteria it is unstable with respect to ordering in μ; thus the first order phase transition in Q produces indirectly a first order phase transition in μ.

The manner in which phase transitions driven by dipolar or octupolar ordering are second order and those driven by quadrupolar ordering are first order may be examined by considering the Landau free energy expansion. Using $\xi = Q/2$ and considering quadrupolar ordering alone, on expanding equation (2.1) in powers of ξ

$$\lambda_{1,2}(\underline{k}) = \frac{1}{2}\left\{ a+b \pm \sqrt{(a-b)^2+4(|c|^2+|d|^2)-2U\xi(a-b)+U^2\xi^2} \right\}$$

$$= \lambda^{\circ}_{1,2}(\underline{k}) \mp \frac{U\xi(a-b)}{\sqrt{((a-b)^2+4(|c|^2+|d|^2))}} \pm \frac{4U^2\xi^2(|c|^2+|d|^2)}{4((a-b)^2+4(|c|^2+|d|^2))^{3/2}}$$

$$\pm \frac{U^3\xi^3(a-b)(|c|^2+|d|^2)}{((a-b)^2+4(|c|^2+|d|^2))^{5/2}} + O(\xi^4) \qquad (2.2)$$

where λ_i° is the paramagnetic energy. The density of states N(E) may be written in terms of $\lambda_i = \lambda_i^{\circ} + \mu_i$, being

$$N(E) = \sum_k (\delta(\lambda_1 - E) + \delta(\lambda_2 - E))$$

$$N(E) = \sum_k \left(\delta(\lambda_1^\circ - E + \mu_1) + \delta(\lambda_2^\circ - E + \mu_2)\right)$$

$$= \sum_k \left(\delta(\lambda_1^\circ - E) + \delta(\lambda_2^\circ - E)\right) + \sum_k \Big(\mu_1 \delta'(\lambda_1^\circ - E)$$

$$+ \frac{\mu_1^2}{2!}\delta''(\lambda_1^\circ - E) + \frac{\mu_1^3}{3!}\delta'''(\lambda_1^\circ - E) + \ldots + \mu_2 \delta'(\lambda_2^\circ - E)$$

$$+ \frac{\mu_2^2}{2!}\delta''(\lambda_2 - E) + \frac{\mu_2^3}{3!}\delta'''(\lambda_1^\circ - E) + \ldots \Big) \qquad (2.3)$$

$$= N_0(E) + N_1 \xi + N_2 \xi^2 + N_3 \xi^3 + \ldots \qquad (2.4)$$

and the total energy E_{tot} may be expressed in terms of these quantities as

$$E_{tot} = \int_0^{\mu(\xi)} E\, N(E)\, dE \qquad (2.5)$$

where $\mu(\xi)$ is the Fermi energy. The linear term in ξ in the N(E) expansion has the coefficient N_1, and from cubic symmetry and equations (2.2) and (2.3) we have

$$N_1 = \frac{u}{8}\frac{d}{dE}\sum_{\underline{k}} \frac{(a-b)}{\sqrt{((a-b)^2 + 4(|c|^2+|d|^2))}}\left(\delta(\lambda_1^\circ - E) - \delta(\lambda_2^\circ - E)\right) \qquad (2.6)$$

which is zero as the term $(a-b)/\sqrt{(a-b)^2 - 4(|c|^2 + |d|^2)}$ has cubic symmetry. However, both N_2 and N_3 are non-zero and are given by

$$N_2 = \sum_{\underline{k}} \frac{u^2(|c|^2+|d|^2)}{((a-b)^2+4(|c|^2+|d|^2))^{3/2}}\left(\delta'(\lambda_1^\circ - E) - \delta'(\lambda_2^\circ - E)\right) + \frac{u^2(a-b)^2}{2\left((a-b)^2+4(|c|^2+|d|^2)\right)}\left(\delta''(\lambda_1^\circ - E) + \delta''(\lambda_2^\circ - E)\right) \qquad (2.7)$$

$$N_3 = \sum_{\underline{k}} \frac{u^3(a-b)(|c|^2+|d|^2)}{((a-b)^2+4(|c|^2+|d|^2))^{5/2}}\left(\delta'(\lambda_1^\circ - E) - \delta'(\lambda_2^\circ - E)\right) - \frac{1}{2}\frac{u^3(a-b)(|c|^2+|d|^2)}{4((a-b)^2+4(|c|^2+|d|^2))^{5/2}}\left(\delta''(\lambda_1^\circ - E) + \delta''(\lambda_2^\circ - E)\right)$$

$$+ \frac{1}{6}\frac{u^3(a-b)^3}{8^3\left((a-b)^2+4(|c|^2+|d|^2)\right)^{3/2}}\left(\delta'''(\lambda_1^\circ - E) - \delta'''(\lambda_2^\circ - E)\right) \qquad (2.8)$$

which do not go to zero as a result of cubic symmetry.

The Fermi energy $\mu(\xi)$ may be found using the conservation of the number of electrons n

$$n = \int_0^{\mu_0} N_0(E)\,dE = \int_0^{\mu} N(E)\,dE$$

Therefore

$$\int_0^{\mu_0} (N(E) - N_0(E))\,dE + \int_{\mu_0}^{\mu} N(E)\,dE = 0$$

and expanding N(E) as in equation (2.4)

$$\xi^2 \int_0^{\mu_0} N_2(E)\,dE + \xi^3 \int_0^{\mu_0} N_3(E)\,dE + \int_{\mu_0}^{\mu} N_0(E)\,dE + O(\xi^4) = 0$$

so that to order ξ^3

$$(\mu - \mu_0)\,N_0(\mu_0) = -\xi^2 \int_0^{\mu_0} N_2(E)\,dE - \xi^3 \int_0^{\mu_0} N_3(E)\,dE + O(\xi^4)$$

The Landau expansion may now be formed by putting this expression for $\mu(\xi)$ into equation (2.5):

$$E_{tot} = \int_0^{\mu_0} E\,N(E)\,dE + \int_{\mu_0}^{\mu} E\,N(E)\,dE$$

$$= \int_0^{\mu_0} E\,N(E)\,dE + (\mu - \mu_0)\,\mu_0\,N_0(E) + O(\xi^4)$$

$$= \int_0^{\mu_0} E\,N(E)\,dE + \mu_0 \left(-\xi^2 \int_0^{\mu_0} N_2(E)\,dE - \xi^3 \int_0^{\mu_0} N_3(E)\,dE \right)$$

so that the cubic term is

$$\xi^3 \int_0^{\mu_0} E\,N_3(E)\,(E - \mu_0)\,dE$$

which as $N_3 \neq 0$ is finite, as neither E nor $(E - \mu_0)$ change sign in the region of integration. The presence of this finite cubic term in Q in the Landau expansion indicates that a first-order phase transition will precede second-order ordering when quadrupolar ordering occurs (see Landau and Lifshitz (1980), p. 451).

For dipolar ordering the linear term in μ is zero, and the quadratic term non-zero. The cubic term in μ is zero as the energy of the system with reversed magnetic moment is the same; as a consequence dipolar ordering occurs as a second-order phase transition.

Thus, considering Figure 2.6 the phase transition is driven by quadrupolar ordering and is first-order, initially with no ordering of a dipolar or octupolar nature. Then at a higher U the appropriate Stoner criteria for instability of the quadrupolar state is reached, which is different from U_p and U_c calculated with respect to the paramagnetic state, and the coupled dipolar and octupolar ordering appear in a second-order phase transition. In this case the dipolar and quadrupolar transitions are in the reverse order to that found in Figure 2.1, in which, after a small second-order phase change in μ inducing a similar phase change in Q we have a large quadrupolar first-order phase change occurring, driving a large first-order phase change in μ. There is another example of a second-order phase change in μ driving a similar change in Q given in Figure 2.7; this is an instability with respect to the compensated moment mode (1,-1,1,-1) occurring at U_c. The bandstructure along various symmetry axes is shown in Figure 2.8, for U = 0.7, and shows how crossing of the bands occurs.

A further way of studying the formation of the magnetic moment displayed in Figure 2.1 is to plot the four projected densities of states $n_\mu(E)$ for a sequence of values of U as done in Figure 2.9. The definition of $n_\mu(E)$ is

$$n_\mu(E) = \frac{1}{N} \sum_{i\underline{k}} a^*_{i\mu}(\underline{k})\, a_{i\mu}(\underline{k})\, f_i(E) \qquad (2.9)$$

where the $a^*_{i\mu}(\underline{k})$ are as defined in equation (1.9), and $f_i(E)$ is the density of states of the i-th band at energy E; the summation is over momenta $\underline{k}$ up to a Fermi level corresponding to E. This version of the model has a canonical bandstructure (ddσ = -1, ddπ = 2/3) and one electron per atom, for which the Fermi level is marked. The hybridization between the four orbitals μ = (3/2,m) can be seen, and also the manner in which there is a transition from four superimposed densities of states in the paramagnetic regime to one filled and three unfilled orbitals in the localized (high U) regime.

2.4 Anisotropy of magnetic moment formation

The case studied along various symmetry axes in Figures 2.1 - 2.3 (ddσ = -1, ddπ = 2/3, n = 1) was used to investigate the anisotropy of magnetic moment formation. From the figures it is clear that moment formation is easiest along the axis [001], and much harder along [110] and [111]. This may be quantified further by calculating the total energy of the moment for various values of U for each axis; the total energy ε_{bt} is given by equation (1.22), and the calculated values are given in Table 2.1. The energy ε_a of the paramagnetic state is

$$\varepsilon_o = \varepsilon_{tot}(U=0) + \frac{3Un}{4}$$

where $\varepsilon_{tot}(U=0) = -0.3705$, and we define the energy ε by

$$\varepsilon = \varepsilon_{tot} - \varepsilon_o$$

with $\varepsilon_1, \varepsilon_2, \varepsilon_3$ referring to the energy for an [001], [110] and [111] moment respectively. The magnetic moment μ along each of these axes is M_1, M_2 and M_3.

A Landau free energy expansion $\varepsilon_{tot}(\underline{M})$ may be performed in the ferromagnetic domain; if we use the first few Kubic harmonic functions we can write down combinations of the components of the magnetic moment $\underline{\mu} = (M_x, M_y, M_z)$ having cubic symmetry:

$$\varepsilon_{tot} = \varepsilon_o + \tfrac{1}{2}A(M_x^2 + M_y^2 + M_z^2) + \tfrac{1}{4}B(M_x^2 M_y^2 + M_y^2 M_z^2 + M_x^2 M_z^2) + \tfrac{1}{4}C(M_x^4 + M_y^4 + M_z^4)$$

The unknown coefficients A,B,C can then be found from the positions and values of the energy at the energy minima:

$$M_1 = \left(-\frac{A}{C}\right)^{1/2} \qquad \varepsilon_1 = -\frac{A^2}{4C}$$

$$M_2 = \left(\frac{-4A}{2C+B}\right)^{1/2} \qquad \varepsilon_2 = -\frac{A^2}{2C+B}$$

Therefore, we can determine these quantities from M_1, and as follows:

$$A = \frac{4\varepsilon_1}{M_1^2}$$

$$B = -\frac{A^2}{\varepsilon_2} - 2C$$

$$C = -\frac{A^2}{4\varepsilon_1}$$

and hence calculate the quantities M_3 and ε_3 from them:

$$M_3 = \left(\frac{-3A}{(B+C)} \right)^{1/2}$$

$$\varepsilon_3 = \frac{-3A^2}{4(B+C)}$$

For the cases with U = 1.3, 1.5 the following are obtained:

U = 1.3	U = 1.5
$\varepsilon_1 = -0.530$	$\varepsilon_1 = -0.6665$
$\varepsilon_2 = -0.524$	$\varepsilon_2 = -0.6489$
$A = -0.9811$	$A = -1.235$
$B = 0.9289$	$B = 1.206$
$C = 0.4540$	$C = 0.5721$
$M_3 = 1.459$	$M_3 = 1.443$
$\varepsilon_3 = -0.522$	$\varepsilon_3 = -0.6433$

This indicates the extent to which a Landau expansion in the ferromagnetic regime relates moment formation in different directions, attempting to reproduce the high degree of anisotropy.

Table 2.1

		[001]	[110]	[111]	ε_0
U = 0	ε_{tot}	- 0.3705	- 0.3705	- 0.3705	- 0.3705
	ε	0	0	0	
	μ	0	0	0	
U = 0.8	ε_{tot}	- 0.07	- 0.08	- 0.07	- 0.075
	ε	+ 0.005	- 0.005	+ 0.005	
	μ	0	0	0	
U = 1.0	ε_{tot}	- 0.01780	0.0048	- 0.004476	0.0045
	ε	- 0.0223	0.00030	- 0.00898	
	μ	1.268	0.000731	0.02824	
U = 1.3	ε_{tot}	0.07183	0.07800	0.07657	0.05745
	ε	- 0.530	- 0.524	- 0.525	
	μ	1.47	1.44	1.43	
U = 1.5	ε_{tot}	0.0585	0.0761	0.0651	0.725
	ε	- 0.6665	- 0.6489	- 0.6599	
	μ	1.47	1.47	1.47	

The results of Table 2.1 reveal the fundamental anisotropy of the model, present in general as well as in this case. The model has planes of high correlation with the magnetic moment aligned perpendicular to these planes, and poor correlation between planes. This anisotropy stems from the strong spin-orbit coupling (assumed infinite for our model). The moments and total energies in Table 2.1 show that the moment forms most easily along [001], with much more difficulty along [111], and with even more difficulty along [110]; this agrees with the concept of planar behaviour, with moments ordering normal to, but not in, the planes.

2.5 Anisotropy in the large U limit

To indicate how anisotropic behaviour arises we can in the region of large U derive an effective Hamiltonian H from our degenerate Hubbard Hamiltonian; we define t_{mn} as the hopping integral between state m on one site and state n on another. Only the hopping integrals between nearest neighbours are assumed to be non-zero, and then, in a similar way to Cyrot & Leon-Caen (1975) we can write H as

$$H = -\sum_{mnm'n'} t_{mn}\, t_{n'm'}\, c^{+}_{n'j}\, c_{m'i}\, c^{+}_{mi}\, c_{nj}$$

$$= -\sum_{mnm'n'} t_{mn}\, t_{n'm'}\, c^{+}_{n'j}\, c_{nj}\, (\delta_{mm'} - c^{+}_{mi}\, c_{m'i})$$

If we put the quantization axis along the line joining the centres then, doing the sum over m',n'

$$H = -\sum_{mn} t_{mm}\, t_{nn}\, c^{+}_{mj}\, c_{mi}\, c^{+}_{ni}\, c_{nj} - \sum_{mn} t_{mm}\, t_{nn}\, c^{+}_{mi}\, c_{mj}\, c^{+}_{nj}\, c_{ni}$$

$$H = -\sum_{mn} t_{mm} t_{nn} c^{+}_{mj} c_{nj} (\delta_{mn} - c^{+}_{ni} c_{mi})$$

$$- \sum_{mn} t_{mm} t_{nn} c^{+}_{mi} c_{ni} (\delta_{mn} - c^{+}_{nj} c_{mj})$$

$$= -\sum_{m} t^{2}_{mm} c^{+}_{mj} c_{mj} + \sum_{mn} t_{mm} t_{nn} c^{+}_{mj} c_{nj} c^{+}_{ni} c_{mi} - \sum_{m} t^{2}_{mm} c^{+}_{mi} c_{mi}$$

$$+ \sum_{mn} t_{mm} t_{nn} c^{+}_{mi} c_{ni} c^{+}_{nj} c_{mj}$$

2.5.1 One-electron case

Now the j = 1/2 case, with m = ± 1/2 and t_{mm} = t, can be looked at specifically, and H reduces to

$$H = \text{constant} + t^{2} (c^{+}_{\uparrow j} c_{\uparrow j} c^{+}_{\uparrow i} c_{\uparrow i} + c^{+}_{\downarrow j} c_{\downarrow j} c^{+}_{\downarrow i} c_{\downarrow i}$$

$$+ c^{+}_{\uparrow j} c_{\downarrow j} c^{+}_{\downarrow i} c_{\uparrow i} + c^{+}_{\downarrow j} c_{\uparrow j} c^{+}_{\uparrow i} c_{\downarrow i})$$

Also using

$$2 S^{z}_{j} = n_{\uparrow j} - n_{\downarrow j}$$

$$n_{j} = n_{\uparrow j} + n_{\downarrow j}$$

$$n_{\uparrow j} = \tfrac{1}{2} n_{j} + S^{z}_{j}$$

$$n_{\downarrow j} = \tfrac{1}{2} n_{j} - S^{z}_{j}$$

then for the one-electron case

$$H = \text{constant} + t^{2} [(\tfrac{1}{2} + S^{z}_{j})(\tfrac{1}{2} + S^{z}_{i}) + (\tfrac{1}{2} - S^{z}_{j})(\tfrac{1}{2} - S^{z}_{i})$$

$$+ S^{+}_{j} S^{-}_{i} + S^{-}_{j} S^{+}_{i}]$$

$$= \text{constant} + 2t^{2} [S^{z}_{j} S^{z}_{i} + \tfrac{1}{2} (S^{+}_{j} S^{-}_{i} + S^{-}_{j} S^{+}_{i})]$$

$$= \text{constant} + 2t^{2} \underline{S}_{j} \cdot \underline{S}_{i}$$

which is the Heisenberg Hamiltonian, as expected.

If we consider one electron in the j = 3/2, d orbital, case we can interpret t_{mm} as follows

$$t_{1/2\,1/2} = t_{-1/2\,-1/2} = \frac{1}{5}\left(2dd\sigma + 3dd\pi\right)$$

$$t_{3/2\,3/2} = t_{-3/2\,-3/2} = \frac{1}{5}\left(dd\sigma + 4dd\delta\right)$$

The first term in the effective Hamiltonian favours occupation of the m = 3/2,-3/2 states if the hopping integrals have the canonical values

$$dd\sigma = -1 \;,\; dd\pi = \frac{2}{3} \;,\; dd\delta \simeq 0$$

giving

$$t_{1/2\,1/2} \simeq 0 \qquad t_{3/2\,3/2} \simeq -\frac{1}{5}$$

Conversely, if $dd\sigma \gg dd\pi, dd\delta$ then occupation of m = 1/2,-1/2 is favoured, and the effective Hamiltonian is

$$\frac{1}{2}UH = -\frac{1}{2}\sum_m t_{mm}^2\left(n_{mj} + n_{mi}\right) + \sum_m t_{mm}^2\, n_{mj}\, n_{mi}$$

$$+ \sum_{m\neq n} t_{mm}\, t_{nn}\, c_{mj}^{+}\, c_{nj}\, c_{ni}^{+}\, c_{mi}$$

$$= -\frac{1}{2}\sum_m t_{mm}^2\left(n_{mj} - n_{mi}\right)^2 + \sum_{m\neq n} t_{mm}\, t_{nn}\, c_{mj}^{+}\, c_{nj}\, c_{ni}^{+}\, c_{mi}$$

If we put

$$t_{1/2\,1/2} = t_{-1/2\,-1/2} = t \qquad t_{3/2\,3/2} = t_{-3/2\,-3/2} \simeq 0$$

then

$$\frac{UH}{2t^2} \simeq -\tfrac{1}{2}(n_{\frac{1}{2}j} - n_{\frac{1}{2}i})^2 - \tfrac{1}{2}(n_{-\frac{1}{2}j} - n_{-\frac{1}{2}i})^2 + c^+_{\frac{1}{2}j} c_{-\frac{1}{2}j} c^+_{-\frac{1}{2}i} c_{\frac{1}{2}i} + c^+_{-\frac{1}{2}j} c_{\frac{1}{2}j} c^+_{\frac{1}{2}i} c_{-\frac{1}{2}i}$$

The space is spanned by the states $|\frac{1}{2}i\ \frac{1}{2}j\rangle, |\frac{1}{2}i\ -\frac{1}{2}j\rangle, |-\frac{1}{2}i\ \frac{1}{2}j\rangle, |-\frac{1}{2}i, -\frac{1}{2}j\rangle$ but there are non-zero matrix elements only between the states $|\frac{1}{2}i\ -\frac{1}{2}j\rangle, |-\frac{1}{2}i\ \frac{1}{2}j\rangle$ (as in Cooper (1982)):

$$\det |\ (UH/2t^2) - \lambda 1\ | = \begin{vmatrix} -1-\lambda & 1 \\ 1 & -1-\lambda \end{vmatrix} = 0$$

$$\lambda = 0, -2$$

where -2 is therefore the ground state. The corresponding wave-function is

$$|\psi\rangle = \frac{1}{\sqrt{2}}\left(|\tfrac{1}{2}i\ -\tfrac{1}{2}j\rangle - |-\tfrac{1}{2}i\ \tfrac{1}{2}j\rangle\right)$$

with the following values for matrix elements

$$\langle\psi|\, J_i^z\, |\psi\rangle = \langle\psi|\, J_j^z\, |\psi\rangle = 0$$

$$\langle\psi|\, \underline{J}_i \cdot \underline{J}_j\, |\psi\rangle = \langle\psi|\, J_i^z J_j^z + \tfrac{1}{2}(J_i^+ J_j^- + J_i^- J_j^+)\, |\psi\rangle$$

$$\langle\psi|\, J_i^z J_j^z\, |\psi\rangle = \frac{1}{2}\left[\langle\tfrac{1}{2}i\ -\tfrac{1}{2}j|\, J_i^z J_j^z\, |\tfrac{1}{2}i\ -\tfrac{1}{2}j\rangle + \langle-\tfrac{1}{2}i\ \tfrac{1}{2}j|\, J_i^z J_j^z\, |-\tfrac{1}{2}i\ \tfrac{1}{2}j\rangle\right]$$

$$= -\frac{1}{4}$$

Then using the operators

$$J_i^+ = \sum_n \sqrt{(J(J+1) - n(n+1))}\, c^+_{n+1\,i}\, c_{ni}$$

$$= \sqrt{3}\, c^+_{-\frac{1}{2}i}\, c_{-\frac{3}{2}i} + 2\, c^+_{\frac{1}{2}i}\, c_{-\frac{1}{2}i} + \sqrt{3}\, c^+_{\frac{3}{2}i}\, c_{\frac{1}{2}i}$$

$$\tau_j^- = \sqrt{3}\, c^+_{-3/2\,j}\, c_{-1/2\,j} + 2\, c^+_{-1/2\,j}\, c_{1/2\,j} + \sqrt{3}\, c^+_{1/2\,j}\, c_{3/2\,j}$$

hence

$$\langle 4 | \tau_i^+ \tau_j^- | 4 \rangle = \langle 4 | \left[\tau_i^+ \tau_j^-, \tfrac{1}{\sqrt{2}} \left(c^+_{1/2\,i}\, c_{-1/2\,j} - c^+_{-1/2\,i}\, c_{1/2\,j} \right) \right] | 0 \rangle$$

$$= 4 \langle 4 | c^+_{1/2\,i}\, c_{-1/2\,i}\, c^+_{-1/2\,j}\, c_{1/2\,j} | 4 \rangle$$

and also, similarly,

$$\langle 4 | \tau_i^- \tau_j^+ | 4 \rangle = 4 \langle 4 | c^+_{-1/2\,i}\, c_{1/2\,i}\, c^+_{1/2\,j}\, c_{-1/2\,j} | 4 \rangle$$

Then, expressing $|4\rangle$ in terms of $|0\rangle$:

$$\langle 4 | \tau_i^+ \tau_j^- | 4 \rangle = 2 \langle 0 | \left(c_{-1/2\,j}\, c_{1/2\,i} - c_{1/2\,j}\, c_{-1/2\,i} \right) c^+_{1/2\,i}\, c_{-1/2\,i}\, c^+_{-1/2\,j}\, c_{1/2\,j}$$

$$\left(c^+_{1/2\,i}\, c^+_{-1/2\,j} - c^+_{-1/2\,i}\, c^+_{1/2\,j} \right) | 0 \rangle$$

$$= 2 \langle 0 | c_{-1/2\,j}\, c_{-1/2\,i}\, c^+_{-1/2\,j}\, c^+_{-1/2\,i} | 0 \rangle$$

$$= -2 \langle 0 | c_{1/2\,j}\, c^+_{-1/2\,j}\, c_{-1/2\,i}\, c^+_{-1/2\,i} | 0 \rangle$$

$$= -2$$

and similarly

$$\langle 4 | \tau_i^- \tau_j^+ | 4 \rangle = -2$$

$$\langle 4 | \underline{\tau}_i \cdot \underline{\tau}_j | 4 \rangle = -\frac{9}{4}$$

Clearly, the consequence of $\langle \underline{J}_i \cdot \underline{J}_j \rangle < 0$ is that the ground state is a superposition of the states with angular momentum perpendicular to the quantization axis

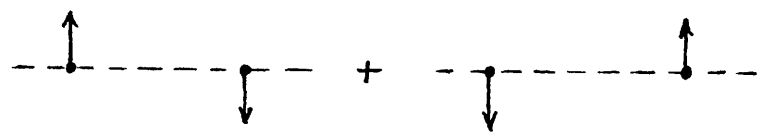

with no $j_z = 3/2$ components (which are along the axis).

If, conversely, we now consider

$$t_{1/2\,1/2} = t_{-1/2\,-1/2} = 0$$

$$t_{3/2\,3/2} = t_{-3/2\,-3/2} = t$$

then

$$\frac{UH}{2t^2} = -\frac{1}{2}(n_{3/2\,j} - n_{3/2\,i})^2 - \frac{1}{2}(n_{-3/2\,j} - n_{-3/2\,i})^2 + c^+_{3/2\,j} c_{-3/2\,j} c^+_{-3/2\,i} c_{3/2\,i} + c^+_{-3/2\,j} c_{3/2\,j} c^+_{3/2\,i} c_{-3/2\,i}$$

so that the wavefunction in this case

$$|\psi\rangle = \frac{1}{\sqrt{2}} \left(|3/2\,i\ -3/2\,j\rangle - |-3/2\,i\ 3/2\,j\rangle \right)$$

Also

$$\langle \psi | J_i^z | \psi \rangle = \langle \psi | J_j^z | \psi \rangle = 0$$

$$\langle \psi | \underline{J}_i \cdot \underline{J}_j | \psi \rangle = \langle \psi | J_i^z J_j^z | \psi \rangle = -\frac{9}{4}$$

with no contribution from $J_i^+ J_j^-, J_i^- J_j^+$. This ground state is a superposition of the states

with only $j_z = 3/2$ components.

2.5.2 Two-electron case

The change in the interaction energy that occurs on going from a ground state of two electrons on each of two atoms to that of one electron on one and three on another is U. The effective Hamiltonian is

$$\frac{UH}{2} = -\frac{1}{2}\sum_m t_{mm}^2 (n_{mj} - n_{mi})^2 + \sum_{m\neq n} t_{mm} t_{nn} c_{mj}^+ c_{nj} c_{ni}^+ c_{mi}$$

In the two limits $t_{\frac{1}{2}\frac{1}{2}} = 0$ or $t_{\frac{3}{2}\frac{3}{2}} = 0$ this two-electron problem has a simple form closely related to the one-electron situation. One electron occupies a m = 3/2 or -3/2 state ($t_{\frac{3}{2}\frac{3}{2}} = 0$) or m = 1/2 or -1/2 state ($t_{\frac{1}{2}\frac{1}{2}} = 0$) passively, whilst the remaining electron behaves as for the case above. A more general solution can be found by taking $t_{3/2\,3/2} \gg t_{1/2\,1/2}$ or $t_{3/2\,3/2} \ll t_{1/2\,1/2}$.

Considering two atoms each with two electrons the total $J^z = J_1^z + J_2^z$ is a constant of the motion; if we look only at the $J^z = 0$ states there are eight, namely if m,n refer to site i and m',n' site j,

$$\phi_1(m,n;m',n') = (3/2, 1/2; -3/2, -1/2)$$

$$\phi_2 = (3/2\ -1/2\ ;\ -3/2\ ,\ 1/2\ )$$

$$\phi_3 = (-3/2\ ,\ 1/2\ ;\ 3/2\ ,\ -1/2\ )$$

$$\phi_4 = (-3/2\ ,\ -1/2\ ;\ 3/2\ ,\ 1/2\ )$$

$$\phi_5 = (1/2, -1/2; 1/2, -1/2)$$

$$\phi_6 = (1/2, -1/2; 3/2, -3/2)$$

$$\phi_7 = (3/2, -3/2; 1/2, -1/2)$$

$$\phi_8 = (3/2, -3/2; 3/2, -3/2)$$

So that in this basis, writing $t_1 = t_{\frac{1}{2}\frac{1}{2}}$, $t_3 = t_{\frac{3}{2}\frac{3}{2}}$, the effective Hamiltonian is

$$H = \left[\begin{array}{cccc|cccc}
(-t_1^2-t_3^2) & t_1^2 & t_3^2 & 0 & 0 & -t_1t_3 & -t_1t_3 & 0 \\
t_1^2 & (-t_1^2-t_3^2) & 0 & t_3^2 & 0 & t_1t_3 & t_1t_3 & 0 \\
t_3^2 & 0 & (-t_1^2-t_3^2) & t_1^2 & 0 & t_1t_3 & t_1t_3 & 0 \\
0 & t_3^2 & t_1^2 & (-t_1^2-t_3^2) & 0 & -t_1t_3 & -t_1t_3 & 0 \\
\hline
0 & 0 & 0 & 0 & 0 & 0 & 0 & 0 \\
-t_1t_3 & t_1t_3 & t_1t_3 & -t_1t_3 & 0 & (-t_1^2-t_3^2) & 0 & 0 \\
-t_1t_3 & t_1t_3 & t_1t_3 & -t_1t_3 & 0 & 0 & (-t_1^2-t_3^2) & 0 \\
0 & 0 & 0 & 0 & 0 & 0 & 0 & 0
\end{array}\right]$$

The signs of the functions ϕ_i resulting from different states are as follows, excluding the rows and columns of zeros:

$\phi_1 = (1/2, 3/2; -3/2, -1/2)$ $\phi_2 = (1/2, 3/2; -3/2, 1/2)$ $\phi_3 = (-3/2, 1/2; -1/2, 3/2)$ $\phi_4 = (-3/2, -1/2; 1/2, 3/2)$ $\phi_6 = (-\frac{1}{2}, \frac{1}{2}; -\frac{3}{2}, \frac{3}{2})$ $\phi_7 = (-\frac{3}{2}, \frac{3}{2}; -\frac{1}{2}, \frac{1}{2})$

$-\phi_7 = (-3/2, 3/2; 1/2, -1/2)$	ϕ_7	ϕ_6	$-\phi_6$	ϕ_3	ϕ_2
$\phi_2 = (-1/2, 3/2; -3/2, 1/2)$	ϕ_1	ϕ_1	ϕ_2	$-\phi_1$	$-\phi_1$
$\phi_3 = (1/2, -3/2; 3/2, -1/2)$	ϕ_4	ϕ_4	ϕ_3	$-\phi_4$	$-\phi_4$
$-\phi_6 = (1/2, -1/2; -3/2, 3/2)$	ϕ_6	ϕ_7	$-\phi_7$	ϕ_2	ϕ_3

and neglecting ϕ_5 and ϕ_8 (which are states with zero energy and do not mix with the other states) we can write H as

$$(\underline{\underline{H}} - \lambda \underline{\underline{1}}) \begin{pmatrix} \underline{x} \\ \underline{y} \end{pmatrix} = \underline{0}$$

$$\underline{\underline{H}} = \begin{pmatrix} \underline{\underline{A}} & \underline{\underline{B}}^T \\ \underline{\underline{B}} & \underline{\underline{C}} \end{pmatrix}$$

$$\underline{\underline{A}}\,\underline{x} + \underline{\underline{B}}^T \underline{y} = \lambda \underline{x}$$

$$\underline{\underline{B}}\,\underline{x} + \underline{\underline{C}}\,\underline{y} = \lambda \underline{y}$$

$$\underline{\underline{A}}\,\underline{x} - \underline{\underline{B}}^T (\underline{\underline{C}} - \lambda \underline{\underline{1}})^{-1} \underline{\underline{B}}\,\underline{x} = \lambda \underline{x}$$

Therefore the problem has become

$$\bar{\underline{\underline{A}}}\,\underline{x} = \lambda \underline{x}$$

$$\bar{\underline{\underline{A}}} = \underline{\underline{A}} - \underline{\underline{B}}^T (\underline{\underline{C}} - \lambda \underline{\underline{1}})^{-1} \underline{\underline{B}}$$

and $\bar{\underline{\underline{A}}}$ can be found approximately by using $t_3 << t_1$ and the one-electron solution to get $\lambda \simeq -2t_1^2$, and then

$$(\underline{\underline{C}} - \lambda \underline{\underline{1}})^{-1} \simeq \underline{\underline{1}} / t_1^2$$

$$\bar{\underline{\underline{A}}} \simeq \underline{\underline{A}} - \underline{\underline{B}}^T \underline{\underline{B}} / t_1^2$$

$$\simeq \begin{pmatrix} -t_1^2 - t_3^2 & t_1^2 + 2t_3^2 & 3t_3^2 & -2t_3^2 \\ t_1^2 + 2t_3^2 & -t_1^2 - 3t_3^2 & -2t_3^2 & 3t_3^2 \\ 3t_3^2 & -2t_3^2 & -t_1^2 - 3t_3^2 & t_1^2 + 2t_3^2 \\ -2t_3^2 & 3t_3^2 & t_1^2 + 2t_3^2 & -t_1^2 - 3t_3^2 \end{pmatrix}$$

Using the approximation $\lambda = -2t_1^2$ and neglecting t_3, the eigenvector $\underline{e}$ is

$$(\bar{\underline{\underline{A}}} - \lambda \underline{\underline{1}})\,\underline{e} = \begin{pmatrix} t_1^2 & t_1^2 & 0 & 0 \\ t_1^2 & t_1^2 & 0 & 0 \\ 0 & 0 & t_1^2 & t_1^2 \\ 0 & 0 & t_1^2 & t_1^2 \end{pmatrix} \begin{pmatrix} a \\ -a \\ b \\ -b \end{pmatrix} = \underline{0}$$

$$a = b \qquad \underline{e} = (1, -1, 1, -1)$$

If t_3 terms are now included the eigenvalue of H is $\lambda = -2t_1^2 - 10t_3^2$:

$$(\underline{\underline{A}} - \lambda \underline{\underline{1}})\underline{e} = \begin{pmatrix} t_1^2+7t_3^2 & t_1^2+2t_3^2 & 3t_3^2 & -2t_3^2 \\ t_1^2+2t_3^2 & t_1^2+7t_3^2 & -2t_3^2 & 3t_3^2 \\ 3t_3^2 & -2t_3^2 & t_1^2+7t_3^2 & t_1^2+2t_3^2 \\ -2t_3^2 & 3t_3^2 & t_1^2+2t_3^2 & t_1^2+7t_3^2 \end{pmatrix} \begin{pmatrix} a \\ -a \\ b \\ -b \end{pmatrix}$$

$$= \underline{0} \qquad a = b$$

$$\underline{e} = (1, -1, 1, -1)$$

and so the ground state is approximately

$$|\psi\rangle = \tfrac{1}{2}(\phi_1 - \phi_2 - \phi_3 + \phi_4)$$

This can be rewritten as

$$|\psi\rangle = \tfrac{1}{2}\left(c^+_{1/2i}\, c^+_{3/2i}\, c^+_{-3/2j}\, c^+_{-1/2j} - c^+_{-1/2i}\, c^+_{3/2i}\, c^+_{-3/2j}\, c^+_{1/2j} \right.$$

$$\left. - c^+_{-3/2i}\, c^+_{1/2i}\, c^+_{-1/2j}\, c^+_{3/2j} + c^+_{-3/2i}\, c^+_{-1/2i}\, c^+_{1/2j}\, c^+_{3/2j} \right) |0\rangle$$

$$= \tfrac{1}{2}\left(c^+_{3/2i}\, c^+_{-3/2j} - c^+_{-3/2i}\, c^+_{3/2j}\right)\left(c^+_{1/2i}\, c^+_{-1/2j} - c^+_{-1/2i}\, c^+_{1/2j}\right)|0\rangle$$

Clearly then

$$\langle\psi|\, \gamma_i^2\, |\psi\rangle = 0$$

Alternatively, if the case where $t_1 \ll t_3$ is considered, then

$$(\underline{\underline{c}} - \lambda \underline{\underline{1}})^{-1} \simeq \underline{\underline{1}} / t_3^2$$

with $\lambda \simeq -2t_3^2$. Then

$$\bar{\underline{A}} = \underline{A} - \underline{B}^T \underline{B} / t_3^2$$

$$= \begin{pmatrix} -3t_1^2 - t_3^2 & 3t_1^2 & t_3^2 + 2t_1^2 & -2t_1^2 \\ 3t_1^2 & -3t_1^2 - t_3^2 & -2t_1^2 & t_3^2 + 2t_1^2 \\ t_3^2 + 2t_1^2 & -2t_1^2 & -3t_1^2 - t_3^2 & 3t_1^2 \\ -2t_1^2 & t_3^2 + 2t_1^2 & 3t_1^2 & -3t_1^2 - t_3^2 \end{pmatrix}$$

provided the states are ordered $\phi_1, \phi_3, \phi_2, \phi_4$. The ground state is then

$$\lambda = -2t_3^2 - 10t_1^2$$

$$|4\rangle = \tfrac{1}{2}(\phi_1 - \phi_2 - \phi_3 + \phi_4)$$

as for the $t_3 \ll t_1$ case. This wave-function has the properties that one pair of electrons couples antiferromagnetically along the axis, whilst the other pair couples antiferromagnetically transversely. In both limiting cases $t_1 \ll t_3$, $t_1 \gg t_3$ the ground state is

$$|4\rangle = \tfrac{1}{2}(c^+_{1/2i} c^+_{-1/2j} - c^+_{-1/2i} c^+_{1/2j})(c^+_{3/2i} c^+_{-3/2j} - c^+_{-3/2i} c^+_{3/2j})|0\rangle$$

Although this high U limit gives antiferromagnetic ordering it is possible that at lower U band overlap effects, included in a more realistic theory, would give ferromagnetic ordering.

However, the principal feature of the ground state derived above is that it has strong bonding between atoms in sheets, and weak bonding between those sheets. The magnetic moments are therefore aligned along < 001 > . Physically the anisotropy, with weakest coupling along the magnetic axis and strongest in the

transverse plane, occurs because the coupling comes from orbital states which pile up charge along the bonding axis while the orbital moment is maximized for states where the charge is piled up in the plane transverse to the moment.

The nature of the anisotropy can be seen more clearly by relating the effective Hamiltonian above to the Coqblin-Schrieffer Hamiltonian (Coqblin & Schrieffer (1969)) and the work of Cooper at al. (Siemann & Cooper (1980), Yang & Cooper (1982), Cooper et al. (1983), Thayamballi & Cooper (1984)). The Coqblin-Schrieffer theory treats the interaction of an f^1 ion with band electrons, using the Anderson Hamiltonian

$$H = H_0 + H_1$$

$$H_0 = \sum_{m\underline{k}} E_{\underline{k}}\, n_{m\underline{k}} + E_0 \sum_m n_m + \frac{U}{2} \sum_{m m'} n_m n_{m'}$$

$$H_1 = \sum_{m\underline{k}} \left(V_{\underline{k}}\, c^+_{m\underline{k}}\, c_m + V^*_{\underline{k}}\, c^+_m\, c_{m\underline{k}} \right)$$

and includes single electron band energies, the configuration energy (without correlation) of the f^1 ion, a Coulomb energy accounting for correlation, and a hybridization energy H_1 regarding the mixing of f and band electrons. Provided $H_1 \ll H_0$ the Schrieffer-Wolf transformation replaces the hybridization interaction by an effective localized electron-band resonant exchange scattering. Taking the scattering as significant only over energies below the f-electron energy and above the Fermi energy, a Hamiltonian H_{fb} giving exchange scattering between the band electrons and a single ion can be derived, of the form

$$H_{fb} = -J \sum_{\underline{k}\underline{k}'} \sum_{mm'} c^{+}_{m'\underline{k}'} c_{m\underline{k}} \left(c^{+}_{m} c_{m'} - \frac{\delta_{mm'}}{(2j+1)} \sum_{m''} n_{m''} \right)$$

Coqblin & Schrieffer (1969) then obtain the two-ion interaction by transforming the band electron states to plane waves, treating two f^1 ions in a sea of band electrons to second order. The resulting interaction is of the RKKY type and is

$$H_{12}(R) = \sum_{mm'} \left\{ E_{12}^{mm'}(R) \left(c^{+1}_{m'} c^{1}_{m} - \frac{\delta_{mm'}}{(2j+1)} \sum_{m''} n^{1}_{m''} \right) \left(c^{+2}_{m} c^{2}_{m'} - \frac{\delta_{mm'}}{(2j+1)} \sum_{m''} n^{2}_{m''} \right) \right\}$$

We shall now show how this Hamiltonian relates to the effective Hamiltonian adopted above; rearranging gives

$$H_{12}(R) = \sum_{m \neq m'} E_{12}^{mm'}(R)\, c^{+1}_{m'} c^{1}_{m} c^{+2}_{m} c^{2}_{m'} + \sum_{m} E_{12}^{mm'}(R) \left(n^{1}_{m} - \frac{n}{(2j+1)} \right) \left(n^{2}_{m} - \frac{n}{(2j+1)} \right)$$

$$= \sum_{m \neq m'} E_{12}^{mm'}(R)\, c^{+1}_{m'} c^{1}_{m} c^{+2}_{m} c^{2}_{m'} + \sum_{m} E_{12}^{mm}(R)\, n^{1}_{m} n^{2}_{m} - \frac{n}{(2j+1)} \sum_{m} E_{12}^{mm}(R) \left(n^{1}_{m} + n^{2}_{m} \right)$$

and this is the effective Hamiltonian of our formalism with

$$E_{12}^{mm'}(R) = t_{mm} t_{m'm'}$$

except for the factor n/(2j+1) instead of 1/2 in the last term, which would agree for a half-filled band, and a constant.

Considering m,m' = ± 1/2 only, as in much of Cooper's work,

this requires $E_{mm'} = t^2_{\frac{1}{2}\frac{1}{2}}$ with a similar lack of dependence on m,m'. In the ground state we have shown that only the m = ± 1/2 states are occupied, and as

$$\sum_{m=-1/2}^{1/2} (n^1_m + n^2_m) = 2n$$

the last term is a constant. It is therefore clear that the physical properties of the exchange interaction that we have considered should be very similar to the Coqblin-Schrieffer case for f^n considered by Cooper.

However, from the analysis above of the one- and two-electron cases the superexchange is antiferromagnetic, whereas Cooper has ferromagnetic ordering; our interaction has similar anisotropy, but has opposite sign.

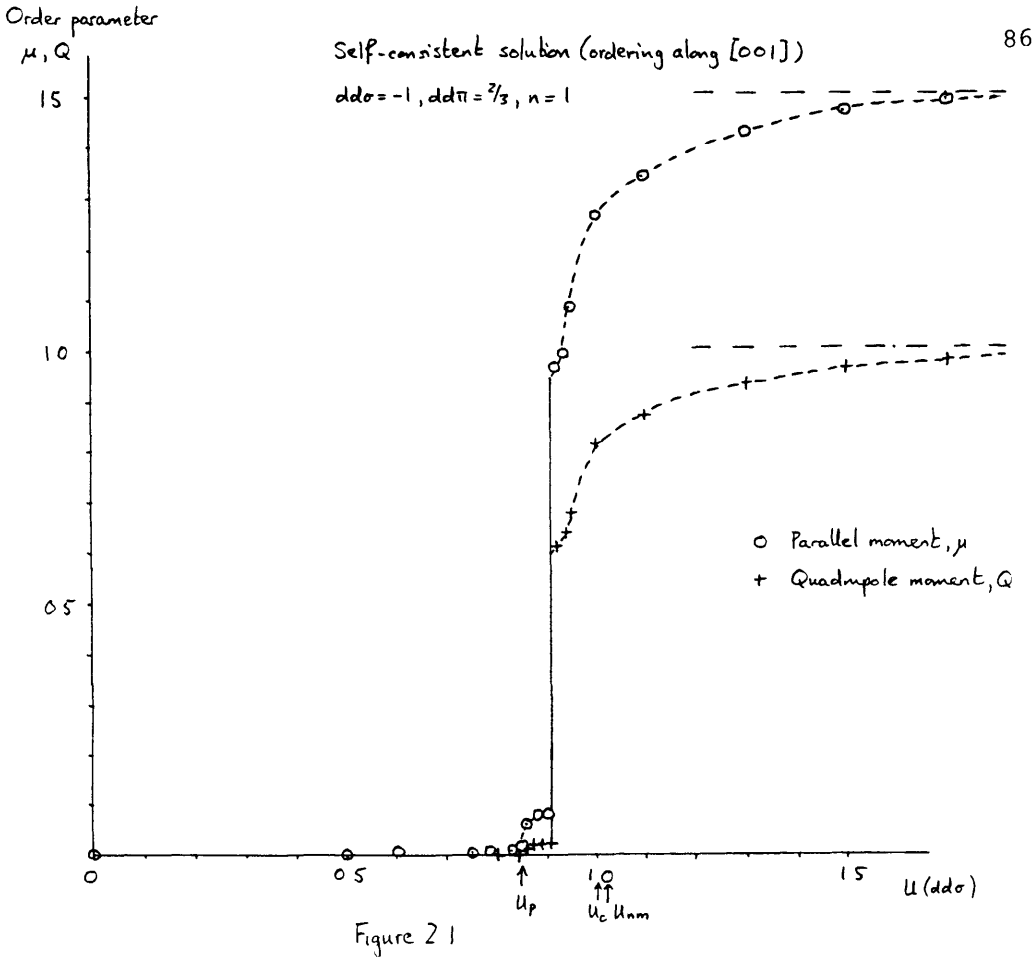

Figure 2 1

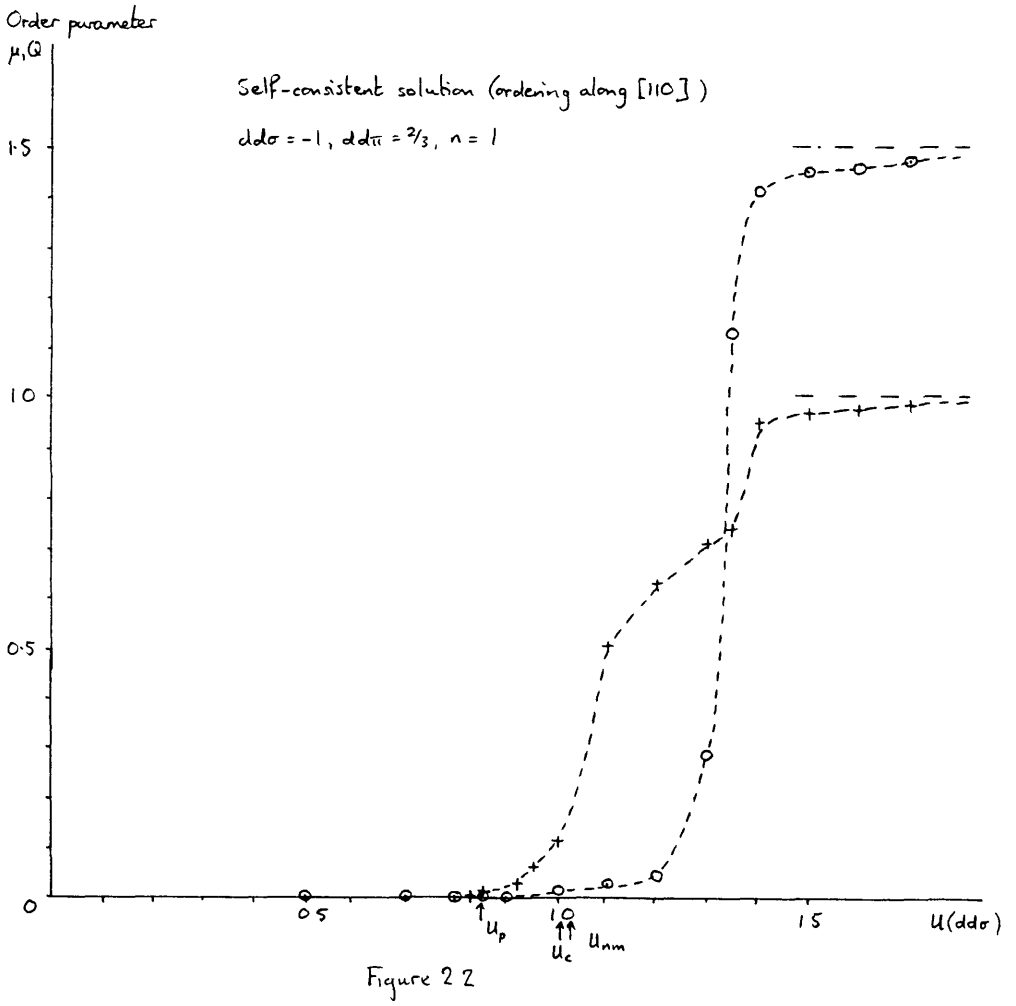

Figure 2 2

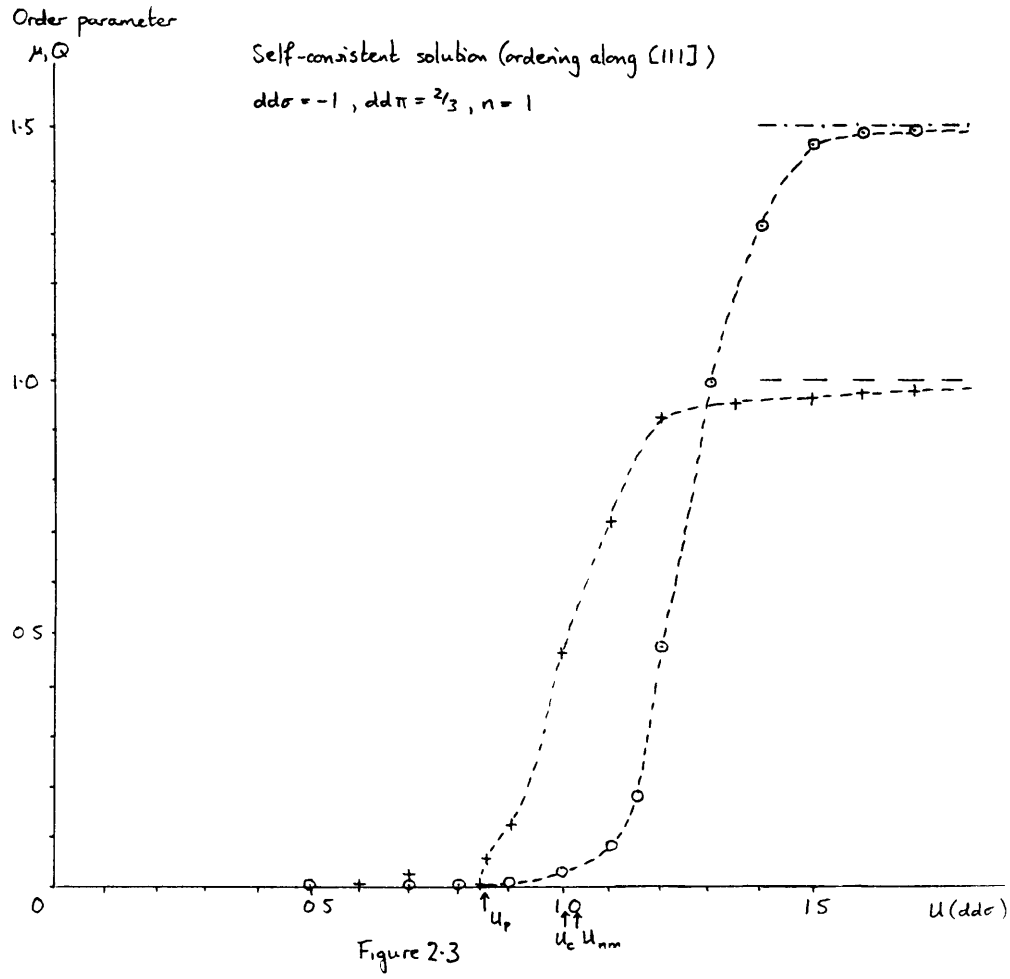

Figure 2·3

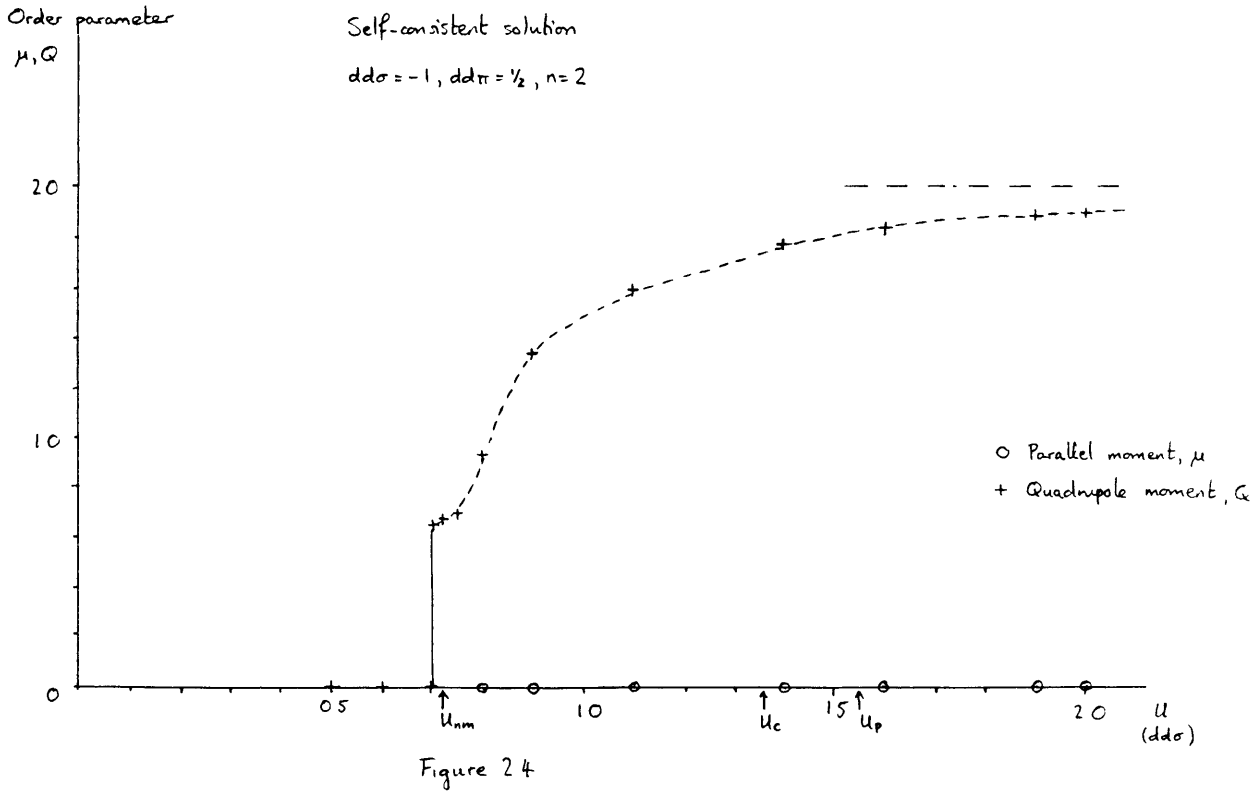

Figure 2·4

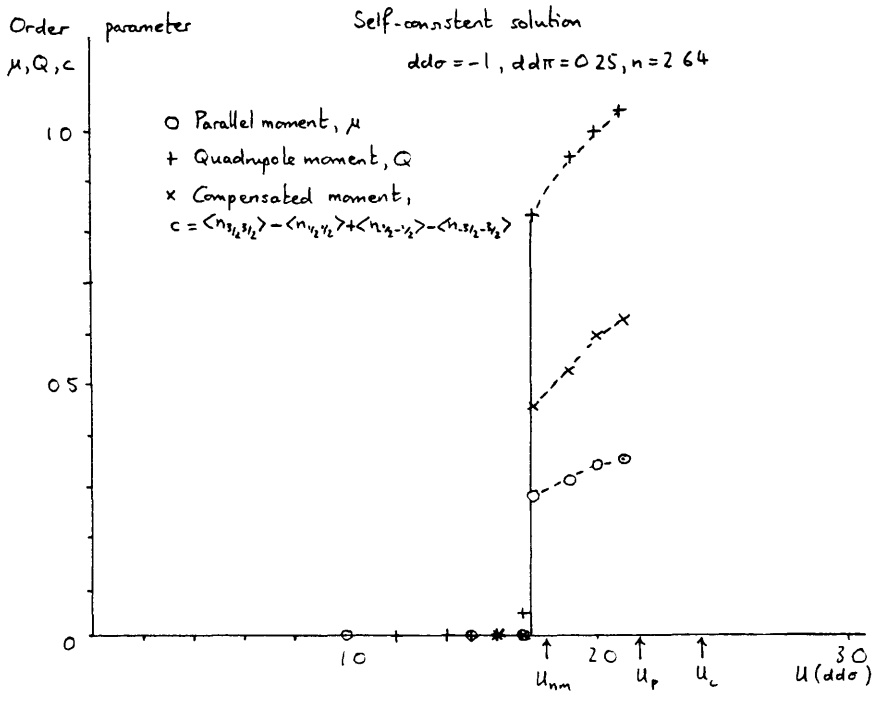

Figure 2.5

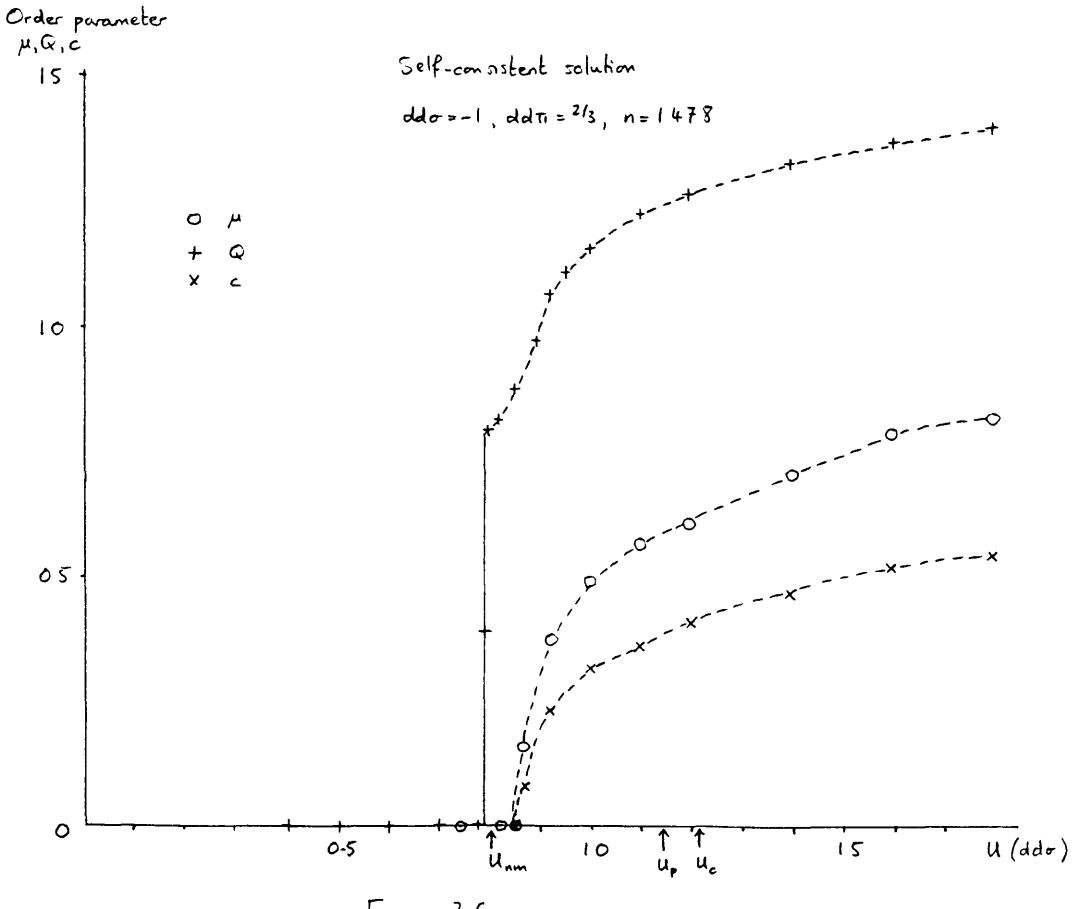

Figure 2.6

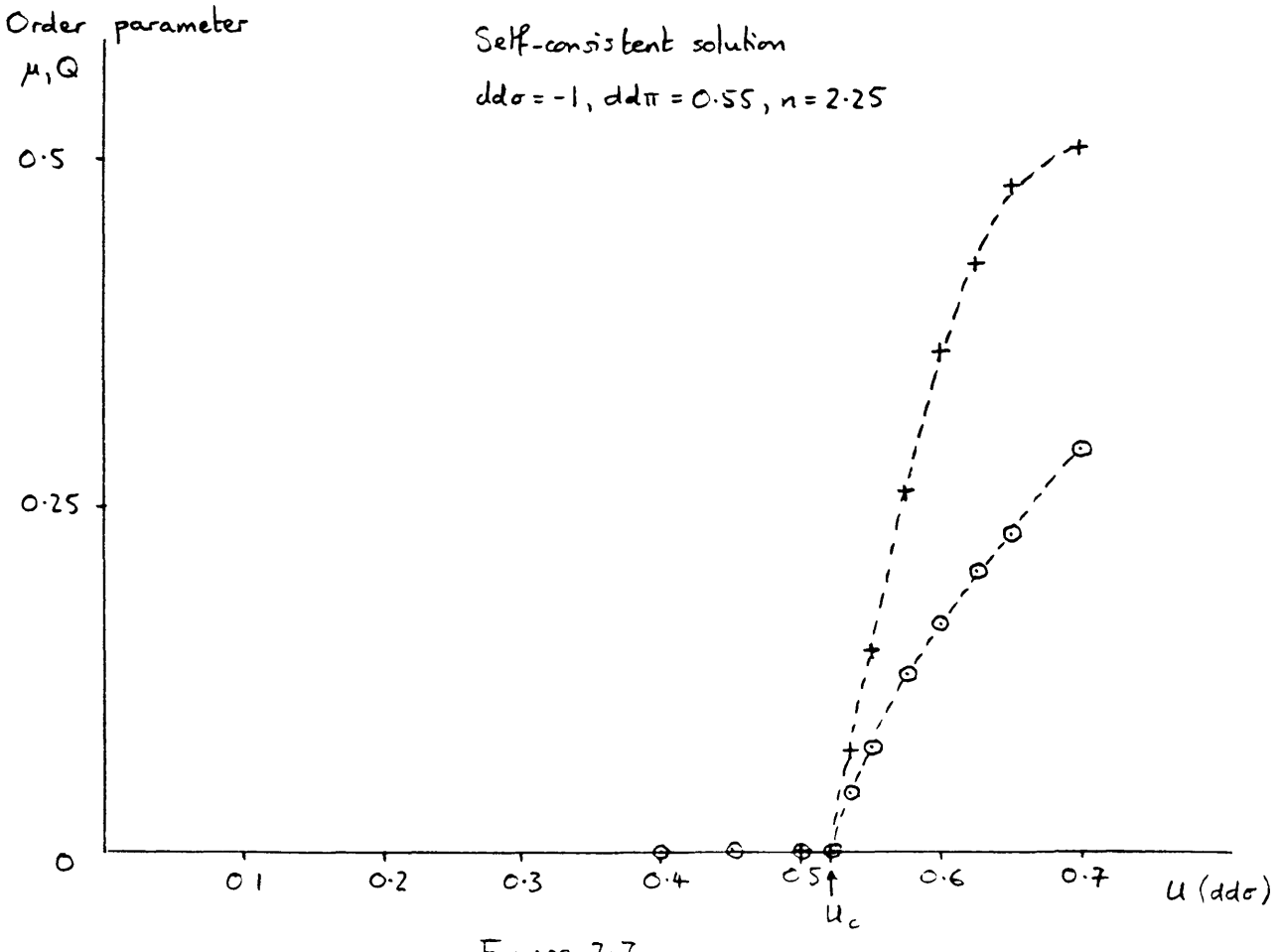
Order parameter
μ, Q
Self-consistent solution
ddσ = -1, ddπ = 0·55, n = 2·25
0·5
0·25
0
0·1
0·2
0·3
0·4
0·5
0·6
0·7
U (ddσ)
Uc

Figure 2·7

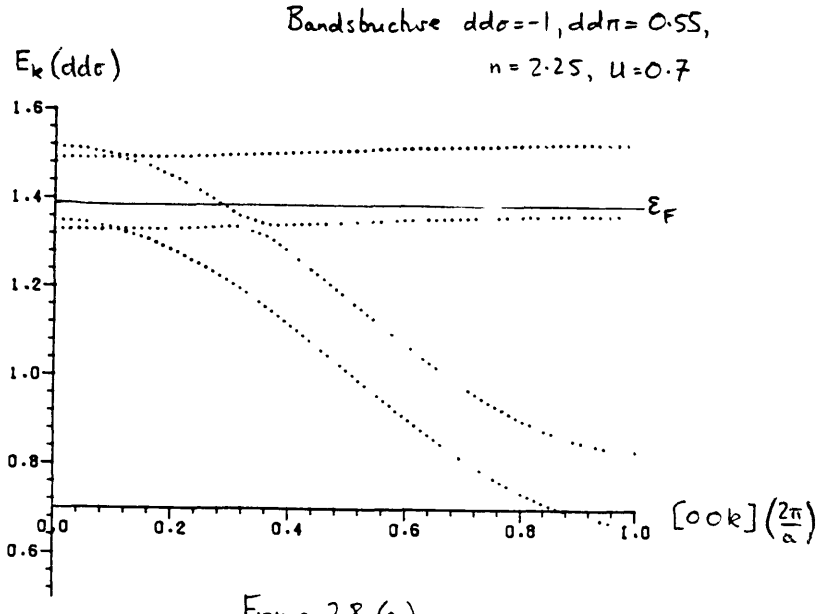

Figure 2.8 (a)

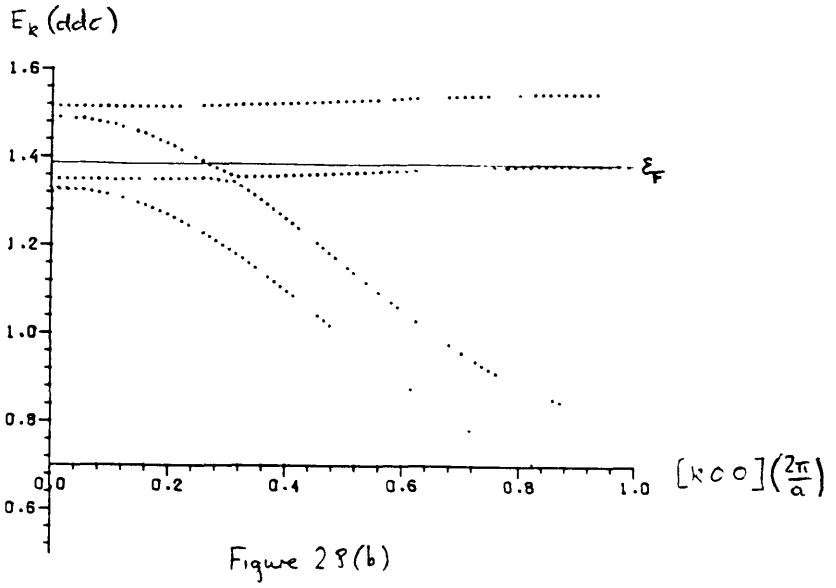

Figure 2.8 (b)

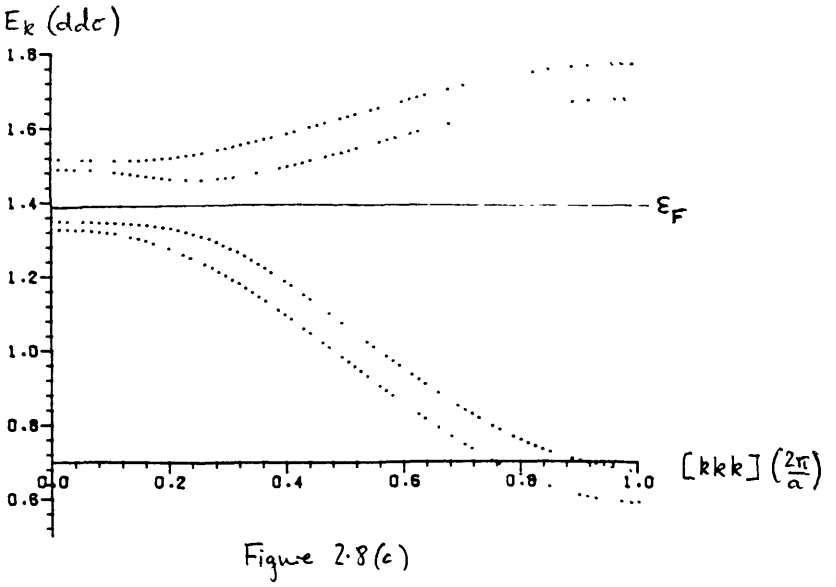

Figure 2.8 (c)

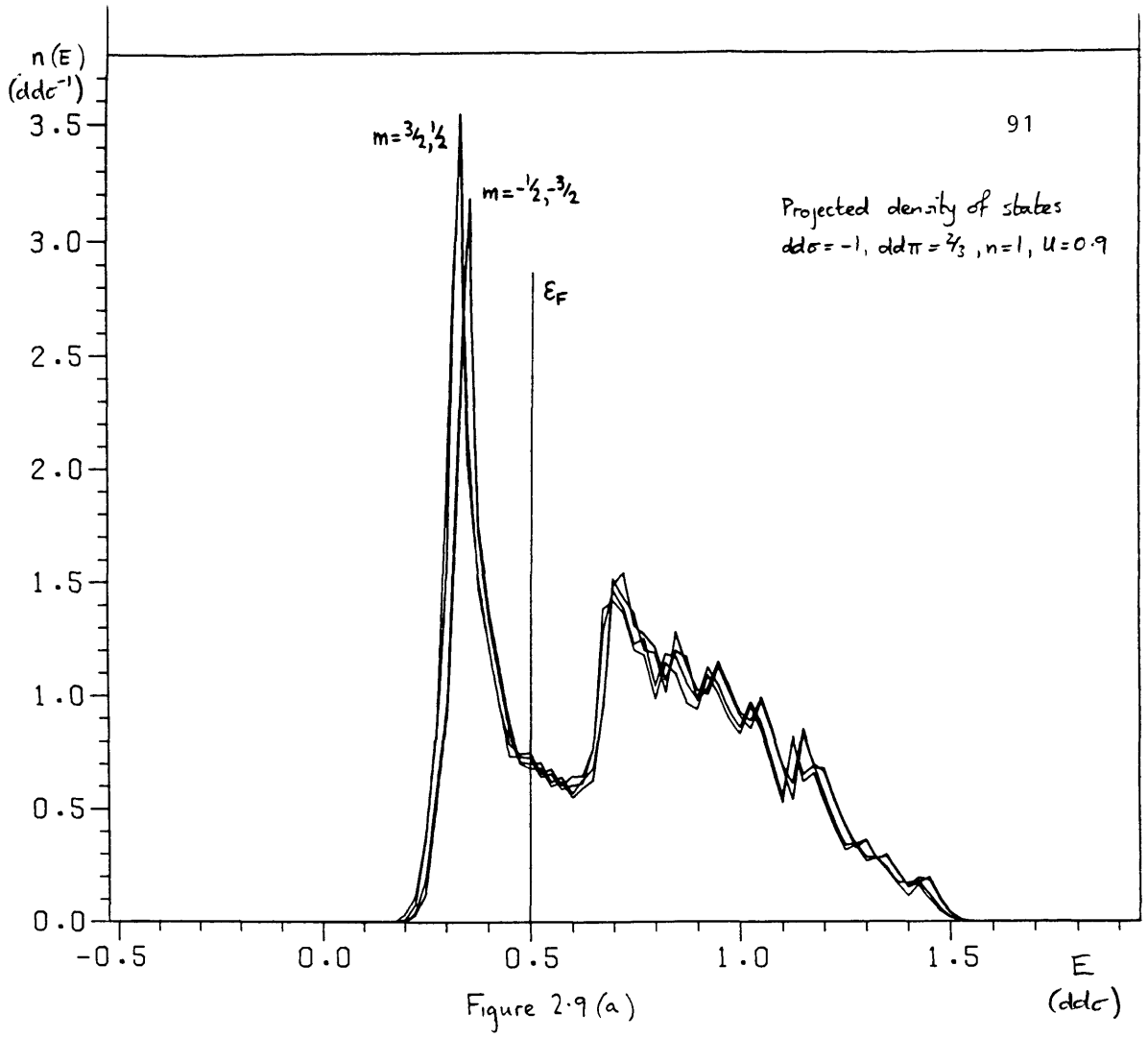

Figure 2·9 (a)

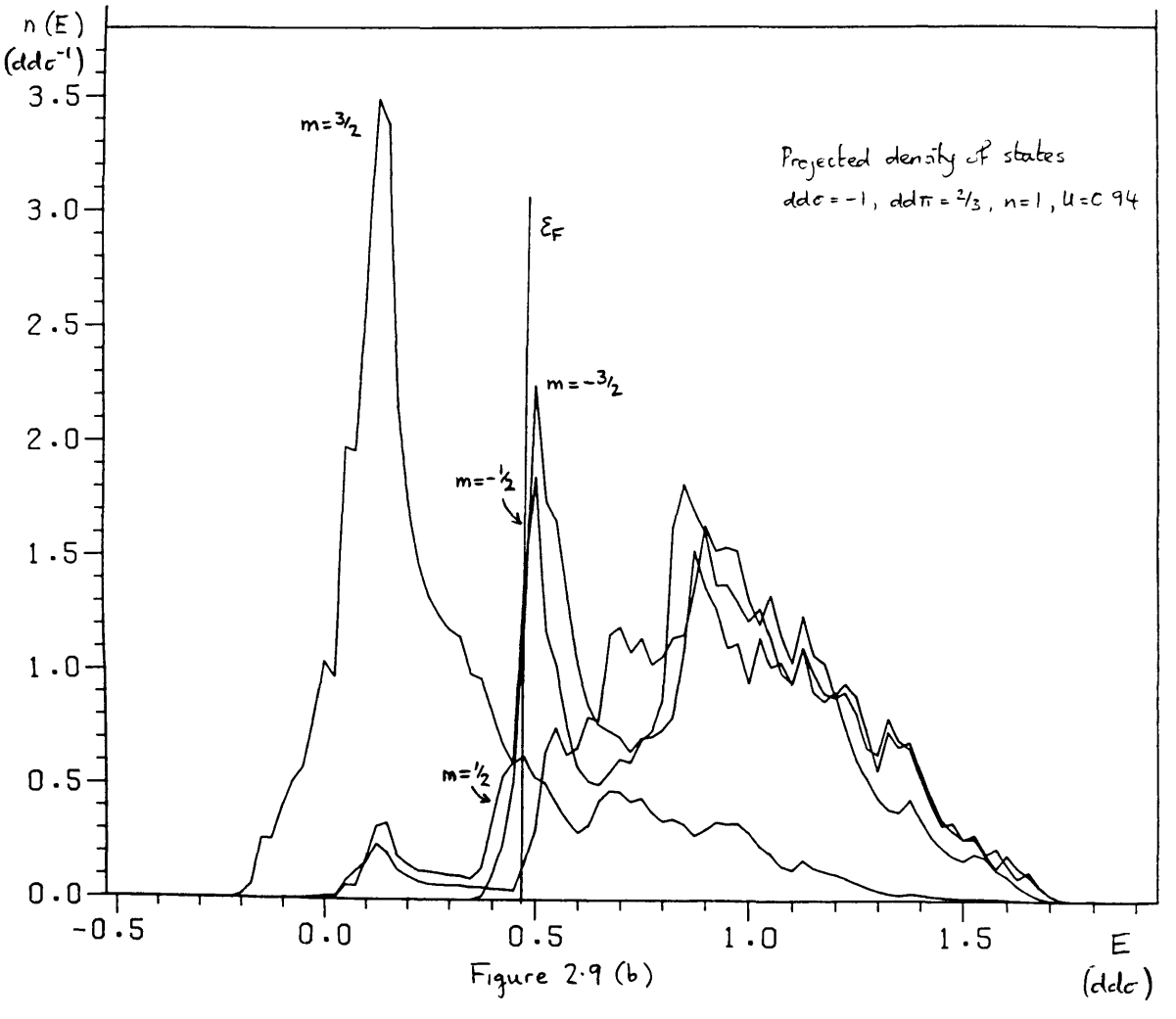

Figure 2·9 (b)

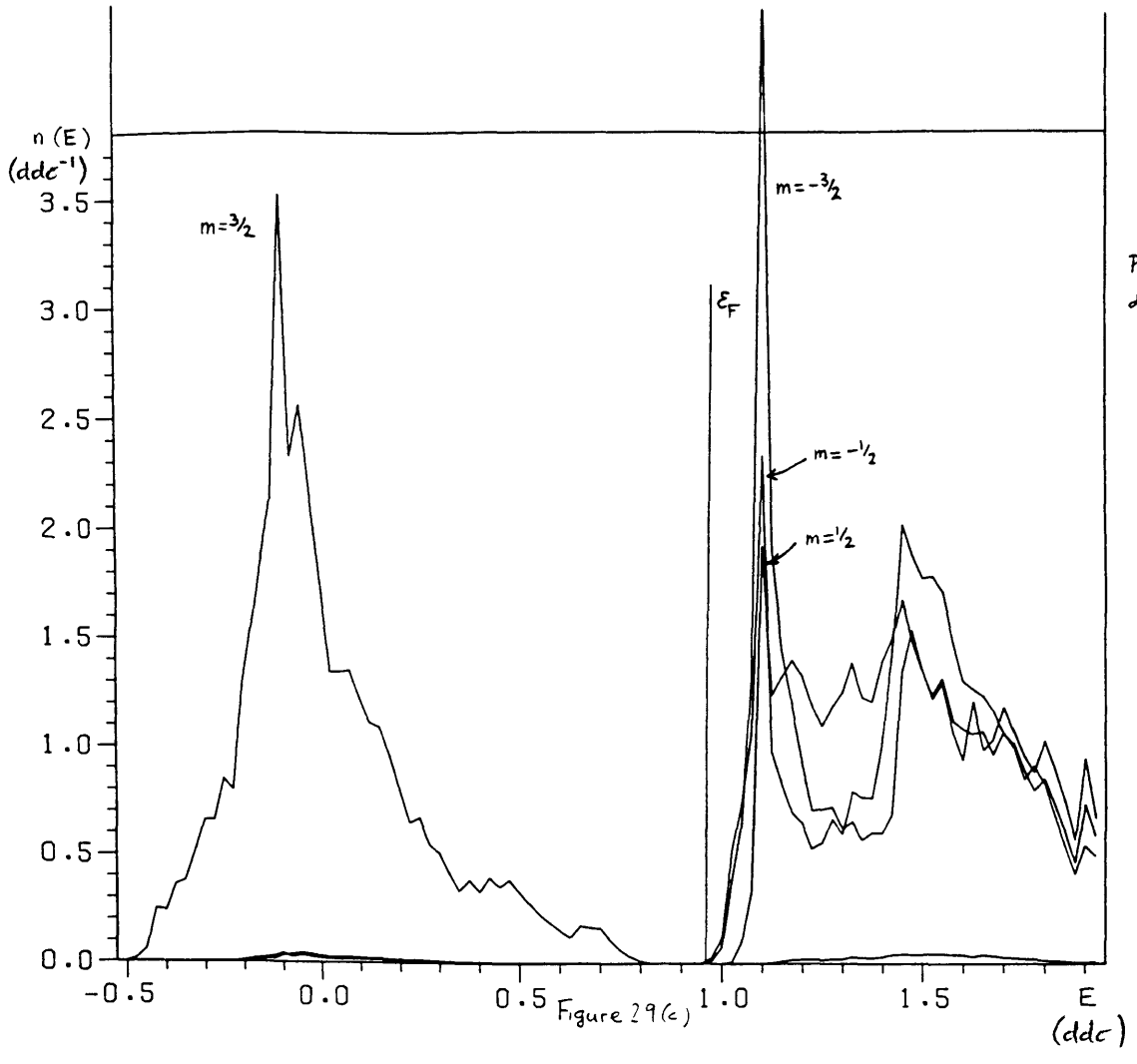

Figure 29(c)

Projected density of states
$dd\sigma = -1$, $dd\pi = 2/3$, $n = 1$, $U = 15$

CHAPTER 3

Anisotropy of the critical scattering and the damping of excitations in the ferromagnetic state

3.1 Introduction

The previous chapter examined the types of ordering which occur as self-consistent HF solutions of our model, and completed the study of the ground state. We now turn to the dynamic properties of the model, and consider numerical solutions for the RPA susceptibility $\chi^{\alpha\beta}(q,\omega)$ in various cases. An outstanding feature of $\mathrm{Im}\,\chi^{\alpha\beta}(q,\omega+i\eta)$, which describes the magnetic scattering, is the high degree of anisotropy, arising similarly to the anisotropic static properties of the model. Experimental neutron scattering work on actinide compounds (Buyers and Holden (1984)) shows a very similar anisotropy.

3.2 Anisotropic critical scattering

The spin correlations in several uranium compounds have been measured near the Néel temperature using neutron scattering techniques. In UN, USb and UAs in particular this critical scattering at low energy displays a marked anisotropy, which can be interpreted in terms of strong correlations within {001} sheets, and weak correlations between sheets.

Uranium nitride (see Table 1.1) has a rock-salt structure and orders with the Type-1 antiferromagnetic structure with the spins along the cube-edge direction. It has the lowest Néel temperature (T_N = 49.5 ± 0.5 K), lowest ordered moment (0.75 μ_B) and lowest U-U distance (3.45 Å) of the pnictides. Uranium arsenide

below 64 K ($0.5T_N$) has a Type-1A antiferromagnetic structure, and between $0.5T_N$ and T_N a Type-1 structure (Buyers et al. (1985)).

Measurements of the critical scattering of UN and UAs in the paramagnetic regime ($T > T_N$) at low energy have revealed it to be longitudinal (Holden et al. (1982a,b), Sinha et al. (1981), Buyers et al. (1985)), so that the fluctuations are parallel to the incipient moments of the ordered phase, with perpendicular fluctuations highly suppressed. Also the fluctuations have spatial anisotropy with the scattering having the form of a cigar-shaped distribution in reciprocal space, with the long axis along the domain direction.

For a Type-1 antiferromagnet the ordering occurs at inequivalent wavevectors and so in UN no two of the domain wavevectors $\underset{\sim}{\tau}_D$ = [100] ($2\pi/a$), [010] ($2\pi/a$), [001] ($2\pi/a$) are related by a wavevector $\underset{\sim}{\tau}_N$ of the fcc reciprocal lattice. Hence the long-wavelength critical scattering associated to a particular incipient ordering can be explored by considering small wavevectors around the appropriate $\underset{\sim}{\tau}_D$.

For ordering as a Type-1 antiferromagnet the ordering wavevector is [001] ($2\pi/a$) and hence a Bragg peak also forms at [110] ($2\pi/a$), as [11$\bar{1}$] ($2\pi/a$) is a reciprocal lattice vector for the fcc lattice, whilst for a Type-1A antiferromagnet [0,0,0.5] ($2\pi/a$) is the ordering wavevector.

Experimental work by Holden et al. (1982a,b) on UN and UAs examined scans made through the [110]($2\pi/a$) point in the radial [$\zeta\zeta$0] and transverse [00ζ] directions at T/T_N = 1.01-1.05, so that the former is parallel to the domain vector, and the latter perpendicular. They find that the distribution is anisotropic, with a width in the neutron scattering peak for UN of 2.8 times

greater along the domain direction than perpendicular to it. The anisotropy similarly observed in USb by Lander, Sinha, Sparlin and Vogt (1978) is greater by a factor of two.

The strength of the planar structure of the fluctuations observed in UN is indicated by the magnitude of the correlation range and the persistence of the critical scattering to high temperatures (correlation is still observable at $1.6T_N$).

The inverse correlation length is extremely small, even well above T_N, and corresponds to correlations between the uranium moments whose range is 5-7 times longer than comparable Heisenberg systems (Holden et al. (1982b)).

The experimental work on UAs revealed even more striking anisotropy (Holden et al. (1982a), Buyers et al. (1985), Sinha et al. (1981)) than in UN. However the structure of the effective exchange interaction is such that the scattering peaks around (1,1,0.3) rather than (110). Mean field analyses (Holden et al. (1982a)) indicate that for spins lying in an (001) correlated sheet the exchange between spin components perpendicular to the sheet is stronger than the exchange between spin components in the sheet by factors of 49 for USb, 37 for UAs and 13 for UN.

The anisotropic nature of the model with a $j = 3/2$ d-states subband and infinite spin-orbit coupling is displayed in its neutron scattering. The critical scattering described above refers to scattering at a temperature slightly greater than the Néel temperature T_N. In our zero temperature formalism we can consider scattering at a U value slightly less than the critical value U_c required for ordering, and this provides an analogue to critical scattering. Just as the experimental critical scattering persisted at tempera-

tures well removed from T_N, that in the model persists to U values well below U_c (at least $U = 0.8\ U_c$).

Using different sets of parameters a wide range of sub-lattice structures was possible as ground-state solutions.

The experimental work on UN was for incipient ordering in a Type-1 antiferromagnetic structure, which has a point at [110] $(2\pi/a)$ equivalent to the ordering wavevector ~~at [110] $(2\pi/a)$~~ so that a peak which finally diverges occurs at that point in reciprocal space. When a constant $\underline{q}$ measurement of the inelastic scattering is made for low energy neutrons $(\hbar\omega \ll \beta^{-1} = kT)$ and no separation of the scattered neutron energies is made, the scattering intensity is proportional to $Re\ \chi^{\alpha\beta}(q,0)$, as is shown below (see also the appendix in Buyers et al. (1985)).

The differential neutron scattering cross-section $d^2\sigma/d\Omega d\omega$ per element of solid angle $d\Omega$, for wavevector transfer $\underline{q} = \underline{k} - \underline{k}'$ from initial momentum $\underline{k}$ to final momentum $\underline{k}'$ and frequency transfer $\omega = E - E'$ is (as in equation (1.41)):

$$\frac{d^2\sigma}{d\Omega d\omega} = \frac{(\gamma r_o)^2}{4} \frac{k'}{k} S(q,\omega)$$

$$S(q,\omega) = g_J^2 f(q)^2 \sum_{\alpha\beta} (\delta_{\alpha\beta} - \hat{q}_\alpha \hat{q}_\beta) S^{\alpha\beta}(q,\omega)$$

where r_o is the electron radius and γ the magnetic moment in nuclear magnetons. The spin-correlation function $S(q,\omega)$ is related (by the fluctuation-dissipation theorem) to the dynamical susceptibility by

$$S^{\alpha\beta}(q,\omega) = \frac{1}{\pi(1-e^{-\beta\omega})} Im\ \chi^{\alpha\beta}(q,\omega)$$

where $\beta = 1/kT$ and

$$S^{\alpha\beta}(q,\omega) = (2\pi)^{-1} \int dt\, e^{-i\omega t} \langle J^{\alpha}_{q}(t)\, J^{\beta}_{-q}(0) \rangle$$

and g_J is the Landé factor and f(q) the form factor. Therefore in the limit of low energy neutrons $(\beta\omega \ll 1)$, summing over undiscriminated energies with $\mathrm{Im}\,\chi^{\alpha\beta}(q,\omega) \neq 0$ for small ω only, the expression for $S^{\alpha\beta}(q,\omega)$ gives on integration

$$\int_{-\omega_{max}}^{\omega_{max}} S^{\alpha\beta}(q,\omega)\, d\omega = \int_{-\omega_{max}}^{\omega_{max}} \frac{\mathrm{Im}\,\chi^{\alpha\beta}(q,\omega)}{\pi\,(1-e^{-\beta\omega})}\, d\omega$$

$$\simeq \int_{-\omega_{max}}^{\omega_{max}} \frac{kT}{\pi\omega}\, \mathrm{Im}\,\chi^{\alpha\beta}(q,\omega)\, d\omega$$

As the maximum neutron frequency ω_{max} lies above the range for which $\mathrm{Im}\,\chi^{\alpha\beta}(q,\omega) \neq 0$ we can approximate this by

$$\int_{-\omega_{max}}^{\omega_{max}} S^{\alpha\beta}(q,\omega)\, d\omega \simeq \frac{kT}{\pi} \int_{-\infty}^{\infty} \frac{\mathrm{Im}\,\chi^{\alpha\beta}(q,\omega)}{\omega}\, d\omega$$

$$\simeq kT\, \mathrm{Re}\,\chi^{\alpha\beta}(q,0)$$

using the Kramers-Kronig relation.

A set of parameters ($\frac{dd\sigma}{} = -1$, $\frac{dd\pi}{} = 2/3$, n=1.2) for the model was found which, on ordering from the paramagnetic state, had a diverging peak in its susceptibility $\chi^{\alpha\beta}(q,0)$ at the [110]

$(2\pi/a)$ for a Type-1 antiferromagnet, and is the Bragg peak in the magnetic critical scattering considered by Holden et al. (1982a,b) for UN, their results being shown in Figure 3.1(c).

The calculations for our model were limited in accuracy (as described below). However, the peaks in $Re\ \chi^{\alpha\beta}(q,0)$ at [110] $(2\pi/a)$, and at several other possible ordering wavevectors, along $[00\zeta]$, $[\zeta\zeta 0]$ and $[\zeta\zeta\zeta]$ were calculated for a variety of values of U. It was found that the susceptibility peak at [110] $(2\pi/a)$ was the first to diverge, doing so at U = 0.72; Figure 3.1(a,b) shows the peak at U = 0.71. Figure 3.2 shows $Re\ \chi^{\alpha\beta}(q,0)$ for two cross-sections through the (110) peak at U = 0.65: the calculations were made for scans in the radial $[\zeta\zeta 0]$ and transverse $[00\zeta]$ directions, and show a peak width in the magnetic critical scattering that is greater by a factor of 2.0 in the domain direction. This bears a fundamental resemblance to Figure 3.1 due to Holden et al. (1982b), both in the alignment of the anisotropy and its degree.

The results displayed in this chapter involved calculations of $\chi^{\alpha\beta}(q,\omega)$ for finite $\underline{q}$ along a symmetry axis in the paramagnetic state or $\chi^{\alpha\beta}(q,\omega)$ for the ferromagnetic state with finite $\underline{\mu}, \underline{q}$ along a symmetry axis. Both types of calculation require breaking of the full cubic symmetry group O_h retaining only invariance of the Hamiltonian under rotations about the appropriate axis C_4. The anisotropic critical scattering calculations involved $\chi^{\alpha\beta}(q,0)$ for a general $\underline{q}$ not along a symmetry axis, breaking all symmetry.

When calculations under lowered symmetry were performed an appropriately enlarged IBZ was used, and thus the storage and

length of time for the calculations was increased. To make these calculations tractable a coarser mesh (lower m parameter) was used, usually m = 6 (as defined in Section 1.9) when retaining rotational symmetry but making many calculations for many ω values. Fewer points in the ω variable could be examined for $Im\,\chi^{zz}(q,\omega+i\eta)$ under such circumstances. When all symmetry was broken but $\omega=0$ m = 7 was used.

In the anisotropic critical scattering the coarse mesh size must be compared to the small $\underline{q}$ displacements about [110](2π/a) considered, and this deficiency led to the inaccuracy and significant scatter in Figures 3.1(a,b) and 3.2. However, the general shape of the peak is discernible, and the presence of strong anisotropy visible.

3.3 Spin-orbit coupling and magnetic excitations

It has been found experimentally that well-defined collective magnetic excitations (spin waves) are absent in UN and US (Holden et al. 1982a, 1982b)); this feature is found in cases of our j = 3/2 fcc d-subband model and should occur also in a j = 5/2 fcc f-subband model of the uranium compounds.

The experimental data referred to consists of inelastic neutron scattering measurements, determined within our formalism by the response functions $Im\,\chi^{\alpha\beta}(q,\omega+i\eta)$ or $\ll J^{\alpha}_{q};J^{\beta}_{-q}\gg_{\omega}$. In the spin-only case, which is a good approximation for 3d metals with small spin-orbit coupling, we have for q = 0 in a ferromagnet a sharp spin wave (Goldstone) mode at $\omega = 0$ because $S^{\alpha}_{q=0}=\sum_i S^{\alpha}_i$ is a constant of the motion. However, when the spin-orbit coupling becomes large $[J^{\alpha}_{q},H]\neq 0$ as J^{α}_{q} does not commute

with the first term in equation (1.1) (J^α_q clearly commutes with the second term, although not in the HF approximation):

$$[J^\alpha_q, H] = \sum_{\mu\underline{k}} \sum_{\nu\eta\underline{k}'} f^\alpha_\mu T_{\nu\eta}(\underline{k}') \left[c^+_{\mu+\alpha\,\underline{k}+\underline{q}} c_{\mu\underline{k}}, c^+_{\nu\underline{k}'} c_{\eta\underline{k}'}\right] \quad (3.1)$$

$$= \sum_{\mu\underline{k}} \sum_{\nu\eta\underline{k}'} f^\alpha_\mu T_{\nu\eta}(\underline{k}') \left(c^+_{\mu+\alpha\,\underline{k}+\underline{q}} \left[c_{\mu\underline{k}}, c^+_{\nu\underline{k}'}\right]_+ c_{\eta\underline{k}'} - c^+_{\nu\underline{k}'} \left[c^+_{\mu+\alpha\,\underline{k}+\underline{q}}, c_{\eta\underline{k}'}\right]_+ c_{\mu\underline{k}}\right)$$

$$= \sum_{\mu\underline{k}} \sum_{\nu\eta} \left(f^\alpha_\mu T_{\mu\eta}(\underline{k}) c^+_{\mu+\alpha\,\underline{k}+\underline{q}} c_{\eta\underline{k}} - f^\alpha_\mu T_{\nu\mu+\alpha}(\underline{k}+\underline{q}) c^+_{\nu\underline{k}+\underline{q}} c_{\mu\underline{k}}\right)$$

$$= \sum_{\mu\underline{k}} \sum_{\nu} \left(f^\alpha_\mu T_{\mu\nu}(\underline{k}) c^+_{\mu+\alpha\,\underline{k}+\underline{q}} c_{\nu\underline{k}} - f^\alpha_\nu T_{\mu\nu+\alpha}(\underline{k}+\underline{q}) c^+_{\mu\underline{k}+\underline{q}} c_{\nu\underline{k}}\right) \quad (3.2)$$

For example, therefore, when q = 0

$$[J^z_0, H] = \sum_{\mu\nu\underline{k}} (\mu - \nu) T_{\mu\nu}(\underline{k}) c^+_{\mu\underline{k}} c_{\nu\underline{k}}$$

which is non-zero because of the off-diagonal terms $T_{\mu\nu}$ which allow electrons to change their m_j value as they hop between atoms. Even in the case where the spin-orbit coupling is significant but not large (i.e. when $(\frac{1}{2} L^\alpha_q + S^\alpha_q)$ is not necessarily proportional to J^α_q) this complication will occur.

Not only is the commutator $[J^z_0, H]$ non-zero, but also J^z_0 has non-zero matrix elements between the ground state $|0\rangle$ and a continuum of single-particle excitation states $|n\rangle$:

$$\langle n | [J^z_0, H] | 0 \rangle = \langle n | J^z_0 H - H J^z_0 | 0 \rangle$$

$$= (E_0 - E_n) \langle n | J^z_0 | 0 \rangle$$

as $(E_0 - E_n)$ is non-zero.

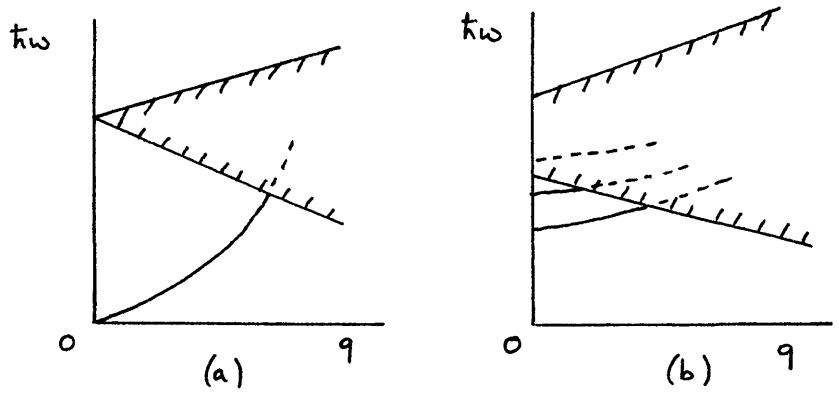

The schematic diagrams show the conventional dispersion relation for the spin-only single-band case (a) with the Stoner continuum of excitations coming to a weightless point at q = 0, and case (b) for our model (see also Figure 3.15). The latter case has the Stoner continuum of single-particle excitations, even at q = 0, extending from a minimum energy which may be quite small (especially on ordering provided U is not too large) to quite high energies, of order of the bandwidth. This continuum between two energies $\hbar\omega$ for which $\mathrm{Im}\,\chi^{zz}(q=0,\omega+i\eta)\neq 0$ has been displayed for several paramagnetic cases in the first chapter, by giving $\mathrm{Im}\,P(\omega)$, $\mathrm{Im}\,Q(\omega)$.

The large anisotropy due to the dominating spin-orbit coupling in the f band can place the potential spin wave in the Stoner continuum. In the case of normal rare-earth systems, or actinide systems with localized f electrons, $\mathcal{J}_0^\alpha$ commutes with the exchange part of the Hamiltonian but single-site crystal anisotropy leads to an anisotropy gap in the spin wave spectrum. However, $\mathcal{J}_0^\alpha$ has matrix elements between sharp crystal field levels, leading to well-defined crystal field excitations at q = 0, and there are no itinerant f electrons to give damping. It is the combination of strong spin-orbit coupling and itinerancy which may wash out spin waves in actinide compounds like ferromagnetic US and similarly in antiferromagnetic UN.

The existence of the continuum at $\omega \neq 0$ implies that the odd moments of the imaginary part of $\chi^{\alpha\beta}(q=0, \omega+i\eta)$ should be non-zero, in contrast to the spin-only single-band case for which they are zero at q = 0.

3.4 The second moment of the shape function

The neutron scattering cross-section is proportional to the dynamical structure factor $S^{\alpha\beta}(q,\omega)$ as shown by equation (1.41), where

$$S^{\alpha\beta}(q,\omega) = \frac{1}{2\pi}\int_{-\infty}^{\infty} dt\, e^{i\omega t} \langle J^{\alpha}_{-q}(0)\, J^{\beta}_{q}(t)\rangle \tag{3.3}$$

and the relaxation shape function $F^{\alpha\beta}(q,\omega)$ is then defined by the relations

$$S^{\alpha\beta}(q,\omega) = \omega\, \chi^{\alpha\beta}(q)\, F^{\alpha\beta}(q,\omega) \tag{3.4}$$

$$F^{\alpha\beta}(q,\omega) = \frac{1}{\omega \chi^{\alpha\beta}(q)} \frac{1}{2\pi}\int_{-\infty}^{\infty} dt\, e^{-i\omega t} \langle [J^{\alpha}_{-q}(0), J^{\beta}_{q}(t)]\rangle \tag{3.5}$$

The frequency moments $F^{\alpha\beta(n)}(q)$ are given by (Marshall and Lowde, 1968):

$$F^{\alpha\beta(n)}(q) = \left[\left(-i \frac{\partial}{\partial t}\right)^n F^{\alpha\beta}(q,t) \right]_{t=0} \tag{3.6}$$

where $F^{\alpha\beta(n)}(q) = \int_{-\infty}^{\infty} F^{\alpha\beta}(q,\omega)\omega^n d\omega$ so that the zeroth and second moments are

$$F^{\alpha\beta(0)} = 1 \tag{3.7}$$

$$F^{\alpha\beta(2)} = -\ddot{F}^{\alpha\beta}(q) \tag{3.8}$$

with the time derivative being evaluated from the commutator

$$\dot{J}^{\alpha}_{q} = -i \left[J^{\alpha}_{q} , H \right]$$

The odd moments of the shape function are zero, and the even moments can be calculated from the expression (3.6) in terms of commutators. Thus for the first moment

$$\chi^{\alpha\beta}(q)\, \dot{F}^{\alpha\beta}(q) = \langle \left[J^{\alpha}_{q} , J^{\beta}_{-q} \right] \rangle = 0 \tag{3.9}$$

and for the second moment

$$\chi^{\alpha\beta}(q)\, \ddot{F}^{\alpha\beta}(q) = i \langle \left[J^{\alpha}_{q} , \dot{J}^{\beta}_{-q} \right] \rangle \tag{3.10}$$

$$= \Big\langle \sum_{\mu \underline{k}} \sum_{\mu' \underline{k}'} \sum_{\nu} \Big[f^{\alpha}_{\mu}\, c^{+}_{\mu+\alpha\, \underline{k}+q}\, c_{\mu \underline{k}} \,,\, \left(f^{\beta}_{\mu'}\, T_{\mu'\nu}(\underline{k}') \right) c^{+}_{\mu'+\beta\, \underline{k}'-q}\, c_{\nu \underline{k}'}$$

$$- f^{\beta}_{\mu}\, T_{\nu\mu'+\beta}(\underline{k}'-q)\, c^{+}_{\nu\, \underline{k}'-q}\, c_{\mu' \underline{k}'} \Big] \Big\rangle \tag{3.11}$$

$$= \Big\langle \sum_{\mu \underline{k}} \sum_{\mu' \underline{k}'} \sum_{\nu} \Big(f^{\alpha}_{\mu}\, f^{\beta}_{\mu'}\, T_{\mu'\nu}(\underline{k}') \Big(c^{+}_{\mu+\alpha\, \underline{k}+q} \left[c_{\mu \underline{k}} , c^{+}_{\mu'+\beta\, \underline{k}'-q} \right]_{+} c_{\nu \underline{k}'}$$

$$- c^{+}_{\mu'+\beta\, \underline{k}'-q} \left[c^{+}_{\mu+\alpha\, \underline{k}+q} , c_{\nu \underline{k}'} \right]_{+} c_{\mu \underline{k}} \Big) - f^{\alpha}_{\mu}\, f^{\beta}_{\mu'}\, T_{\nu\mu'+\beta}(\underline{k}'-q)$$

$$\Big(c^{+}_{\mu+\alpha\, \underline{k}+q} \left[c_{\mu \underline{k}} , c^{+}_{\nu\, \underline{k}'-q} \right]_{+} c_{\mu' \underline{k}'} - c^{+}_{\nu\, \underline{k}'-q} \left[c^{+}_{\mu+\alpha\, \underline{k}+q} , c_{\mu' \underline{k}'} \right]_{+} c_{\mu \underline{k}} \Big) \Big\rangle \tag{3.12}$$

$$= \sum_{\mu\nu \underline{k}} \sum_{m} \Big(f^{\alpha}_{\mu}\, f^{\beta}_{\mu-\beta}\, T_{\mu-\beta\,\nu}(\underline{k}+q)\, a^{*}_{m\,\mu+\alpha}(\underline{k}+q)\, a_{m\nu}(\underline{k}+q) \langle n_{m\,\underline{k}+q} \rangle$$

$$- f^{\alpha}_{\mu}\, f^{\beta}_{\nu}\, T_{\nu\mu+\alpha}(\underline{k}+q)\, a^{*}_{m\nu+\beta}(\underline{k})\, a_{m\mu}(\underline{k}) \langle n_{m\underline{k}} \rangle - f^{\alpha}_{\mu}\, f^{\beta}_{\nu}\, T_{\mu\nu+\beta}(\underline{k})\, a^{*}_{m\,\mu+\alpha}(\underline{k}+q)$$

$$a_{m\nu}(\underline{k}+q) \langle n_{m\,\underline{k}+q} \rangle + f^{\alpha}_{\mu}\, f^{\beta}_{\mu+\alpha}\, T_{\nu\mu+\alpha+\beta}(\underline{k})\, a^{*}_{m\nu}(\underline{k})\, a_{m\mu}(\underline{k}) \langle n_{m\underline{k}} \rangle \Big) \tag{3.13}$$

Therefore, this expression allows $\chi^{\alpha\beta}(q)\ddot{F}^{\alpha\beta}(q)$ to be calculated, and from equation (3.5)

$$\chi^{\alpha\beta}(q=0)\ddot{F}^{\alpha\beta}(q=0) = -\frac{1}{\pi}\int_{-\infty}^{\infty}\omega\, \mathrm{Im}\chi^{\alpha\beta}(0,\omega)\,d\omega \qquad (3.14)$$

so that this can be compared with calculations of this integral based upon $\chi^{\alpha\beta}(q,\omega)$ curves. This calculation was done at q = 0 for several values of the parameters (see Table 3.1); it was found to be non-zero in the paramagnetic regime, and fell towards zero for larger U. The agreement with the first moment of the imaginary part of the susceptibility, taken from $\mathrm{Im}\chi^{\alpha\beta}(0,\omega)$ calculations, seemed reasonable as they gave for the case $dd\sigma$ = -1, $dd\pi$ = 2/3, n = 1.0, U = 0.94 (Figure 3.16):

$$\int_{-\infty}^{\infty}\omega\, \mathrm{Im}\chi^{zz}(0,\omega)\,d\omega = 1.13$$

and for the case $dd\sigma$ = - 1, $dd\pi$ = 0.55, n = 2.25, U = 0.7 (Figure 3.12):

$$\int_{-\infty}^{\infty}\omega\, \mathrm{Im}\chi^{zz}(0,\omega)\,d\omega = 1.34$$

Table 3.1

		U			
		0.0	0.7	0.94	3.0
$-dd\pi/dd\sigma$ = 2/3 n = 1.0, U = 0.94	$-\pi\,\mathrm{Im}\chi^{zz}(0)\ddot{F}^{zz}(0)$	3.2	-	1.04	0.06
$-dd\pi/dd\sigma$ = 0.55 n = 2.25, U = 0.7	$-\pi\,\mathrm{Im}\chi^{zz}(0)\ddot{F}^{zz}(0)$	3.5	1.22	-	0.09

The high U limit should correspond to the localized spin-only case, so that it is expected that $\ddot{F}^{\alpha\beta}(q=0)$ tends to zero. Considering the case with n = 1, we can examine this limit analytically at high U using equation (3.13). The interaction term in the HF Hamiltonian H dominates

$$H = \sum_{\mu\nu\underline{k}} T_{\mu\nu}(\underline{k})\, c^{+}_{\mu\underline{k}} c_{\nu\underline{k}} + U \sum_{\mu\nu\underline{k}} (n\delta_{\mu\nu} - \langle n_{\mu\nu}\rangle)\, c^{+}_{\mu\underline{k}} c_{\nu\underline{k}}$$

so that the eigenstates tend to the states $|\mu\underline{k}\rangle$ of definite total angular momentum. The expansion coefficients $a_{n\mu}(\underline{k}) \to \delta_{n\mu}$ and the bandstructure has bands with energies of multiples of U which are either completely filled or unfilled. For n = 1 there is a filled $m_j = +3/2$ band at about $\hbar\omega \sim 0$ and three unfilled bands at $\hbar\omega \sim U$, which only $\langle n_{3/2\,3/2}\rangle = 1$ and all other $\langle n_{\mu\nu}\rangle = 0$ so that H tends to

$$H = \begin{pmatrix} 0 & 0 & 0 & 0 \\ 0 & U & 0 & 0 \\ 0 & 0 & U & 0 \\ 0 & 0 & 0 & U \end{pmatrix} + O(T_{\mu\nu})$$

Therefore, at q = 0,

$$\chi^{\alpha\beta}(q=0)\,\ddot{F}^{\alpha\beta}(q=0) = \sum_{\mu\underline{k}} \left(f^{\alpha}_{\mu} f^{\beta}_{\mu-\beta}\, T_{\mu-\beta\,\mu+\alpha}(\underline{k}) \langle n_{\mu+\alpha\,\mu+\alpha}\rangle \right.$$

$$- f^{\alpha}_{\mu} f^{\beta}_{\mu-\beta}\, T_{\mu-\beta\,\mu+\alpha}(\underline{k}) \langle n_{\mu\mu}\rangle - f^{\alpha}_{\mu} f^{\beta}_{\mu+\alpha}\, T_{\mu\,\mu+\alpha+\beta}(k) \langle n_{\mu+\alpha\,\mu+\alpha}\rangle$$

$$\left. + f^{\alpha}_{\mu} f^{\beta}_{\mu+\alpha}\, T_{\mu\,\mu+\alpha+\beta}(k) \langle n_{\mu\mu}\rangle \right)$$

$$= 0$$

so that the first moment of $\mathrm{Im}\,\chi^{\alpha\beta}(0,\omega)$ tends to zero as U rises and the continuum becomes a narrow band of falling weight about $\hbar\omega = U$ (see Figure 3.15). This high U case corresponds to increasing localization in which the itinerancy is suppressed, removing the combination of itinerancy and spin-orbit coupling.

3.5 Susceptibility calculations and sum rules

The calculations of the susceptibility $\chi^{\alpha\beta}(q,\omega)$ may be checked from several relations with other quantities. The Kramers-Kronig relation can be used to see whether $\mathrm{Re}\,\chi^{\alpha\beta}(q,\omega)$ and $\mathrm{Im}\,\chi^{\alpha\beta}(q,\omega)$, which are calculated independently as described in Section 1.9, are consistent:

$$\mathrm{Re}\,\chi^{\alpha\beta}(q,\omega) = \frac{1}{\pi}\int_{-\infty}^{\infty} \frac{\mathrm{Im}\,\chi^{\alpha\beta}(q,\omega')}{(\omega-\omega')}\,d\omega' \qquad (3.16)$$

This was done successfully for q = 0 and for finite q in several cases, agreement being to within ± 5%.

Also, from the results in Chapter 1 in the paramagnetic regime $\chi^{\alpha\beta}(0,\omega\to 0)$ may be compared with its value calculated from P(0) and Q(0), and $\chi^{\alpha\beta}(q\to 0,0)$ with that calculated from P(0), Q(0), P^S and Q^S. These agreed well in several cases which were tried; for example, for the bandstructure with $dd\sigma = -1$, $dd\pi = 2/3$ and n = 2 at U = 0 the susceptibility calculation gave

$$\mathrm{Re}\,\chi^{zz}(q\to 0,0) = 5.863$$

whilst

$P(0) = 0.3177$ $\qquad$ $P^S = 0.2085$

$Q(0) = 0.2426$ $\qquad$ $Q^S = 0.2558$

hence from these integrals

$$\mathrm{Re}\,\chi^{zz}(q\to 0,0) = 2P(0) + 8Q(0) + 12Q^S + 3P^S$$

$$= 5.846$$

which is agreement to about ± 0.5%.

3.6 The damping of spin waves

In a similar manner to the use of the d states j = 3/2 subband, we can also investigate the HF solution using a basis of the f states j = 5/2 subband, and the ground state solutions are relevant to our discussion of spin-wave damping. The establishment of the f states j = 5/2 subband Hamiltonian is described in Appendix C, where it is shown that the representation of the j = 5/2 manifold with full cubic symmetry is the sum of the fourfold irreducible representation Γ_8^- and the twofold Γ_7^-.

The ground state HF solution of a canonical $5f_{5/2}$ subband with n = 3 and infinite spin-orbit coupling assumed may be calculated; the magnetic moment along [001] is plotted against U in Figure 3.3. Also the bandstructure along various symmetry directions for various values of U together with the projected density of states of the six $(5/2,m_j)$ orbitals (these are defined by equation (2.9)) are shown in Figures 3.4-3.11. In the paramagnetic state at U = 0 the bandstructure (Figure 3.4) can be seen to have Kramers' degeneracy and also to have a fourfold and twofold degeneracy at the origin of k-space Γ. The projected density of states (Figure 3.5) has three distinct twofold curves, as there are now

two irreducible representations from which the $n_\mu(E)$ are derived.

Considering the expression for the interacting susceptibility $\mathrm{Im}\chi^{\alpha\beta}(q,\omega+i\eta)$ derived above in Chapter 1, it can be seen that at q = 0 the continuum of single-particle Stoner excitations (with $\mathrm{Im}\chi^{\alpha\beta}(0,\omega+i\eta)\neq 0$) extends from a minimum $\omega=\omega_0$ to maximum $\omega=\omega_1$ as follows. The energy $\hbar\omega_0$ is given by the smallest vertical transition between a filled and unfilled state allowed by the HF self-consistent bandstructure; the energy $\hbar\omega_1$ is correspondingly given by the largest such allowed transition.

The canonical $5f_{5/2}$ bandstructures obtained for magnetization in the [001] direction (Figures 3.6-3.11) indicate that for a large range of U parameters $\hbar\omega_0$ is small $(\hbar\omega_0 \simeq 0.04\,ff\sigma)$ whilst $\hbar\omega_1$ is large $(\hbar\omega_1 \simeq ff\sigma)$. For a $5f_{5/2}$ bandwidth of 1 eV, with $ff\sigma$ = 0.5 eV, this would give $\hbar\omega_0 \simeq 20$ meV.

Therefore, even for low-lying excitations there is a continuous range of single-particle modes for the excitations to decay into, as the continuum extends to such low energies. This provides a mechanism for heavy spin wave damping within such systems.

On examining the susceptibility $\mathrm{Im}\chi^{zz}(q,\omega+i\eta)$ to observe this damping we chose to perform calculations on the simpler $d_{3/2}$ subband, with the examples selected to have a continuum extending to low energies, that is a bandstructure with bands crossing close to the Fermi level.

The model with the parameters $dd\sigma$ = -1, $dd\pi$ = 0.55, n = 2.25 was investigated. The self-consistent solution for the order parameters μ and Q are given in Figure 2.7; a second-order phase transition occurs at the instability U_c = 0.52, and a compensated moment (the (1, -1, 1, -1) mode in equation (1.84)) forms.

At U = 0.7 this moment is strong enough to give a magnetic moment μ = 0.29, and the bandstructures along a variety of symmetry axes are given in Figure 2.8. The Fermi level is quite close to a crossing of two bands, and considering transitions between filled and unfilled states the continuum for which $Im\chi^{zz}(0,\omega+i\eta) \neq 0$ can be seen to extend down at least to $\hbar\omega_0 = 0.04dd\sigma$. On calculating $Im\chi^{zz}(0,\omega+i\eta)$ this is non-zero down to an energy of $\hbar\omega_0 = 0.02dd\sigma$ (see Figure 3.13), which for a bandwidth of 1 eV is an energy of 20meV. The dispersion relation, showing the continuum domain for which $Im\chi^{zz}(q,\omega+i\eta) \neq 0$ and the energy of the excitation modes for $q < 0.4(2\pi/a)$ is given in Figure 3.15(a). The continuum remains reasonably unchanged at q ≠ 0, but at low $\hbar\omega$ intra-band excitations become important once $q > 0.02(2\pi/a)$ and meet the continuum at $q \simeq 0.1(2\pi/a)$.

In Figure 3.12 the first excitation mode should fall at the point indicated by the lowest energy arrow (where $\det|\underline{\underline{1}} + \underline{\underline{\Gamma}}\underline{\underline{\Omega}}| = 0$) and a broad ill-defined peak is seen. The region of phase space ($\underline{k}$-space) contributing to this process is shown (by the extent of the broadening of the delta function) to be large enough to give very strong damping. The weight of the damped delta function indicated is 0.048 of the weight of the whole continuum. Figure 3.13 shows a more detailed version of the excitation peak using a more accurate solution. Figure 3.14 shows a similar peak for a different example, and it displays an even greater degree of damping. In both cases there are further excitation modes at higher energies which are difficult to discern in the continuum (see Figure 3.12).

Also there are cases where the continuum starts at higher energies, and in Figure 3.15(b,c,d) the dispersion relation and

values of $\mathrm{Im}\chi^{zz}(q,\omega+i\eta)$ are displayed for $dd\sigma = -1$, $dd\pi = 2/3$, n = 1. The sequence begins with a dispersion relation for this n = 1 canonical bandstructure case at U = 0.9 which has just changed from paramagnetic to very weakly ordered (aligned moment). This is followed by a weakly ferromagnetic case, at U = 0.94, showing how the continuum broadens and rises to higher energy with $\hbar\omega_0$ being lifted at higher $\underline{q}$. Finally, U = 1.5 represents the strongly ferromagnetic case, with the continuum rising in energy. In the high U limit the continuum becomes a band about $\hbar\omega = U$. The appearance of $\mathrm{Im}\chi^{zz}(q,\omega+i\eta)$ for this case at $q = 0{\cdot}0\left(\frac{2\pi}{a}\right), 0{\cdot}2\left(\frac{2\pi}{a}\right), 0{\cdot}4\left(\frac{2\pi}{a}\right)$ are shown in Figure 3.16, with the position of the excitation modes indicated by arrows.

In Figure 3.15(d) the features of the high U limiting case have started to emerge. At U = 1.6 the filled lower band and unfilled upper bands no longer overlap, and the intraband contribution to $\mathrm{Im}\chi^{zz}(q,\omega+i\eta)$ vanishes. This leaves the excitation modes which have moved to low energy exposed, and in this high U limit we return to undamped well-defined spin waves, as the itinerant model reaches its localized limit. Amongst the uranium pnictides and chalcogenides, UTe provides an example where the lattice parameter is sufficiently high as to make the system more highly localized, and sharp well-defined spin waves have been observed (Buyers et al. (1980)).

3.7 Conclusions

The current chapter and two preceding chapters have been concerned with establishing a model which, by combining itinerancy and strong spin-orbit coupling, possesses many of the unusual

magnetic properties of light actinide compounds. Treated at the HF-RPA level of approximation numerical methods have been developed to give the ground state and dynamical properties (via the generalized susceptibility $\chi^{\alpha\beta}(q,\omega)$) of the model for a wide variety of the variable parameters, which are principally $dd\pi/dd\sigma$, n and U. The ground state calculations reveal the circumstances that favour quadrupolar ordering (which is related to the orbital degeneracy) or alternatively magnetic solutions with various types of spin ordering. The strong spin-orbit coupling gives rise to strong anisotropy displayed in both static (moment formation) and dynamic (critical scattering) properties and also in a large anisotropy gap in energy between excitation modes at q = 0 and the ground state. Furthermore, our analysis of the paramagnetic and ordered states indicated how the Stoner continuum has considerable width in energy $\hbar\omega$, and for d or f subbands which have U slightly greater than required for ordering, often extends down to low energies. Hence the anisotropy gap is sufficient in typical ferromagnetic cases to place the excitation mode in this continuum of single-particle excitations, even at q = 0, and that a mechanism for strong spin-wave damping exists as excitation modes in the continuum on calculation have heavy damping. In the localized (high U) limit a transition to undamped spin waves occurs as is observed in more localized actinide compound systems.

The effects of spin-orbit coupling in our model can be seen only for the spin-orbit parameter λ in $\lambda \underline{L}\cdot\underline{S}$ taken to be infinite. It would be of interest to be able to do calculations for intermediate values of λ in order to see the transition between the weakly and strongly coupled cases. However, this would require taking a much larger basis of states than just a f state j = 5/2 subband, and would be computationally difficult.

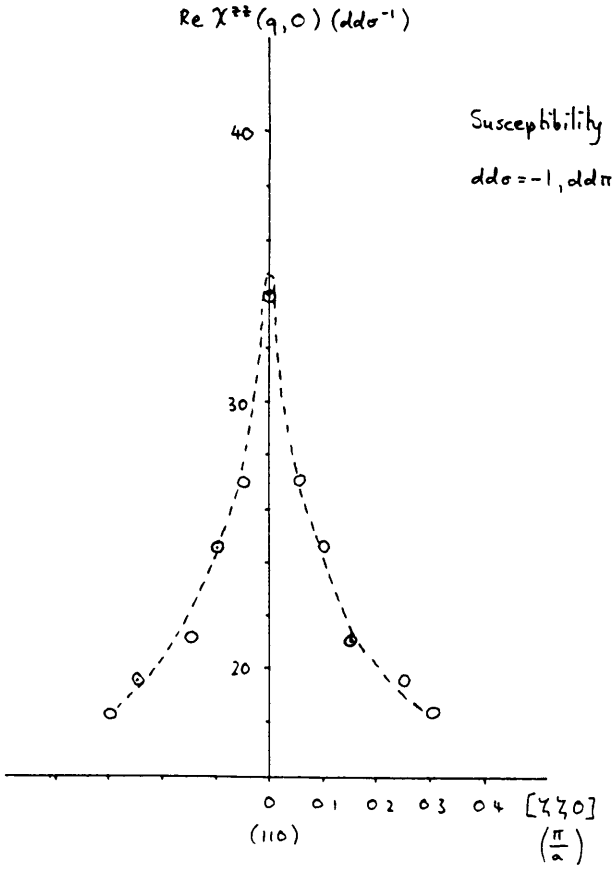

Figure 3·1 (a)

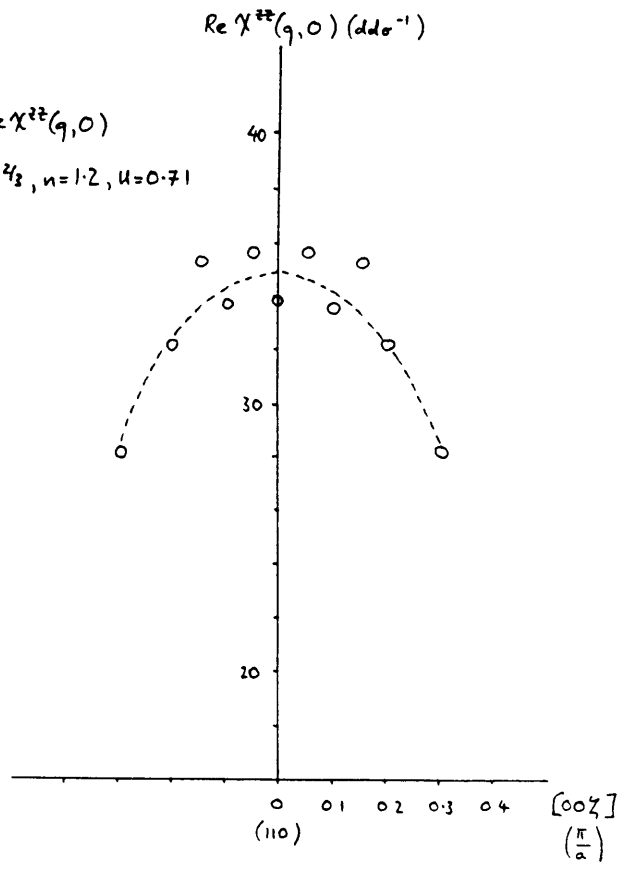

Figure 3·1 (b)

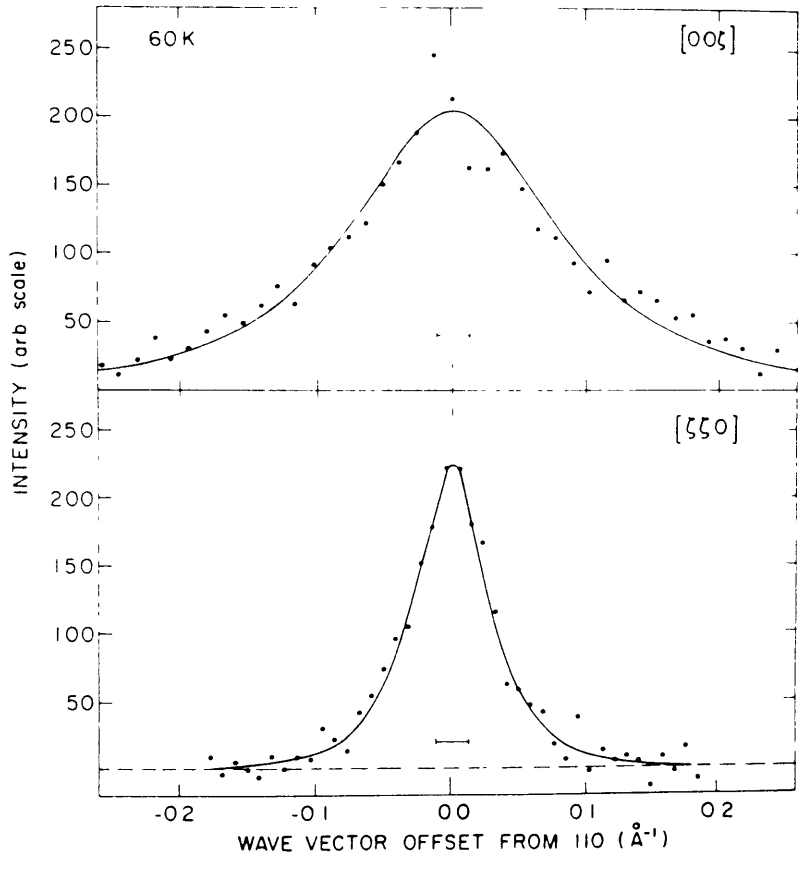

Fig. 3.1(c) Anisotropy of critical scattering in uranium nitride measured with a triple-axis spectrometer operated at constant $\nu = 0$ (Holden et al., 1982b)

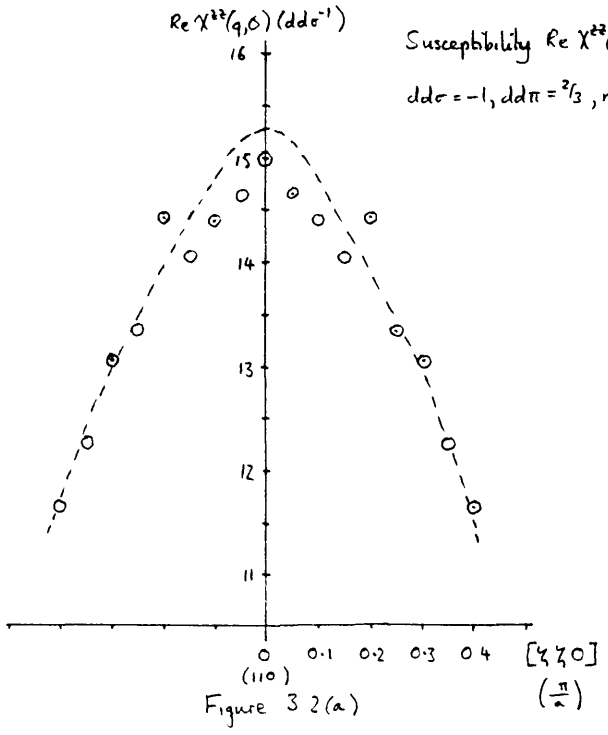

Figure 3·2(a)

Susceptibility Re $\chi^{22}(q,0)$

ddσ = −1, ddπ = ²/₃, n = 1·2, U = 0·65

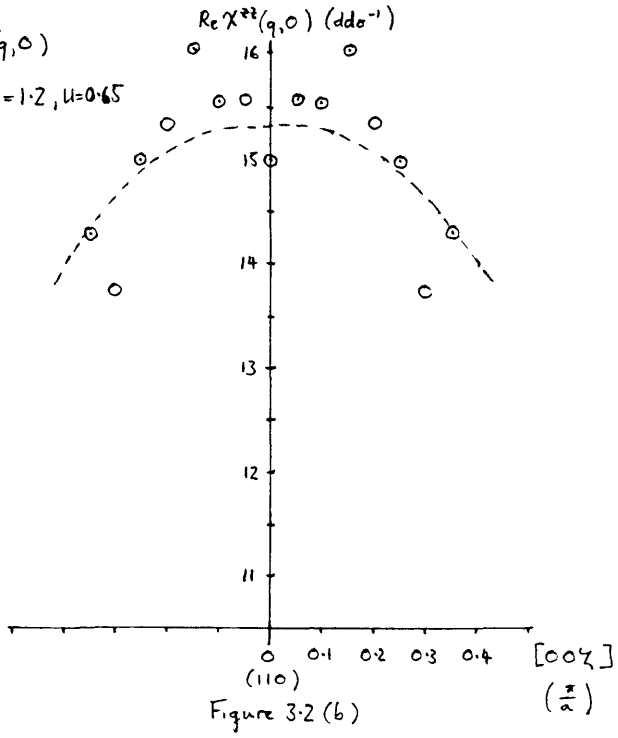

Figure 3·2(b)

Magnetic moment μ

Canonical f band, n = 3

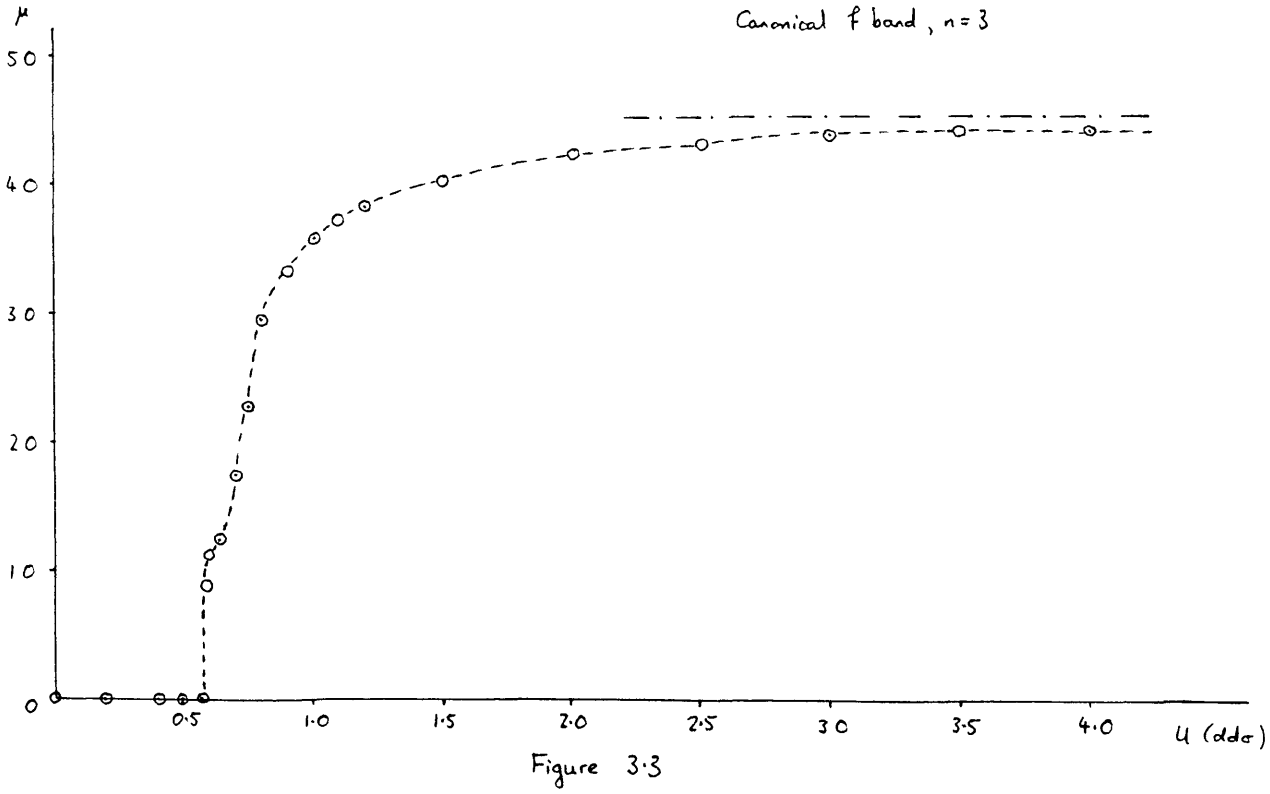

Figure 3·3

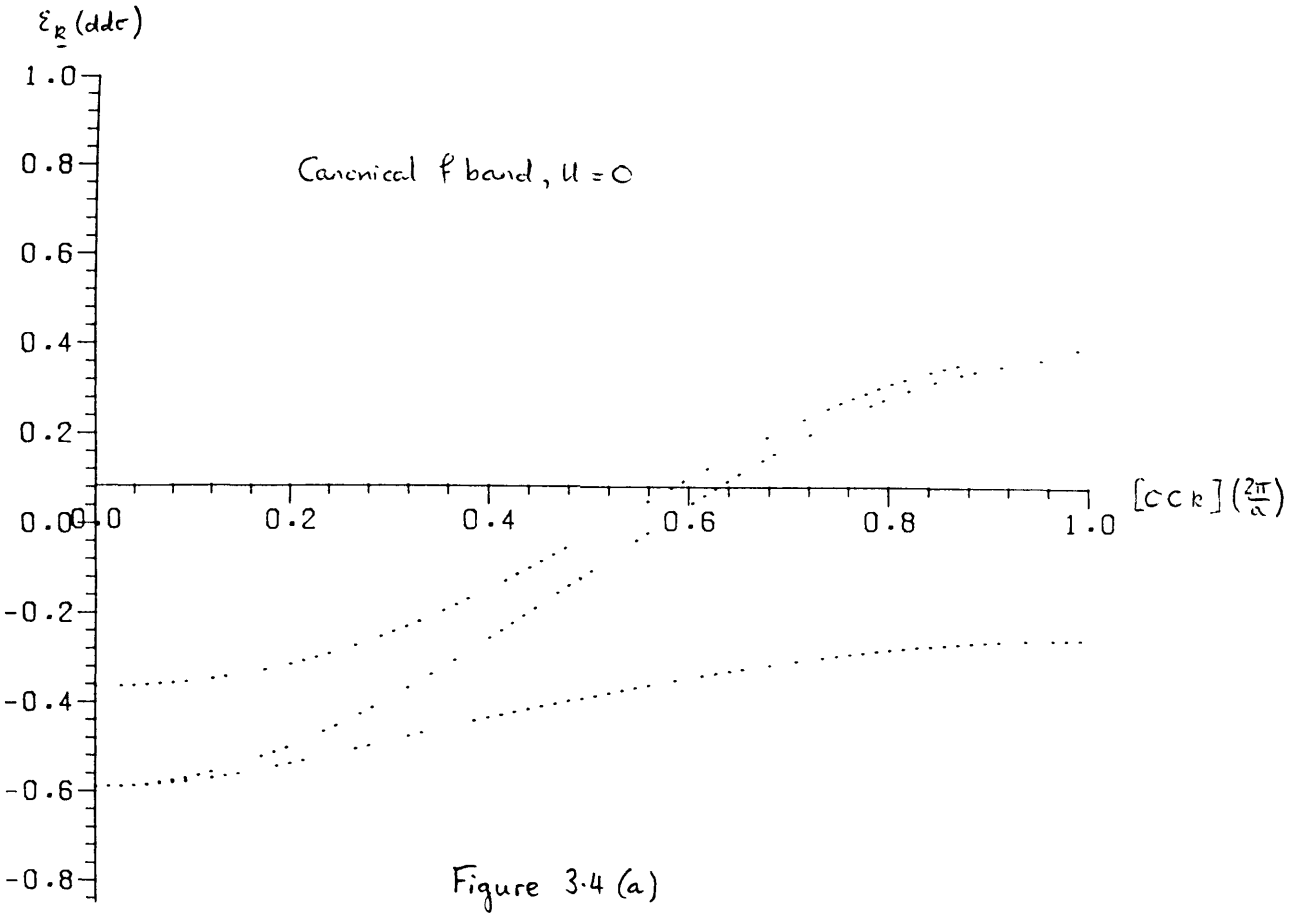
$\varepsilon_{\underline{k}}$ (ddc)
Canonical f band, U = 0
1.0
0.8
0.6
0.4
0.2
0.0
-0.2
-0.4
-0.6
-0.8
0.0
0.2
0.4
0.6
0.8
1.0
[c c k] ($\frac{2\pi}{a}$)

Figure 3.4 (a)

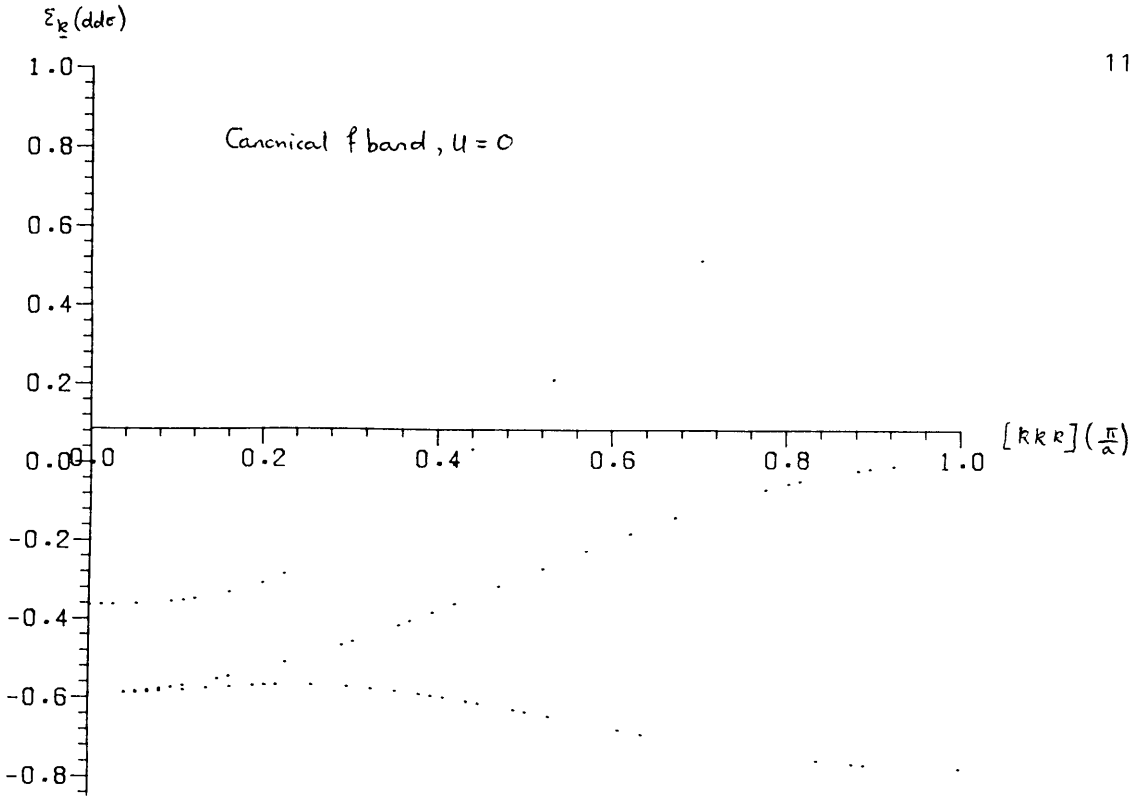

Figure 3.4 (b)

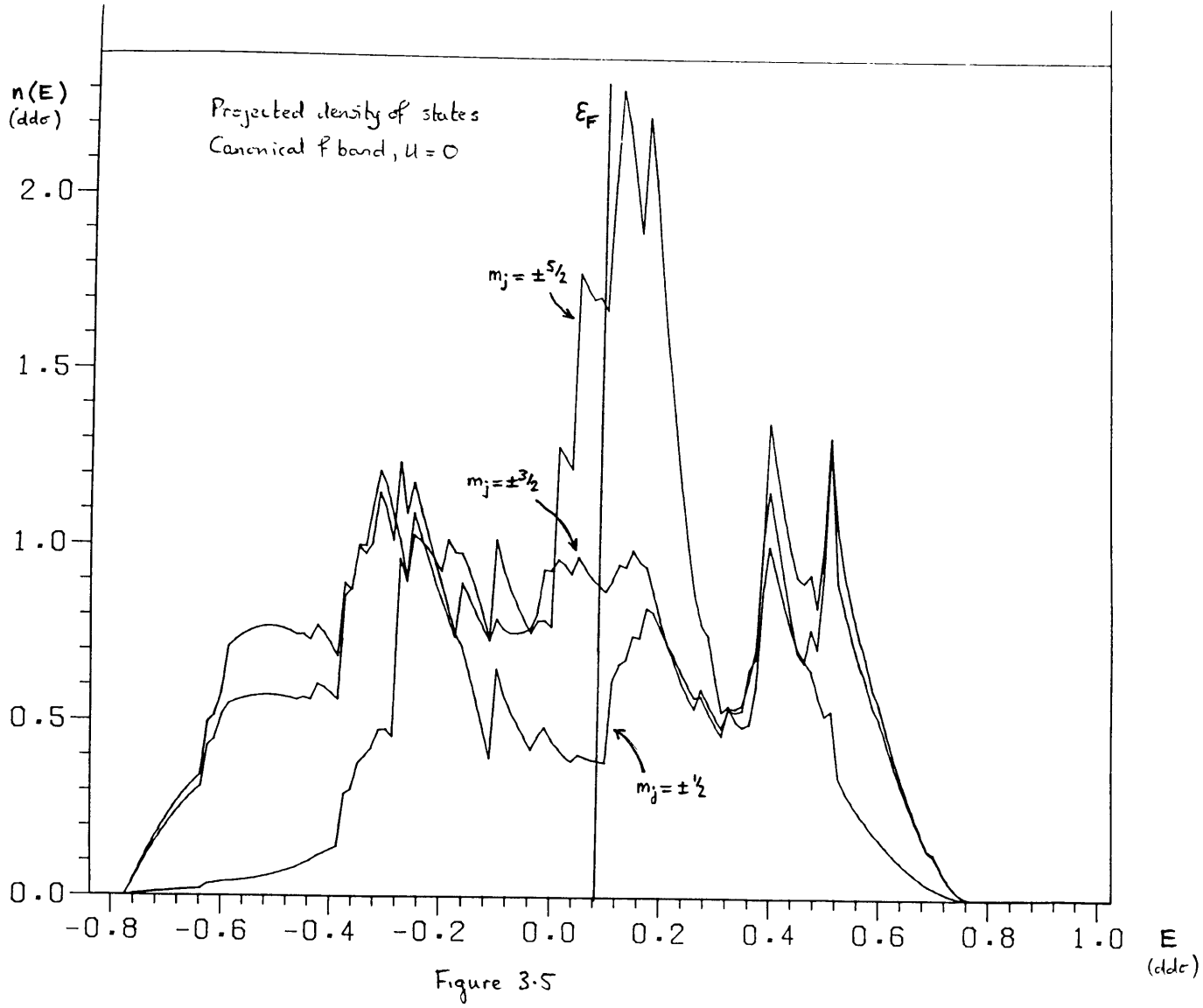

Figure 3.5

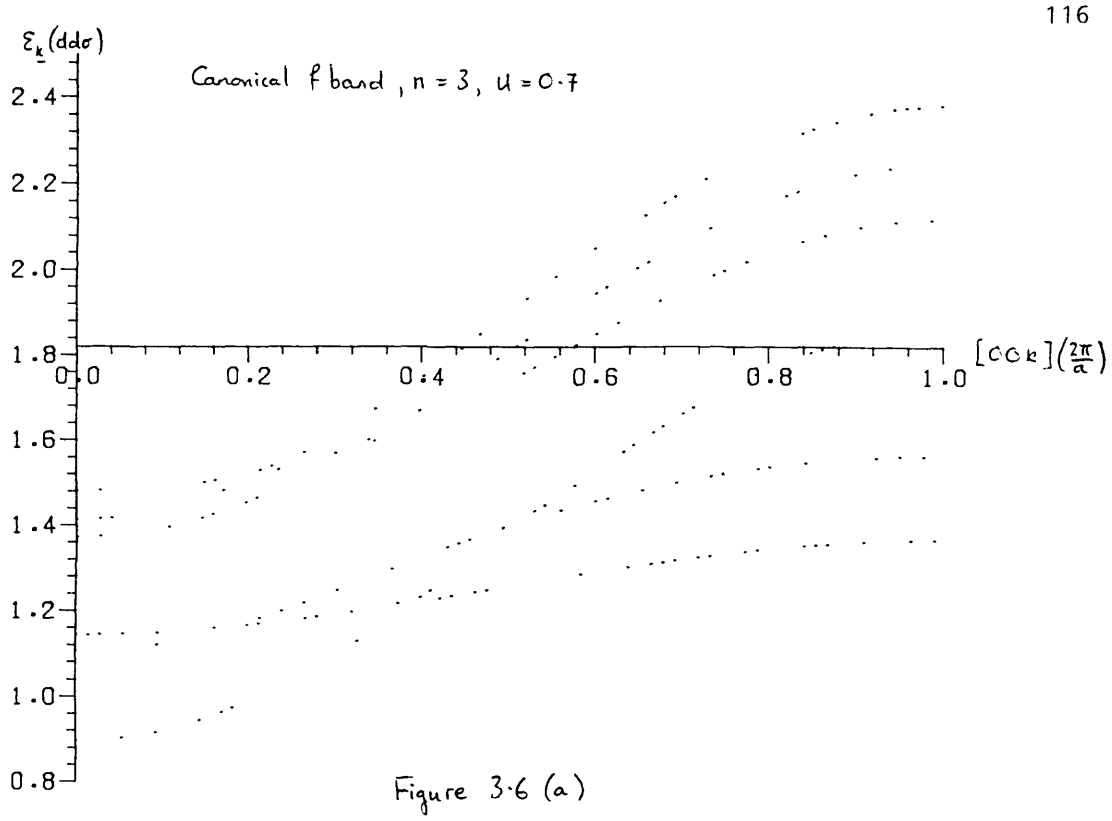

Figure 3·6 (a)

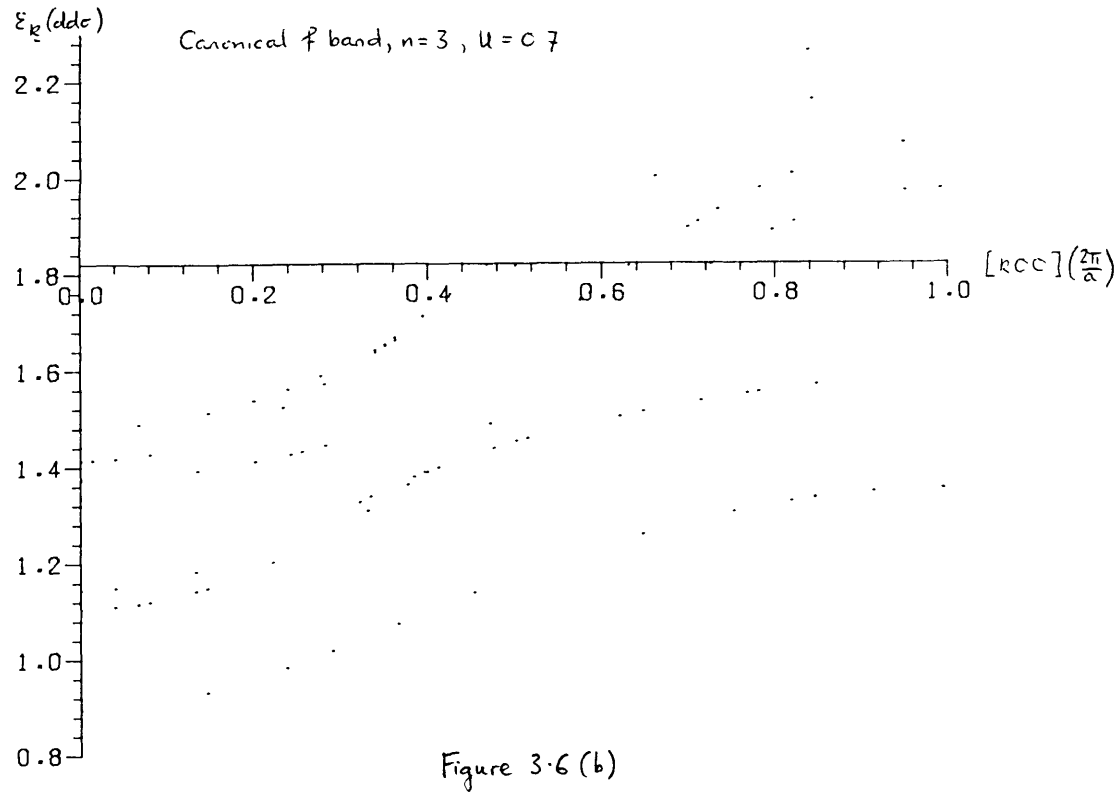

Figure 3·6 (b)

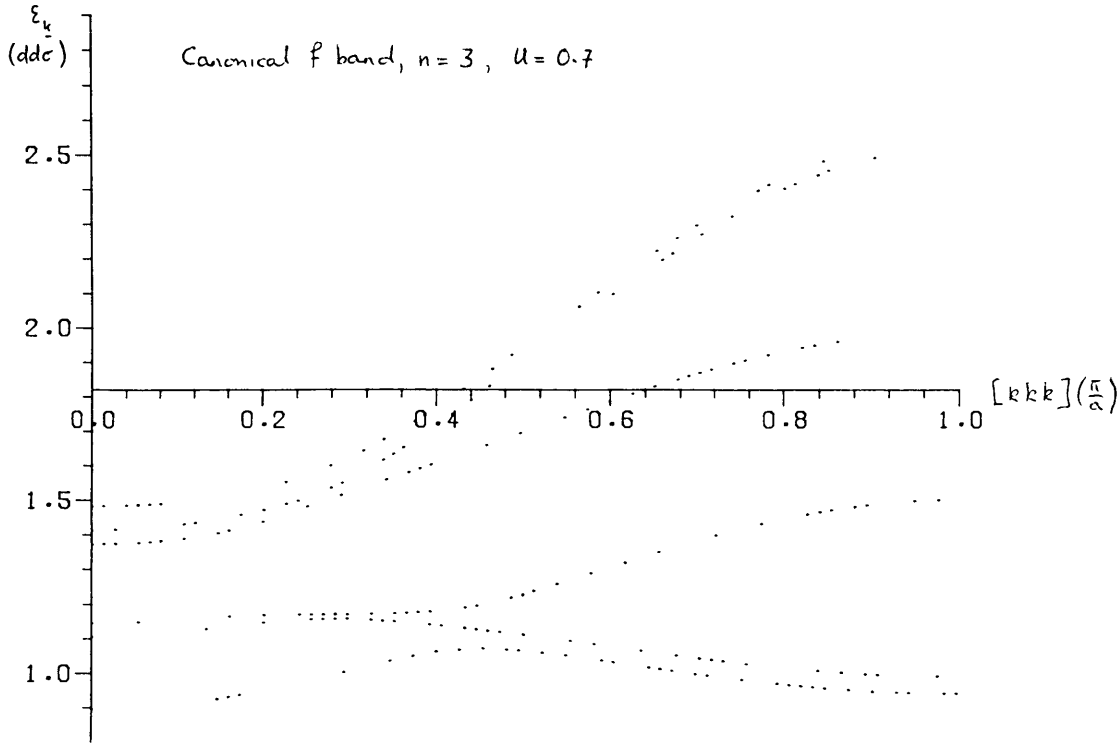

Figure 3.6 (c)

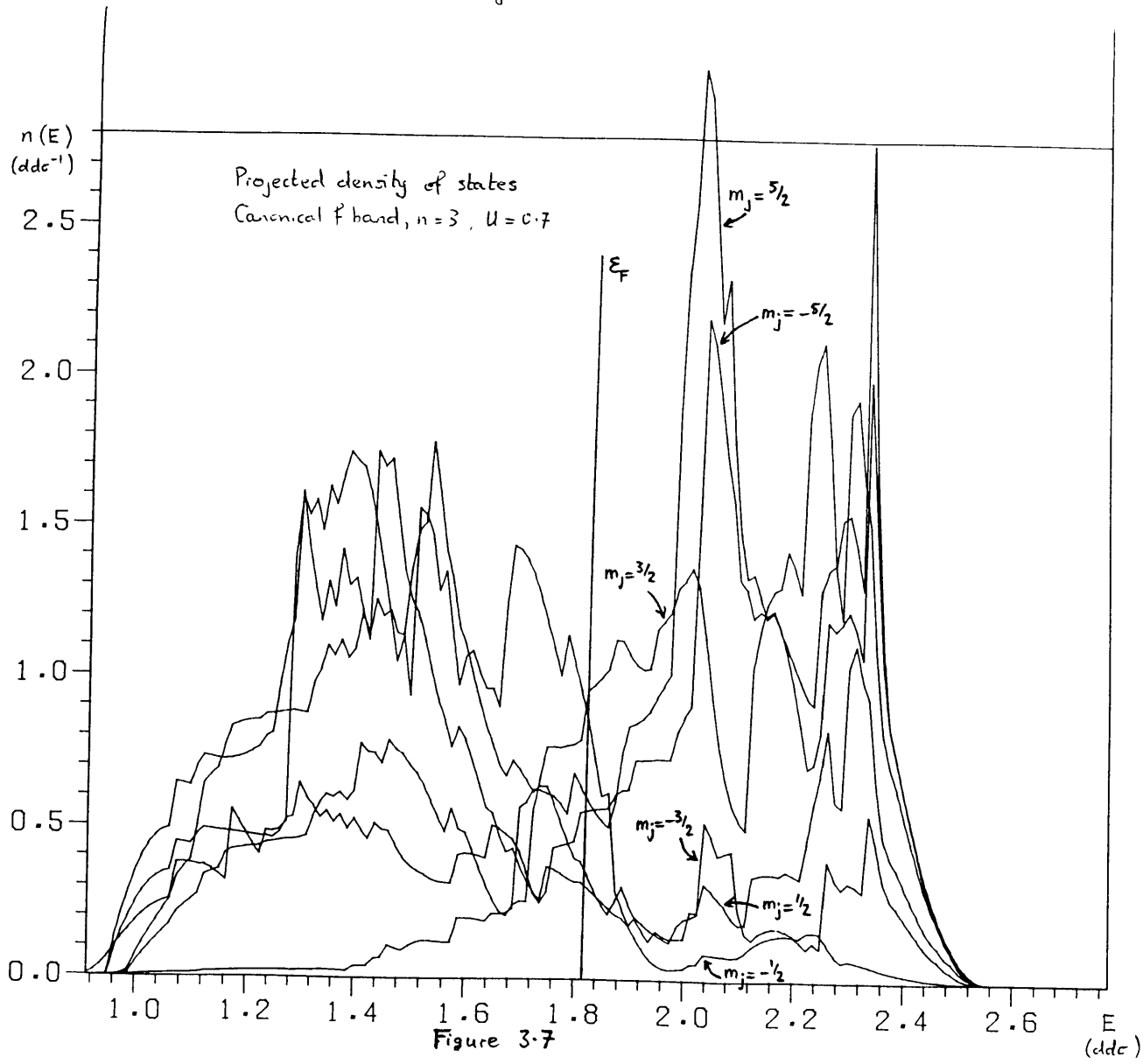

Figure 3.7

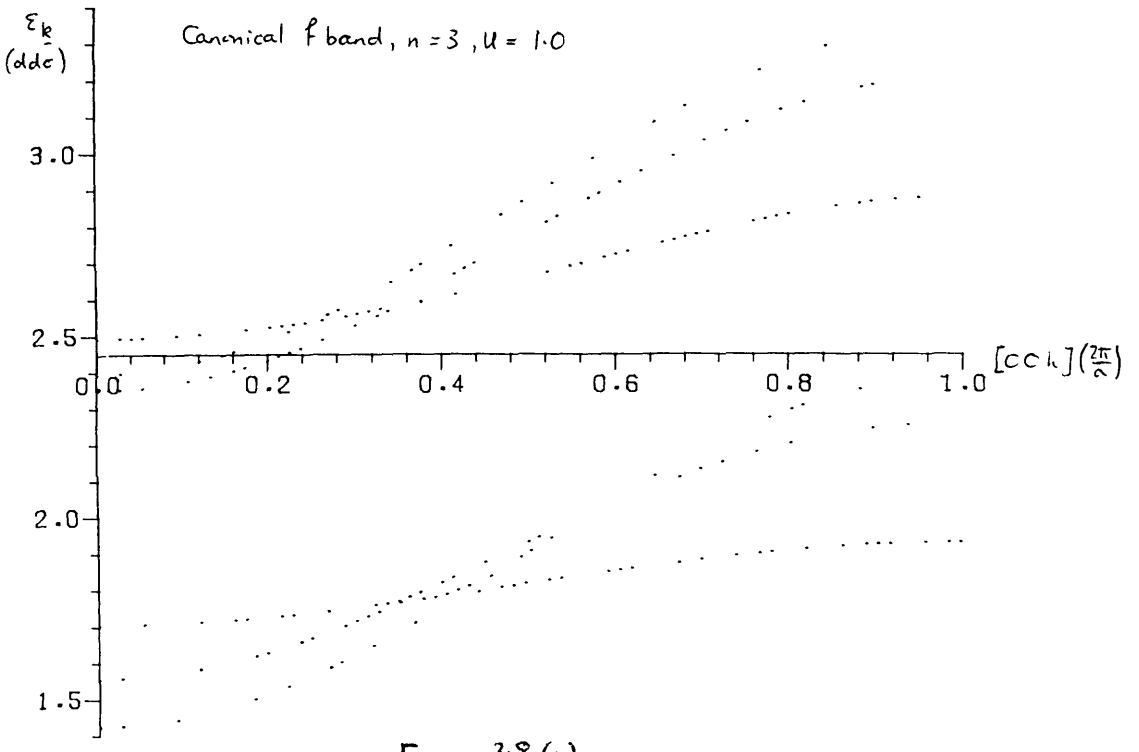

Figure 3.8 (a)

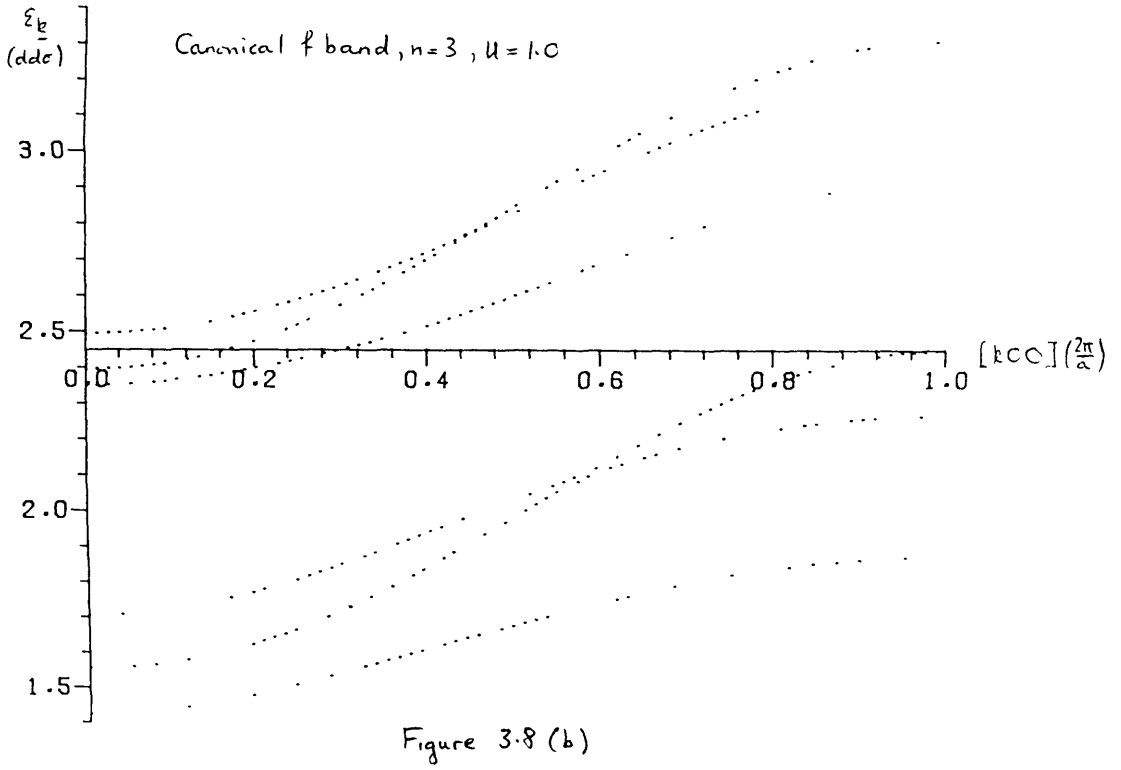

Figure 3.8 (b)

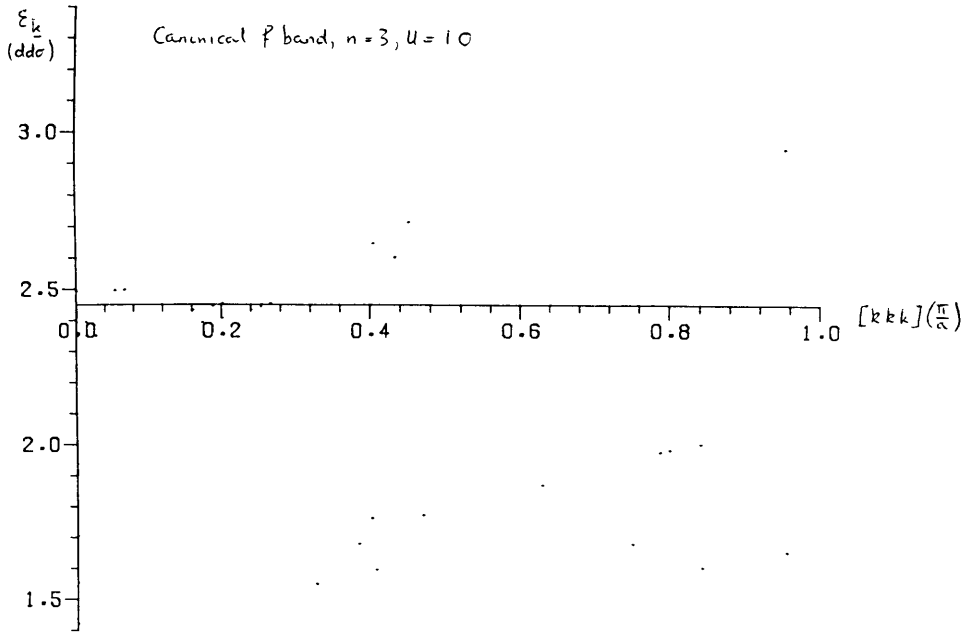

Figure 3.8 (c)

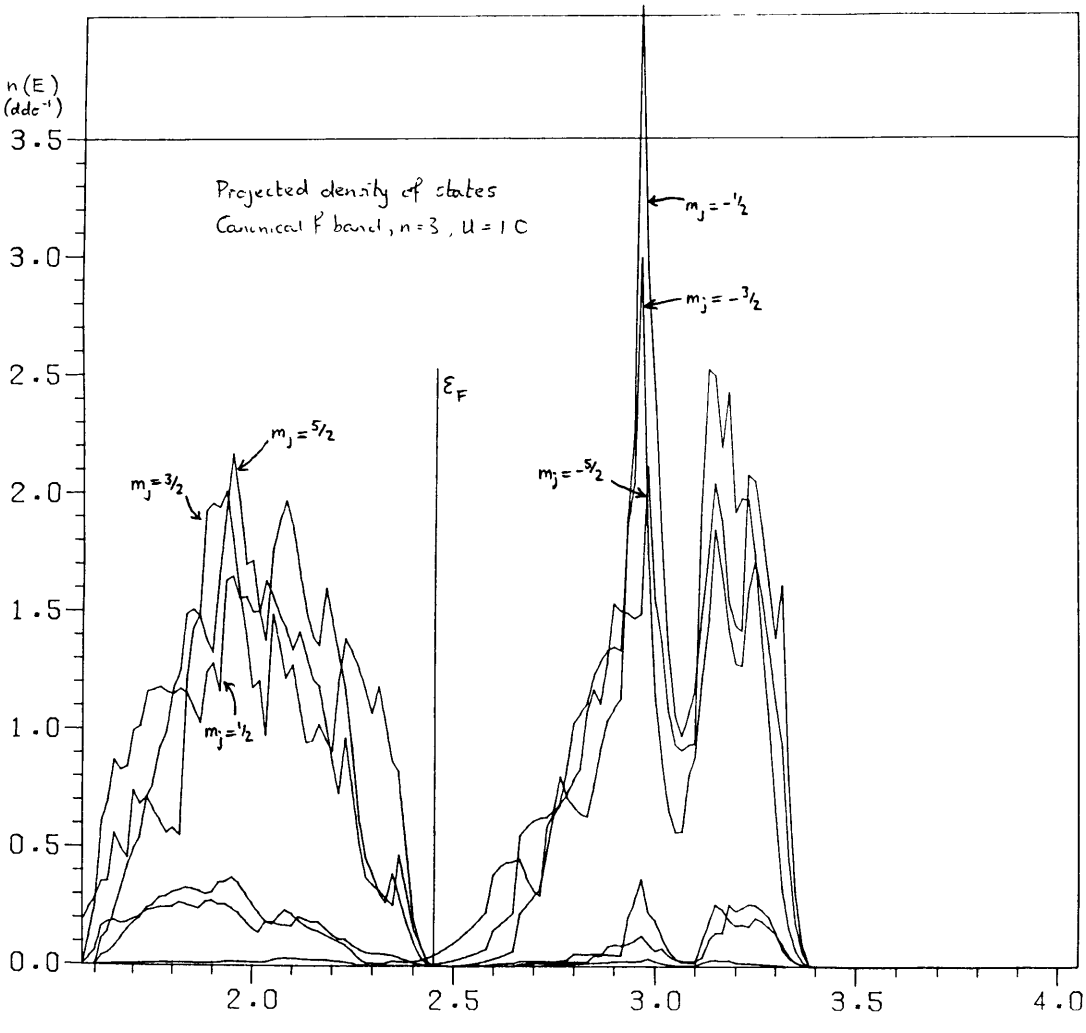

Figure 3.9

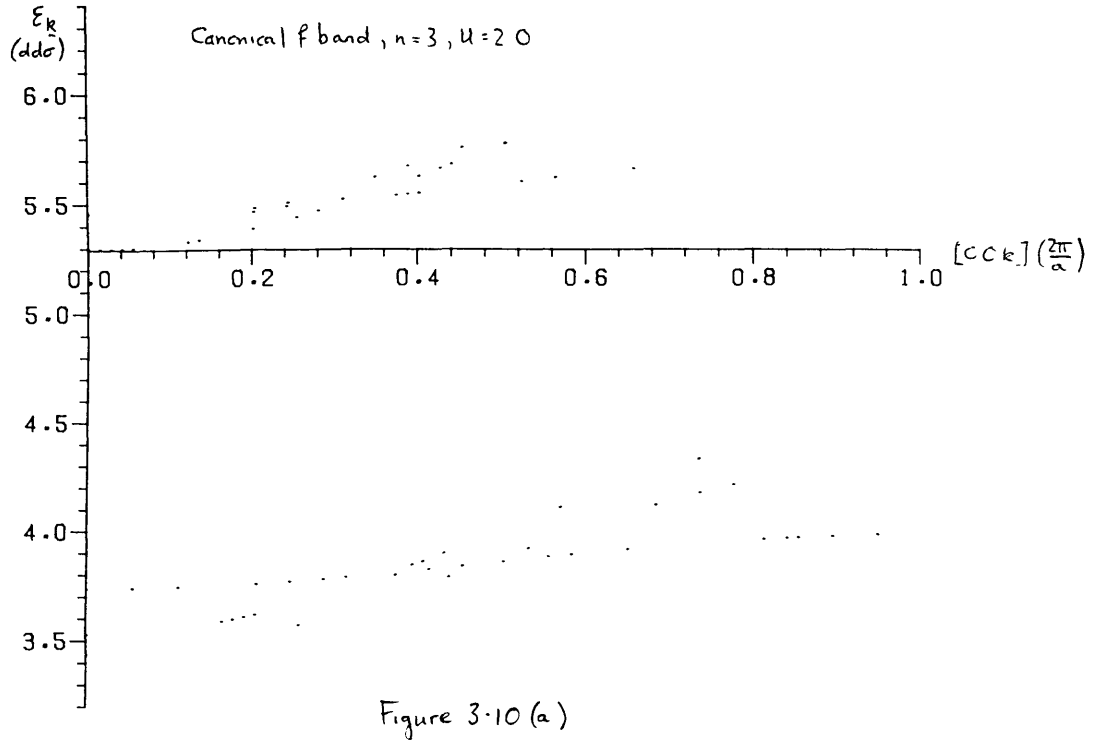

Figure 3·10 (a)

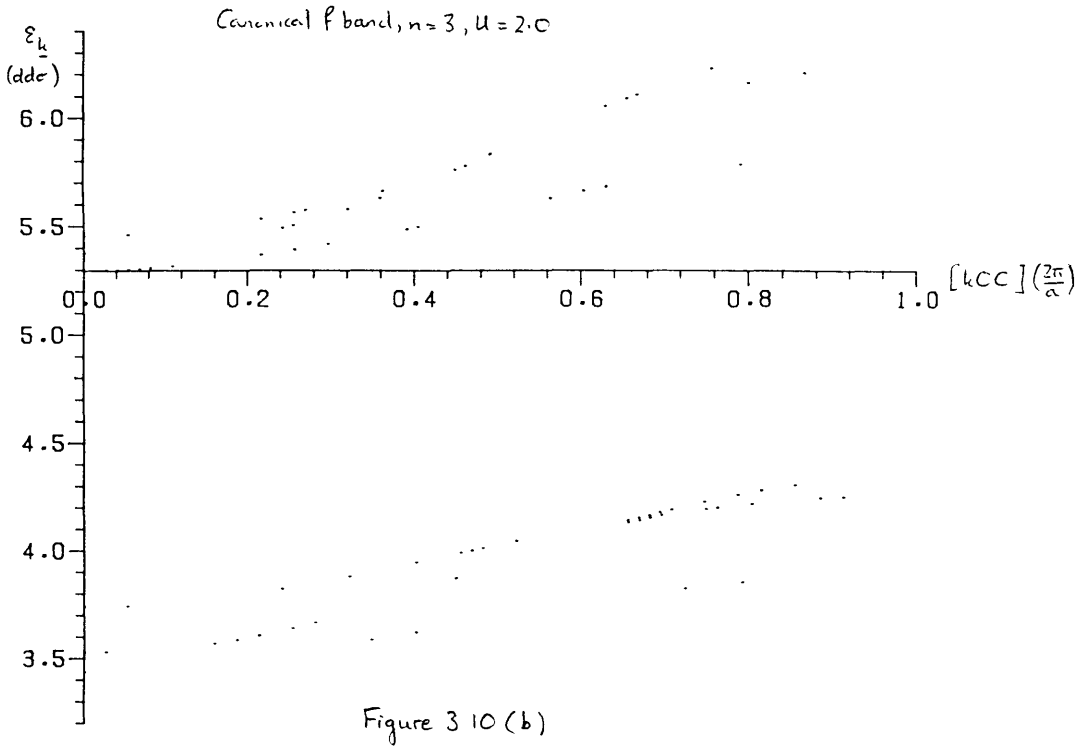

Figure 3.10 (b)

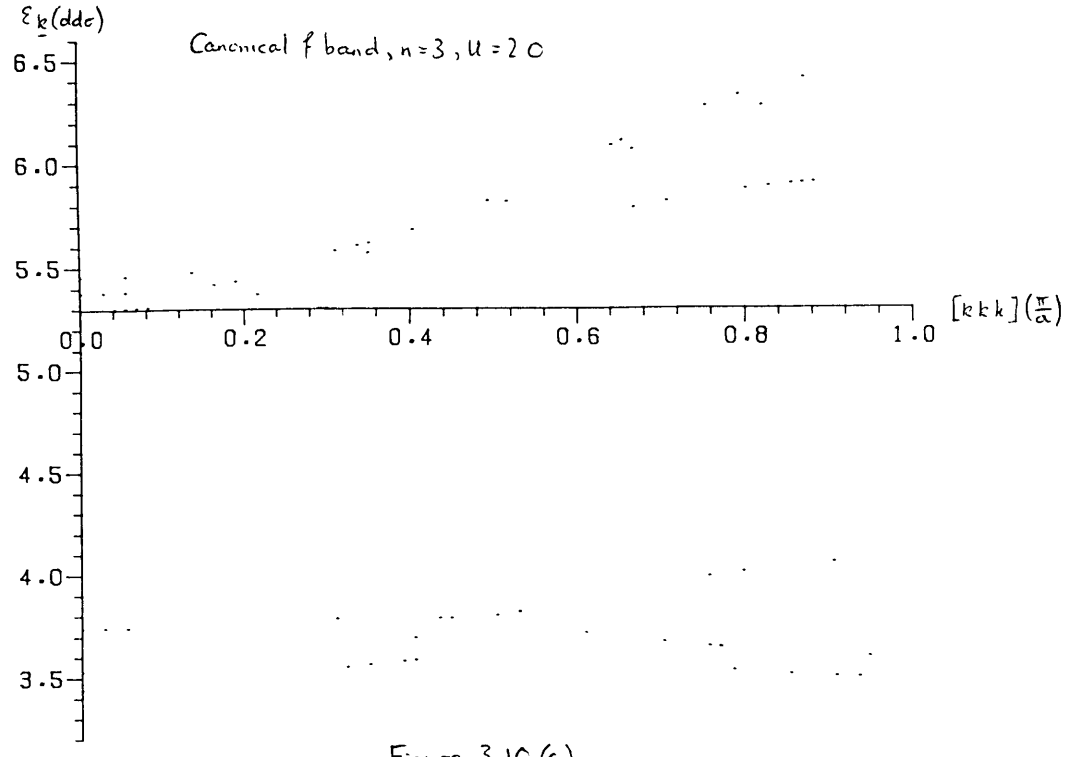

Figure 3 10 (c)

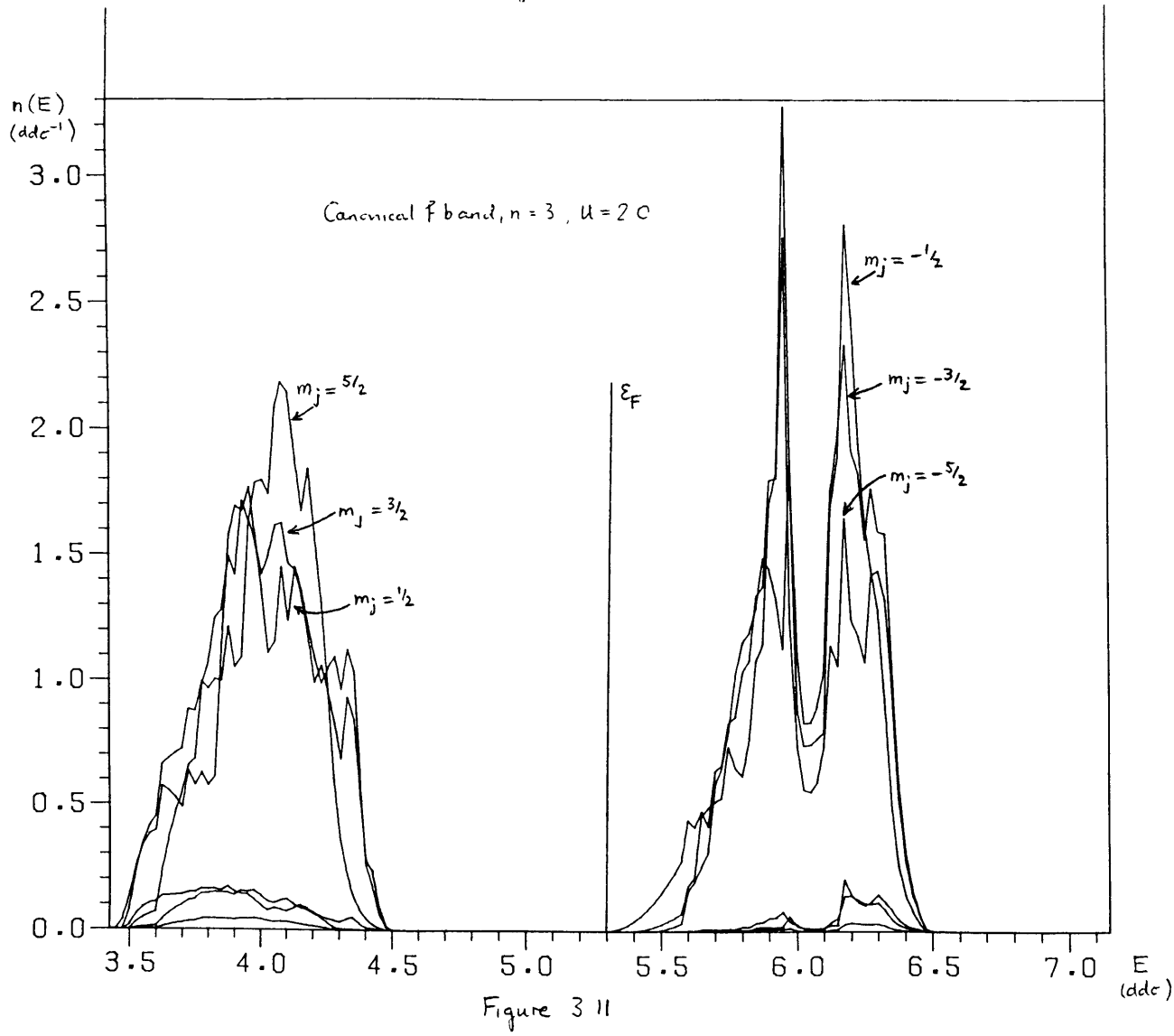

Figure 3 11

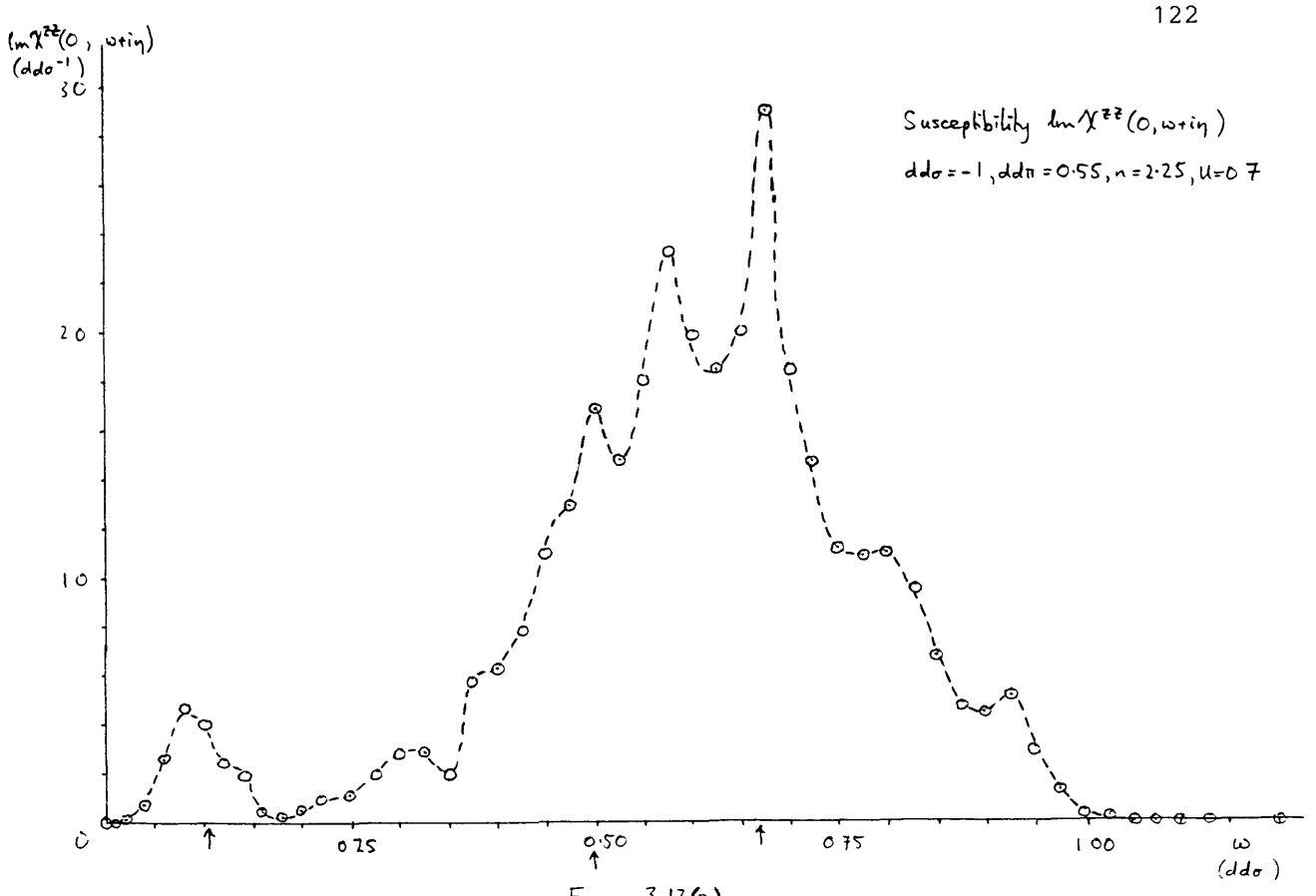

Figure 3 12(a)

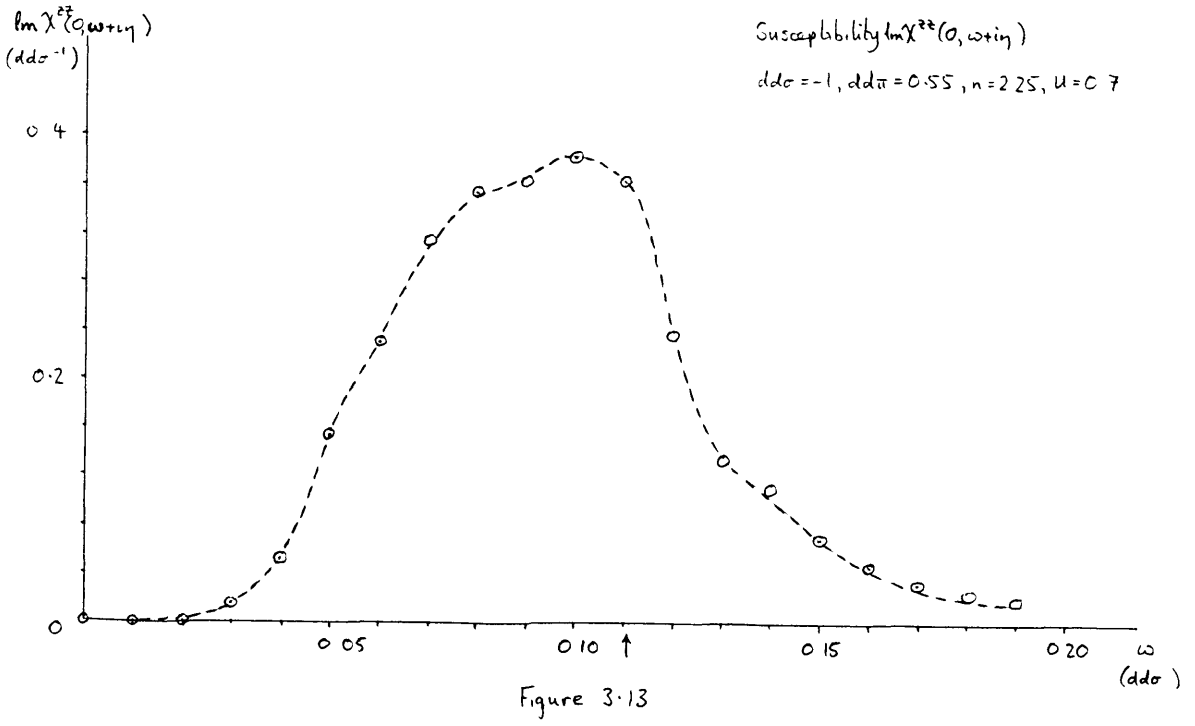

Figure 3·13

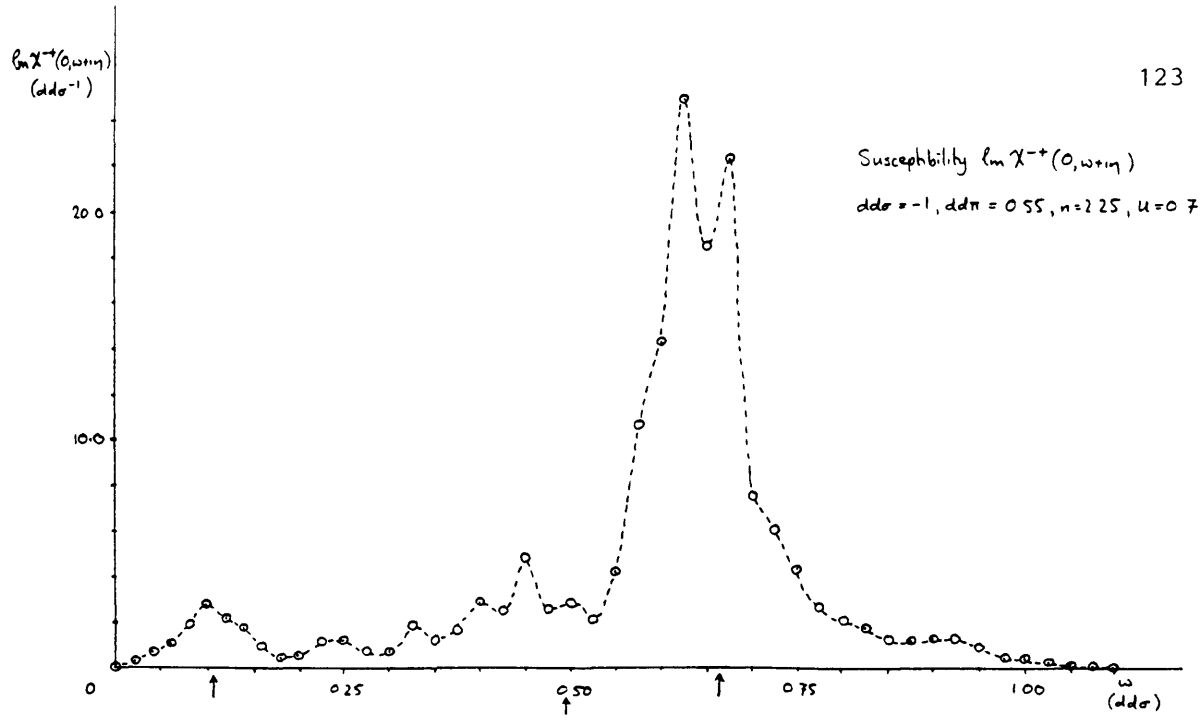

Figure 3.12 (b)

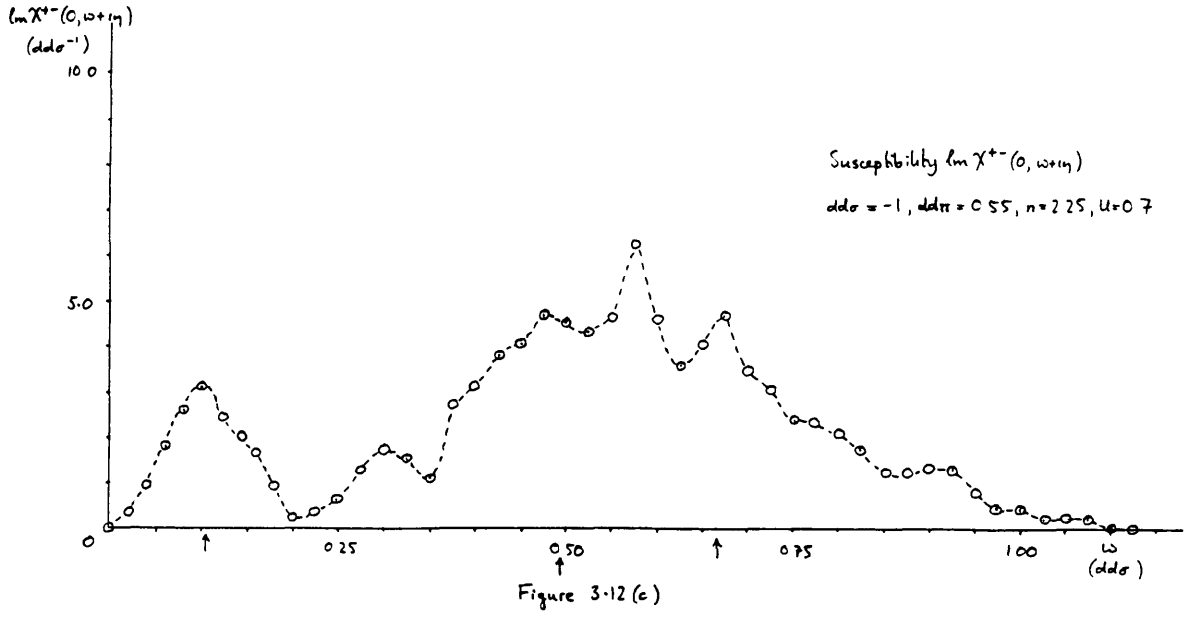

Figure 3.12 (c)

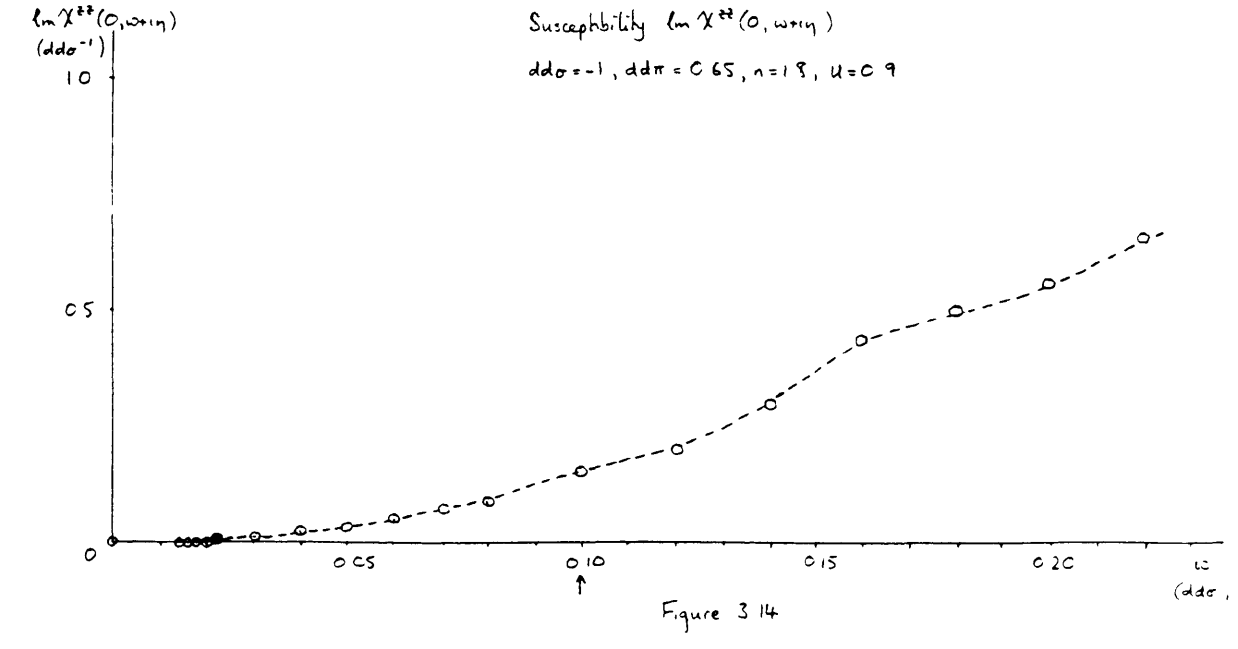

Figure 3.14

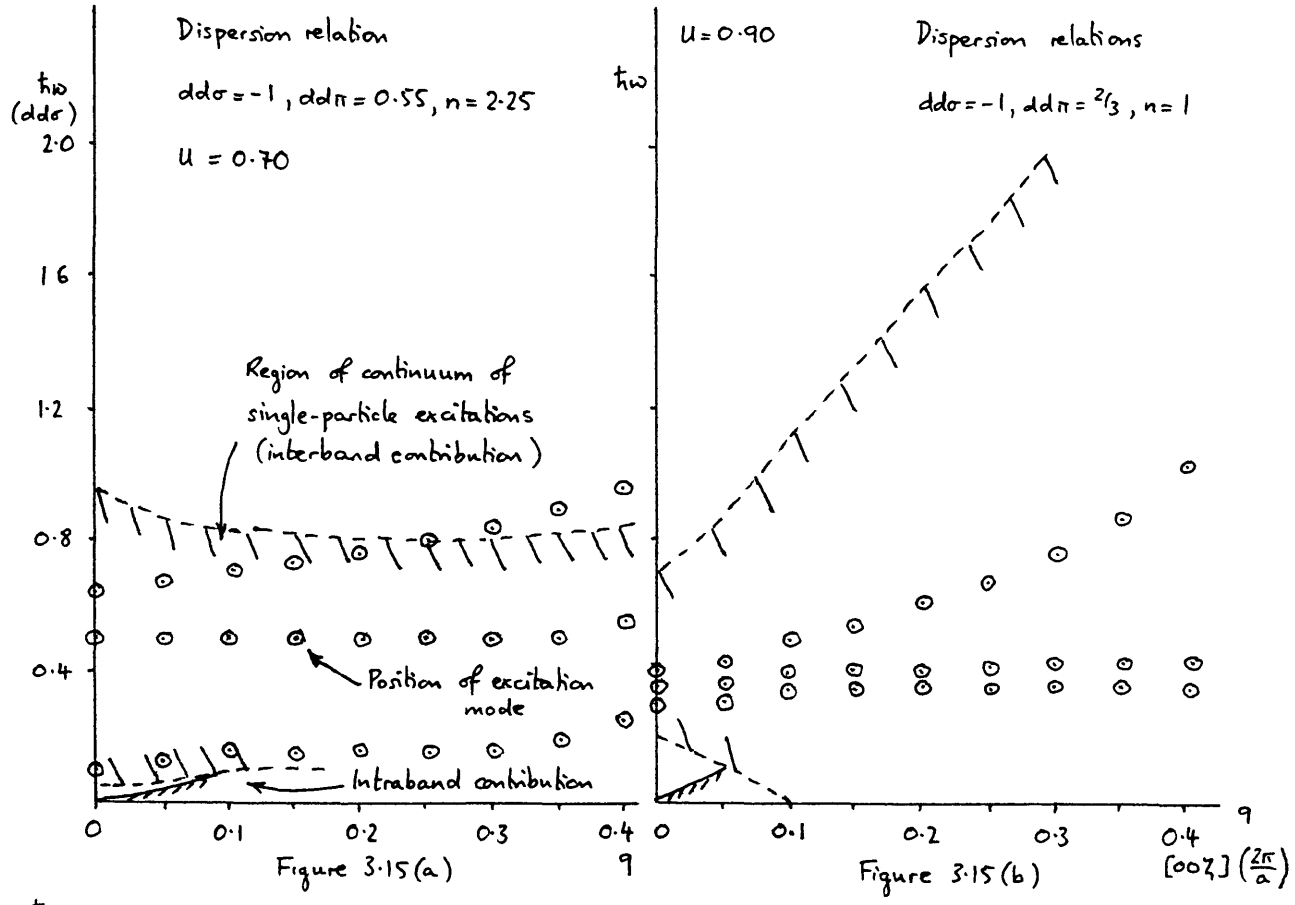

Figure 3.15(a)

Figure 3.15(b)

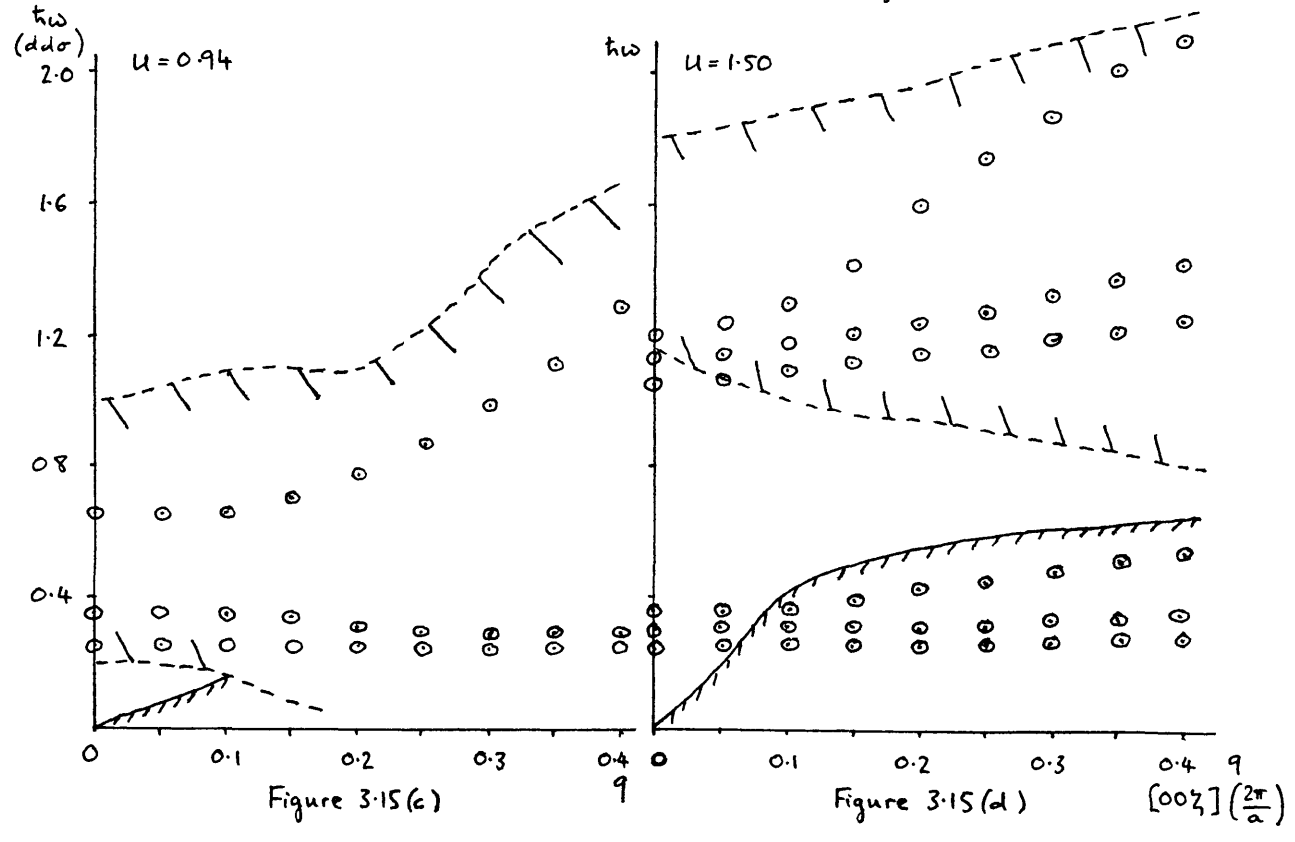

Figure 3.15(c)

Figure 3.15(d)

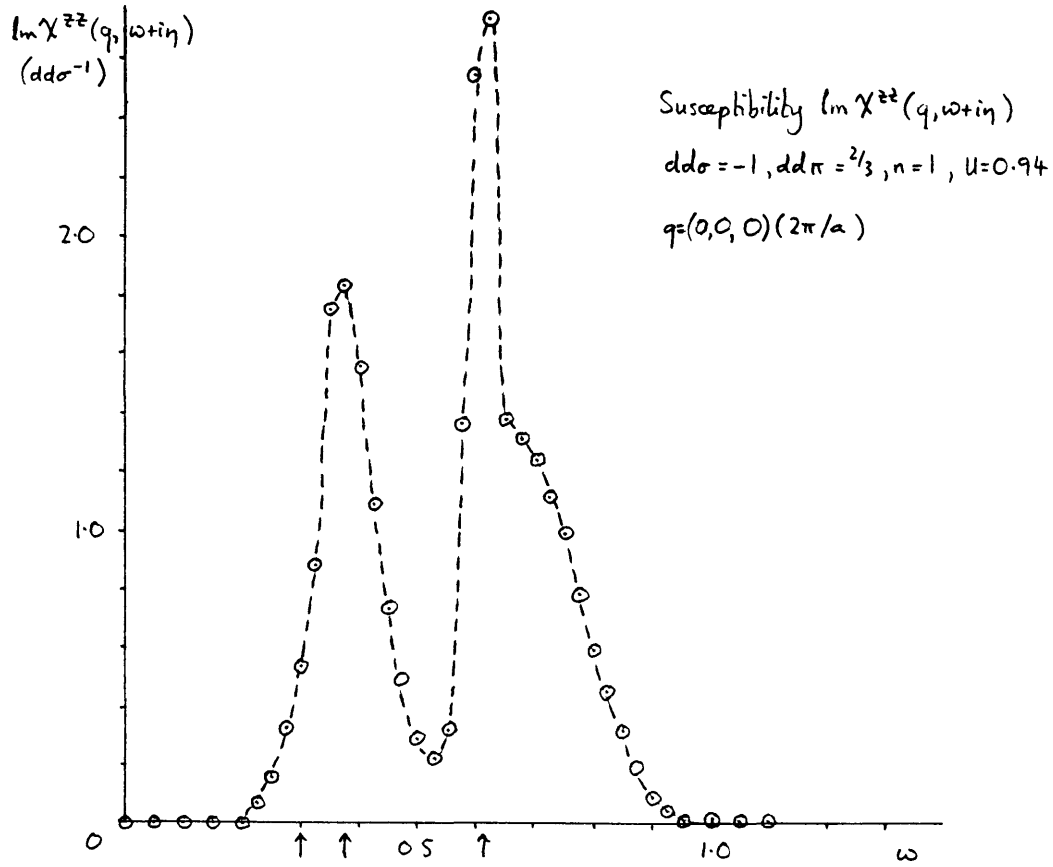

Figure 3·16 (a)

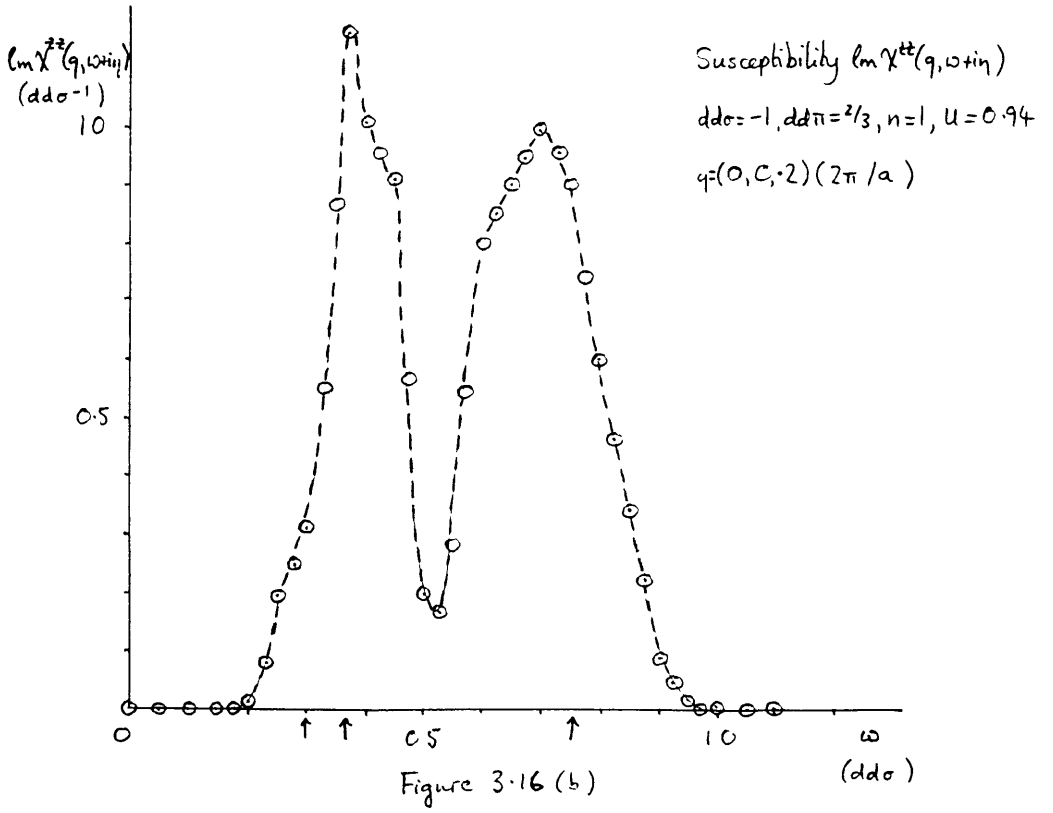

Figure 3·16 (b)

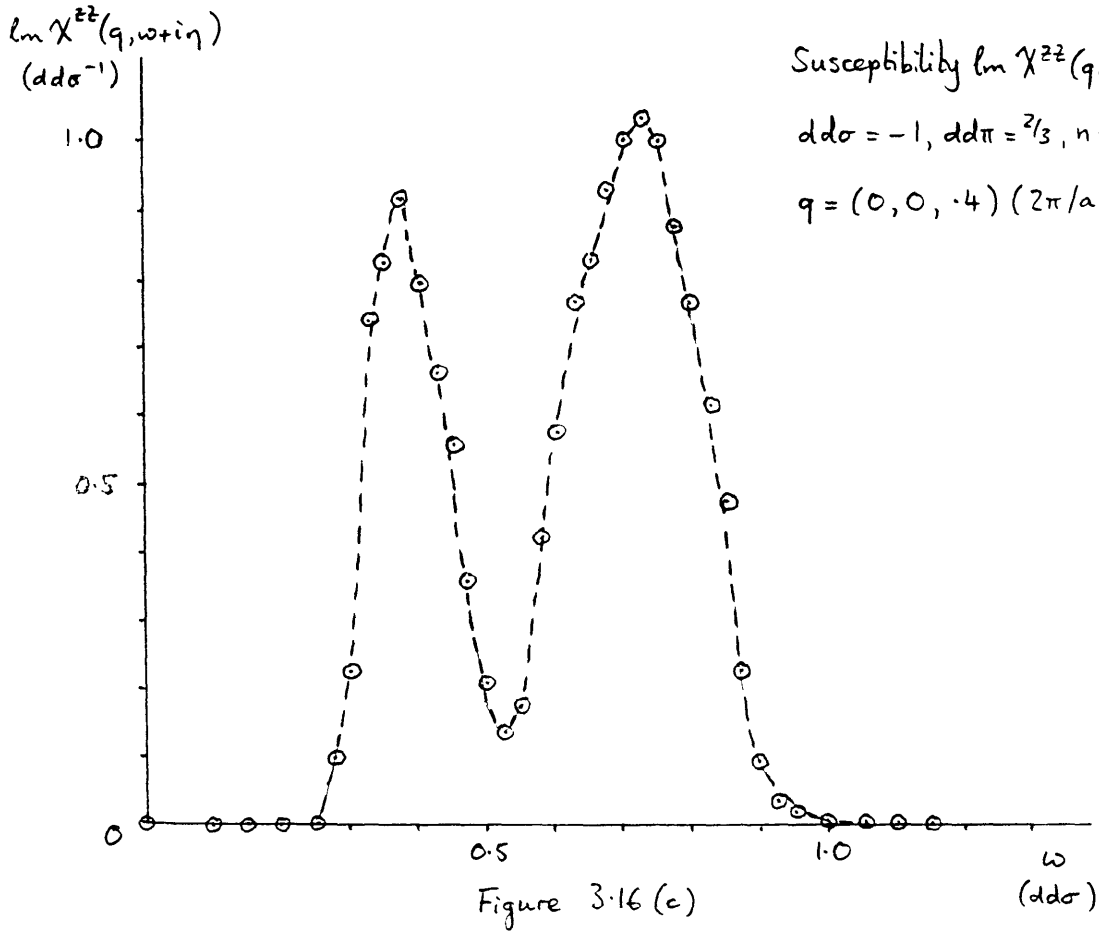
Im $\chi^{zz}(q,\omega+i\eta)$
(ddσ⁻¹)
1·0
0·5
0
0·5
1·0
ω
(ddσ)
Susceptibility Im $\chi^{zz}(q,\omega+i\eta)$
ddσ = −1, ddπ = 2/3, n = 1, U = 0·94
q = (0, 0, ·4) (2π/a)

Figure 3·16 (c)

CHAPTER 4

Magnetic excitations and the electron mass enhancement

4.1 Introduction

The previous chapters have shown how a model of actinide magnetism combining itinerancy and large spin-orbit coupling (assumed infinite) may be established, deriving the static and dynamic properties at the HF-RPA level of approximation. The excitation modes of the system interact with the itinerant electrons, and the effects of this upon the electrons are far from negligible in some cases. One important effect can be enhancement of the electron effective mass by interaction with an excitation mode lying at low energy, and we calculate the magnitude of this in this chapter. This enhancement is of interest because of the recent discovery of 'heavy-fermion' systems amongst actinide compounds, which display a range of highly unusual properties including exceptionally high mass enhancement of the electrons.

4.2 Heavy-fermion systems

Superconductivity in the high-effective-mass ($\sim 200\ m_e$) electrons in $CeCu_2Si_2$ was discovered by Steglich in 1979, and since then much effort has been spent in searching for and characterizing such 'heavy-fermion' systems. There are eight heavy-fermion systems presently known, including superconductors ($CeCu_2Si_2$, UBe_{13}, UPt_3), magnets ($NpBe_{13}$, U_2Zn_{17}, UCd_{11}) and materials with no apparent ordering ($CeAl_3$, $CeCu_6$). These f-electron materials can be seen (Table 4.1) to have enormous specific heat γ values (450-1600 mJ/mol K^2), large values of the low-temperature magnetic

susceptibility (8 - 50 x 10^{-3} emu/mol G), maxima in the resistivity at low temperatures with large ρ_{max} values (100-200 Ω cm) and unusual temperature dependencies of their specific heats below 10K. The experimental data currently available is fully reviewed in Stewart (1984). The three superconducting heavy fermion systems (HFS) possess such unusual properties that p-wave pairing of the superconducting electrons has been proposed, rather than BCS s-wave pairing.

Typically, the mass enhancement m*/m ~ 200 from γ, which means that m*/m is of the order of 30 times the band mass. The Wilson ratio R is of order unity in HFS, as it is for a non-interacting Fermi liquid with g = 2, J = 1/2 (i.e. spin only):

$$R = \frac{\pi^2 k^2 \chi(T=0)}{g^2 \mu_B^2 \gamma J(J+1)}$$

where k is the Boltzmann constant, g the Landé factor and μ_B the Bohr magneton for an electron. Thus χ is large due to a large quasi particle effective mass m*, and not because of exchange enhancement.

There are similarities in the behaviour of actinide HFS to that of ^{3}He, being a complex superfluid system with orbital degrees of freedom. The theory of the superfluid A and B phases of ^{3}He has been reviewed by Leggett (1975), and the orbital dynamics investigated by Leggett et al. (1976), Combescot et al. (1976) and Wölfle (1976).

Theoretical models which have currently emerged include three

Table 4.1.

	$d_{f\ atom-f\ atom}$ (Å)	γ (mJ/mol K^2)	T_c (superconducting) (K)
$CeCu_2Si_2$	4.1	1100	0.6
UBe_{13}	5.13	1100	0.97
UPt_3	4.1	452	0.54
$CeAl_3$	4.43	1620	no ordering above 0.05 K
$CeCu_6$	4.83	~ 1600	"
$NpBe_{13}$	5.13	Magnetic transitions below 10 K. Large estimated γ above magnetic ordering temperature	> 900 "
U_2Zn_{17}	4.39		535 "
UCd_{11}	6.56		840 "

types. A half-filled Hubbard band near a metal-insulator (localization) transition was considered by Brinkman and Rice (1970) using Gutzwiller's method and this was then applied by Vollhardt (1984) to ^{3}He systems. Secondly, a nearly-half-filled Hubbard band at high U was studied by Rice et al. (1985); in analogy with ^{3}He, and using Brinkman-Rice theory for a strongly correlated Fermi liquid, they argue (along with Anderson (1984)) that superconductivity in UBe_{13} is of a p-wave nature. Recently, Rice and Ueda (to be published) have investigated a periodic Anderson model whilst still using the Gutzwiller method.

The third approach has been to consider the Anderson lattice in the Kondo limit, and this has been pursued by Razafimandimby et al. (1984) with particular reference to $CeCu_2Si_2$. This model should apply to $CeCu_2Si_2$, which is generally thought to show Hubbard splitting in the f band between a peak corresponding to the f^1 final state and another corresponding to the f^2 final state, indicating high correlation effects. XPS-BIS measurements have also been performed on UBe_{13} by Wuilloud et al. (1984) and by contrast there is no clear separation of peaks, but merely one broad peak. This indicates weaker correlation in UBe_{13} than $CeCu_2Si_2$, and a reasonably broad 5f band, of order 3eV bandwidth. This situation in UBe_{13} and more particularly UPt_3 (Stewart (1984)), although no UPt_3 BIS measurements appear to be published to date, make it reasonable to adopt an itinerant model, treated at the HF-RPA level. Using the model considered in previous chapters we proceed to describe how mass enhancement may occur by interaction with low-lying excitation modes of the model. The possible types of mode include magnetic and quadrupolar; however, the quadrupolar

modes can be seen from equations (1.81)-(1.83) to be always lower in energy. Also, if $\rho(E_f)$ is the quasiparticle density of states and F_o^a the Landau parameter, then

$$\chi = \frac{2\mu_B^2 \rho(E_f)}{1 + F_o^a}$$

so that the strong exchange enhancement that occurs near to a ferromagnetic transition makes $\chi/\gamma \gg 1$; and for HFS the Wilson ratio is $\chi/\gamma \sim 1$. Thus, it is likely that mass enhancement effects in compounds like UPt_3 are best modelled within our formalism by considering interactions between the conduction electrons and a low-lying quadrupolar mode.

4.3 Magnetic excitations and the electronic mass enhancement

Conduction electrons can acquire an increase in their effective mass m* due to interactions with different low-lying excitations of the solid. Calculations have been done for mass enhancements due to the electron-phonon interaction (Abrikosov, Gorkov & Dzyaloshinski (1963)) or the interaction with paramagnons (Doniach & Engelsberg (1966)), in which the excitations occur in the conduction electron system itself. It has been shown that there is a similar mass enhancement mechanism by which magnetic excitons can contribute (White & Fulde (1981) and Fulde & Jensen (1983)). The effect of the mass enhancement on the specific heat was considered at finite temperature, and the theory generalized to ferromagnetically ordered systems.

In its simplest form the Green's function of an interacting electron system is given by $G(\underline{k},\omega)$ where

$$G(\underline{k},\omega) = \frac{1}{\omega - \varepsilon_{\underline{k}} - \Sigma(\underline{k},\omega)}$$

and $\varepsilon_{\underline{k}}$ is the kinetic energy of an electron of momentum $\underline{k}$ calculated from the Fermi surface, $\Sigma(\underline{k},\omega)$ the mass operator containing all irreducible scattering events of the electron with its surroundings. The quasiparticle excitations give rise to the poles of $G(\underline{k},\omega)$. The effective mass m* is defined for the excitations close to the Fermi surface at $\underline{k} = \underline{k}_f$, and is given by

$$\frac{1}{m^*} = \frac{1}{k_f} \left.\frac{\partial E(\underline{k})}{\partial \underline{k}}\right|_{\underline{k}=\underline{k}_f}$$

where E(k) are the poles of $G(\underline{k},\omega)$

$$E(\underline{k}) = \varepsilon_{\underline{k}} + \Sigma(\underline{k}, E(\underline{k}))$$

and so if

$$\frac{m}{k_f} \left.\frac{\partial \Sigma(\underline{k},\omega)}{\partial \underline{k}}\right|_{\underline{k}=\underline{k}_f} \ll 1$$

$$\frac{dE(\underline{k})}{dk} = \frac{d\varepsilon_k/dk}{1 - \left.\frac{\partial \Sigma}{\partial \varepsilon}\right|_{E_f}}$$

then

$$\frac{m^*}{m} = \frac{N^*(E_f)}{N(E_f)} = 1 - \left.\frac{\partial \Sigma(\underline{k}_f,\omega)}{\partial \omega}\right|_{\omega=0}$$

The fact that m*/m is real is ensured by the imaginary part of $\Sigma(\underline{k},\omega)$ vanishing like ω^2 for quasiparticles close to the Fermi surface. A substantial mass enhancement will occur when $\Sigma(\underline{k},\omega)$ results from interactions of conduction electrons with excitations of sufficiently low energies, so that $\Sigma(\underline{k},\omega)$ varies rapidly with ω

close to $\omega = 0$.

In the formalism used previously to derive the HF equations and RPA result, we require an expression for the $\underline{k}$ and ω dependence of $\Sigma_{\alpha\beta}(\underline{k},\omega)$, where α,β are orbitals in the (j,m_j) basis. The non-interacting Green's function $G^0_{\alpha\beta}(\underline{k},t)$ is defined as

$$G^0_{\alpha\beta}(\underline{k},t) = -i \langle T[c_{\underline{k}\alpha}(t)\, c^+_{\underline{k}\beta}(0)\,] \rangle \tag{4.1}$$

where

$$c^+_{\underline{k}\alpha} = \sum_n a^*_{n\alpha}(\underline{k})\, c^+_{\underline{k}n}$$

hence

$$\begin{aligned} G^0_{\alpha\beta}(\underline{k},t) &= -i \sum_{mn} a_{m\alpha}(\underline{k}) a^*_{n\beta}(\underline{k}) \langle T[c_{\underline{k}m}(t) c^+_{\underline{k}n}(0)] \rangle \\ &= \sum_n a_{n\alpha}(\underline{k}) a^*_{n\beta}(\underline{k}) G^0_n(k) \\ G^0_n(k) &= \delta_{mn} \langle T[c_{\underline{k}m}(t) c^+_{\underline{k}n}(0)] \rangle \end{aligned} \tag{4.2}$$

The second order contribution to $\Sigma_{\alpha\beta}$ of the diagram

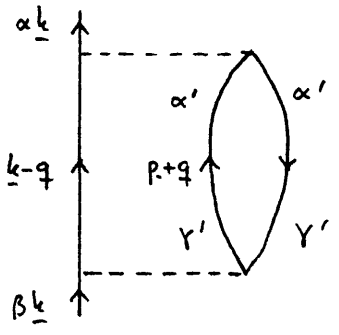

is, by the Feynman rules

$$\Sigma^{(2)}_{\alpha\beta}(k) = \left(\frac{i}{\hbar}\right)^2 (2\pi)^{-8}(-1) \sum_{\alpha'\gamma'} \int d^4p \int d^4q \left(\frac{U}{N}\right)^2 G^0_{\alpha\beta}(k-q)\, G^0_{\gamma'\alpha'}(p)\, G^0_{\alpha'\gamma'}(p+q) \tag{4.3}$$

The integral over p_0 can be expressed in terms of previously defined quantities $G_{\alpha\beta,\gamma\delta}(q,\omega)$, $\Gamma_{\alpha\beta,\delta\gamma}(q,\omega)$ as follows

$$\frac{1}{2\pi}\int dp_0\, G^0_{\gamma'\alpha'}(p)\,G^0_{\alpha'\gamma'}(p+q) = \sum_{mn} a_{m\gamma'}(p)\,a^*_{m\alpha'}(p)$$

$$a_{n\alpha'}(p+q)\,a^*_{n\gamma'}(p+q)\,\frac{1}{2\pi}\int dp_0\, G^0_m(p)\,G^0_n(p+q)$$

$$= i\sum_{mn}\left\{\frac{(1-f_{mp})f_{np+q}}{E_{np+q}-E_{mp}-q_0+i\eta} + \frac{f_{mp}(1-f_{np+q})}{E_{mp}-E_{np+q}+q_0+i\eta}\right\} \tag{4.4}$$

$$a_{m\gamma'}(p)\,a^*_{m\alpha'}(p)\,a_{n\alpha'}(p+q)\,a^*_{n\gamma'}(p+q)$$

and integrating over p completely, for unit volume,

$$\frac{1}{(2\pi)^4}\int d^4p\, G^0_{\alpha'\gamma'}(p)\,G^0_{\alpha'\gamma'}(p+q) = i\hbar\sum_{mnp} a_{m\gamma'}(p)\,a^*_{m\alpha'}(p)$$

$$a_{n\alpha'}(p+q)\,a^*_{n\gamma'}(p+q)\left\{\frac{(1-f_{mp})f_{np+q}}{E_{np+q}-E_{mp}-\hbar q_0+i\eta} + \frac{f_{mp}(1-f_{np+q})}{E_{mp}-E_{np+q}+\hbar q_0+i\eta}\right\} \tag{4.5}$$

$$= -i\hbar\,\Gamma^{(\tau)}_{\gamma'\gamma',\alpha'\alpha'}(q) \tag{4.6}$$

where the time-ordered non-interacting response function $\Gamma^{(\tau)}_{\alpha\beta,\delta\gamma}(q)$ is defined by

$$\Gamma^{(\tau)}_{\alpha\beta,\delta\gamma}(q) = -\sum_{mnp} a^*_{n\alpha}(p+q)\,a_{m\beta}(p)\,a^*_{m\gamma}(p)\,a_{n\delta}(p+q)$$

$$\left\{\frac{(1-f_{mp})f_{np+q}}{E_{np+q}-E_{mp}-\hbar q_0+i\eta} + \frac{f_{mp}(1-f_{np+q})}{E_{mp}-E_{np+q}+\hbar q_0+i\eta}\right\} \tag{4.7}$$

Therefore the contribution to $\Sigma^{(2)}_{\alpha\beta}(k)$ is

$$\Sigma^{(2)}_{\alpha\beta}(k) = -\frac{i}{\hbar}\left(\frac{U}{N}\right)^2\int\frac{d^4q}{(2\pi)^4}\,G^0_{\alpha\beta}(k-q)\,\Gamma^{(\tau)}_{\gamma'\gamma',\alpha'\alpha'}(q) \tag{4.8}$$

for this single second-order diagram. More generally we can consider the set of diagrams

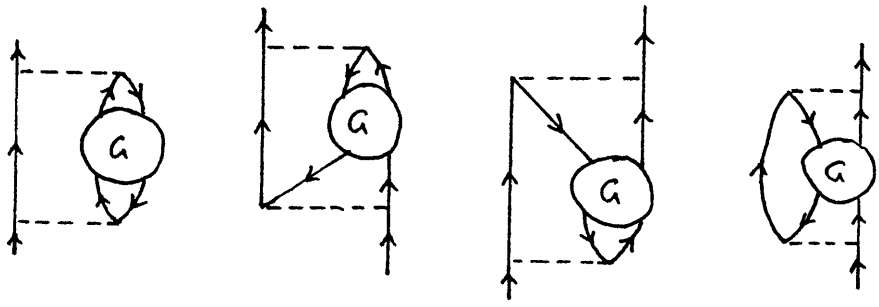

where G is a general interaction representing the RPA ladder. Thus, for the second-order diagrams

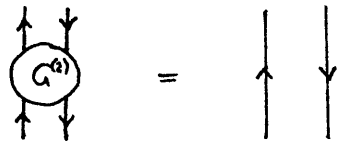

which means that these diagrams are double-counted in the series, and for the third-order diagrams

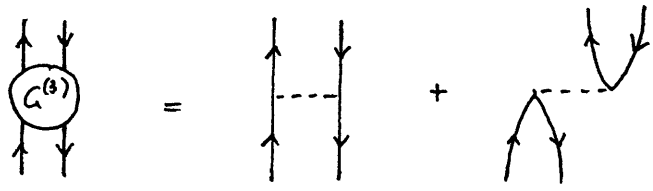

so that these (and, incidentally, all higher order) diagrams are unique. Removing the double-counting of the second-order diagrams gives for the full contribution to the self-energy $\Sigma_{\alpha\beta}(k)$

$$\Sigma_{\alpha\beta}(k) = \Sigma^{HF}_{\alpha\beta}(k) - \frac{i}{\hbar}\left(\frac{U}{N}\right)^2 \sum_{\substack{\xi\mu \\ \alpha'\beta'\gamma'\delta'}} (\delta_{\alpha\xi}\delta_{\beta'\alpha'} - \delta_{\alpha\alpha'}\delta_{\beta'\xi})$$

$$\times (\delta_{\beta\mu}\delta_{\gamma'\delta'} - \delta_{\beta\gamma'}\delta_{\mu\delta'}) \int d^4q \frac{1}{(2\pi)^4} G^0_{\xi\mu}(k-q)\left\{G^{(\tau)}_{\gamma'\delta',\beta'\alpha'}(q) - \frac{1}{2}\Gamma_{\gamma'\delta',\alpha'\beta'}(q)\right\} \quad (4.9)$$

where $G^{(\tau)}_{\alpha\beta,\gamma\delta}(q)$ is the interacting time-ordered response function corresponding to $\Gamma^{(\tau)}_{\alpha\beta,\delta\gamma}(q)$.

The non-local nature of $\Sigma_{\alpha\beta}(\underline{k},\omega)$ is an awkward complication which may be removed. Calculations of the dispersion curves for the quadrupolar mode lying at low energy, for example Figure 4.12, show that the modes vary little in energy with $\underline{q}$. This indicates that a straightforward local approximation $\Sigma_{\alpha\beta}(\omega)$ to the self-energy correction to HF would be reasonably good:

$$\Sigma_{\alpha\beta}(\omega) = \frac{1}{N}\sum_{\underline{k}}\left[\Sigma_{\alpha\beta}(\underline{k},\omega) - \Sigma^{HF}_{\alpha\beta}(\underline{k},\omega)\right] \qquad (4.10)$$

Defining a local interacting susceptibility $T_{\gamma'\delta',\alpha'\beta'}(\omega-\omega')$ by

$$T_{\gamma'\delta',\alpha'\beta'}(\omega-\omega') = \frac{1}{N}\sum_{\underline{k}}\left\{G^{(\tau)}_{\gamma'\delta',\beta'\alpha'}(\underline{k},\omega-\omega') - \frac{1}{2}\Gamma^{(\tau)}_{\gamma'\delta',\alpha'\beta'}(\underline{k},\omega-\omega')\right\} \qquad (4.11)$$

we can rewrite equation (4.9) as

$$\Sigma_{\alpha\beta}(\omega) = -\frac{i}{\hbar}\left(\frac{U}{N}\right)^2 \sum_{\substack{\xi\mu \\ \alpha'\beta'\gamma'\delta'}} (\delta_{\alpha\xi}\delta_{\beta'\alpha'} - \delta_{\alpha\alpha'}\delta_{\beta'\xi})(\delta_{\beta\mu}\delta_{\gamma'\delta'} - \delta_{\beta\gamma'}\delta_{\mu\delta'})$$

$$\frac{1}{(2\pi)^4}\int d^3k'\,d\omega'\; T_{\gamma'\delta',\alpha'\beta'}(\omega-\omega')\,G^{\circ}_{\xi\mu}(\underline{k}',\omega') \qquad (4.12)$$

On differentiating this equation with respect to ω at $\omega=0$ we obtain

$$\left.\frac{\partial\Sigma_{\alpha\beta}(\omega)}{\partial\omega}\right|_{\omega=0} = -\frac{i}{\hbar}\left(\frac{U}{N}\right)^2 \sum_{\substack{\xi\mu \\ \alpha'\beta'\gamma'\delta'}} (\delta_{\alpha\xi}\delta_{\beta'\alpha'} - \delta_{\alpha\alpha'}\delta_{\beta'\xi})$$

$$(\delta_{\beta\mu}\delta_{\gamma'\delta'} - \delta_{\beta\gamma'}\delta_{\gamma\delta'}) \int \frac{d^3k'\,d\omega'}{(2\pi)^4}\, T_{\gamma'\delta',\alpha'\beta'}(-\omega')\frac{\partial}{\partial\omega'}G^{\circ}_{\xi\mu}(\underline{k}',\omega') \qquad (4.13)$$

Considering $G^{\circ}_{\xi\mu}(\underline{k}',\omega')$, from its definition by equation (4.2),

$$G^{\circ}_{\xi\mu}(\underline{k}',\omega') = \sum_n a_{n\xi}(\underline{k}')\, a^{*}_{n\mu}(\underline{k}')\, G^{\circ}_{n}(\underline{k}',\omega') \tag{4.14}$$

$$= \sum_n a_{n\xi}(\underline{k}')\, a^{*}_{n\mu}(\underline{k}') \left\{ \frac{\theta(\omega')}{\omega' - \hbar^{-1}E_{n\underline{k}'} + i\delta} + \frac{\theta(-\omega')}{\omega' - \hbar^{-1}E_{n\underline{k}'} - i\delta} \right\} \tag{4.15}$$

so that on differentiation

$$\frac{\partial G^{\circ}_{\xi\mu}(\underline{k}',\omega')}{\partial\omega'} = \sum_n a_{n\xi}(\underline{k}')\, a^{*}_{n\mu}(\underline{k}') \left\{ \frac{\delta(\omega')}{\omega' - \hbar^{-1}E_{n\underline{k}'} + i\delta} \right.$$

$$\left. + \frac{\delta(-\omega')}{\omega' - \hbar^{-1}E_{n\underline{k}'} - i\delta} - \frac{\theta(\omega')}{(\omega' - \hbar^{-1}E_{n\underline{k}'} + i\delta)^2} - \frac{\theta(-\omega')}{(\omega' - \hbar^{-1}E_{n\underline{k}'} - i\delta)^2} \right\} \tag{4.16}$$

We now wish to make an approximation which is equivalent to the following:

$$\int dE_{\underline{k}'} \frac{\partial}{\partial\omega'} G(\underline{k}',\omega') = -2\pi i\,\delta(\omega') - \left[\frac{\theta(\omega')}{\omega' - E_{\underline{k}'} + i\delta} + \frac{\theta(-\omega')}{\omega' - E_{\underline{k}'} - i\delta} \right]_{-\mu}^{\infty}$$

$$= -2\pi i\,\delta(\omega') + \frac{2}{\omega' + \mu}$$

$$\simeq -2\pi i\,\delta(\omega')$$

where μ is the Fermi energy. From equation (4.16), then

$$\frac{\partial}{\partial\omega'} G^{\circ}_{\xi\mu}(\underline{k}',\omega') \simeq \sum_n a_{n\xi}(\underline{k}')\, a^{*}_{n\mu}(\underline{k}') \left\{ \frac{1}{-\hbar^{-1}E_{n\underline{k}'} + i\delta} + \frac{1}{\hbar^{-1}E_{n\underline{k}'} + i\delta} \right\} \delta(\omega') \tag{4.17}$$

$$\simeq \sum_n a_{n\xi}(\underline{k}')\, a^{*}_{n\mu}(\underline{k}') \left\{ -2\pi i\hbar\,\delta(E_{n\underline{k}'})\,\delta(\omega') \right\} \tag{4.18}$$

provided the term $2/(\omega'+\mu)$ is small. Therefore equation (4.13) can be approximated by

$$\left.\frac{\partial \sum_{\alpha\beta}(\omega)}{\partial\omega}\right|_{\omega=0} \simeq -\frac{i}{\hbar}\left(\frac{U}{N}\right)^2 \sum_{\substack{\xi\mu \\ \alpha'\beta'\gamma'\delta'}} (\delta_{\alpha\xi}\delta_{\beta'\alpha'} - \delta_{\alpha\alpha'}\delta_{\beta'\xi})$$

$$\times(\delta_{\beta\mu}\delta_{\gamma'\delta'} - \delta_{\beta\gamma'}\delta_{\mu\delta'}) \int \frac{d^3k'}{(2\pi)^3}(-i\hbar)\sum_n a_{n\xi}(\underline{k}')\, a_{n\mu}(\underline{k}')\,\delta(E_{nk'})\, T_{\gamma'\delta',\alpha'\beta'}(0) \tag{4.19}$$

$$\simeq -\frac{i}{\hbar}\left(\frac{U}{N}\right)^2 \sum_{\substack{\xi\mu \\ \alpha'\beta'\gamma'\delta'}} (\delta_{\alpha\xi}\delta_{\beta'\alpha'} - \delta_{\alpha\alpha'}\delta_{\beta'\xi'})(\delta_{\beta\mu}\delta_{\gamma'\delta'} - \delta_{\beta\gamma'}\delta_{\mu\delta'})$$

$$(-i\hbar)\frac{N}{4}\, N(0)\, \delta_{\xi\mu}\, T_{\gamma'\delta',\alpha'\beta'}(0) \tag{4.20}$$

where N(O) is the density of states at the Fermi surface. Therefore, on simplifying this expression,

$$\left.\frac{\partial \sum_{\alpha\beta}(\omega)}{\partial\omega}\right|_{\omega=0} = -\frac{1}{4}U^2 N(0) \sum_{\xi\alpha'\beta'\gamma'\delta'} (\delta_{\alpha\xi}\delta_{\beta'\alpha'} - \delta_{\alpha\alpha'}\delta_{\beta'\xi})$$

$$(\delta_{\beta\xi}\delta_{\gamma'\delta'} - \delta_{\beta\gamma'}\delta_{\xi\delta'})\frac{1}{N}\, T_{\gamma'\delta',\alpha'\beta'}(0) \tag{4.21}$$

$$= -\frac{1}{4}U^2 N(0) \sum_{\alpha'\beta'\gamma'\delta'} (\delta_{\alpha\beta}\delta_{\beta'\alpha'}\delta_{\gamma'\delta'} + \delta_{\beta'\delta'}\delta_{\alpha\alpha'}\delta_{\beta\gamma'}$$

$$- \delta_{\beta\beta'}\delta_{\alpha\alpha'}\delta_{\gamma'\delta'} - \delta_{\alpha\delta'}\delta_{\beta'\alpha'}\delta_{\beta\gamma'})\frac{1}{N}\, T_{\gamma'\delta',\alpha'\beta'}(0) \tag{4.22}$$

Using $t_{\gamma'\delta',\alpha'\beta'}$, defined by

$$t_{\gamma'\delta',\alpha'\beta'} = \frac{1}{N}\, T_{\gamma'\delta',\alpha'\beta'}(0) \tag{4.23}$$

the derivative of the self-energy is

$$\left.\frac{\partial \Sigma_{\alpha\beta}}{\partial \omega}\right|_{\omega=0} = -\frac{1}{4} U^2 N(0) \left\{ \delta_{\alpha\beta} \sum_{\alpha'\gamma'} t_{\gamma'\gamma',\alpha'\alpha'} + \sum_{\beta'} t_{\beta\beta',\alpha\beta'} - \sum_{\gamma'} t_{\gamma'\gamma',\alpha\beta} - \sum_{\alpha'} t_{\beta\alpha,\alpha'\alpha'} \right\} \quad (4.24)$$

The local nature of the self-energy means that we would expect it to be diagonal. This is true when U = 0 as $\sum_q \Gamma_{\alpha\beta,\gamma\delta}(q,\omega)$ only has non-zero terms of the form $\Gamma_{\alpha\beta,\alpha\beta}$, so that only $t_{\alpha\beta,\alpha\beta} \neq 0$ in equation (4.24). However, it is not clear when U ≠ 0 how to prove that $\sum_q G_{\alpha\beta,\delta\gamma}(q,\omega)$ only has non-zero terms $G_{\alpha\beta,\beta\alpha}$. In practice, numerical calculations show that this is true, and therefore from equation (4.24)

$$\left.\frac{\partial \Sigma_{\alpha\beta}(\omega)}{\partial \omega}\right|_{\omega=0} = -\frac{1}{4} U^2 N(0) \delta_{\alpha\beta} \sum_{\gamma'} \left\{ \sum_{\alpha'} t_{\gamma'\gamma',\alpha'\alpha'} + t_{\beta\gamma',\alpha\gamma'} - t_{\gamma'\gamma',\alpha\beta} - t_{\beta\alpha,\gamma'\gamma'} \right\} \quad (4.25)$$

Numerically we also find that this expression (4.25) is independent of α, and therefore the appropriate expression for the mass enhancement m*/m derived from a local self-energy is

$$\frac{m^*}{m} = 1 - \frac{1}{4} \mathrm{tr} \left.\frac{\partial \Sigma_{\alpha\alpha}}{\partial \omega}\right|_{\omega=0}$$

$$= 1 + \frac{1}{16} U^2 N(0) \sum_{\alpha'\gamma'} \left(2 t_{\gamma'\gamma',\alpha'\alpha'} + t_{\alpha'\gamma',\alpha'\gamma'} \right) \quad (4.26)$$

which may be evaluated from the RPA calculations of $\Gamma_{\alpha\beta,\gamma\delta}(q,0)$ and $C_{\alpha\beta,\delta\gamma}(q,0)$.

4.4 Computational results

In the previous section an expression was derived for the mass enhancement m*/m in terms of the matrix $t_{\alpha\beta,\gamma\delta}$

$$\frac{m^*}{m} = 1 + \frac{1}{16} U^2 N(0) \sum_{\alpha'\gamma'} (2 t_{\gamma'\gamma',\alpha'\alpha'} + t_{\alpha'\gamma',\alpha'\gamma'})$$

As mentioned in the introduction to this chapter, this expression may become large close to a second-order phase transition, whether magnetic or quadrupolar, but it is the latter that is particularly of interest. This is because interaction with a non-magnetic low-lying mode can enhance m*/m whilst leaving the Wilson ratio close to unity; also the lowest-lying mode is quadrupolar, as described in section 1.9. However, as shown in section 2.2, when considering phase transitions to ordered states, quadrupolar ordering occurs as a first-order phase transition due to the finite cubic term in Q in the Landau expansion. Therefore, a set of parameters for the model was sought which gave rise to the Stoner criterion for the quadrupolar mode being lowest ($U_{nm} < U_p, U_c$), with the first-order phase transition occurring at a value of U only slightly lower than U_{nm}. This would allow a region of U values for which the ground state was paramagnetic but still quite close to a quadrupolar second-order phase transition, with divergence of the $t_{\alpha\beta,\gamma\delta}$.

Table 4.2 shows a range of cases considered; any solutions having U_{nm} reasonably large and N(0) not too small were of interest,

including two sets of parameters which fulfilled the criteria and gave rise to large mass enhancements.

The first case ($dd\sigma = -1$, $dd\pi = 2/3$, n = 1.478) had the self-consistent ground state indicated in Figure 2.6. The first-order phase transition occurred at U = 0.78, very close to the predicted second-order instability at U = 0.79. Equation (4.26) involves an implicit sum over $\underline{q}$; if we write this explicitly we have

$$\frac{m^*}{m} = 1 + \frac{1}{16} U^2 N(0) \sum_{\underline{q}} \sum_{\alpha'\gamma'} \left\{ 2 T'_{\gamma'\gamma';\alpha'\alpha'}(\underline{q},0) + T'_{\alpha'\gamma';\alpha'\gamma'}(\underline{q},0) \right\} \tag{4.27}$$

where

$$T'_{\alpha\beta,\gamma\delta}(\underline{q},\omega) = C^{(T)}_{\alpha\beta,\delta\gamma}(\underline{q},\omega) - \tfrac{1}{2} \Gamma^{(T)}_{\alpha\beta,\gamma\delta}(\underline{q},\omega) \tag{4.28}$$

Therefore, at a given point in $\underline{q}$-space we can calculate the contribution $(m^*/m)(\underline{q})$ to the mass enhancement:

$$\left(\frac{m^*}{m}\right)(\underline{q}) = 1 + \frac{1}{16} U^2 N(0) \sum_{\alpha'\gamma'} \left\{ 2 T_{\gamma'\gamma';\alpha'\alpha'}(\underline{q},0) + T'_{\alpha'\gamma';\alpha'\gamma'}(\underline{q},0) \right\} \tag{4.29}$$

with

$$\frac{m^*}{m} = \frac{1}{N} \sum_{\underline{q}} \left(\frac{m^*}{m}\right)(\underline{q}) \tag{4.30}$$

Figure 4.1 shows $(m^*/m)(\underline{q})$ plotted along the symmetry axes [001] and [111] for U = 0.78, and this does not vary very much with $\underline{q}$. As an approximation $(m^*/m)(\underline{q})$ was taken to be constant at

Table 4.2

$-\beta/\alpha$	n	U_{nm}	R=N(O)/4	ε_F
0.25	1.27	1.85	0.525	- 0.40
	1.63	1.46	0.609	- 0.24
	1.97	1.16	0.728	- 0.12
	2.22	1.31	0.322	0.00
	2.31	1.47	0.138	0.10
	2.44	1.60	0.196	0.30
	2.64	1.79	0.3345	0.50
0.35	1.1	1.3	0.77	- 0.41
0.55	0.905	0.34	3.77	- 0.333
	1.97	0.69	0.104	0.08
0.6667	0.56	0.38	3.5	- 0.3914
	1.478	0.79	0.3674	- 0.145
	2.82	1.12	0.903	0.2

a value at least 7.0 so that the total mass enhancement m*/m = 7.0.

It is necessary also to ensure that when the phase change occurs the quadrupolar mode ordering is uniform, with no sublattice formation: that it is a type of orbital ferromagnetism rather than antiferromagnetism, as the self-consistent ground state solution is for the uniform system with no sublattice formation catered for. The susceptibility for the quadrupolar mode was defined in equation (1.95), and in Figure 4.2 we display $\chi_Q(q,\omega)$ for q along the [001] axis at U = 0.65 and U = 0.73 approaching the phase transition. The function peaks at q = 0, and would eventually diverge at q = 0 at U = 0.79.

In Figure 4.3 the susceptibility functions $P(\omega)$ and $Q(\omega)$ defined by equations (1.39)-(1.40) are shown, and in Figure 4.4 these are combined in a graph of $\chi^{zz}(0,\omega)$ at U = 0. The position of the excitation modes at q = 0 can be calculated from equations (1.81)-(1.83) using the $P(\omega), Q(\omega)$ curves, and by calculating $\chi_Q(0,\omega)$ at a series of values of U. In Figure 4.5 the $Im\chi_Q(0,\omega)$ continuum is shown at U = 0.35, with a very strong peak at the position of the quadrupolar mode; as U increases the modes move lower in energy, and Figure 4.6 shows this mode approaching the lower edge of the continuum at U = 0.5. The edge is reached at U = 0.60, and the delta function mode then separates from the continuum; the situation at U = 0.74 is shown in Figure 4.7, with the position of the mode and the shape of the remaining continuum (the scale of this Figure should be noted).

The strength of the delta function once it has become separated may be calculated as follows. The susceptibility $\chi_Q(0,\omega)$ is

$$\chi_Q(0,\omega) = \frac{8(P+Q)}{1-2u(P+Q)} = \frac{8S}{1-2uS} \tag{4.31}$$

where S = (P + Q); if S' and S" are the real and imaginary parts of S then

$$\mathrm{Im}\,\chi_Q(0,\omega) = \frac{4\pi}{u} \frac{2uS''}{\pi[(1-2uS')^2+(2uS'')^2]} \tag{4.32}$$

so that the singular part $\mathrm{Im}\,\chi_Q^s$ of $\mathrm{Im}\,\chi_Q$ is

$$\mathrm{Im}\,\chi_Q^s(0,\omega+i\eta) = \frac{4\pi}{u}\,\delta(1-2uS') \tag{4.33}$$

$$= \frac{4\pi}{u}\,\delta\left(1-2uS'+(\omega-\omega_0)\left(-2u\frac{dS'}{d\omega}\right)\right)$$

$$= \frac{4\pi}{u}\,\frac{1}{\left(2u\frac{dS'}{d\omega}\right)}\,\delta(1-2uS')$$

$$= \frac{2\pi}{u^2\left(dS'/d\omega\right)}\,\delta(1-2uS') \tag{4.34}$$

Using $S(\omega) = \frac{1}{8}\chi^{zz}_{u=0}(0,\omega)$ the calculated weight of the quadrupolar mode at U = 0.74 is 28. The calculated weight of the isolated mode as it leaves the continuum at U = 0.61 is 6.0; the weight from Figure 4.6 at U = 0.5 is 6.5, and from Figure 4.7 at U = 0.35 is 7.0, giving reasonable agreement as regards continuity of the delta function strength as it leaves the continuum. Also from Figure 4.4 $(dS'/d\omega)$ tends to zero as $\omega \to 0$, so that by equation (4.34) the strength of the mode increases as it falls to lower energies. Thus in the region of U = 0.74 - 0.78 the system has a very strong low-lying quadrupolar mode (for q = 0). The position of this mode against U is shown in Figure 4.8. Clearly,

the high mass enhancement of about 7.0 at U = 0.78 is related to the role of this mode in the system, which is at $\omega = 0.03$ and has a weight of 32, at q = 0. The dispersion relation for the modes of the system at U = 0.74 is shown in Figure 4.12, and the quadrupolar mode remains at low energy for the full range of $\underline{q}$ along the [00q] axis. The graphs of $Im\chi^{zz}(q,\omega+i\eta)$ at $q = 0.9(2\pi/a)$ in Figure 4.13 indicate how the weight of the continuum remains in this low energy region.

Another case which gave rise to a substantial mass enhancement was $dd\sigma = -1$, $dd\pi = 0.25$, n = 2.64. The self-consistent ground state solution is shown in Figure 2.5, giving the variation magnetic and quadrupolar order parameters with U. The first-order phase transition which precedes the second-order criterion at $U_{nm} = 1.79$ occurs at U = 1.70. In the region U = 1.40 - 1.70 the system is paramagnetic but is close enough to the second-order quadrupolar instability for the terms $G_{\alpha'\gamma',\alpha'\gamma'}(q,0)$ to be significantly enhanced. In Figure 4.9 we show the mass enhancement $(m^*/m)(\underline{q})$ along the [001] axis for U = 1.45 and U = 1.49. In order to investigate whether formation of a sublattice occurs, the susceptibility for the mode to which the system is tending $\chi_Q(q,0)$ was calculated, and is shown in the same Figure 4.9; it peaks at q = 0 as U approaches the critical value so that uniform quadrupolar ordering occurs as chosen for the ground state calculation.

The contribution to the mass enhancement possesses full cubic symmetry but varies strongly with $\underline{q}$. In order to integrate $(m^*/m)(\underline{q})$ over the Brillouin zone the mass enhancement curves were fitted to a function $f(\underline{q})$ constructed from the first few Kubic terms, which are the simplest polynomials with cubic symmetry:

$$f(q) = \tfrac{1}{2}A\,(q_x^2 + q_y^2 + q_z^2) + \tfrac{1}{4}B\,(q_x^2 q_y^2 + q_y^2 q_z^2 + q_x^2 q_z^2)$$
$$+ \tfrac{1}{4}C\,(q_x^4 + q_y^4 + q_z^4) + \tfrac{1}{4}D\,(q_x^4 q_y^4 + q_y^4 q_z^4 + q_x^4 q_z^4) + E$$

and the best fit that could be obtained was with

A = - 40.55	D = - 4000
B = 400.0	E = 3.8
C = 208.8	

The curves for f($\underline{q}$) along the symmetry axes [001] and [111] are shown in Figure 4.9. On integrating this function over the Brillouin zone using 10277 points we obtained 5.84, and this is a good approximation to the full mass enhancement (m*/m) by equation (4.48).

Considering the quadrupolar mode giving rise to this enhancement its position may be calculated from the susceptibility functions $P(\omega), Q(\omega)$ for the system plotted in Figure 4.10. The quadrupolar mode is visible in Figure 4.11 of $\mathrm{Im}\,\chi_Q(0,\omega)$ at U = 0.6 and has a weight of 5.2. When U reaches U = 1.0 the mode separates from the continuum and continues to fall in energy as U increases, as in Figure 4.14. When U = 1.49 the quadrupole mode at q = 0 is at $\omega \simeq 0.4$ and has a weight of 7.1, and as it is not particularly low-lying in energy it gives a mass enhancement contribution of (m*/m)(q=0) = 3.8. Along symmetry axes, where they reach the Brillouin zone boundary, (m*/m)($\underline{q}$) becomes large, although considering the dispersion relation in Figure 4.13 the quadrupole mode at those q values has not come down to a low energy. The mass enhancement was also calculated for values of U closer to U = 1.70; however, it does not change very significantly.

From Figure 4.14, which displays the position of the quadrupolar mode as the system approaches ordering, it can be seen that the mode never does reach very low energies even at U = 1.70 and this explains why m*/m only rises slowly from U = 1.45 to U = 1.70, and the generally lower enhancement in this case, compared to that with the previous set of parameters.

4.5 Conclusions

Having previously established the basic static and dynamic properties of our model containing itinerancy and spin-orbit coupling, and the importance of quadrupolar ordering, we have sought to estimate the correction to the HF electron mass due to interactions between the electrons and all the excitation modes of the system. This has been shown to give rise to large mass enhancements in the paramagnetic state on approaching a quadrupolar phase transition; this is related to the movement down to low energies of the quadrupolar excitation mode, which has a high delta function weight and is uniformly low-lying throughout $\underline{q}$-space.

The model contains two basic features of light actinide compounds in being itinerant with spin-orbit coupling, and so possesses some relevance to the heavy-fermion systems UBe_{13} and particularly UPt_3. Thus, the mechanism we have described for large electron mass enhancement within the model may be the mechanism giving rise to the experimental results for m*/m described in section 4.2. The renormalization of the f-band (and the electron band mass) would mean that the simple model enhancement of m*/m ~ 7 may be compared with an enhancement m*/m' ~ 30 upon the band mass m' in UPt_3. It is quite possible, even without accurately

modelling the crystal structure of UPt_3, that an f-states model would have lower-lying excitation modes, thus giving rise to significantly higher enhancements via this mechanism.

The superconductivity in HFS has been the subject of investigation recently, and it has been speculated (Anderson (1984)) by several authors that in UBe_{13} and UPt_3 it is p-wave in nature, bearing in mind the symmetry properties. Investigation of the superconducting state of our model would be of interest in this respect, in displaying the influence of spin-orbit coupling.

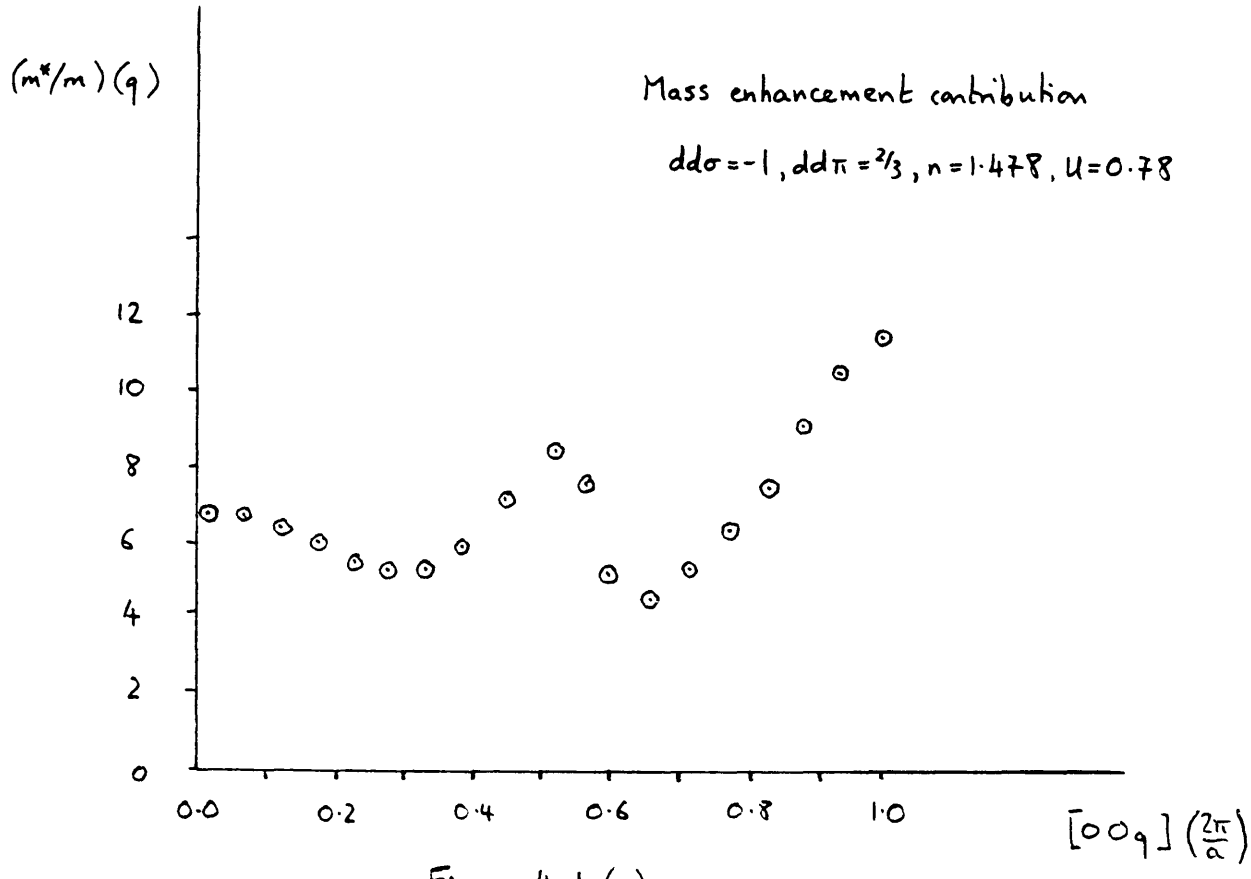

Figure 4·1 (a)

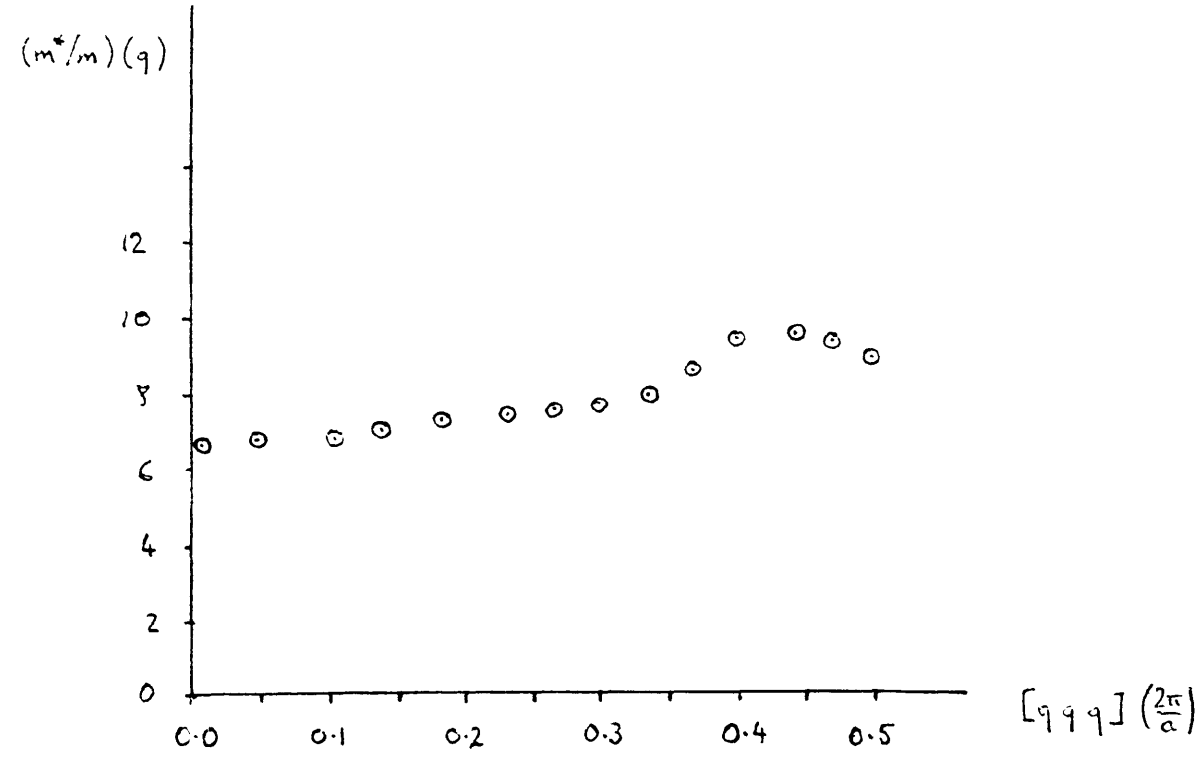

Figure 4·1 (b)

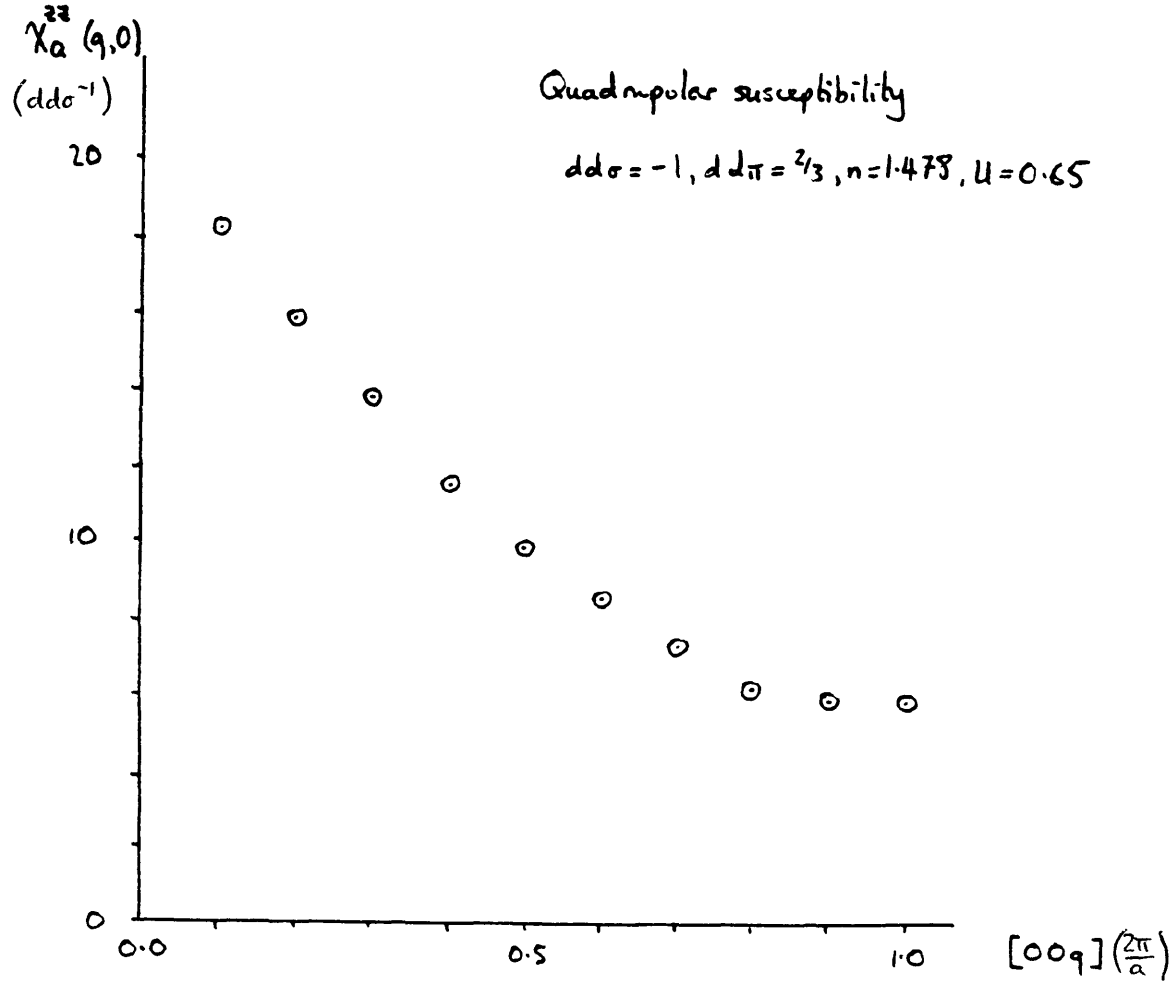

Figure 4.2 (a)

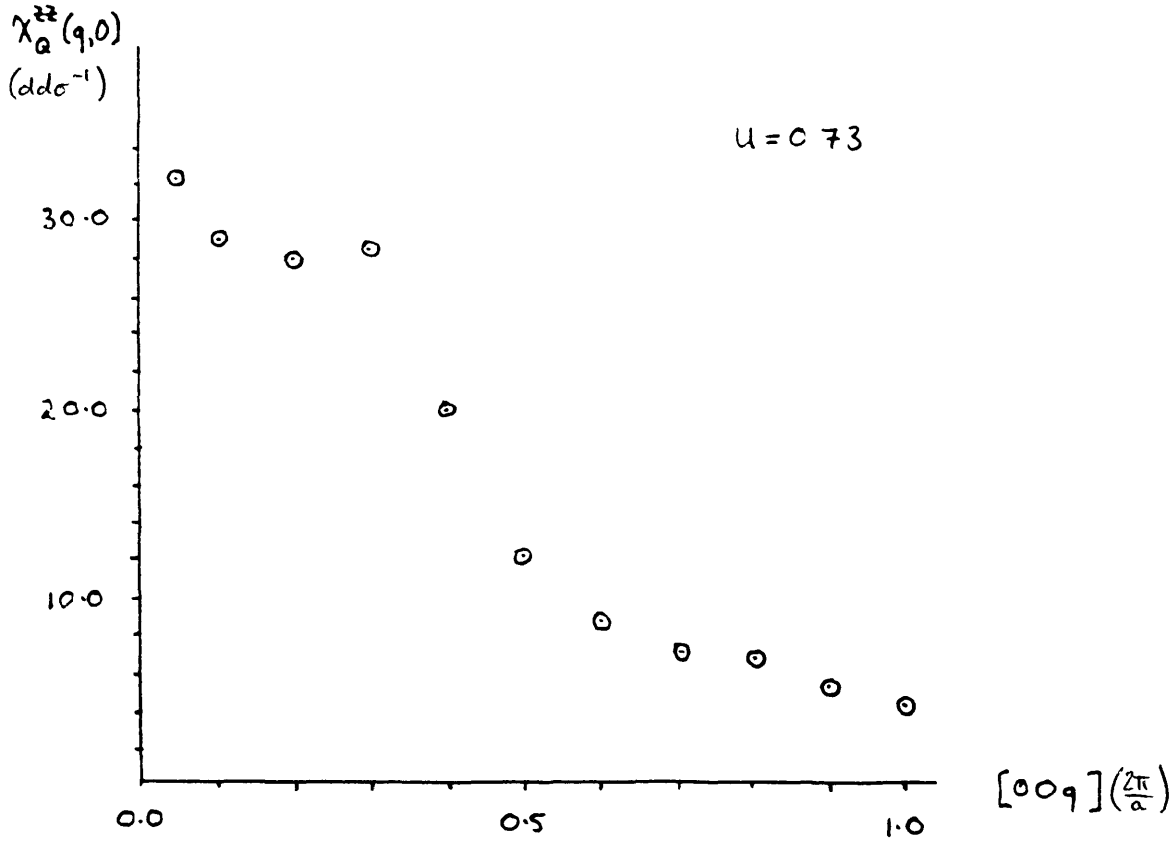

Figure 4.2 (b)

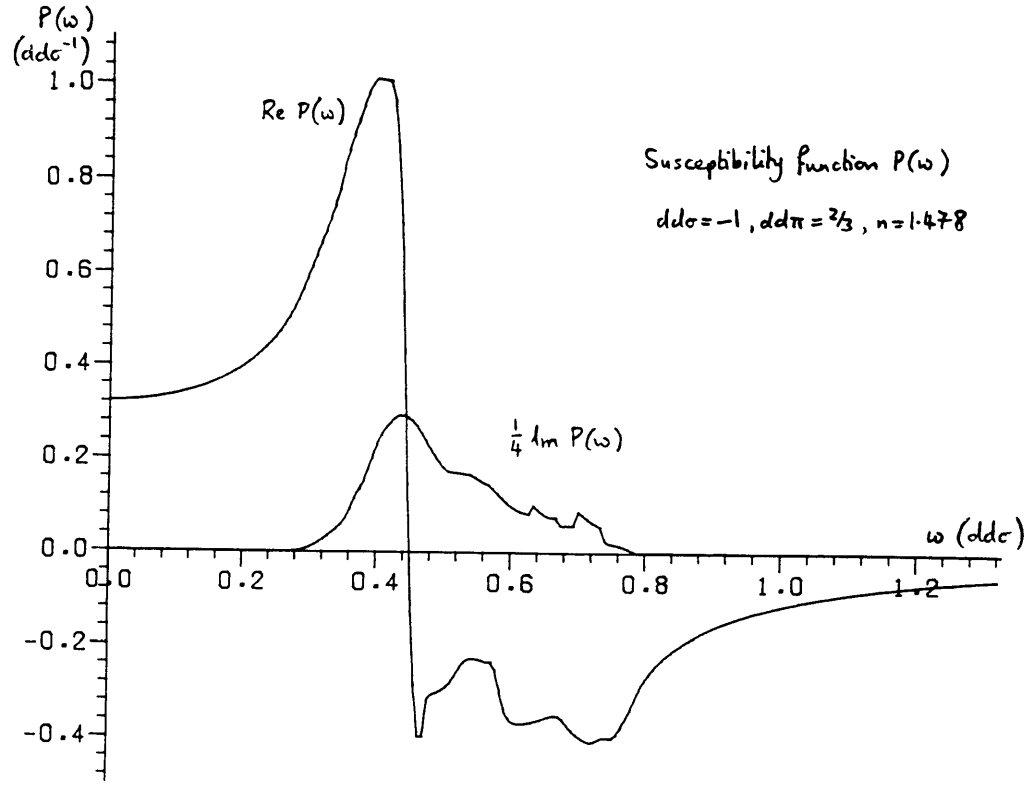

Figure 4.3 (a)

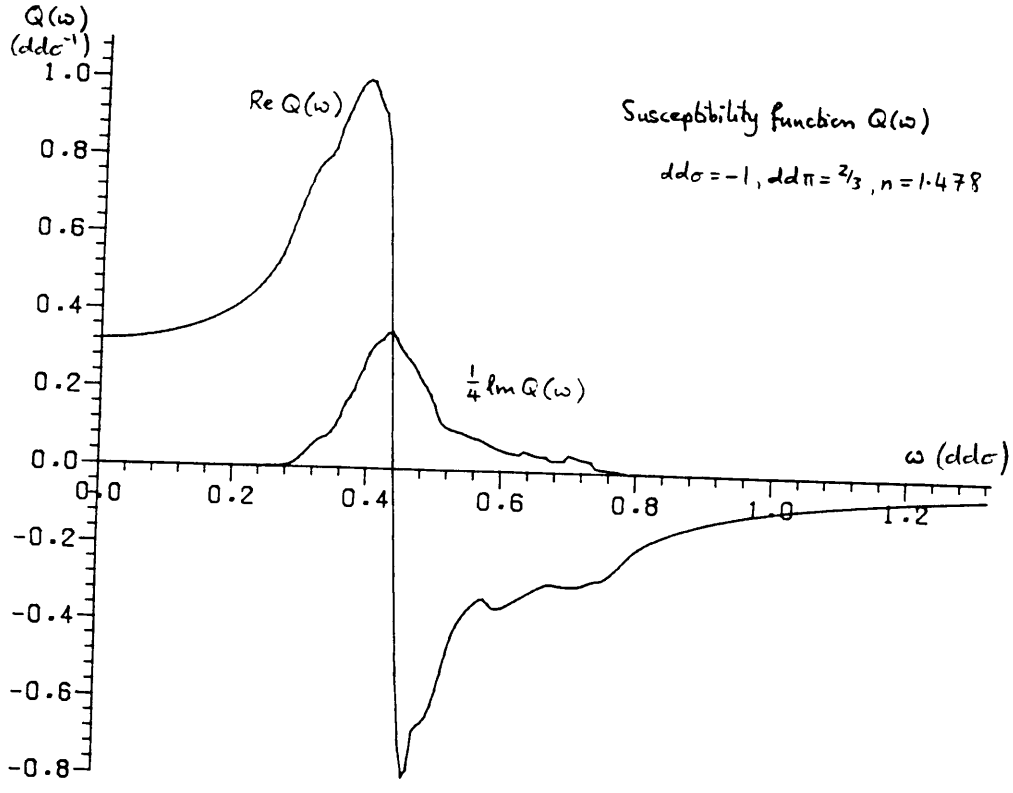

Figure 4.3 (b)

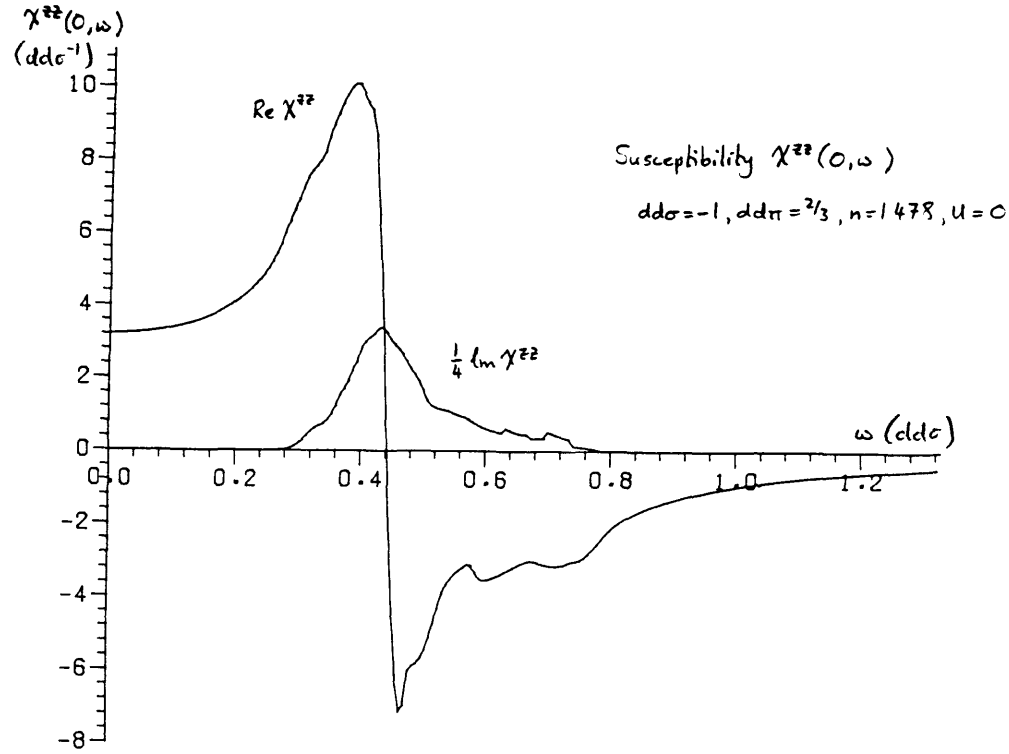

Figure 4 4

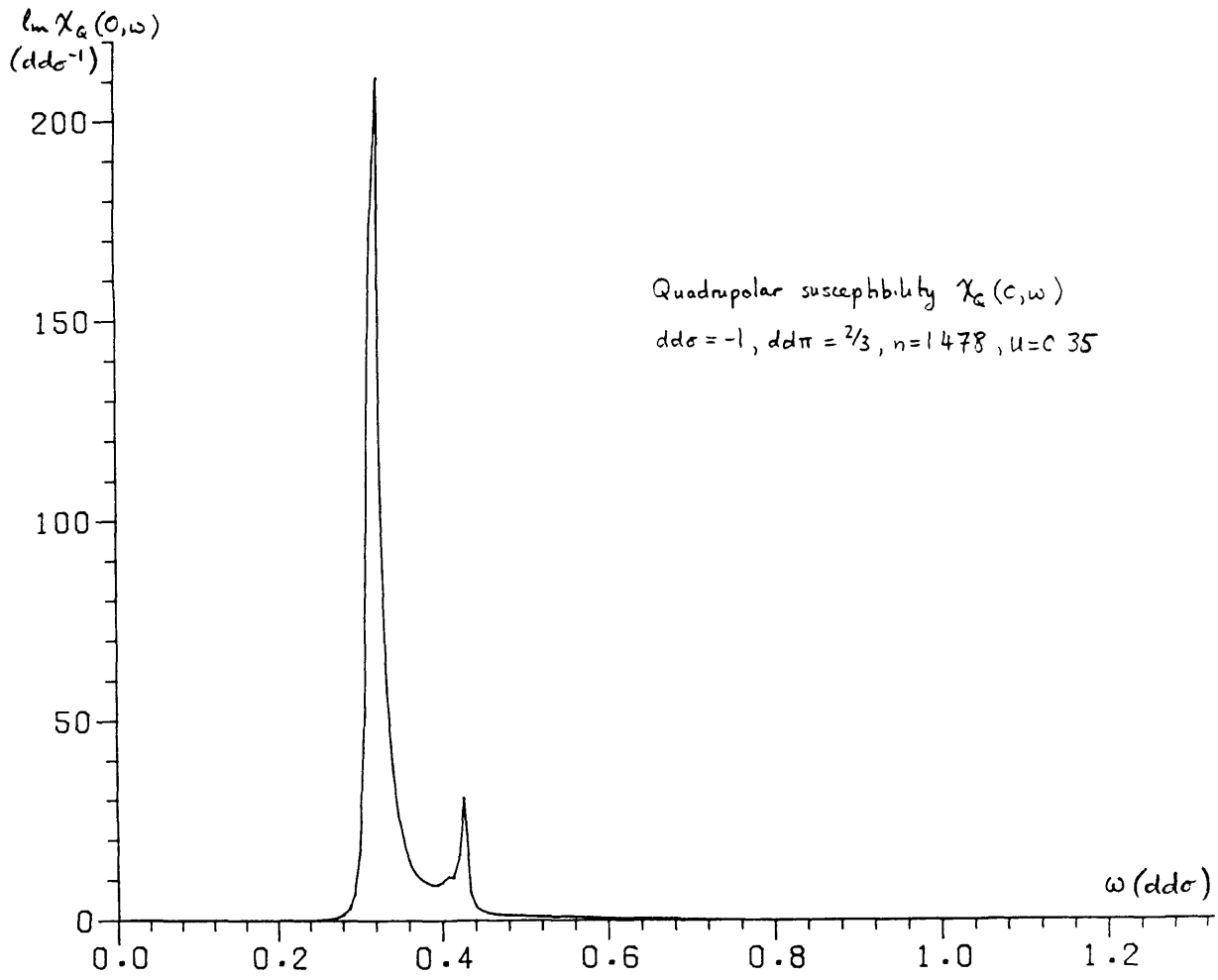

Figure 4 5

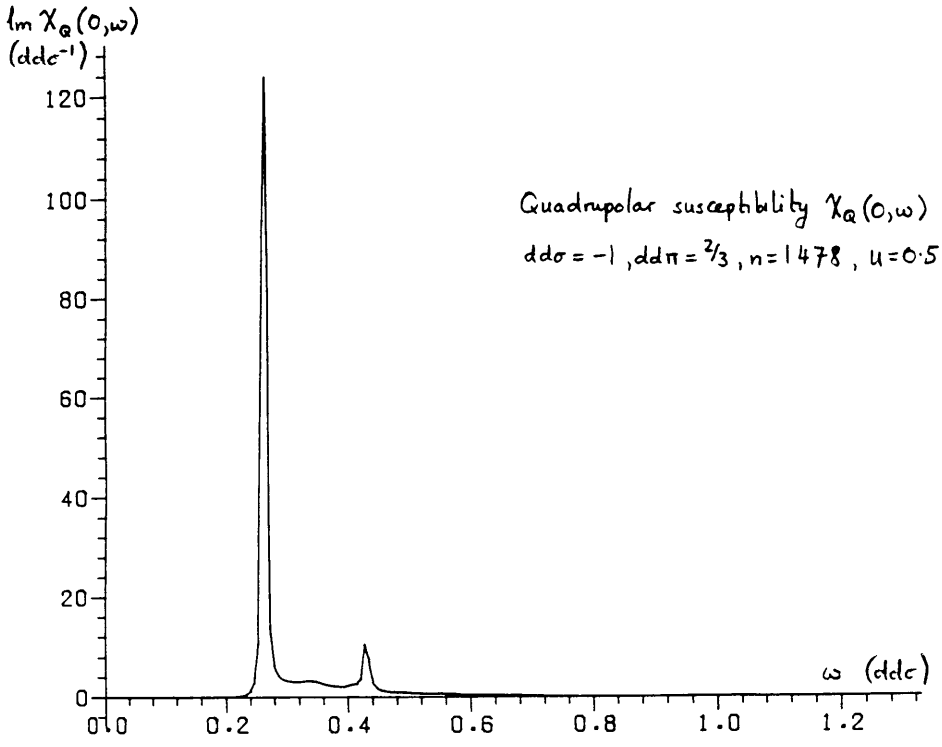

Figure 46

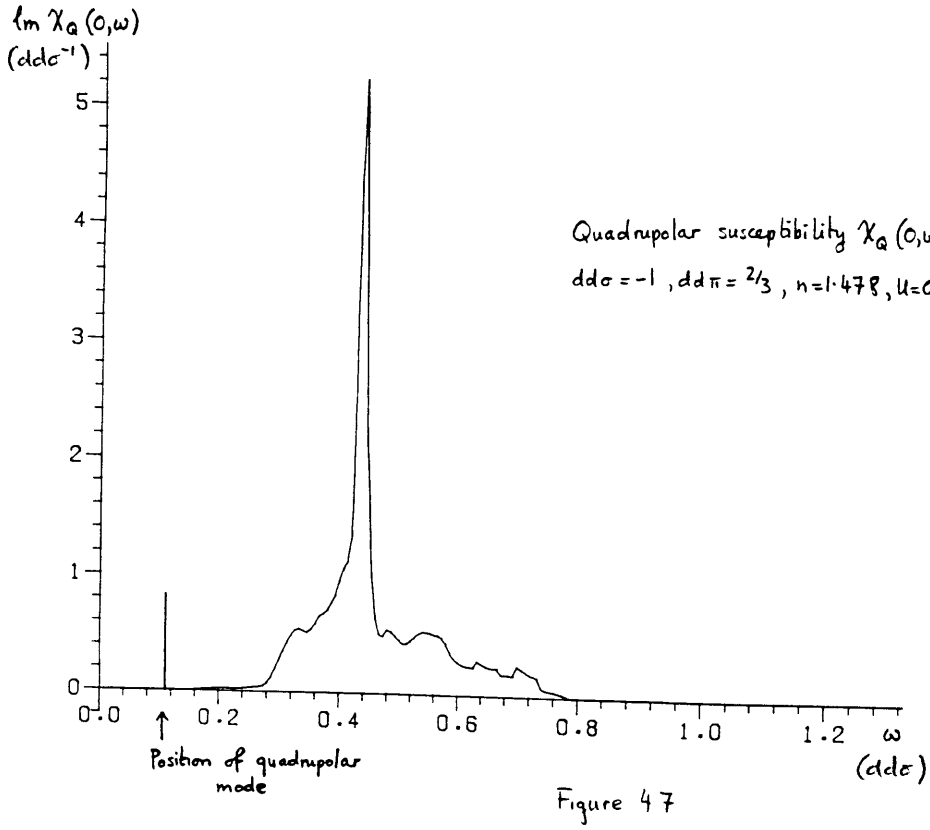

Figure 47

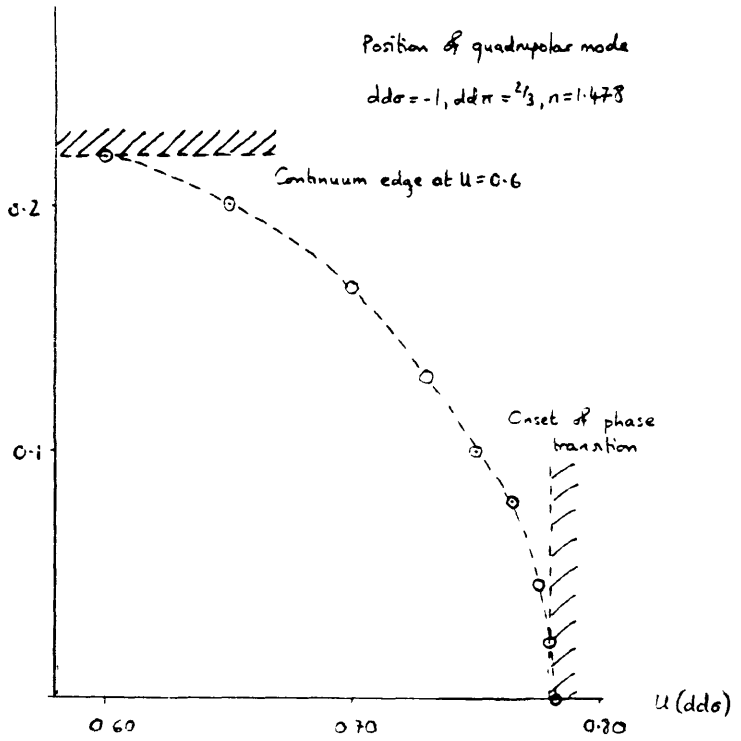

Figure 4.8

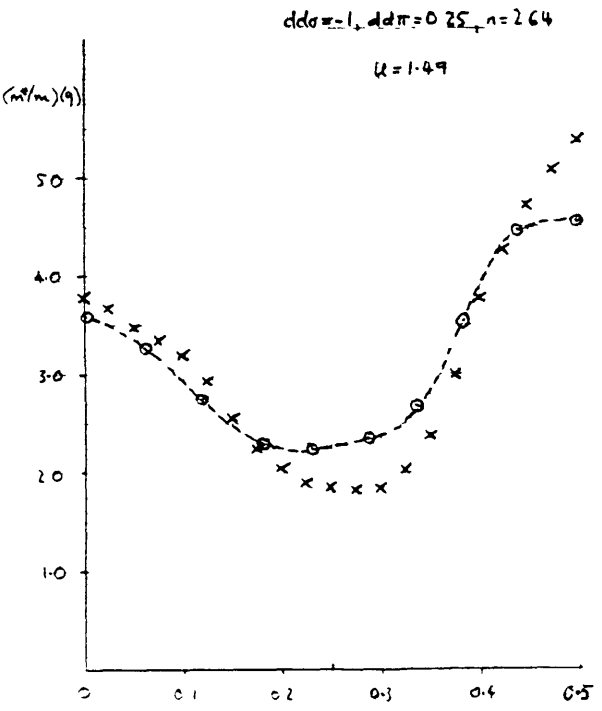

Figure 4.9 (b)

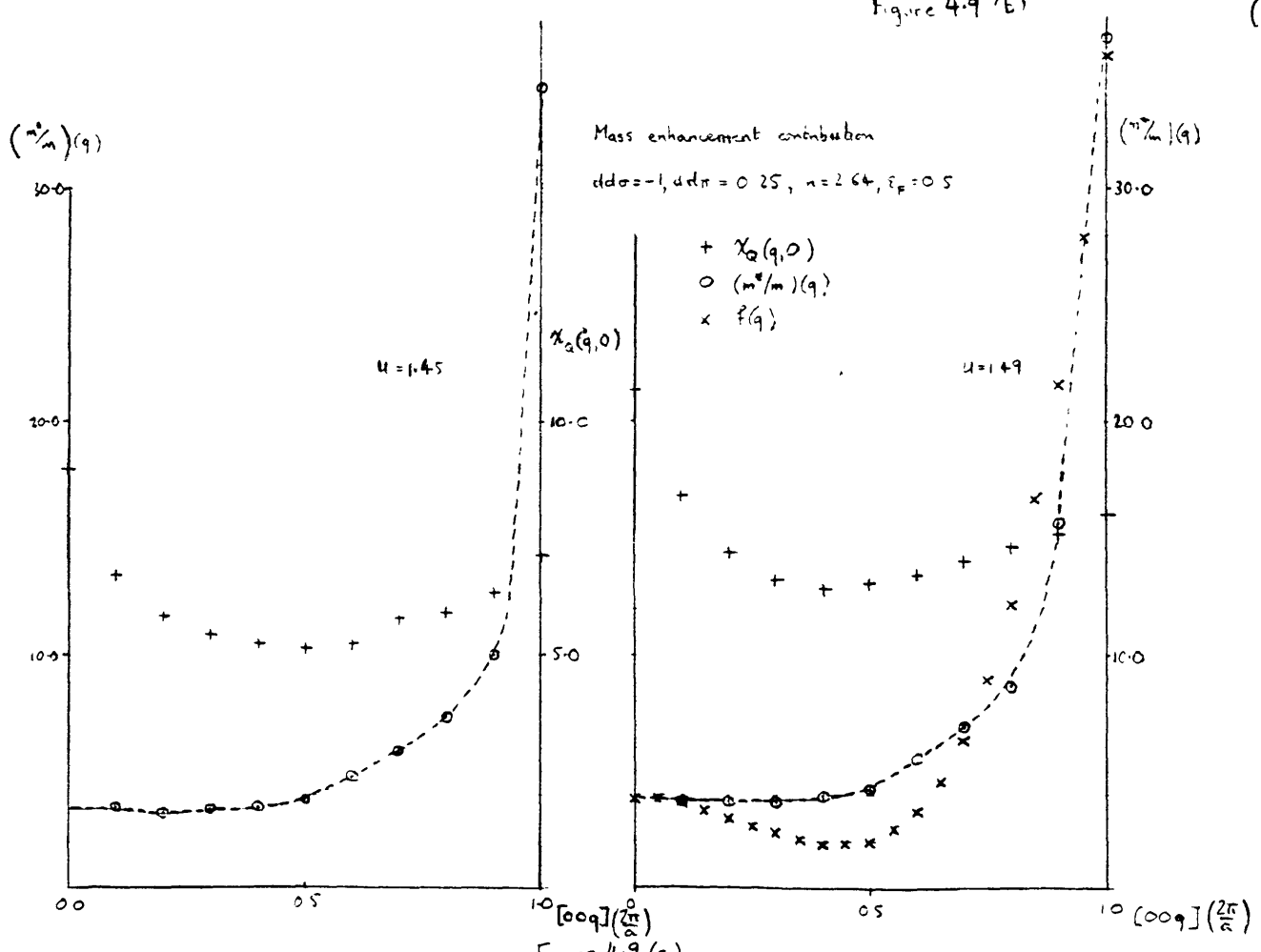

Figure 4.9 (a)

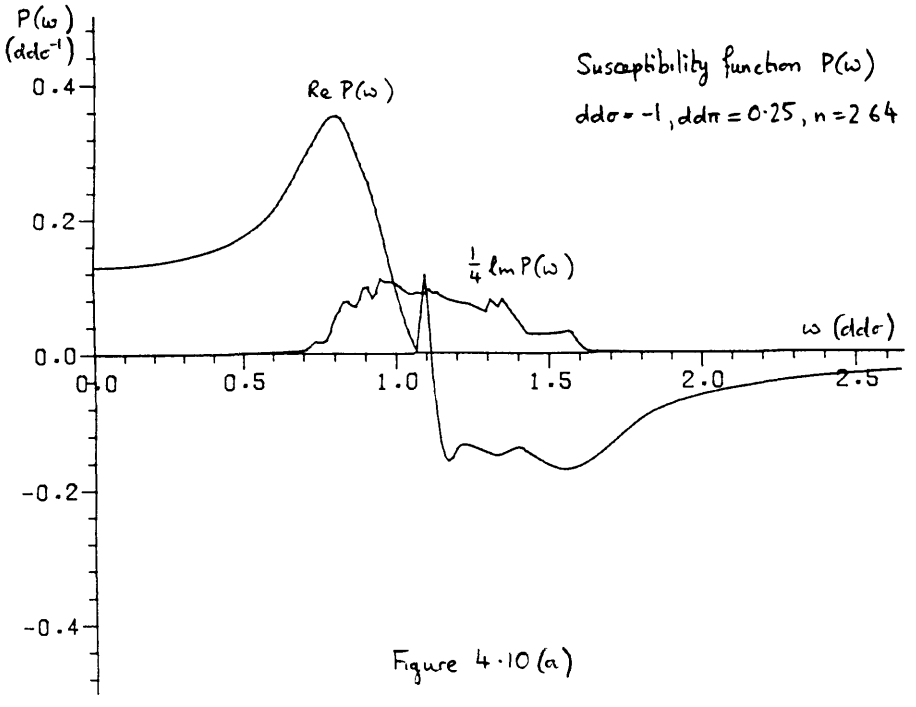

Figure 4.10 (a)

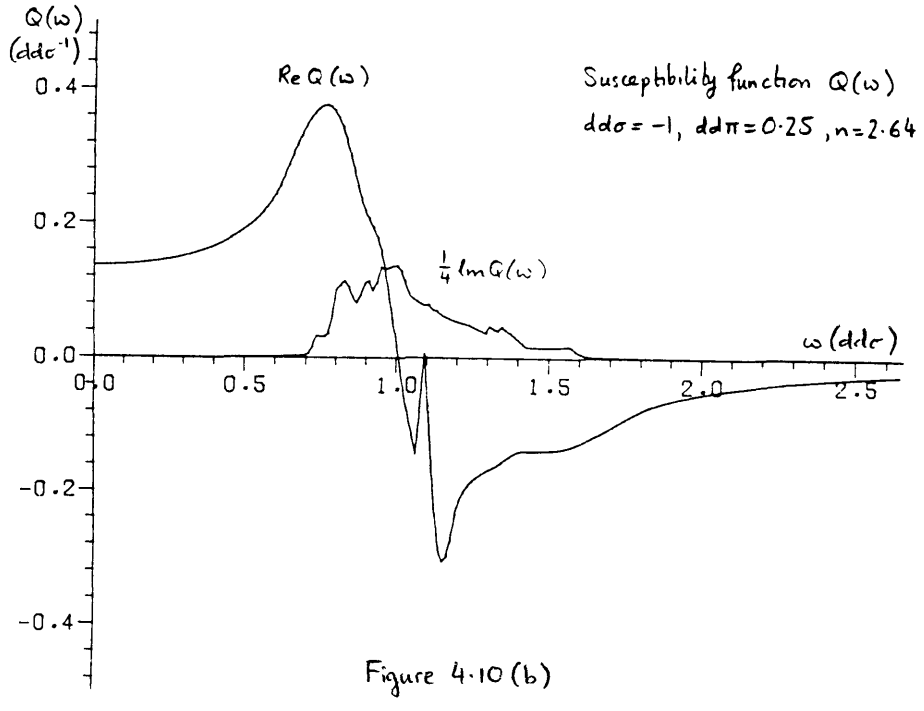

Figure 4.10 (b)

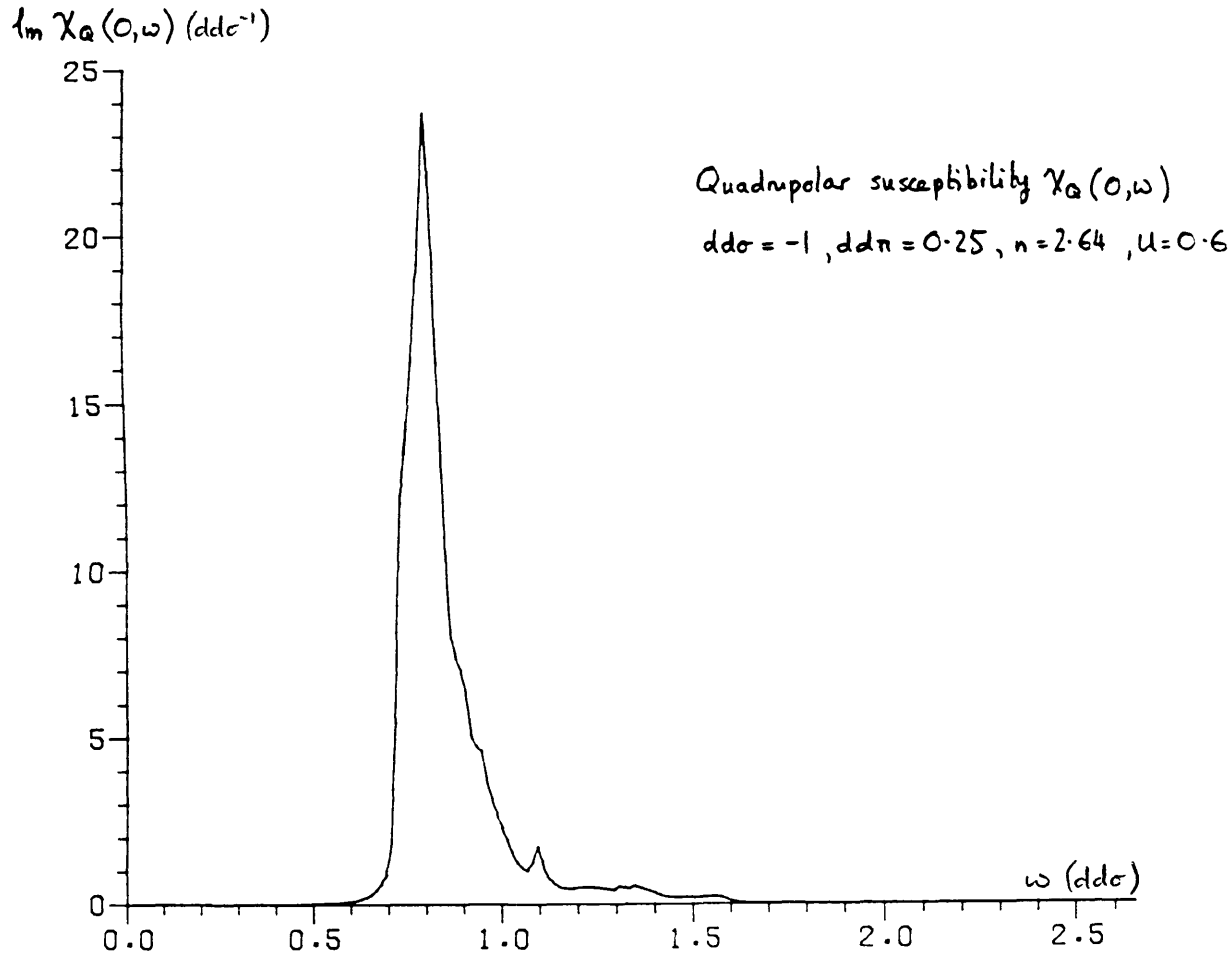
Im $\chi_Q(0,\omega)$ (ddσ⁻¹)
25
20
15
10
5
0
0.0
0.5
1.0
1.5
2.0
2.5
ω (ddσ)
Quadrupolar susceptibility $\chi_Q(0,\omega)$
ddσ = -1 , ddπ = 0·25 , n = 2·64 , U = 0·6

Figure 4·11

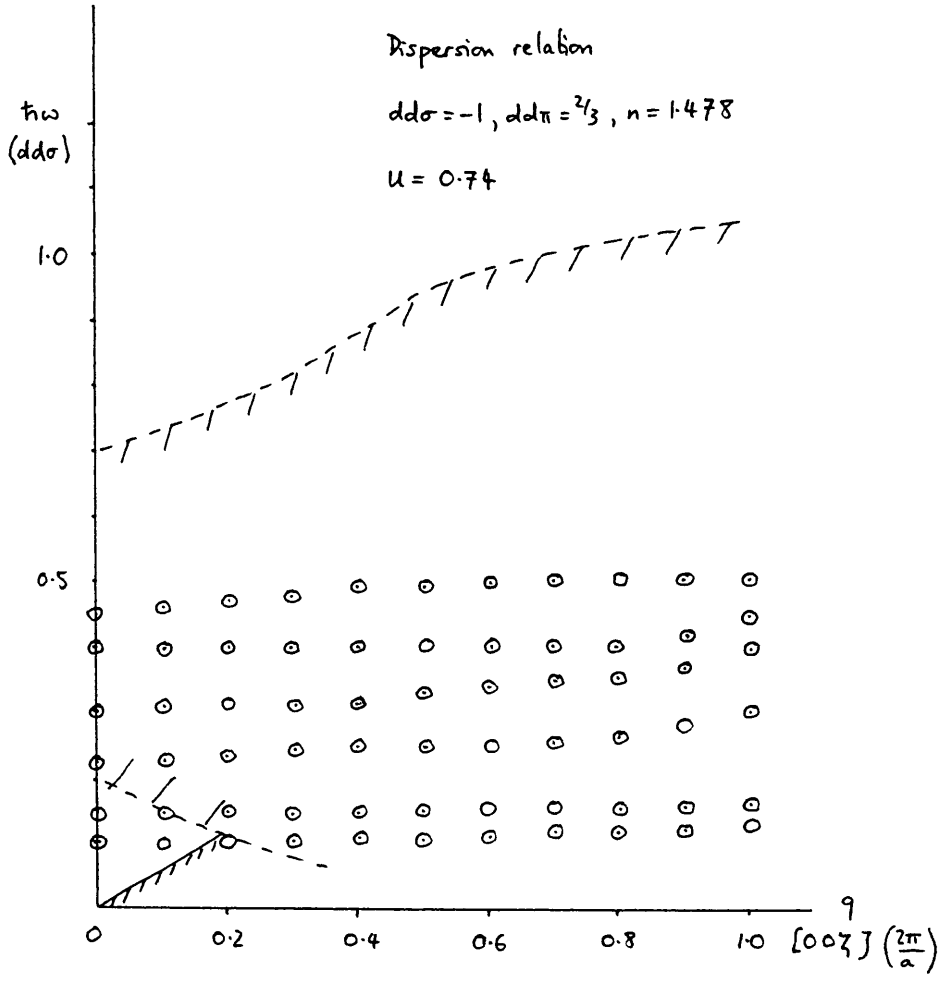

Figure 4.12 (a)

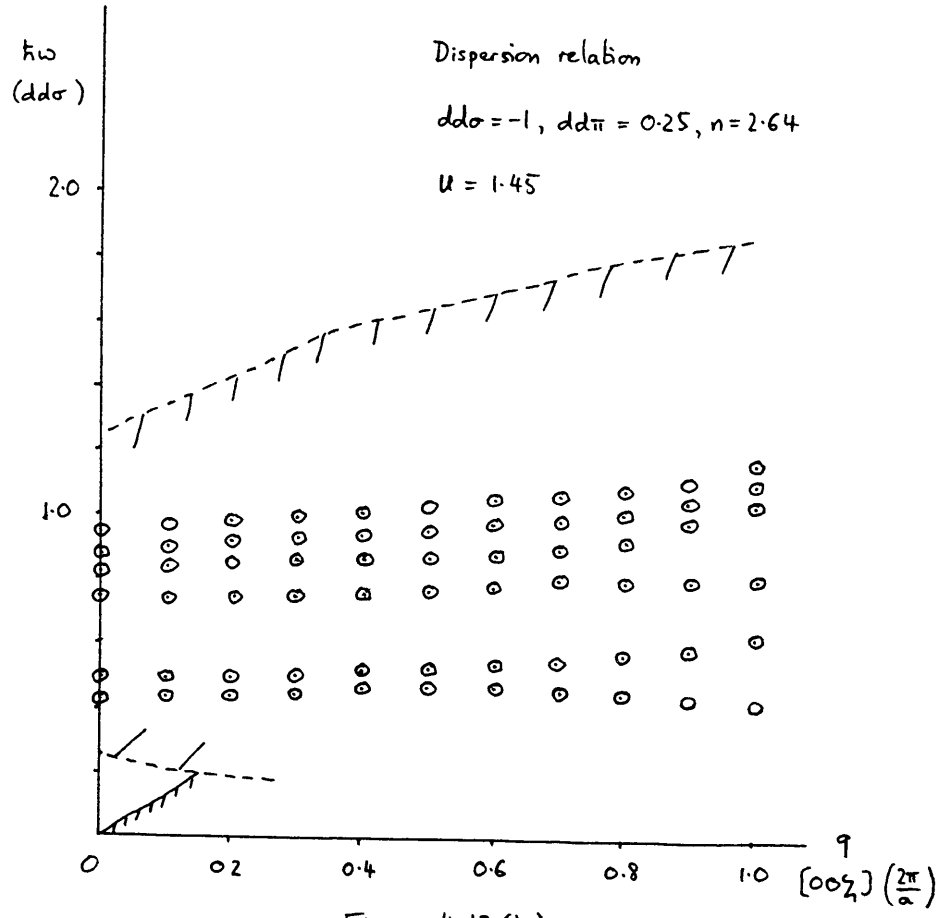

Figure 4.12 (b)

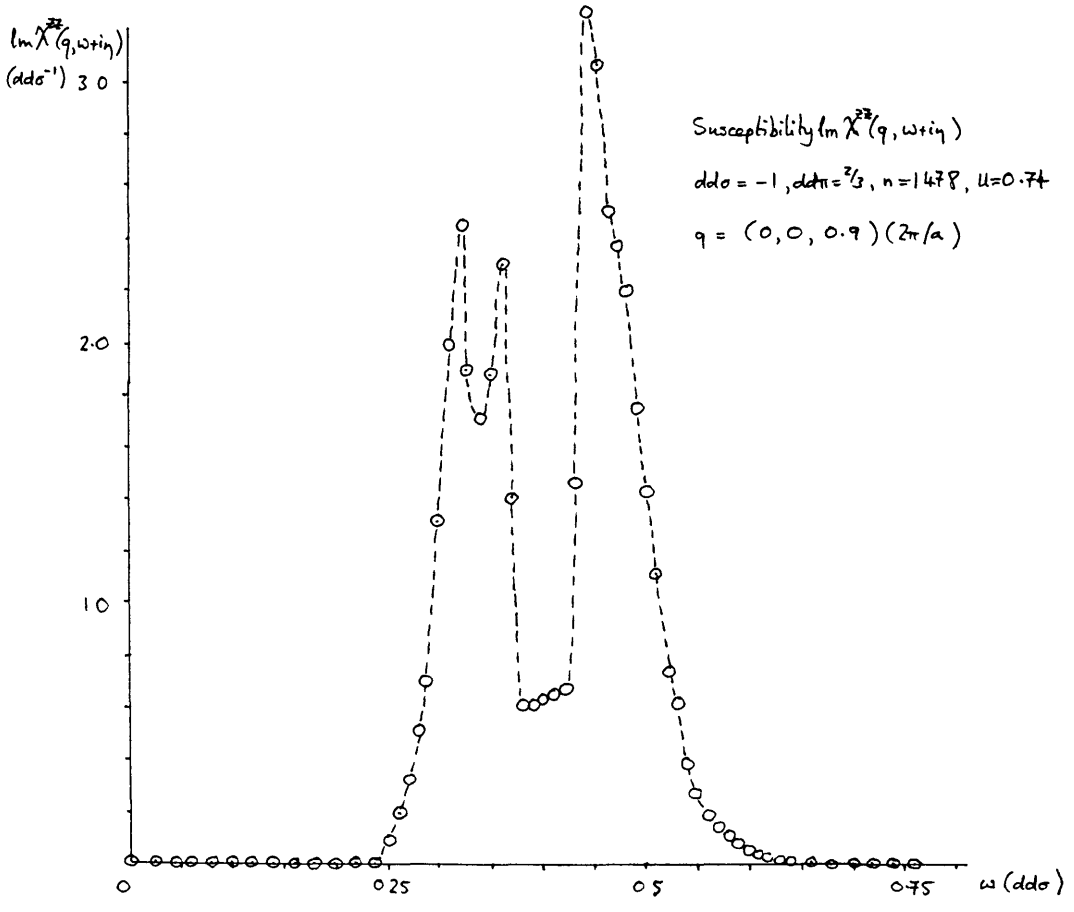

Figure 4.13

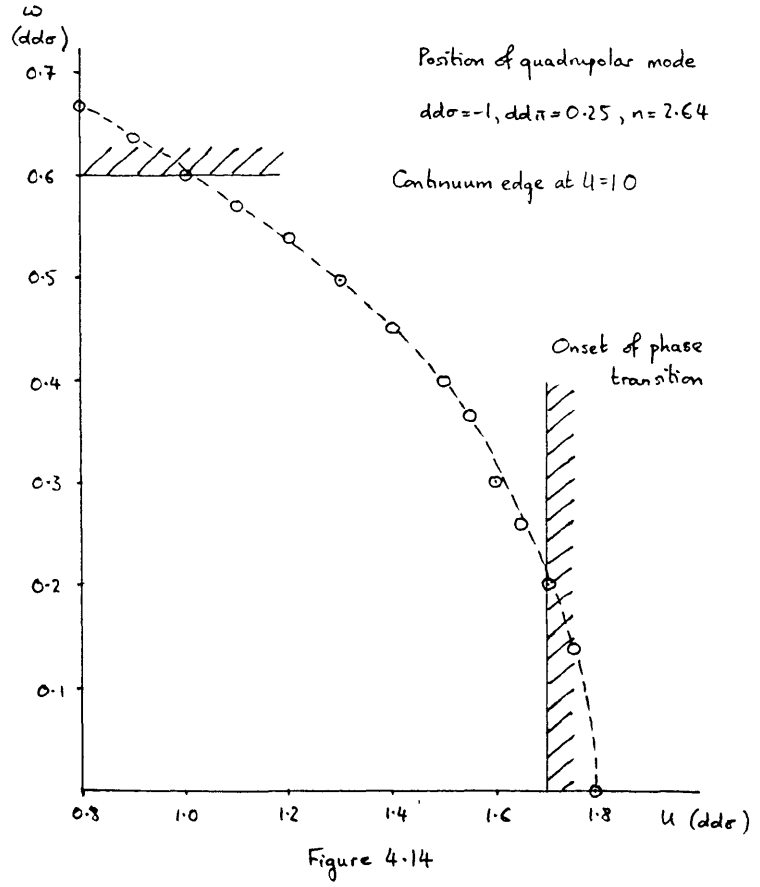

Figure 4.14

APPENDIX A

Symmetry properties of $\langle n_{\mu\nu} \rangle$

The HF Hamiltonian has been shown (equation (1.16)) to be

$$H = \sum_{\mu\nu\underline{k}} \left\{ T_{\mu\nu}(\underline{k}) + U(n\delta_{\mu\nu} - \langle n_{\mu\nu} \rangle) \right\} c^{+}_{\mu\underline{k}} c_{\nu\underline{k}}$$

where

$$\langle n_{\mu\nu} \rangle = \frac{1}{N} \sum_{i\underline{p}} a^{*}_{i\nu}(\underline{p}) a_{i\mu}(\underline{p}) f_{i\underline{p}}$$

Considering the basis functions for the d states, and using Table A.1, we have the representations of the states without spin to be $\Gamma_{12} \oplus \Gamma_{25'}$, where

$$\left.\begin{array}{l} 2z^2 - x^2 - y^2 \\ x^2 - y^2 \end{array}\right\} \Gamma_{12}$$

$$\left.\begin{array}{l} xy \\ yz \\ xz \end{array}\right\} \Gamma_{25'}$$

as shown in general texts on group theory and quantum mechanics, such as Callaway (1974).

Now, putting in the spin, and using Table A.2 and BSW notation we have

$$(\Gamma_{12} \oplus \Gamma_{25'}) \otimes D^{(1/2)} = \Gamma_8^{+} \oplus \Gamma_8^{+} \oplus \Gamma_7^{+} \qquad \text{(A.1)}$$

Considering now only the j = 3/2 subband, with the representation $D_{\mu\nu}(R)$ for a symmetry operation R

$$a_{i\mu}(R\underline{k}) = D_{\mu\nu}(R)\, a_{i\nu}(\underline{k})$$

it is true that D must be a sum of a_i irreducible representations Γ_i:

$$D = \sum_i a_i \Gamma_i$$

From (A.1) one may deduce, as D is of dimension 4, that $D = \Gamma_8^+$; however, this can be shown in detail as follows.

If we define the character of the elements α of the irreducible representations by (as in Callaway (1974))

$$\chi_i(\alpha) = \sum_j [\alpha]_{i,jj}$$

then the character of D is

$$\chi(\alpha) = \sum_i a_i \chi_i(\alpha)$$

Now for a group of order g and irreducible representation of dimension d(i)

$$\sum_\alpha [\alpha]^*_{i',j'j'} [\alpha]_{i,jj} = \frac{g}{d(i)} \delta_{ii'} \delta_{jj'}$$

$$\sum_\alpha \chi_i^*(\alpha) \chi_{i'}(\alpha) = \frac{g}{d(i)} \delta_{ii'} \sum_{jj'} \delta_{jj'} = g\delta_{ii'}$$

$$a_j = \frac{1}{g} \sum_\alpha \chi_j^*(\alpha) \chi(\alpha)$$

where we sum over the elements α ; alternatively, we sum over the classes r:

$$a_j = \frac{1}{g} \sum_{\alpha} \chi_j^*(\alpha)\chi(\alpha) \qquad (A.2)$$

where N_r is the dimension of the class.

We now construct the character table of D, which has the classes E, C_4^2, C_4, C_2, C_3. Hence we have the character table

	E	C_4^2	C_4	C_2	C_3	JE	JC_4^2	JC_4	JC_2	JC_3
D	4	0	0	0	-1	4	0	0	0	-1

where clearly J does not change the sign of the basis functions as they are even. Clearly then from (A.2) and Table A.2 $D = \Gamma_8^+$ as

$$\langle n_{\mu\nu} \rangle = \sum_R \sum_{\underline{k}' \text{IBZ}} \sum_m a_{m\mu}(R\underline{k}') a^*_{m\nu}(R\underline{k}') \langle n_{m\underline{k}'} \rangle$$

$$= \sum_R \sum_{\underline{k}' \text{IBZ}} \sum_{m\eta\xi} D^*_{\nu\xi}(R) D_{\mu\eta}(R) a_{m\eta}(\underline{k}') a^*_{m\xi}(\underline{k}') \langle n_{m\underline{k}'} \rangle$$

$$= \sum_R \sum_{\underline{k}' \text{IBZ}} \sum_{m\eta\xi} \left(\sum_i a_i \Gamma^{(i)}_{\nu\xi}(R) \right) \left(\sum_j a_j \Gamma^{(j)}_{\mu\eta}(R) \right) a_{m\eta}(\underline{k}') a_{m\xi}(\underline{k}') \langle n_{m\underline{k}'} \rangle$$

$$= \sum_{\substack{\underline{k}' m \\ \text{IBZ}}} \sum_{\eta\xi} \sum_{ij} a_i a_j \delta_{ij} \delta_{\nu\mu} \delta_{\xi\eta} \frac{g}{d(i)} a_{m\eta}(\underline{k}') a^*_{m\xi}(\underline{k}') \langle n_{m\underline{k}'} \rangle$$

$$= \sum_{\substack{\xi \underline{k}' m \\ \text{IBZ}}} \sum_i \delta_{\mu\nu} a_i^2 \frac{g}{d(i)} a_{m\xi}(\underline{k}') a^*_{m\xi}(\underline{k}') \langle n_{m\underline{k}'} \rangle$$

$$= \delta_{\mu\nu} \sum_i \left(a_i^2 \frac{g}{d(i)} \right) \sum_{\substack{\xi \underline{k}' m \\ \text{IBZ}}} a_{m\xi}(\underline{k}') a^*_{m\xi}(\underline{k}') \langle n_{m\underline{k}'} \rangle$$

$$\langle n_{\mu\nu} \rangle = \left(\sum_i a_i^2 \frac{g}{d(i)} \right) \delta_{\mu\nu} \sum_{\substack{\xi \underline{k}' m \\ 1BZ}} a_{m\xi}(\underline{k}') a^*_{m\xi}(\underline{k}') \langle n_{m\underline{k}'} \rangle \quad \text{(A.3)}$$

and $a_i = 1$ with $i = 1,1$ so that $g = d(i) = 4$

$$\langle n_{\mu\nu} \rangle = \delta_{\mu\nu} \sum_{\substack{\xi \underline{k}' m \\ 1BZ}} a_{m\xi}(\underline{k}') a^*_{m\xi}(\underline{k}') \langle n_{m\underline{k}'} \rangle$$

Here we have used the great orthogonality theorem which states that for irreducible representations $\Gamma^{(\lambda)}$

$$\sum_R \Gamma^{(\lambda)*}_{\alpha\beta}(R) \, \Gamma^{(\mu)}_{\gamma\delta}(R) = \frac{g}{d(\lambda)} \delta_{\alpha\gamma} \delta_{\beta\delta} \delta_{\lambda\mu}$$

where $d(\lambda)$ is the dimension of $\Gamma^{(\lambda)}$ and the irreducible representations $\Gamma^{(\lambda)}$, $\Gamma^{(\mu)}$ belong to a group of g elements.

Hence we have shown that $\langle n_{\mu\nu} \rangle$ is diagonal, and (by Schurr's lemma) is proportional to the identity. Clearly in the paramagnetic state, if n is the total number of electrons,

$$\langle n_{\mu\nu} \rangle = \delta_{\mu\nu} \frac{n}{4}$$

If we now break the existing full cubic symmetry by applying a $\underline{B}$ field along [001], or equivalently letting a moment form along [001], then from Falicov and Ruvalds (1968) using Table A.2, as the symmetry operations are about the point Γ in $\underline{k}$-space

$$\Gamma_8^+ \rightarrow \gamma_1^+ \oplus \gamma_2^+ \oplus \gamma_3^+ \oplus \gamma_4^+ \quad \text{(A.4)}$$

$$D_{\mu\nu}(R) = \delta_{\mu\nu} D_\mu(R) \rightarrow \gamma_1^+ \oplus \gamma_2^+ \oplus \gamma_3^+ \oplus \gamma_4^+$$

with character table ($\alpha = \frac{1}{\sqrt{2}}(1+i)$):

$\mu \backslash R$	E	$A=C_4$	$B=C_4^2$	$C=C_4^3$	$\mathcal{J}E$	$\mathcal{J}A$	$\mathcal{J}B$	$\mathcal{J}C$
Γ_1^+	1	α	i	$-\alpha^*$	1	α	i	$-\alpha^*$
Γ_2^+	1	α^*	$-i$	$-\alpha$	1	α^*	$-i$	$-\alpha$
Γ_3^+	1	$-\alpha$	i	α^*	1	$-\alpha$	i	α^*
Γ_4^+	1	$-\alpha^*$	$-i$	α	1	$-\alpha^*$	$-i$	α

Also we can choose 6 points in $\underline{k}$ space from which the 48 cubic symmetry points are generated by the above 8 operations; these points indicate how to construct the new irreducible Brillouin zone (IBZ) from the IBZ with full cubic symmetry:

x	y	z
x	z	-y
y	x	-z
z	-y	x
z	x	y
z	y	-x

Hence the full BZ can be visited from the IBZ by going to each of the above 6 points and calculating the eigenvectors and eigenvalues; for each of the 8 symmetry-related points $a^*_{m\mu}(\underline{k})\,a_{m\mu}(\underline{k})$ and $E_{m\underline{k}}$ are then equal.

Similarly, for moments along [110], [111] we can do calculations as outlined in Tables A.3 and A.4.

The matrix $T_{\mu\nu}(\underline{k})$ has to be transformed by rotating the axis of quantization from [001] to [110] or [111], and this is done by the transformation for the angular momentum manifold $\underline{J}$

under rotation through $\underline{\theta}$:

$$a_{n\mu'}(\underline{k}) = \left(e^{\frac{i}{\hbar}\underline{\theta}\cdot\underline{J}} \right)_{\mu'\mu} a_{n\mu}(\underline{k})$$

The new z-axis then lies along the axis of quantization and the symmetry axis under consideration. In that basis $\langle n_{\mu\nu} \rangle$ is then again diagonal.

From equation (A.4) above we have four one-dimensional representations acting, and by Schurr's lemma each is proportional to the identity (trivially). Hence four scalars, with one constraint that they add up to n, now determine the elements of $\langle n_{\mu\nu} \rangle$ (which by equation (A.3) is still diagonal).

Table A.1

CHARACTER TABLE FOR THE CUBIC GROUP O_h

Representation				BSW[a] ·	E	$3C_4^2$	$6C_4$	$6C_2$	$8C_3$	J	$3JC_4^2$	$6JC_4$	$6JC_2$	$6JC_3$
BSW[a]	EWK[b]	Bethe[c]	Basis	Koster[d] ·	E	$3C_2$	$6C_4$	$6C_{2'}$	$8C_3$	I	$3\sigma_h$	$6S_4$	$6\sigma_d$	$8S_6$
Γ_1	A_{1g}	Γ_1	1		1	1	1	1	1	1	1	1	1	1
Γ_2	A_{2g}	Γ_2	$x^4(y^2-z^2)+y^4(z^2-x^2)+z^4(x^2-y^2)$		1	1	−1	−1	1	1	1	−1	−1	1
Γ_{12}	E_g	Γ_3	x^2-y^2											
			$2z^2-x^2-y^2$		2	2	0	0	−1	2	2	0	0	−1
Γ_{15}	T_{1u}	$\Gamma_{4'}$	x, y, z		3	−1	1	−1	0	−3	1	−1	1	0
Γ_{25}	T_{2u}	$\Gamma_{5'}$	$z(x^2-y^2)$		3	−1	−1	1	0	−3	1	1	−1	0
$\Gamma_{1'}$	A_{1u}	$\Gamma_{1'}$	$xyz[x^4(y^2-z^2)+y^4(z^2-x^2)+z^4(x^2-y^2)]$		1	1	1	1	1	−1	−1	−1	−1	−1
$\Gamma_{2'}$	A_{2u}	$\Gamma_{2'}$	xyz		1	1	−1	−1	1	−1	−1	1	1	−1
$\Gamma_{12'}$	E_u	$\Gamma_{3'}$	$xyz(x^2-y^2)$		2	2	0	0	−1	−2	−2	0	0	1
$\Gamma_{15'}$	T_{1g}	Γ_4	$xy(x^2-y^2)$		3	−1	1	−1	0	3	−1	1	−1	0
$\Gamma_{25'}$	T_{2g}	Γ_5	xy, yz, zx		3	−1	−1	1	0	3	−1	−1	1	0

[a] Bouckaert *et al* (1936).
[b] Eyring *et al* (1944)
[c] Bethe (1929).
[d] Koster (1957)

Table A.2

CHARACTERS OF THE ADDITIONAL REPRESENTATIONS OF THE DOUBLE GROUP O_h

Representation	Class E	$\bar{E}$	$(C_4^2, \bar{C}_4^2)$	C_4	$\bar{C}_4$	$(\bar{C}_2, C_2)$	C_3	$\bar{C}_3$
Γ_6^+	2	−2	0	$2^{1/2}$	$-2^{1/2}$	0	1	−1
Γ_7^+	2	−2	0	$-2^{1/2}$	$2^{1/2}$	0	1	−1
Γ_8^+	4	−4	0	0	0	0	−1	1
Γ_6^-	2	−2	0	$2^{1/2}$	$-2^{1/2}$	0	1	−1
Γ_7^-	2	−2	0	$-2^{1/2}$	$2^{1/2}$	0	1	−1
Γ_8^-	4	−4	0	0	0	0	−1	1
	J	$\bar{J}$	$(JC_4^2, \bar{J}\bar{C}_4^2)$	JC_4	$\bar{J}\bar{C}_4$	$(JC_2, \bar{J}\bar{C}_2)$	JC_3	$\bar{J}\bar{C}_3$
Γ_6^+	2	−2	0	$2^{1/2}$	$-2^{1/2}$	0	1	−1
Γ_7^+	2	−2	0	$-2^{1/2}$	$2^{1/2}$	0	1	−1
Γ_8^+	4	−4	0	0	0	0	−1	1
Γ_6^-	−2	2	0	$-2^{1/2}$	$2^{1/2}$	0	−1	1
Γ_7^-	−2	2	0	$2^{1/2}$	$-2^{1/2}$	0	−1	1
Γ_8^-	−4	4	0	0	0	0	1	−1

$$\Gamma_1 \times D^{(1/2)} = \Gamma_6^+ \qquad \Gamma_{1'} \times D^{(1/2)} = \Gamma_6^-$$
$$\Gamma_2 \times D^{(1/2)} = \Gamma_7^+ \qquad \Gamma_{2'} \times D^{(1/2)} = \Gamma_7^-$$
$$\Gamma_{12} \times D^{(1/2)} = \Gamma_8^+ \qquad \Gamma_{12'} \times D^{(1/2)} = \Gamma_8^-$$
$$\Gamma_{15} \times D^{(1/2)} = \Gamma_6^- + \Gamma_8^- \qquad \Gamma_{15'} \times D^{(1/2)} = \Gamma_6^+ + \Gamma_8^+$$
$$\Gamma_{25} \times D^{(1/2)} = \Gamma_7^- + \Gamma_8^- \qquad \Gamma_{25'} \times D^{(1/2)} = \Gamma_7^+ + \Gamma_8^+$$

Table A.3

Moment along [110]

$$\Gamma_8^+ \rightarrow 2Y_1^+ \oplus 2Y_2^+$$

	E	A	JE	JA
Y_1^+	1	i	1	i
Y_2^+	1	-i	1	-i

$A = C_2$

New IBZ is old IBZ x 12 as follows:

x	y	z
-x	-y	z
x	-y	-z
-x	y	-z
x	-z	y
x	z	-y
z	y	-x
-z	y	x
z	-y	x
-x	z	y
-z	-y	-z
-x	-z	-y

Table A.4

Moment along [111]

$$\Gamma_8^+ \rightarrow 2\Gamma_1^+ \oplus \Gamma_2^+ \oplus \Gamma_3^+$$

	E	A	B	$\mathcal{I}$E	$\mathcal{I}$A	$\mathcal{I}$B
Γ_1^+	1	-1	1	1	-1	1
Γ_2^+	1	$-\omega^2$	ω	1	$-\omega^2$	ω
Γ_3^+	1	$-\omega$	ω^2	1	$-\omega$	ω^2

$A = C_3 \quad B = C_3^2 \quad \omega = \frac{1}{2}(-1+i\sqrt{3})$

New IBZ consists of old IBZ x 8 as follows:

x	y	z
-x	-y	z
x	-y	-z
-x	y	-z
-y	x	z
y	-x	z
x	-z	y
-y	-x	-z

Quantization axis is [111] and so $T_{\mu\nu}(\underline{4})$ requires rotation $\theta = 70°32'4''$.

APPENDIX B

Hartree-Fock equations with a Hund's rule term

The Hamiltonian that was adopted above

$$H = \sum_{\mu\nu\underline{k}} T_{\mu\nu}(\underline{k})\, c^{+}_{\mu\underline{k}}\, c_{\nu\underline{k}} + U \sum_{i} \sum_{\mu<\nu} n_{\mu i}\, n_{\nu i}$$

does not take into account Hund's rule coupling, and the calculation of moments compared with their experimental values (Brooks, private communication) indicate that this interaction may well be significant. The form of such a term in the Hamiltonian H_h must be invariant under rotation, and distinguish between the orbitals with $m_j = \pm 3/2$ and $m_j = \pm 1/2$ without distinguishing between $m_j = +3/2, -3/2$ or $m_j = +1/2, -1/2$; thus Kramers' degeneracy and invariance under time reversal are to be retained. A suitable Hamiltonian is

$$H_h = H + U' \sum_{i} \underline{J}_i \cdot \underline{J}_i \qquad \text{(B.1)}$$

where U' is an energy parameter, alongside U and the Slater-Koster hopping integrals. Writing H_h in a more suitable basis, the Hartree-Fock single-particle Hamiltonian can be derived

$$H_h = H + U' \sum_{i} \left(\tfrac{1}{2} J_i^{+} J_i^{-} + \tfrac{1}{2} J_i^{-} J_i^{+} + J_i^{z^2} \right) \qquad \text{(B.2)}$$

and this can be expressed as

$$H_h = H + U' \sum_{i} \left(J_i^{+} J_i^{-} + J_i^{z^2} + \tfrac{1}{2} [J_i^{-}, J_i^{+}] \right) \qquad \text{(B.3)}$$

$$H = H_h + \frac{U'}{2}\sum_i J_i^{z2} + U'\sum_i \left(f_\mu^+ f_\nu^- c_{\mu+1i}^+ c_{\mu i} c_{\nu-1i}^+ c_{\nu i} \right. \qquad \text{(B.4)}$$
$$\left. + f_\mu^o f_\nu^o c_{\mu i}^+ c_{\mu i} c_{\nu i}^+ c_{\nu i} \right)$$

using the scalar Clebsch-Gorden coefficient f_μ^α as defined in equation (1.46). Then, similarly to above,

$$\left[\sum_\mu a_{n\mu}(\underline{k})\, c_{\mu\underline{k}}^+ , H_h \right] = -E_{n\underline{k}} \sum_\mu a_{n\mu}(\underline{k})\, c_{\mu\underline{k}}^+ \qquad \text{(B.5)}$$

$$\left[c_{\mu\underline{k}}^+ , (J_i^+ J_i^- + J_i^{z2}) \right] = \frac{1}{\sqrt{N}} e^{i\underline{k}\cdot\underline{R}_i} \left(\left[c_{\mu i}^+ , f_\lambda^+ f_\nu^- c_{\lambda+1i}^+ c_{\lambda i} \right. \right. \qquad \text{(B.6)}$$
$$\left. \times c_{\nu-1i}^+ c_{\nu i} \right] + \left. \left[c_{\mu i}^+ , f_\lambda^o f_\nu^o c_{\lambda i}^+ c_{\lambda i} c_{\nu i}^+ c_{\nu i} \right] \right)$$

$$= -\frac{1}{\sqrt{N}} e^{i\underline{k}\cdot\underline{R}_i} \left\{ f_\mu^+ f_\nu^- c_{\mu+1i}^+ c_{\nu-1i}^+ c_{\nu i} + f_\lambda^+ f_\mu^- c_{\lambda+1i}^+ c_{\lambda i} c_{\mu-1i}^+ \right. \qquad \text{(B.7)}$$
$$\left. + f_\mu^o f_\nu^o c_{\mu i}^+ c_{\nu i}^+ c_{\nu i} + f_\lambda^o f_\mu^o c_{\lambda i}^+ c_{\lambda i} c_{\mu i}^+ \right\}$$

and so working entirely in $\underline{k}$-space,

$$\sum_i \left[c_{\mu\underline{k}}^+ , (J_i^+ J_i^- + J_i^{z2}) \right] = -\frac{1}{N} \sum_{\underline{k}_1 \underline{k}_2 \lambda\nu} \left\{ f_\mu^+ f_\nu^- c_{\mu+1\underline{k}_1}^+ c_{\nu-1\underline{k}_2} c_{\nu\, \underline{k}_1+\underline{k}_2-\underline{k}} \right. \qquad \text{(B.8)}$$
$$+ f_\lambda^+ f_\mu^- c_{\lambda+1\underline{k}_1}^+ c_{\lambda\, \underline{k}_1+\underline{k}_2-\underline{k}} c_{\mu-1\underline{k}_2}^+ + f_\mu^o f_\nu^o c_{\mu\underline{k}_1}^+ c_{\nu\underline{k}_2}^+ c_{\nu\, \underline{k}_1+\underline{k}_2-\underline{k}}$$
$$\left. + f_\lambda^o f_\mu^o c_{\lambda\underline{k}_1}^+ c_{\lambda\, \underline{k}_1+\underline{k}_2-\underline{k}} c_{\mu\underline{k}_2}^+ \right\}$$

This expression is now put in terms of the $C_{m\underline{k}}^+$ basis, and the RPA applied. Then using

$$\sum_\mu a_{n\mu}(\underline{k}) \left[c_{\mu\underline{k}}^+ , H_h \right] = -E_{n\underline{k}}\, c_{n\underline{k}}^+ \qquad \text{(B.9)}$$

and from (provided the states $|\mu\underline{k}\rangle$ form a complete set)

$$c^{+}_{n\underline{k}}|0\rangle = |n\underline{k}\rangle = \sum_{\mu} |\mu\underline{k}\rangle\langle\mu\underline{k}|n\underline{k}\rangle$$

$$= \sum_{\mu} a_{n\mu}(\underline{k})\,|\mu\underline{k}\rangle \qquad \text{(B.10)}$$

we obtain, placing the terms from the $\left(H + \frac{U'}{2}\sum_i J_i^z\right)$ term in the description 'other terms':

$$E_{n\underline{k}}\, a_{n\alpha}(\underline{k}) = \text{other terms} - \sum_{\underline{k}_1 \ell\mu\nu\lambda} \frac{U'}{N} \Big\{ f^{+}_{\mu} f^{-}_{\alpha+1}\, a^{*}_{\ell\mu+1}(\underline{k}_1)\, a_{\ell\alpha+1}(\underline{k}_1)$$

$$+ f^{+}_{\alpha-1} f^{-}_{\mu}\, a_{\ell\alpha-1}(\underline{k}_1) a^{*}_{\ell\mu-1}(\underline{k}_1) + f^{o}_{\mu} f^{o}_{\alpha}\, a^{*}_{\ell\mu}(\underline{k}_1) a_{\ell\alpha}(\underline{k}_1) + f^{o}_{\alpha} f^{o}_{\mu}\, a_{\ell\alpha}(\underline{k}_1) a^{*}_{\ell\mu-1}(\underline{k}_1)$$

$$- f^{+}_{\mu} f^{-}_{\nu}\, a^{*}_{\ell\nu-1}(\underline{k}_1) a_{\ell\nu}(\underline{k}_1) - f^{+}_{\lambda} f^{-}_{\mu}\, a^{*}_{\ell\lambda+1}(\underline{k}_1) a_{\ell\lambda}(\underline{k}_1) - f^{o}_{\mu} f^{o}_{\nu}\, a^{*}_{\ell\nu}(\underline{k}_1) a_{\ell\nu}(\underline{k}_1)$$

$$- f^{o}_{\lambda} f^{o}_{\mu}\, a^{*}_{\ell\lambda}(\underline{k}_1) a_{\ell\lambda}(\underline{k}_1) \Big\}\, a_{n\mu}(\underline{k})\, f_{\ell\underline{k}_1} \qquad \text{(B.11)}$$

Hence the Hartree-Fock potential $V_{\lambda\mu}$ is

$$V_{\lambda\mu} = \text{other terms} + \frac{U'}{N} \Big\{ 2 f^{o}_{\mu} f^{o}_{\lambda} \langle n_{\lambda\lambda}\rangle - (f^{+}_{\lambda} f^{-}_{\mu} + f^{o}_{\lambda} f^{o}_{\mu})\langle n_{\lambda\mu-1}\rangle$$

$$- (f^{+}_{\mu-1} f^{-}_{\lambda} + f^{o}_{\mu} f^{o}_{\lambda})\langle n_{\lambda\mu}\rangle \Big\} \qquad \text{(B.12)}$$

Using the diagonal property of $\langle n_{\lambda\mu}\rangle$ we have

$$V_{\lambda\mu} = \text{other terms} - \frac{U'}{N} (f^{+}_{\lambda} f^{-}_{\lambda+1} + f^{o}_{\lambda} f^{o}_{\lambda+1} + f^{+}_{\lambda-1} f^{-}_{\lambda}$$

$$+ f^{o}_{\lambda} f^{o}_{\lambda})\, \delta_{\lambda\mu}\langle n_{\lambda\lambda}\rangle \qquad \text{(B.13)}$$

$$V_{\lambda\mu} = \text{other terms} - \frac{U'}{N}\Big\{ \lambda(2\lambda+1) + \Big(\tfrac{3}{2}\tfrac{5}{2} - \lambda(\lambda+1)\Big) + \Big(\tfrac{3}{2}\tfrac{5}{2} - \lambda(\lambda-1)\Big)\Big\}\delta_{\lambda\mu}\langle n_{\lambda\lambda}\rangle \qquad \text{(B.14)}$$

$$= \text{other terms} - \frac{U'}{N}\left(\lambda + \frac{15}{2}\right)\delta_{\lambda\mu}\langle n_{\lambda\lambda}\rangle \qquad \text{(B.15)}$$

and so the potential $V_{\lambda\mu}$ including the Hund's interaction is

$$V_{\lambda\mu} = \Big\{ U\left(n\delta_{\mu\mu} - \langle n_{\mu\mu}\rangle\right) + \frac{U'}{2}\mu\langle n_{\mu\mu}\rangle - U'\left(\mu + \frac{15}{2}\right)\langle n_{\mu\mu}\rangle \Big\}\delta_{\lambda\mu} \qquad \text{(B.16)}$$

$$= \Big\{ Un\delta_{\mu\mu} - \left(U + \frac{15}{2}U'\right)\langle n_{\mu\mu}\rangle - \frac{U'}{2}\mu\langle n_{\mu\mu}\rangle \Big\}\delta_{\lambda\mu} \qquad \text{(B.17)}$$

This gives a single-particle Hamiltonian which, as it includes a $-\frac{U'}{2}\mu\langle n_{\mu\mu}\rangle$ term, forms a quadrupolar-ordered state less easily (depending upon U'/U) with respect to the magnetic ordering.

APPENDIX C

Slater-Koster matrix for the f states subband (j = 5/2)

For the Slater-Koster kinetic energy matrix $T_{\mu\nu}(\underline{k})$ appropriate for the $l = 3$, s = 1/2 f states there are (in the context of high spin-orbit coupling) two subbands, with j = 7/2 and j = 5/2. The canonical values of the ff hopping integrals are given in Anderson (1978, 1979) and Brooks (1980), and allow $ff\pi$, $ff\delta$ and $ff\phi$ to be expressed in terms of $ff\sigma$:

$$ff\sigma = 1$$

$$ff\pi = -\frac{3}{4}$$

$$ff\delta = \frac{3}{20}$$

$$ff\phi = -\frac{1}{20}$$

In a similar manner to Sharma (1979), Takegahara et al. (1980) and Lendi (1974) we can use the basis states

$$\phi_1 = 2\sqrt{15}\, C\, xyz = i\frac{1}{\sqrt{2}}(-Y_{32} + Y_{3-2})$$

$$\phi_2 = Cx(5x^2 - 3r^2) = \frac{1}{4}(-\sqrt{5}Y_{33} + \sqrt{3}Y_{31} - \sqrt{3}Y_{3-1} + \sqrt{5}Y_{3-3})$$

$$\phi_3 = Cy(5y^2 - 3r^2) = \frac{1}{4}i(-\sqrt{5}Y_{33} - \sqrt{3}Y_{31} - \sqrt{3}Y_{3-1} - \sqrt{5}Y_{3-3})$$

$$\phi_4 = Cz(5z^2 - 3r^2) = Y_{30} \qquad \text{(C.1)}$$

$$\phi_5 = \sqrt{15}\, C\, x(y^2 - z^2) = \frac{1}{4}(\sqrt{3}Y_{33} + \sqrt{5}Y_{31} - \sqrt{5}Y_{3-1} - \sqrt{3}Y_{3-3})$$

$$\phi_6 = \sqrt{15}\, C\, y(z^2 - x^2) = \frac{1}{4}i(-\sqrt{3}Y_{33} + \sqrt{5}Y_{31} + \sqrt{5}Y_{3-1} - \sqrt{3}Y_{3-3})$$

$$\phi_7 = \sqrt{15}\, C\, z(x^2 - y^2) = \frac{1}{\sqrt{2}}(Y_{32} + Y_{3-2})$$

where

$$C = \left(\frac{7}{16\pi}\right)^{1/2} r^{-3}$$

Hence, using the states in the j = 5/2 subband only, and the decomposition of states $|j m_j\rangle$ into states $|\ell s\rangle$:

$$\begin{aligned}
|5/2\ 5/2\rangle &= \sqrt{\tfrac{6}{7}}\,|3\ -1/2\rangle - \sqrt{\tfrac{1}{7}}\,|2\ 1/2\rangle \\
|5/2\ 3/2\rangle &= \sqrt{\tfrac{5}{7}}\,|2\ -1/2\rangle - \sqrt{\tfrac{2}{7}}\,|1\ 1/2\rangle \\
|5/2\ 1/2\rangle &= \sqrt{\tfrac{4}{7}}\,|1\ -1/2\rangle - \sqrt{\tfrac{3}{7}}\,|0\ 1/2\rangle \\
|5/2\ -1/2\rangle &= \sqrt{\tfrac{3}{7}}\,|0\ -1/2\rangle - \sqrt{\tfrac{4}{7}}\,|-1\ 1/2\rangle \\
|5/2\ -3/2\rangle &= \sqrt{\tfrac{2}{7}}\,|-1\ 1/2\rangle - \sqrt{\tfrac{5}{7}}\,|-2\ 1/2\rangle \\
|5/2\ -5/2\rangle &= \sqrt{\tfrac{1}{7}}\,|-2\ -1/2\rangle - \sqrt{\tfrac{6}{7}}\,|-3\ 1/2\rangle
\end{aligned} \tag{C.2}$$

we can write the form of $T_{\mu\nu}(\underline{k})$ (in the basis $|5/2\ 5/2\rangle, |5/2\ 3/2\rangle, |5/2\ 1/2\rangle, \ldots |5/2\ -5/2\rangle$) as

$$T_{\mu\nu}(\underline{k}) = \left(\begin{array}{ccc:ccc}
a & d & e & f & g & 0 \\
d^* & b & i & j & 0 & g \\
e^* & i^* & c & 0 & j & -f \\
\hdashline
f^* & j^* & 0 & c & -i & e \\
g^* & 0 & j^* & -i^* & b & -d \\
0 & g^* & -f^* & e^* & -d^* & a
\end{array}\right) \tag{C.3}$$

where the $(-1)^m$ in the definition of the spherical harmonic implies that

$$\begin{aligned}
|1\ s\rangle &= -\langle -1\ s|^* \\
|3\ s\rangle &= -\langle -3\ s|^*
\end{aligned}$$

Kramers' degeneracy implies that $T_{\mu-\mu}(\underline{k}) = 0$, and stems from invariance under time reversal.

Then, the following matrix elements were calculated:

$$(\phi_1/\phi_1) = (xyz/xyz) = (\cos\xi\cos\eta + \cos\eta\cos\zeta + \cos\xi\cos\zeta)\left(\tfrac{5}{2}pp\pi + \tfrac{3}{2}pp\phi\right)$$

$$(\phi_1/\phi_4) = (xyz/z(5z^2-3r^2)) = \tfrac{\sqrt{15}}{2}\sin\xi\sin\eta\,(pp\pi - pp\phi)$$

$$(\phi_1/\phi_7) = (xyz/z(x^2-y^2)) = 0$$

$$(\phi_4/\phi_2) = (z(5z^2-3r^2)/x(5x^2-3r^2)) = \sin\xi\sin\zeta\left(-\tfrac{1}{8}pp\sigma + \tfrac{27}{16}pp\pi - \tfrac{15}{8}pp\delta + \tfrac{5}{16}pp\phi\right)$$

$$(\phi_4/\phi_3) = (z(5z^2-3r^2)/y(5y^2-3r^2)) = \sin\eta\sin\zeta\left(-\tfrac{1}{8}pp\sigma + \tfrac{27}{16}pp\pi - \tfrac{15}{8}pp\delta + \tfrac{5}{16}pp\phi\right)$$

$$(\phi_4/\phi_4) = (z(5z^2-3r^2)/z(5z^2-3r^2)) = (\cos\zeta\cos\xi + \cos\zeta\cos\eta)\left(\tfrac{1}{8}pp\sigma + \tfrac{27}{16}pp\pi + \tfrac{15}{8}pp\delta + \tfrac{5}{16}pp\phi\right) + \cos\xi\cos\eta\left(\tfrac{3}{2}pp\pi + \tfrac{5}{2}pp\phi\right)$$

$$(\phi_7/\phi_2) = (z(x^2-y^2)/x(5x^2-3r^2)) = \sqrt{15}\sin\xi\sin\zeta\left(\tfrac{1}{8}pp\sigma - \tfrac{3}{16}pp\pi - \tfrac{1}{8}pp\delta + \tfrac{3}{16}pp\phi\right)$$

$$(\phi_7/\phi_3) = (z(x^2-y^2)/y(5y^2-3r^2)) = \sqrt{15}\sin\eta\sin\zeta\left(-\tfrac{1}{8}pp\sigma + \tfrac{3}{16}pp\pi + \tfrac{1}{8}pp\delta - \tfrac{3}{16}pp\phi\right)$$

$$(\phi_7/\phi_4) = (z(x^2-y^2)/z(5z^2-3r^2)) = \sqrt{15}(\cos\xi\cos\zeta - \cos\eta\cos\zeta)\left(-\tfrac{1}{8}pp\sigma - \tfrac{3}{16}pp\pi + \tfrac{1}{8}pp\delta + \tfrac{3}{16}pp\phi\right)$$

$$(\phi_7/\phi_5) = (z(x^2-y^2)/x(y^2-z^2)) = \sin\xi\sin\zeta\left(\tfrac{15}{8}pp\sigma - \tfrac{5}{16}pp\pi + \tfrac{1}{8}pp\delta - \tfrac{27}{16}pp\phi\right)$$

$$(\phi_7/\phi_6) = (z(x^2-y^2)/y(z^2-x^2)) = \sin\eta\sin\zeta\left(\tfrac{15}{8}pp\sigma - \tfrac{5}{16}pp\pi + \tfrac{1}{8}pp\delta - \tfrac{27}{16}pp\phi\right)$$

$$(\phi_7/\phi_7) = (z(x^2-y^2)/z(x^2-y^2)) = (\cos\xi\cos\zeta + \cos\zeta\cos\eta)\left(\tfrac{15}{8}pp\sigma + \tfrac{5}{16}pp\pi + \tfrac{1}{8}pp\delta + \tfrac{27}{16}pp\phi\right) + 4\cos\xi\cos\eta\,pp\delta$$

and hence using (C.1) and (C.2) to express $T_{\mu\nu}(\underline{k})$ in terms of $\langle ls \mid T \mid l's' \rangle$ gave the following

$$a = A\,(1{\cdot}07143\,pp\sigma + 1{\cdot}78571\,pp\pi + 0{\cdot}92857\,pp\delta + 0{\cdot}21429\,pp\phi) + (B+C) \times (0{\cdot}26789\,pp\sigma + 0{\cdot}80358\,pp\pi + 1{\cdot}37500\,pp\delta + 1{\cdot}55357\,pp\phi)$$

$$b = A\,(0{\cdot}21429\,pp\sigma + 0{\cdot}92857\,pp\pi + 1{\cdot}78571\,pp\delta + 1{\cdot}07143\,pp\phi) + (B+C) \times (0{\cdot}91071\,pp\sigma + 1{\cdot}30357\,pp\pi + 0{\cdot}44643\,pp\delta + 1{\cdot}33929\,pp\phi)$$

$$c = A\,(0{\cdot}42857\,pp\sigma + 0{\cdot}71429\,pp\pi + 0{\cdot}71429\,pp\delta + 2{\cdot}14286\,pp\phi) + (B+C) \times (0{\cdot}53571\,pp\sigma + 1{\cdot}32143\,pp\pi + 1{\cdot}60714\,pp\delta + 0{\cdot}53571\,pp\phi)$$

$$d = (E - iD)(0.47916\,ff_\sigma + 0.79860\,ff_\pi + 0.15972\,ff_\delta - 1.43747\,ff_\phi)$$

$$e = (B - C)(0.16941\,ff_\sigma - 0.16941\,ff_\pi - 0.84704\,ff_\delta + 0.84704\,ff_\phi)$$
$$+ iF(-0.67763\,ff_\sigma - 0.67763\,ff_\pi + 0.67763\,ff_\delta + 0.67763\,ff_\phi)$$

$$f = (E + iD)(-0.33882\,ff_\sigma - 0.45175\,ff_\pi + 0.79057\,ff_\delta)$$

$$g = A(-0.47916\,ff_\sigma - 0.15972\,ff_\pi + 1.11803\,ff_\delta - 0.47916\,ff_\phi)$$
$$+ (B+C)(0.11979\,ff_\sigma + 0.03993\,ff_\pi - 0.27951\,ff_\delta + 0.11979\,ff_\phi)$$
$$+ iF(-0.65884\,ff_\sigma + 0.25456\,ff_\pi + 0.65884\,ff_\delta - 0.25456\,ff_\phi)$$

$$i = (E - iD)(0.45457\,ff_\sigma + 0.55558\,ff_\pi - 0.25254\,ff_\delta - 0.75761\,ff_\phi)$$

$$j = (B - C)(-0.53033\,ff_\sigma - 0.47982\,ff_\pi + 0.63135\,ff_\delta + 0.37881\,ff_\phi)$$
$$+ iF(-0.30305\,ff_\sigma - 0.70711\,ff_\pi - 0.50508\,ff_\delta + 1.51523\,ff_\phi)$$

$$A = \cos\xi\cos\eta \qquad C = \cos\eta\cos\zeta \qquad E = \sin\xi\sin\zeta$$
$$B = \cos\xi\cos\zeta \qquad D = \sin\eta\sin\zeta \qquad F = \sin\xi\sin\eta$$

Also it can be shown that the representation D of the

of the six j = 5/2 subband states is a sum of the irreducible

representations

$$D = \Gamma_7^- \oplus \Gamma_8^-$$

From the states given at equation (C.1), using BSW notation,

$$(\Gamma_{25} \oplus \Gamma_{25} \oplus \Gamma_{2'}) \otimes D^{(1/2)} = 2(\Gamma_7^- \oplus \Gamma_8^-) \oplus \Gamma_7^- \qquad \text{(C.4)}$$

and from the character table of D

	E	$\bar{E}$	C_4^2	C_4	$\bar{C}_4$	C_2	C_3	$\bar{C}_3$
D	6	-6	0	$-\sqrt{2}$	$\sqrt{2}$	0	0	0

	J	$\bar{J}$	JC_4^2	JC_4	$\bar{J}\bar{C}_4$	JC_2	JC_3	$\bar{J}\bar{C}_3$
D	-6	6	0	$\sqrt{2}$	$-\sqrt{2}$	0	0	0

and using the character tables of the likely irreducible representations Γ_i found in equation (C.4) we can decompose D into a_i irreducible representations Γ_i . Thus

$$D = \sum_i a_i \Gamma_i$$

where the character $\chi(\alpha)$ of the elements α is

$$\chi(\alpha) = \sum_i a_i \chi_i(\alpha)$$

Then the coefficients a_i are given by

$$a_i = \frac{1}{g} \sum_r N_r \chi_i^*(r) \chi(r)$$

summing over classes r to give

$$D = \Gamma_7^- \oplus \Gamma_8^- .$$

REFERENCES

Abrikosov A.A., Gorkov L.P. and Dzyaloshinski I.E., 'Methods of Quantum Field Theory in Statistical Physics', Prentice-Hall (1963).

Adachi H. and Imoto S., J.N. Sci. Tech. **6** (7), 371 (1969).

Allen S.J., Phys. Rev. B **166**, 2, 530 (1968); **167**, 2, 492 (1968).

Anderson O.K., Klose W. and Nohl H., Phys. Rev. B **17**, 3, 1209 (1978).

Anderson O.K. Pure & Appl. Chem. **52**, 93 (1979).

Anderson P.W., Sol. St. Phys. **14** (1963).

Anderson P.W., Phy. Rev. B **30**, 1549 (1984).

Brinkman W.F. and Rice T.M., Phys. Rev. B **2**, 10, 4302 (1970).

Brookes M.S.S., Physica, **102B**, 51 (1980).

Brookes M.S.S., J. Phys. F. **14**, 639, 653, 857 (1984).

Brookes M.S.S. and Kelly P.J., to be published (1985).

Buyers W.J., Murray A.F., Holden T.M., Svensson E.C., Du Plessis P. de V., Lander G.H. and Vogt O., Physica **102B**, 291 (1980).

Buyers W.J., Murray A.F., Jackman J.A., Holden T.M., Du Plessis P. de V. and Vogt O., J. Appl. Phys.**52**, 2222 (1981).

Buyers W.J. and Holden T.H., Ch. 4 of 'Handbook on the Physics and Chemistry of the Actinides', edited by A.J. Freeman and G.H. Lander, North Holland (1985).

Callaway J., 'Quantum Theory of the Solid State', Academic Press, New York (1974).

Callaway J., Chatterjee A.K., Singhal S.P. and Ziegler A., to be published.

Combercot M. and Combercot R., Phys. Rev. Lett. **37**, 6, 388 (1976).

Cooke J.F., Lynn J.W. and Davies H.L., Sol. St. Comm. **20**, 799 (1976).

Cooke J.F., Phys. Rev. B **7**, 1108 (1973).

Cooke J.F., Lynn J.W. and Davies H.L., Phys. Rev. B **21**, 4118 (1980).

Cooper B.R., JMMM, **29**, 230 (1982).

Cooper B.R., Thayamballi P., Spirlet J.C., Müller W. and Vogt O., Phys. Rev. Lett. **51**, 26, 2418 (1983).

Coqblin B. and Schrieffer J.R., Phys. Rev. **185**, 847 (1969).

Cyrot M., and Lyon-Caen C., J. Phys. C. **6**, L247 (1973); J. Phys. Paris **36**, 253 (1975).

Doniach S. and Engelsberg S., Phys. Rev. Lett. **17**, 750 (1966).

Edwards D.M., Vancouver Conference Proceedings (1984).

Erdös P. and Robinson J.M., 'The Physics of Actinide Compounds', Plenum Press, London (1983).

Falica L.M. and Ruvalds J., Phys. Rev. **172**, 2, 498 (1968).

Fournier J.M., Beille J., Boeuf A., Wedgwood A., Physica **102B**, 282 (1980).

Fulde P. and Jensen J., Phys. Rev. B **27**, 7, 4085 (1983).

Hodges L., Ehrenreich H. and Lang N.D., Phys. Rev. **152**, 2, 505 (1966).

Holden T.M., Buyers W.J.L., Svensson E.C., Jackman J.A. and Murray A.F., J. Appl. Phys. **53** (3), 1967 (1982a).

Holden T.M., Buyers W.J.L., Svensson E.C. and Lander G.H., Phys. Rev. B **26**, 6227 (1982b).

Inagaki S. and Kubo R., Int. J. Magnetism **4**, 139 (1973).

Izuyama T., Kim D. and Kubo R., J. Phys. Soc. Japan **18**, 1025 (1963).

Khomskii D.I. and Kugel K.I., Sol. St. Comm. **13**, 763 (1973).

Knott H.W., Lander G.H., Mueller M.H. and Vogt O., Phys. Rev. B **21**, 4159 (1980).

Kugel K.I. and Khomskii D.I., Sov. Phys. Solid State **15**, 7 (1974).

Lander G.H. and Mueller M.H., Phys. Rev. B **10**, 1994 (1974).

Lander G.H., Sinha S.K., Sparlin D.M. and Vogt O., Phys. Rev. Lett. **40**, 523 (1978).

Lander G.H. and Stirling W.G., Phys. Rev. B **21**, 436 (1980).

Leggett A.J., Rev. Mod. Phys. **47**, 2, 331 (1975).

Leggett A.J. and Tagaki S., Phys. Rev. Lett. **36**, 23, 1379 (1976).

Lehmann G. and Tant M., Phys. Status Solidi **54**, 469 (1972).

Lendi K., Phys. Rev. B **9**, 6, 2433 (1974).

Levy P.M., Morin P. and Schmitt D., Phys. Rev. Lett. **42**, 21, 1417 (1979).

Loewenhaupt M., Lander G.H., Murani A.P. and Murasik A., J. Phys. C. **15**, 6199 (1982).

Long C. and Wang Y-L., Phys. Rev. B **3**, 5, 1656 (1971).

Lowde R.D. and Windsor C.G., Adv. Phys. **19**, 813 (1970).

Marshall W. and Lovesey S.W., 'Theory of Thermal Neutron Scattering', Clarendon, Oxford (1971).

Marshall W. and Lowde R.D., Rep. Prog. Phys. **31** (2), 705 (1968).

Morin P. and Schmitt D., Phys. Rev. B **23**, 11, 5936 (1981); J. Appl. Phys. **52** (3), 2090 (1981).

Morin P. and Schmitt D., J. Phys. F. **8**, 951 (1978).

Norton P.R., Tapping R.L., Creber D.K. and Buyers W.J.L., Phys. Rev. B **21**, 2572 (1980).

Rajogopal A.K. and Callaway J., Phys. Rev. B **7**, 5, 1912 (1973).

Rath J. and Freeman A.J., Phys. Rev. B **11**, 6, 2109 (1975).

Rice T.M., Ueda K., Ott H.R. and Rudigier H., Phys. Rev. B **31**, 1, 594 (1985).

Razafimandimby H., Fulde P. and Keller J., Z. f. Physik B **54**, 111 (1984).

Sharma R.R., Phys. Rev. B **19**, 6, 2813 (1979).

Siemann R. and Cooper B.R., Phys. Rev. Lett. **44**, 15, 1015 (1980).

Sinha S.K., Lander G.H., Shapiro S.M. and Vogt O., Phys. Rev. B **23**, 4556 (1981).

Sivardiere J. and Blume M., Phys. Rev. B **5** (3), 1126 (1972).

Slater J.C. and Koster G.F., Phys. Rev. **94**, 1498 (1954).

Stewart G.R., Rev. Mod. Phys. **56**, 4, 755 (1984).

Stirling W.G., Lander G.H. and Vogt O., Physica **102B**, 249 (1980).

Takegahara K., Aoki Y. and Yanase A., J. Phys. C. **13**, 583 (1980).

Teitelbaum H.H. and Levy P.M., Phys. Rev. B **14** (7), 3058 (1976).

Thayamballi P. and Cooper B.R., J. Appl. Phys. **55** (6), 1829 (1984).

Vollhardt D., Rev. Mod. Phys. **56**, 99 (1984).

Vosko S.H. and Perdew J.P., Can. J. Phys. **53**, 1385 (1975).

Weinberger P., Mallett C.P., Podloucky R. and Nechel A., J. Phys. C.**13**, 173 (1980).

White R.M. and Fulde P., Phys. Rev. Lett. **47**, 21, 1540 (1981).

Wölfle P., Phys. Rev. Lett. **37**, 19, 1279 (1976).

Wuilloud E., Baer Y., Ott H.R., Fisk Z. and Smith J.L., Phys. Rev. B **29**, 9, 5228 (1984).

Yang D. and Cooper B.R., J. Appl. Phys. **53** (3), 1988 (1982).

Zubarev D.N., Sov. Phys. Usp. **3**, 320 (1960).